

Development of an *in vitro* gingivitis model

Thesis submitted by

Joanna Maria Wiecek

For the degree of

DOCTOR OF PHILOSOPHY

in the

Faculty of Medical Sciences

University College London

Division of Microbial Diseases

UCL Eastman Dental Institute

256 Gray's Inn Road

London WC1X 8LD

UK

Declaration

I hereby certify that the work embodied in this thesis is the result of my own investigation. Where the information was derived from other sources, I confirm that this has been indicated in the thesis.

The contents have not been submitted for any other qualification.

Signed

Date

Acknowledgements

My sincere appreciation goes to Dr David Spratt whom I would like to thank for being a great supervisor and a great friend. I would like to express my appreciation for his invaluable guidance, assistance, and support throughout the period of this project, and for proofreading this thesis. The knowledge I have gained from our discussions over the past years has been instrumental in the success of this research project, it would have been truly impossible without him.

I would like to express my deepest gratitude to Don White for funding this project and his continuous support. I am most appreciative for the countless brainstorming sessions and the knowledge he has shared. The positive attitude shown by him throughout the entirety of this project has truly inspired me to persevere and endure throughout this PhD programme.

I would like to acknowledge the financial, academic and technical support provided by University College London and Procter & Gamble (Impact Scholarship).

stay hungry stay foolish

Abstract

Gingivitis a gum disease, affects 50-90% of the adult population worldwide, if left untreated gingivitis can lead to periodontitis. However, even though gingivitis is highly prevalent, the pathogenicity of the disease is still poorly understood; highlighting the need for a reliable and reproducible *in vitro* gingivitis model which could help elucidate clinically important questions and provide a better understanding of gingivitis aetiology. In this study the original Constant Depth Film Fermentor (CDFF) was modified to create a Triple-CDFF (T-CDFF) allowing concurrent growth of oral biofilms that can be treated separately in a controlled, flexible environment. Several mechanical changes were implemented to increase the model's reliability, reproducibility and manoeuvrability; including improving airtightness of the model by applying better seals, re-shaping model parts to increase portability. A standardised experimental methodology was devised; this included sampling procedures to allow reliable and reproducible growth of oral biofilms across the individual units of this system. Biofilms obtained from T-CDFF under health and disease conditions were screened for eight bacteria; using qPCR primers for *S. sanguinis*, *V. dispar*, *N. subflava*, *S. mutans*, *L.casei*, *F. nucleatum*, *P. intermedia*, and *A. naeslundii*. To investigate the presence of other bacteria associated with gingivitis such as *T. denticola*, *P. gingivalis*, a trypsin-like-protease assay was applied. Next generation sequencing combined with metabolomics gave a better understanding of the bacterial changes occurring during simulated disease progression. In conclusion, this study has successfully (i) developed and validated a new complex *in vitro* T-CDFF system and also (ii) showed great potential for modelling gingivitis *in vitro*; although further verification needed. The system was considered reliable and shows a great potential for being used as a standardised model for testing dentifrices and antimicrobials.

Table of content

| | |
|--|----|
| Abstract..... | 7 |
| List of Figures..... | 17 |
| List of Tables..... | 27 |
| 1 CHAPTER..... | 33 |
| Introduction..... | 33 |
| 1.1 Oral cavity..... | 35 |
| 1.2 Dental plaque formation..... | 36 |
| 1.2.1.1 Enamel Pellicle Formation..... | 37 |
| 1.2.1.2 Initial colonization..... | 37 |
| 1.2.1.3 Biofilm maturation..... | 38 |
| 1.3 Periodontal diseases and the oral microbiota..... | 39 |
| 1.3.1 Gingivitis..... | 39 |
| 1.3.2 Periodontitis..... | 41 |
| 1.3.3 Plaque hypotheses of periodontal diseases..... | 43 |
| 1.3.4 Oral microbiome..... | 46 |
| 1.3.4.1 Gingivitis microbiome..... | 47 |
| 1.3.5 Reductionist approach..... | 49 |
| 1.3.6 Cultivation methods..... | 50 |
| 1.3.7 Culture independent methods..... | 51 |
| 1.3.7.1 PCR..... | 51 |
| 1.3.7.2 Quantitative PCR (qPCR)..... | 52 |
| 1.3.7.3 Fluorescence In Situ Hybridisation (FISH)..... | 52 |
| 1.3.7.4 DNA – DNA hybridisation checkerboard..... | 53 |
| 1.4 Holistic approaches..... | 54 |

| | | |
|-----------|---|----|
| 1.4.1 | Proteomics | 54 |
| 1.4.2 | Transcriptomics | 55 |
| 1.4.3 | Genomics | 56 |
| 1.4.4 | Next generation sequencing | 56 |
| 1.4.4.1 | 454 platform using pyrosequencing | 57 |
| 1.4.4.2 | SOLiD platform based on Ligation | 58 |
| 1.4.4.3 | Illumina platform based on sequencing by synthesis | 59 |
| 1.4.5 | Metabolomics | 61 |
| 1.4.5.1 | ¹ H NMR spectroscopy | 62 |
| 1.4.5.2 | Mass spectrometry based techniques..... | 63 |
| 1.4.5.2.1 | Liquid chromatography – mass spectrometry | 63 |
| 1.4.5.2.2 | Gas chromatography – mass spectrometry (GC - MS)..... | 64 |
| 1.5 | Complex <i>in vitro</i> models | 65 |
| 1.5.1 | The Chemostat | 66 |
| 1.5.2 | The Robbins device | 67 |
| 1.5.3 | Calgary Biofilm Device (CBD) | 68 |
| 1.5.4 | Multiple Sorbarod Device | 68 |
| 1.5.5 | CDC Biofilm reactor..... | 70 |
| 1.5.6 | Constant Depth Film Fermentor (CDFF) | 72 |
| 1.6 | Aims of the project | 74 |
| 2 | CHAPTER | 75 |
| 2.1 | Triple-Constant Depth Film Fermentor model (T-CDFF) | 77 |
| 2.2 | Model description..... | 78 |
| 2.2.1 | T-CDFF construction..... | 78 |
| 2.2.2 | T-CDFF set-up..... | 81 |

| | | |
|---------|--|----|
| 2.2.3 | T-CDFE calibration process..... | 83 |
| 2.2.4 | T-CDFE scheme of work | 84 |
| 2.3 | Experimental protocol | 88 |
| 2.3.1 | Standardized inoculum | 88 |
| 2.3.1.1 | Dual-species inoculum..... | 88 |
| 2.3.1.2 | Microcosm inoculum | 89 |
| 2.3.2 | Artificial saliva | 89 |
| 2.3.3 | Conditions to model oral health | 89 |
| 2.3.4 | Conditions to model gingivitis | 89 |
| 2.3.5 | T-CDFE sampling and sample processing..... | 90 |
| 2.3.5.1 | Biofilm sampling | 90 |
| 2.3.5.2 | Effluent sampling..... | 91 |
| 2.4 | Culture methods | 92 |
| 2.5 | Culture independent molecular methods | 93 |
| 2.5.1 | DNA extraction - bead beating protocol..... | 93 |
| 2.5.2 | Triplex quantitative Polymerase Chain Reaction (qPCR)..... | 94 |
| 2.5.2.1 | Quantitative Polymerase Chain Reaction (qPCR) standards | 96 |
| 2.5.3 | Duplex quantitative Polymerase Chain Reaction (qPCR)..... | 96 |
| 2.5.3.1 | Quantitative Polymerase Chain Reaction (qPCR) standards | 97 |
| 2.6 | 16S rRNA genomics..... | 97 |
| 2.7 | Metabolomics | 98 |
| 2.7.1 | Enzymatic assays..... | 98 |
| 2.7.1.1 | Acid and alkaline phosphatase assays..... | 98 |
| 2.7.1.2 | Trypsin – like – protease assay | 99 |
| 2.7.2 | ¹ H Nuclear Magnetic Resonance Spectroscopy (NMR) | 99 |

| | | |
|---------|--|-----|
| 2.7.2.1 | Sample preparation and processing..... | 99 |
| 3 | CHAPTER..... | 101 |
| 3.1 | Introduction..... | 103 |
| 3.2 | Materials and Methods..... | 105 |
| 3.2.1 | Methodology overview..... | 105 |
| 3.2.1.1 | Methodology 1..... | 105 |
| 3.2.1.2 | Methodology 2..... | 105 |
| 3.2.1.3 | Methodology 3..... | 105 |
| 3.2.1.4 | Methodology 4..... | 105 |
| 3.2.2 | CDFD sampling and data processing..... | 106 |
| 3.2.3 | Statistical analysis..... | 106 |
| 3.3 | T-CDFD results..... | 107 |
| 3.3.1 | Model development..... | 107 |
| 3.4 | Model validation..... | 109 |
| 3.4.1 | Methodology 1..... | 109 |
| 3.4.2 | Methodology 2..... | 112 |
| 3.4.3 | Methodology 3..... | 112 |
| 3.4.4 | Methodology 4..... | 115 |
| 3.4.4.1 | Investigation of the oral community developed in the T-CDFD model | 116 |
| 3.4.4.2 | Investigation of the repeatability of the T-CDFD model..... | 119 |
| 3.5 | Discussion..... | 121 |
| 3.5.1 | Development process..... | 121 |
| 3.5.2 | Validation process..... | 122 |
| 3.5.3 | Investigation of the reproducibility of the model..... | 126 |
| 3.6 | Conclusion..... | 129 |

| | | |
|---------|---|-----|
| 4 | CHAPTER | 131 |
| 4.1 | Introduction | 133 |
| 4.2 | T-CDFD Methodology | 135 |
| 4.2.1 | The experimental set-up..... | 135 |
| 4.2.2 | The experimental conditions | 135 |
| 4.2.3 | T-CDFD sampling..... | 136 |
| 4.2.4 | Statistical analysis | 137 |
| 4.2.4.1 | Reproducibility among units..... | 137 |
| 4.2.4.2 | Differences between health and disease | 138 |
| 4.2.5 | Functional approach to investigating the gingivitis associated shifts | 139 |
| 4.2.5.1 | Filter assays..... | 139 |
| 4.2.5.2 | Microcosm biofilm retrieved from T-CDFD..... | 139 |
| 4.3 | Results..... | 141 |
| 4.3.1 | Bacterial shifts from simulated health to gingivitis | 141 |
| 4.3.1.1 | Culture methods..... | 141 |
| 4.3.1.2 | Culture independent methods | 144 |
| 4.3.2 | Investigating the reproducibility of T-CDFD model..... | 149 |
| 4.3.3 | Functional approach to investigate the gingivitis associated shifts | 151 |
| 4.3.3.1 | Filter assay | 151 |
| 4.3.3.2 | Alkaline phosphatase..... | 151 |
| 4.3.3.3 | Trypsin – like – protease..... | 152 |
| 4.3.4 | Enzymatic assays on biofilm samples retrieved from T-CDFD | 152 |
| 4.4 | Discussion..... | 155 |
| 4.4.1 | Microbial trends in simulated gingivitis onset..... | 155 |
| 4.4.2 | Culture methods to analyse the gingivitis associated shifts..... | 156 |

| | | |
|---------|---|-----|
| 4.4.3 | Molecular methods to analyse the gingivitis associated shifts | 157 |
| 4.4.4 | Functional approach to investigate the gingivitis associated shifts | 161 |
| 4.4.5 | Reproducibility of the bacterial shifts in the T-CDFF model..... | 162 |
| 4.5 | Conclusion..... | 165 |
| 5 | CHAPTER | 167 |
| 5.1 | Introduction | 169 |
| 5.2 | Materials and Methods..... | 171 |
| 5.2.1 | CDFF experimental set-up..... | 171 |
| 5.2.2 | CDFF experimental conditions | 171 |
| 5.3 | CDFF sampling..... | 171 |
| 5.3.1 | Biofilm | 171 |
| 5.3.2 | Effluent..... | 172 |
| 5.4 | Post-experimental data analysis..... | 173 |
| 5.4.1 | Differences between health and disease | 173 |
| 5.4.2 | Statistical analysis | 173 |
| 5.5 | Results..... | 175 |
| 5.5.1 | Bacterial shifts..... | 175 |
| 5.5.1.1 | Culture independent methods | 175 |
| 5.5.1.2 | Bacteria implicated in gingivitis..... | 176 |
| 5.5.1.3 | The <i>Actinomyces</i> spp. - <i>Streptococcus</i> spp. cross-over | 178 |
| 5.5.1.4 | Bacteria implicated in oral health | 181 |
| 5.6 | <i>In vitro</i> gingivitis modelling – a functional approach..... | 183 |
| 5.6.1 | Enzymatic assays..... | 183 |
| 5.6.2 | ¹ H NMR Metabolomics approach | 184 |
| 5.7 | Discussion..... | 197 |

| | | |
|-----------|---|-----|
| 5.7.1 | Microbial trends in simulated gingivitis onset..... | 199 |
| 5.7.2 | Functional approach | 201 |
| 5.8 | Conclusion..... | 205 |
| 6 | CHAPTER | 207 |
| 6.1 | Introduction | 209 |
| 6.2 | Methodology..... | 211 |
| 6.2.1 | The experimental set-up and conditions..... | 211 |
| 6.2.2 | CDF sampling..... | 212 |
| 6.2.2.1 | Biofilm..... | 212 |
| 6.2.2.2 | Effluent | 212 |
| 6.2.3 | Statistical analysis | 213 |
| 6.3 | Results..... | 215 |
| 6.3.1 | Real-time PCR study to investigate the gingivitis associated shifts..... | 215 |
| 6.3.2 | Biofilm | 215 |
| 6.3.3 | Effluent data | 220 |
| 6.3.4 | Genomic approach to investigate the gingivitis associated shifts..... | 223 |
| 6.3.4.1 | Biofilm data..... | 223 |
| 6.3.4.1.1 | Phyla composition | 223 |
| 6.3.4.1.2 | Genus and species composition..... | 227 |
| 6.3.4.2 | Effluent data | 230 |
| 6.3.4.2.1 | Phyla composition | 231 |
| 6.3.4.2.2 | Genus and species composition..... | 235 |
| 6.3.5 | Functional approach to investigate the health-gingivitis associated shifts..... | 239 |
| 6.3.6 | Qualitative Analysis..... | 239 |
| 6.3.6.1 | Experiment 1 unit 1 (simulated health conditions only) | 239 |

| | | |
|---------|--|-----|
| 6.3.6.2 | Experiment 1 unit 3 (health – gingivitis conditions)..... | 240 |
| 6.3.6.3 | Experiment 2 unit 1 (simulated health conditions only) | 245 |
| 6.3.6.4 | Experiment 2 unit 3 (health – gingivitis conditions)..... | 246 |
| 6.4 | Discussion..... | 251 |
| 6.4.1 | Methodology choice | 251 |
| 6.4.2 | Methodology optimisation | 252 |
| 6.4.3 | Experimental problems encountered | 253 |
| 6.4.4 | Real-time PCR study to investigate the health-gingivitis associated shifts | 254 |
| 6.4.5 | Genomic approach to investigate the health-gingivitis associated shifts | 255 |
| 6.4.6 | Functional approach to investigate the health-gingivitis associated shifts..... | 259 |
| 6.5 | Conclusion..... | 261 |
| 7 | Final Discussion..... | 263 |
| 7.1 | Project background..... | 263 |
| 7.2 | Summary of main findings | 265 |
| 7.3 | Conclusions and future work | 269 |
| 8 | References | 271 |

List of Figures

- Figure 1.1 presents two periodontal diseases: A) gingivitis and B) periodontitis (adapted from Scannapieco 2013). A – red, tender and swollen gums and bleeding; B – swollen and red gums, bleeding receding gums, loose teeth etc
- Figure 1.2 Scheme of ecological plaque hypothesis (modified from Marsh 1994)
- Figure 1.3 Close-up of the Modified Robbins Device (MRD) (adapted from Coenye *et al.* 2011).
- Figure 1.4 Schematic diagram of the multiple Sorbarod Device (adapted from McBain *et al.* 2005).
- Figure 1.5 The CDC reactor (A) (adapted from Lewis *et al.* 2010) and its experimental set-up (B), where two CDC reactors are coupled with a medium bottle (adapted from Coenye & Nelis 2010).
- Figure 1.6 CDFF system (adapted from Wilson 1999).
- Figure 2.1 A) The standard CDFF - the prototype of T-CDFF, B) Top plate with 3 liquid inlets, gas inlet and sampling port. C) Turntable with 15 gaps for pans. D) Bottom plate with a waste output and a spindle to attach the gear box to.
- Figure 2.2 The comparison of the two models. A) CDFF model, B) T-CDFF units on the right Three liquid inlets encircled in red. Gas inlet encircled in yellow and Sampling port encircled in green.
- Figure 2.3 shows the T-CDFF model housed on the motor.
- Figure 2.4 Figures A – I present the CDFF set-up. Figure J presents the tools used with the CDFF set-up and sampling process.
- Figure 2.5 presents the experimental set-up of the T-CDFF model
- Figure 2.6 presents a simplified T-CDFF set-up. Inoculation flask and pumps for inoculum delivery are encircled in green; the same pumps were re-used for

artificial saliva delivery. GCF flasks and pumps are encircled in pink.

- Figure 2.7 Generalised T-CDFF experimental conditions.
- Figure 3.1 The T-CDFF model with the major modifications. A) T-CDFF model with 3 units housed on a single motor housing, B) The enlargement of a single unit with the mechanical modifications highlighted and explained below.
- Figure 3.2 The total number of *S. sanguinis* (blue line) and *A. naeslundii* (red line) in each unit of the T-CDFF model. Error bars represent the standard error calculated on n=6. *n=6 refers to two biological and three technical replicates
- Figure 3.3 A) Lack of seals on screw caps and faulty waste output seals were responsible for the lack of air tightness. B) Domed nuts were responsible for the lack of air-tightness of the glass vessel, replaced by the non-domed nuts.
- Figure 4.1 The experimental design of T-CDFF experiments. The health conditions were run for 9 days and then switched to 14 days of gingivitis conditions.
- Figure 4.2 shows the experimental set-up with a new multi-channel pump which substituted the single pumps used in delivering the inoculum and the artificial saliva to each T-CDFF unit.
- Figure 4.3 shows the T-CDFF sampling pan with 5 discs, each designated for different analysis.
- Figure 4.4 presents the viable counts for the total number of anaerobes and aerobes in each T-CDFF unit during two individual experiments across health and disease conditions. The data from two sampling points in health (day 5 and day 7) and two sampling points in disease (day 18 and day 23) were averaged to present the change in viable counts for each unit in time in two T-CDFF experiments (n=2). *n=2 refers to two technical replicates.
- Figure 4.5 presents the viable counts for the total number of *Actinomyces* spp. and *Streptococcus* spp. in each T-CDFF unit in two individual experiments across health and disease conditions. The data from two sampling points in health

(day 5 and day 7) and two sampling points in disease (day 18 and day 23) were averaged to present the change in viable counts for the total *Actinomyces* spp. and *Streptococcus* spp. for each unit in time for both T-CDFE experiments (n=2). *n=2 refers to two technical replicates.

Figure 4.6 shows the alkaline phosphatase activity of *P. gingivalis* over time. The axis on the left shows the total bacterial counts [CFUs / mL]; the right-hand axis shows the optical density change over time that represents the metabolic activity of *P. gingivalis* (n=2). *n=2 refers to two technical replicates.

Figure 4.7 shows the trypsin-like-protease activity of *P. gingivalis* over time. The axis on the left shows the total bacterial counts [CFUs / mL]; the right-hand axis shows the optical density change over time that represents the metabolic activity of *P. gingivalis* (n=2). *n=2 refers to two technical replicates.

Figure 5.1 shows the experimental design of the CDFE experiment.

Figure 5.2 presents the sampling pan with 5 discs, each designated for different analysis.

Figure 5.3 The total number of bacteria detected in the biofilm and the effluent samples collected throughout the simulated health, transition and gingivitis conditions in the CDFE experiment. Health conditions are shown in red, transition in green and gingivitis in blue. Blue line shows the total number of cells in the effluent samples; green line shows the total number of cells in the biofilm samples (n=3). *n=3 refers to three technical replicates.

Figure 5.4 shows the total numbers of *F. nucleatum* detected in the biofilm and the effluent samples collected throughout the simulated health, transition and gingivitis conditions in the CDFE experiment. Health conditions are encircled in red, transition in green and gingivitis in blue. Blue line shows the total number of cells in the effluent samples; green line shows the total number of cells in biofilm samples (n=3). *n=3 refers to three technical replicates.

Figure 5.5 shows the total numbers of *P. intermedia* detected in the biofilm and the effluent samples collected throughout the simulated health, transition and

gingivitis conditions in the CDFE experiment. Health conditions are encircled in red, transition in green and gingivitis in blue. Blue line shows the total number of cells in the effluent samples; green line shows the total number of cells in biofilm samples (n=3). n=3 refers to three technical replicates.

Figure 5.6 shows the total numbers of *L. casei* detected in the biofilm and the effluent samples collected throughout the simulated health, transition and gingivitis conditions in the CDFE experiment. The health conditions are encircled in red, transition in green and gingivitis in blue. Blue line shows the total number of cells in the effluent samples; green line shows the total number of cells in the biofilm samples (n=3). n=3 refers to three technical replicates.

Figure 5.7 presents the cell numbers for *A. naeslundii* (blue line) and *S. sanguinis* (green line) detected in the biofilm samples collected throughout the simulated health, transition and gingivitis conditions from the CDFE experiment. The health conditions are encircled in red, transition in green and gingivitis in blue (n=3). n=3 refers to three technical replicates.

Figure 5.8 presents the cell number for *A. naeslundii* (violet line) and *S. sanguinis* (light green line) detected in the effluent samples collected throughout the health, transition and gingivitis conditions from the CDFE experiment. The health conditions are encircled in red, transition in green and gingivitis in blue (n=3). n=3 refers to three technical replicates.

Figure 5.9 shows the PCA analysis applied to the biofilm and the effluent samples. Two biofilm samples (health and disease) are marked as 'New' and highlighted in orange. The effluent samples are highlighted in red, green and blue according to the experiment phase (1-red=health, 2-green=transition, 3-blue=gingivitis). PCA analysis and this Figure were performed by Dr Michael Canon (Procter & Gamble).

Figure 5.10 shows the PCA analysis applied to the effluent samples only. Samples are highlighted according to the experimental phase (1-black=health, 2-red=transition, 3-blue=gingivitis). PCA analysis and this Figure were

performed by Dr Michael Canon (Procter & Gamble).

Figure 5.11 shows the orthogonal PLS analysis applied to the effluent samples and how the analysis is growth dependent. Samples are highlighted according to the experimental phase (1-red=health, 2-green=transition, 3-blue=gingivitis). OPLS analysis and this Figure were performed by Dr Michael Canon (Procter & Gamble).

Figure 5.12 presents the change in propionate levels across the experimental phases. Health conditions – red line, transition conditions – green line, gingivitis conditions – blue line. The averaged health, transition and gingivitis lines represent the differences among the conditions.

Figure 5.13 presents the change in butyrate levels across the experimental phases. Health conditions – red line, transition conditions – green line, gingivitis conditions – blue line. The averaged health, transition and gingivitis lines represent the differences among the conditions.

Figure 5.14 presents the change in ethanol levels across the experimental phases. Health conditions - red line, transition conditions - green line, gingivitis conditions - blue line. The averaged health, transition and gingivitis lines represent the differences among the conditions.

Figure 6.1 presents the experimental conditions for each of the T-CDFF units. Unit 1 served as control and underwent the health conditions for 30 days. Unit 2 was run under health conditions for 9 days and then under enhanced gingivitis conditions (gingivitis+) by providing anaerobic gas conditions instead of micro-aerophylic gas conditions that were used in chapter 4 and 5 (Chapter 2, Section 2.3.4 and Chapter 4, Section 4.2.2). Unit 3 was run under health conditions for 9 days and then under 'gingivitis++' methodology that was defined by higher levels of the artificial GCF (130 μ L / min) and anaerobic gas conditions (Chapter 2, Section 2.3.4).

Figure 6.2 A) presents the data for total bacteria and the total cell number of *S. sanguinis* detected in the biofilm samples collected over time in T-CDFF experiment 1 and B) experiment 2. The violet line (Universal) represents

the total bacteria detected in unit 1; the yellow line (Universal) represents the total bacteria in unit 3. The blue line represents the total amount of *S. sanguinis* detected in unit 1; green line represents the amount of *S. sanguinis* in unit 3. Dotted line represents the conditions change from health to extended health or gingivitis introduced at day 9*. Standard errors are presented as error bars (n=6); n=6 refers to two biological and three technical replicates.

Figure 6.3

A) presents the data for total bacteria and the total cell number of *S. sanguinis* detected in the effluent samples collected over time in T-CDFE experiment 1 and B) experiment 2. The violet line (Universal) represents the total bacteria detected in unit 1; the yellow line (Universal) represents the total bacteria in unit 3. The blue line represents the total amount of *S. sanguinis* detected in unit 1; green line represents the amount of *S. sanguinis* in unit 3. Dotted line represents the conditions change from health to extended health or gingivitis introduced at day 9*. Standard errors are presented as error bars (n=6); n=6 refers to two biological and three technical replicates.

Figure 6.4

presents the phyla composition of the biofilm samples retrieved from T-CDFE experiment 1, unit 1 and unit 3. Figure 6.4 A) presents the data from experiment 1, unit 1 across the health and the extended health conditions. Figure 6.4 B) presents the data from experiment 1, unit 3 across the health and gingivitis conditions. Blue represents the TM7, red represents the Firmicutes, green represents the Actinobacteria and violet the Proteobacteria. Dotted line represents the change in conditions from the health to the extended health or gingivitis conditions introduced at day 9. N=1 refers to one biological sample.

Figure 6.5

presents the phyla composition of the biofilm samples retrieved from T-CDFE experiment 2, unit 1 and unit 3. Figure 6.5 A) presents the data from experiment 2, unit 1 across the health and the extended health conditions. Figure 6.5 B) presents the data from experiment 2, unit 3 across the health and gingivitis conditions. Blue represents the TM7, red represents the Firmicutes, green represents the Actinobacteria and violet the

Proteobacteria. Dotted line represents the change in conditions from the health to the extended health or gingivitis conditions introduced at day 9. N=1 refers to one biological sample.

Figure 6.6 presents the phyla composition of the effluent samples retrieved from T-CDFE experiment 1, unit 1 and unit 3. Figure 6.6 A) presents the data from experiment 1, unit 1 across the health and the extended health conditions. Figure 6.6 B) presents the data from experiment 1, unit 3 across the health and gingivitis conditions. Blue represents the TM7, red represents the Firmicutes, green represents the Actinobacteria and violet the Proteobacteria. Dotted line represents the change in conditions from the health to the extended health or gingivitis conditions introduced at day 9.

Figure 6.7 presents the phyla composition of the effluent samples retrieved from T-CDFE experiment 2, unit 1 and unit 3. Figure 6.7 A) presents the data from experiment 2, unit 1 across the health and the extended health conditions. Figure 6.7 B) presents the data from experiment 1, unit 3 across the health and gingivitis conditions. Blue represents the TM7, red represents the Firmicutes, green represents the Actinobacteria and violet the Proteobacteria. Dotted line represents the change in conditions from the health to the extended health or gingivitis conditions introduced at day 9.

Figure 6.8 presents the results of the OPLS analysis on NMR data retrieved from unit 1, experiment 1.

Figure 6.9 presents the OPLS analysis performed on the effluent samples retrieved from the health and gingivitis conditions in unit 3, experiment 1. Health is represented as blue; gingivitis is represented as green. Sample collected at day 7 was an outlier and was removed from the analysis.

Figure 6.10 presents the components discriminating between the health and gingivitis clusters. Trimethylamine is presented in blue; Pyruvate in red; Propionate in green and Butyrate in violet. Dotted line represents the change in conditions from the health to the gingivitis conditions introduced at day 9.

Figure 6.11 presents the levels of formate that were discriminating across the health-disease phase. Dotted line represents the change in conditions from the health to the gingivitis conditions introduced at day 9.

- Figure 6.12 presents the levels of alanine that were discriminating across the health-disease phase. Dotted line represents the change in conditions from the health to the gingivitis conditions introduced at day 9.
- Figure 6.13 presents the levels of lactate that were discriminating across the health-disease phase. Dotted line represents the change in conditions from the health to the gingivitis conditions introduced at day 9.
- Figure 6.14 presents the levels of ethanol that were discriminating across the health-disease phase. Dotted line represents the change in conditions from the health to the gingivitis conditions introduced at day 9.
- Figure 6.15 presents the OPLS analysis equivalent to the one performed on the NMR data from unit 3, experiment 1 shown in Figure 6.9 and unit 3, experiment 2 shown in Figure 6.16. Samples retrieved from health conditions are represented in blue and samples from the extended health are represented in green.
- Figure 6.16 presents the OPLS analysis performed on the effluent samples retrieved from the health and the gingivitis conditions in unit 3, experiment 2. Health is represented as blue; gingivitis is represented as green. This figure is equivalent to Figure 6.9 (unit 3, experiment 1).
- Figure 6.17 presents the levels of succinate that were discriminating across the health-disease phase. Dotted line represents the change in conditions from the health to the gingivitis conditions introduced at day 9.
- Figure 6.18 presents the levels of trimethylamine that were discriminating across the health-disease phase. Dotted line represents the change in conditions from the health to the gingivitis conditions introduced at day 9.
- Figure 6.19 presents the levels of formate that were discriminating across the health-disease phases. Dotted line represents the change in conditions from the health to the gingivitis conditions introduced at day 9.
- Figure 6.20 presents the levels of acetate that were discriminating across the health-disease conditions. Dotted line represents the change in conditions from the health to the gingivitis conditions introduced at day 9.

List of Tables

| | |
|-----------|---|
| Table 1.1 | Mechanism and advantages/disadvantages of NGS sequencers (Claesson <i>et al.</i> 2010; Zhang <i>et al.</i> 2011; Quail <i>et al.</i> 2012; Liu <i>et al.</i> 2012; Life Technologies Inc. 2014; Illumina Inc. 2015; Roche Inc. 2015). |
| Table 2.1 | The specification of CDFF and T-CDFF model. |
| Table 2.2 | Selective and non-selective media used for T-CDFF experiments. |
| Table 2.3 | FLV, NAP and SSU triplexes consisted of: <i>F. nucleatum</i> , <i>L. casei</i> and <i>V. dispar</i> (FLV); <i>N. subflava</i> , <i>A. naeslundii</i> and <i>P. intermedia</i> (NAP); and <i>S. sanguinis</i> , <i>S. mutans</i> and Universal (SSU). Bases shown in brackets are locked nucleic acid bases. |
| Table 2.4 | Cycling conditions for triplex qPCR. |
| Table 2.5 | Cycling conditions for duplex qPCR. |
| Table 3.1 | presents the description of the mechanical modifications applied to the T-CDFF model. |
| Table 3.2 | shows the numbers for the total bacteria and the health associated bacteria in both CDFF and the T-CDFF's unit. The numbers are expressed as cells / biofilm with a standard error presented in brackets (n=6). n=6 refers to two biological and three technical replicates. |
| Table 3.3 | shows the numbers for the gingivitis associated bacteria in both CDFF and the T-CDFF's unit. The numbers are expressed as cells / biofilm with a standard error presented in brackets (n=6). n=6 refers to two biological and three technical replicates. |
| Table 3.4 | The number of total bacteria and <i>S. sanguinis</i> in each unit of the T-CDFF. The amount of bacteria is expressed as cells / biofilm with standard error presented in brackets (n=6). n=6 refers to two biological and three technical replicates. |
| Table 3.5 | The number of cells for <i>N. subflava</i> and <i>V. dispar</i> in each unit of the T-CDFF. |

| | |
|-----------|--|
| | The number of bacteria are expressed as cells / biofilm with a standard error presented in brackets (n=6). *n=6 refers to two biological and three technical replicates. |
| Table 3.6 | The number of cells for the gingivitis associated bacteria <i>F. nucleatum</i> , <i>A. naeslundii</i> and <i>P. intermedia</i> in each unit of T-CDFF. The numbers of bacteria are expressed as cells / biofilm with a standard error presented in brackets (n=6). n=6 refers to two biological and three technical replicates. |
| Table 3.7 | Statistical analysis of the data set from the T-CDFF experiment (methodology 4). Abbreviations: 1–Unit 1, 2–Unit 2 and 3–Unit 3. |
| Table 4.1 | shows the cell number for the total bacteria detected by triplex qPCR using universal primers in the biofilm samples collected from each T-CDFF unit over time. The standard error is shown in brackets (n=6). Blue line indicates the introduction of gingivitis conditions at day 9. *n=6 refers to two biological and three technical replicates. |
| Table 4.2 | presents the total cell number of the health associated bacteria and <i>S. mutans</i> detected by triplex qPCR primers in biofilm samples collected from each unit over time. The standard error is shown in brackets (n=6). Blue lines indicate the introduction of gingivitis conditions at day 9. *n=6 refers to two biological and three technical replicates. |
| Table 4.3 | presents the total cell number of the gingivitis associated bacteria detected by triplex qPCR primers in biofilm samples collected from each unit over time. The standard error is shown in brackets (n=6). Blue lines indicate the introduction of gingivitis conditions at day 9. *n=6 refers to two biological and three technical replicates. |
| Table 4.4 | presents the statistical analysis applied to the qPCR data. A) UNIANOVA output for the analysis performed for 6 T-CDFF units. B) The residuals plotted against the frequency that showed a normal distribution as expected. C) The residuals plotted against the predicted value showed a symmetric distribution. |

| | |
|-----------|--|
| Table 4.5 | shows the ALPase activity in biofilms collected from three CDFF units in two separate experiments. The health conditions: day 1, day 5 and day 7; disease conditions: day 18 and day 23. Blue line indicates the introduction of gingivitis conditions at day 9. |
| Table 4.6 | present the volumes and hydraulic retention times calculated for both CDFF and T-CDFF. |
| Table 5.1 | The total number of health associated bacteria detected in the biofilm in the CDFF experiment. The average for each species is calculated based on three technical replicates (n=3); ND - not detected. Blue line indicates the conditions change. Samples collected at day 1, 5 and 7 were retrieved from health, while samples from day 20 and 25 were retrieved from gingivitis conditions. |
| Table 5.2 | shows the total number of the health associated bacteria detected in the effluent samples. The average for each species is calculated based on three technical replicates (n=3); ND - not detected. NDA – no data available. Red line indicates the introduction of transition conditions at day 7; Blue line indicates the introduction of gingivitis conditions at day 12. |
| Table 5.3 | The ALPase activity in the biofilm collected at different time points. The enzymatic assay was performed on a single (1x) or concentrated biofilm suspension (3x). Δ – delta activity over time (n=2). n=2 refers to two technical replicates. |
| Table 6.1 | presents the total cell numbers for <i>S. mutans</i> , <i>N. subflava</i> , <i>A. naeslundii</i> detected in the biofilm samples collected from unit 1 and unit 3 in the T-CDFF experiment 1 and 2. Unit 1 was maintained in the health conditions throughout the time; unit 3 was exposed to the health conditions for 9 days and then the conditions were changed to gingivitis and maintained for 21 days. <i>V. dispar</i> , <i>F. nucleatum</i> , <i>P. intermedia</i> and <i>L. casei</i> were not detected in the biofilm samples and thus are not presented in this table. Blue line indicates the introduction of extended health /gingivitis conditions at day 9. ND - not detected. The standard error is shown in brackets (n=6). n=6 refers to two biological and three technical replicates. |

Table 6.2

presents the phylogenetic composition of biofilm collected from experiments 1 and 2, units 1 and 3 in health (H), extended health (EH) and gingivitis conditions (G). The biofilm samples collected from health/extended health/gingivitis were averaged to compare the species proportions between the H-EX and H-G phases. The numbers highlighted in yellow indicate that specific species was not present in all the samples used to calculate an average.

Table 6.3

presents the phylogenetic composition of effluent samples from experiments 1 and 2, units 1 and 3 in health (H), extended health (EH) and gingivitis conditions (G). The effluent samples collected from health/extended health/gingivitis were averaged to compare the species proportions between the H-EX and H-G phases. The numbers highlighted in yellow indicate that specific species was not present in all the samples used to calculate an average.

Abbreviations

| | |
|--------------|---|
| AIDS | Acquired immune deficiency syndrome |
| ALP | Alkaline phosphatase |
| BAPNA | N α -Benzoyl-L-arginine-4-nitroanilide hydrochloride |
| CBA | Columbia Blood Agar |
| CDFF | Constant Depth Film Fermentor |
| CFAT agar | Cadmium Fluoride Acriflavin Tellurite agar |
| CTAB | Cetyltrimethylammonium |
| DNA | Deoxyribonucleic acid |
| dsDNA | double stranded deoxyribonucleic acid |
| dNTP | Deoxynucleotide triphosphate |
| EDTA | Ethylenediaminetetraacetic acid |
| EPS | Extracellular polysaccharide |
| Ext. | Exterior |
| FAA | Fastidious Anaerobe Agar |
| GC | Gas Chromatography |
| GCF | Gingival crevicular fluid |
| HA | Hydroxyapatite |
| HIV | Human immunodeficiency virus |
| Int. | Interior |
| IL | Interleukin |
| MES buffer | (2-(N-morpholino) ethane sulphonic acid) buffer |
| MMP-9 | Matrix metalloproteinase 9 |
| MS | Mass Spectroscopy |
| M-S | Mitis – Salivarius |
| NMR | Nucleic Magnetic Resonance |
| LC | Liquid Chromatography |
| PBS | Phosphate Buffered Saline |
| PCA | Principal Component Analysis |
| PCR | Polymerase Chain Reaction |
| PEG | PolyEthylene Glycol |
| <i>p</i> NP | <i>p</i> -nitrophenol |
| <i>p</i> NPP | <i>p</i> -nitrophenyl disodium orthophosphate |
| PLS | Partial Least Square |

| | |
|----------------|--|
| PTFE | Polytetrafluoroethylene |
| RPMI medium | Roswell Park Memorial Institute medium |
| rRNA | Ribosomal Ribonucleic acid |
| spp. | Species (plural) |
| T-CDFF | Triple-Constant Depth Film Fermentor |
| TLR4 | Toll-like receptor 4 |
| T _m | Melting temperature |
| TNF-alpha | Tumor necrosis factor alpha |
| TLP | Trypsin-like-protease |
| qPCR | quantitative Polymerase Chain Reaction |

Units

| | |
|-----|----------------------|
| bp | Base pair |
| °C | Degree Celsius |
| CFU | Colony Forming Units |
| g | Gravitational force |
| h | Hour |
| kb | Kilobase |
| min | Minute |
| mL | Mililitre |
| mM | Milimolar |
| nM | Nanomolar |
| nm | Nanometer |
| OD | Optical density |
| s | Second |
| µg | Microgram |
| µL | Microlitre |
| µm | Micrometre |

1 CHAPTER

Introduction

1.1 Oral cavity

The human body is composed of approximately 10^{14} cells of which about 10% are mammalian. The remaining are the resident microorganisms of the host (Marsh 2003; Marsh *et al.* 2011). The human mouth is one of the richest and most diverse communities, where the number of bacteria exceeds the human population on earth (Olsen 2006). They are found either on distinct mucosal surfaces such as lips, cheek, tongue, palate or external hard non-shedding surfaces such as teeth, all of which support microbial colonisation. Each of these surfaces is environmentally different; therefore the bacteria associated with these sites differ in metabolism and thus the sites vary in microbial composition (Marsh 2003; Marsh *et al.* 2011).

Predominantly, our knowledge of the microbial diversity in the oral cavity has been shaped by culture methods, which have estimated that there are approximately 250 species present in the mouth (Paster *et al.* 2006). The technological shift from culture based methods to next generation sequencing has revealed much higher richness than previously anticipated. It is estimated that there are approximately 700 different species in the oral cavity, roughly 400 of which have been found in periodontal pocket while the remaining ones are present in other niche areas within the mouth. Additionally, of the estimated 700 species approximately 100-200 are common between individuals; thus there can be significant differences found among the individuals (Paster *et al.* 2006; Dewhirst *et al.* 2010).

The microorganisms present in the oral cavity have been referred to as the oral microflora or oral microbiota; recently, a new term of oral microbiome was introduced by Joshua Lederberg “to signify the ecological community of commensal, symbiotic, and pathogenic microorganisms that literally share our body space and have been all but ignored as determinants of health and disease” (Dewhirst *et al.* 2010). The relationship between humans and their respective oral microbiome, comes into being early on in our existence (Jenkinson & Lamont 2005). Vertical transmission from the mother to the child occurs first at birth, and the delivery method determines which microorganisms will be encountered first by the new-born (Dominguez-Bello *et al.*

2010). It has been reported that vaginally born infants show higher taxonomic diversity at 3 months than caesarean Section deliveries and that caesarean Section babies acquire *S. mutans* approximately 1 year before vaginally born babies (Li *et al.*, 2005). As the child grows, it develops new habitats for microbial colonization such as tooth surfaces and gingival tissues; nonetheless horizontal transmission from people sharing the same environment also contributes to oral diversity (Kohler & Andreen 1994; Li *et al.*, 2005).

The mouth has two major types of surfaces which can be colonised by bacteria, shedding and non-shedding surfaces. The first are mucosal surfaces and the second are mineralised tooth surfaces. Due to this, the bacteria which colonise these two distinctly different regions differ in concentration and nature. As with all microbial communities, the health and species composition of the community is dependent on the supply of nutrients, the environmental pH, the supply of oxygen and the relationships within the community (Kolenbrander *et al.* 2002; Marsh 2003; Olsen 2006; ten Cate 2006). All of the mouth's surfaces are covered in bacterial biofilms, which are called dental plaque when formed on the non-shedding surfaces of the teeth. Dental plaque has been recognised as the main aetiological factor in periodontal disease progression and was extensively investigated in the 19th century (Miller 1891; cited by Zarco *et al.* 2012; cited by Wade 2013). Its formation and complex structure are explained below.

1.2 Dental plaque formation

Plaque is a complex multi-microbial community embedded in extracellular polysaccharide matrix (Marsh 2004; Marsh 2005). It is a dynamic and heterogenous community formed by initial colonizers, that adhere tightly to the pellicle present on the tooth surface, followed by secondary and late successors that form the multi-species community (Marsh 2004; Marsh 2005; Shao and Demuth 2010). Development and maturation of the dental community is driven by microbial competition as well as the interspecies communication (Kolenbrander *et al.* 2002; Marsh 2004; Marsh 2005; Kolenbrander *et al.* 2006; Zarco *et al.* 2012). There are a number of hypotheses as to why bacteria form biofilms. The primary reason is defence, the adage 'safety in

numbers' goes some way to explaining this as biofilms exhibit a resistance to mechanical forces, such as experienced during mastication, and show resistance to the natural washing action of saliva. The microorganisms inside the biofilm matrix are able to withstand the antimicrobial agents in some cases to a concentration 100 times higher than those required to kill planktonic forms (Jefferson 2004). Existing as a biofilm also allows microorganisms to withstand antimicrobial penetration (Stewart & Costerton 2001; Gilbert *et al.* 2002; Toole & Stewart 2005), host immune responses such as phagocytosis (Hentzer *et al.* 2003; Costerton *et al.* 2003; Hall-Stoodley *et al.* 2004) and as a community they can endure changes in pH and starvation of nutrients (Marsh *et al.* 1983; Jenkinson & Lamont 2005; Olsen 2006; Strelkova *et al.* 2013). The formation of dental biofilms comprises several stages that are explained below.

1.2.1.1 Enamel Pellicle Formation

The first step of plaque development is the formation of a salivary pellicle on the enamel surface of the tooth. The pellicle is formed between seconds and minutes after exposure to saliva and is primarily composed of mucinous glycoproteins (Liljemark 2000; Bowen & Koo 2011). Secondary constituents derived from saliva that adhere to the tooth surface include proline-rich proteins, lysozyme, peroxidase, amylase, cystatins, statherin, IgA, IgG, glucosyltransferases and mucin (Bennick 1982; Rölla *et al.* 1983; Rykke *et al.* 1990; Liljemark 2000; Bowen & Koo 2011). All of these substances create a layer of 0.1-1.0 μm thickness that is attached to the enamel by hydrogen bonds (Liljemark 2000). It acts as a specific and selective surface for binding of indigenous oral bacteria, therefore only bacteria with high affinity to the pellicle are found as a pioneer species (Liljemark 2000; Bowen & Koo 2011).

1.2.1.2 Initial colonization

The above mentioned constituents of the pellicle are recognised as receptors by the initial colonisers. Therefore, bacteria which are transported to the enamel surface vicinity either by fluid flow, chemotaxis or Brownian motion (Kolenbrander *et al.* 2002; Kolenbrander *et al.* 2006; Samaranyake 2002), bind to the receptors present in the pellicle via Van der Waal's forces, electrostatic and hydrogen bonds. Bacterial

colonisation often starts with aerobic pioneer colonisers such as streptococci, in particular *Streptococcus salivarius*, *S. mitis* and *S. oralis* (Liljemark 2000) which constitute between 60% to 90% of the bacterial community in the first 4 hours of colonisation. Other early colonisers include *Veillonella* spp., *Actinomyces* spp., *Haemophilus* spp., and *Propionibacterium* spp. (Kolenbrander *et al.* 2002; Kolenbrander *et al.* 2006). These organisms provide a suitable environment for successors by adjusting the local conditions by their metabolic activity, for example they adjust the local pH and E_h and produce nutrients or by-products needed by subsequent microorganisms. Nowadays, it is known that bacterial colonisation and co-aggregation is based on bacterial adhesion-receptor signalling, which is vital to bacterial communication and leads to a spatiotemporal development that can eventually result in a diverse bacterial community and biofilm maturation (Kolenbrander *et al.* 2002; Samaranayake 2002; Olsen 2006; Kolenbrander *et al.* 2006; Marsh *et al.* 2011).

1.2.1.3 Biofilm maturation

An abundant multi-layer bacterial structure is formed within 8-12 hours (Liljemark 2000) and is based on co-adhesion between pioneer species that act as a substratum to successive colonisers. *Fusobacterium nucleatum* seems to play an important role in bridging the early and late colonisers as it co-aggregates with both (Kolenbrander *et al.* 2002; Kolenbrander *et al.* 2006); all the late colonisers including *Porphyromonas gingivalis*, *Treponema denticola*, and *Aggregatibacter actinomycetemcomitans* coaggregate with *F. nucleatum* but not necessarily with each other (Samaranayake 2002; Kuboniwa & Lamont 2010). This would explain why fusobacteria are often found in both healthy and diseased sites (Kolenbrander *et al.* 2002). These bacteria-to-bacteria interactions are based on recognition of specific adhesins by receptors found on microbial surface. This allows the creation of connections either between identical or different species. Single bacteria can have more than one receptor or adhesion. However, they tend to bind to metabolically compatible species. This leads to the formation of a complex three dimensional multi-species bacterial community in which bacteria are related metabolically and embedded in an extracellular polysaccharide

(EPS) matrix that protects them from detrimental environment or antimicrobial agents (Liljemark 2000; Kuboniwa & Lamont 2010; Marsh *et al.* 2011).

1.3 Periodontal diseases and the oral microbiota

Periodontal diseases are widespread and a serious problem among the adult population worldwide, affecting approximately 32% of all adults in USA (~33 million people/per annum) (Brown *et al.* 2000). It has been hypothesized that they're might be a link with other illnesses such as heart disease, diabetes or arthritis; therefore the prevention and treatment of periodontal diseases are crucial for the quality of life and well-being of an individual (Pihlstrom *et al.* 2005). From a pathological point of view, periodontal diseases are defined as any inherited or acquired disorder which results in inflammation of the tissues surrounding and supporting the teeth including the gingiva or periodontal ligaments. However, the term periodontal disease generally refers to the two most common conditions: periodontitis and gingivitis (Loesche & Grossman 2001; Armitage 2003; Pihlstrom *et al.* 2005).



Figure 0.1 presents two periodontal diseases: A) gingivitis and B) periodontitis (adapted from Scannapieco 2013). A – red, tender and swollen gums and bleeding; B – swollen and red gums, bleeding, receding gums, loose teeth etc

1.3.1 Gingivitis

Gingivitis is a highly prevalent periodontal disease affecting 50-90% of adults worldwide. It is reversible and the mildest form of periodontal disease that is principally-caused by lack of oral hygiene resulting in dental plaque accumulation on the surfaces of teeth adjacent to gingiva. It does not affect the supporting structures of the teeth but can itself proceed to periodontitis (Trombelli *et al.* 2004; Pihlstrom *et al.*

2005). Gingivitis is clinically defined by the presence of gingival inflammation without the loss of the connective tissue while periodontitis is defined by inflammation of the gingiva with additional pathological detachment of collagen fibres from cementum, junctional epithelium and finally bone resorption (Loesche & Grossman 2001; Armitage 2003; Pihlstrom *et al.* 2005).

Gingivitis is the most prevalent disease of the periodontum with the two most common forms being chronic marginal gingivitis and plaque-induced gingivitis. As stated above, gingivitis begins with a lack of oral hygiene, which leads to plaque increasing in both thickness and coverage eventually leading to gingival inflammation. The gingival sulcus increases in depth (becoming a periodontal pocket) allowing more space for bacterial accumulation in the presence of nutrient-rich gingival crevicular fluid. It is thought that gingivitis is caused by an imbalance among resident microbiota which leads to environmental changes and alterations in gene expression. The overall results of these changes are that the gingivitis inducing pathogens are able to outcompete the health associated bacteria (see also Section 2.5). However, the exact mechanism is not well characterised yet (Olsen 2006; Paster *et al.* 2006). Although the plaque accumulation is thought to be a major causative factor for gingivitis, there are several systemic factors that can trigger or modulate gingivitis progression. These can be divided into metabolic, environmental, genetic or other factors. The metabolic factors are usually associated with endocrine changes. Therefore, the hormonal changes that occur during puberty or pregnancy can have an impact on plaque-gingivitis relationship. Environmental factors include smoking or tobacco usage, vitamin C deficiency or excessive use of antibiotics. The individual differences in terms of genetics and immune response to infection may also play a role. As an example, several clinical studies have associated the MMP-9, IL-1, IL-6, IL-18 polymorphism with increased susceptibility to gingivitis (Goodson *et al.* 2000; Trombelli *et al.* 2004; Moreira *et al.* 2007; Scapoli *et al.* 2007; Holla *et al.* 2008; Vokurka *et al.* 2008). However, the significance of genetic factors in modulation of the individual's susceptibility to gingivitis remains to be established. Other factors include infections such as HIV/AIDS, physiological or emotional stress, Down's syndrome (Trombelli *et al.* 2004).

The clinical assessment of gingival inflammation is based on several clinical parameters. A visual assessment includes observing the physical status of gingiva by assessing the colour change, surface anatomy and bleeding tendency. To aid the process several indices have been introduced for the clinical evaluation of gingival inflammation. These include papilla, marginal, attached index (PMA), the papillary bleeding index (PBI) and the gingival index (GI) introduced by Loe & Silness (1963). The use of the above mentioned indices have demonstrated the extent of severity between plaque deposits and the severity of gingivitis (Tatakis & Trombelli 2004).

The main therapy for gingivitis patients is aimed at removing the aetiological factors to reduce or eliminate the inflammation and then subsequently allow the gingival tissues to heal (He & Shi 2009). As dental plaque is the primary aetiological factor for disease progression, mechanical or chemical plaque removal techniques can be successfully used as a preventative approach (Lamster 2006). The removal of dental plaque and calculus can be performed by regular daily hygiene applied by hand, sonic, ultrasonic instrument, and supplemented by professional cleaning and supragingival scaling (Van Der Weijden *et al.* 2002; Santos 2003). The addition of topical anti-plaque agents in the form of dentifrices or mouthwashes to a gingivitis-treatment programme for patients with inadequate plaque control can help reduce the problem (Allaker & Douglas 2009) (Santos 2003). These active substances include thymol, menthol, eucalyptol, methyl salicylate, triclosan and chlorhexidine digluconate (Santos 2003; Allaker & Douglas 2009).

1.3.2 Periodontitis

Periodontitis is a complex chronic infectious disease which affects the supporting tissue of the teeth. The onset of disease occurs through bacterial infection which if left untreated can result in irreversible loss of tissue and bone (Loos *et al.* 2005). Periodontitis can be defined as the presence of gingival inflammation at sites where there has been a pathological detachment of collagen fibres from the cementum and the junctional epithelium has migrated apically. The inflammatory events which are associated with connective tissue attachment loss also lead to the resorption of coronal portions of the tooth supporting alveolar bone (Savage *et al.*, 2009). Recent

refinement of the above definition included an inflamed pathological pocket ≥ 4 mm deep with a presence of bone loss (van der Velden 2005). However, this definition does not account for the number of inflamed sites.

The symptoms associated with periodontitis described above, such as gingivitis, bleeding, loss of connective tissue and bone attachment are generally assessed by a set of measurements including bleeding on probing (BOP), pocket probing depth (PPD) and bone loss assessed radiographically (van der Velden 2005; Savage *et al.* 2009). In terms of age, epidemiological studies have reported periodontitis to affect a substantial number of adults under the age of 20 years, and a greater number of adults after the age of 35-40 years (Timmerman & Van der Weijden 2006). Susceptibility to periodontitis can be increased by particular risk factors: pre-existing and long standing gingivitis, smoking or tobacco use, gender, age, hormonal changes, diabetes, pregnancy, and genetic susceptibility (Haber *et al.* 1993; Genco 1996; Loos *et al.* 2005; Timmerman & Van der Weijden 2006). Several clinical studies have suggested that genetic factors can modulate host susceptibility and can be linked with an effect on disease progression. Examples include the IL-1, IL-2, IL-4, IL-10, TNF-alpha and TLR4 polymorphisms that were reported to be associated with periodontal diseases (Trombelli *et al.* 2004; Kinane *et al.* 2005; Kinane *et al.* 2006; Scapoli *et al.* 2007; Nibali *et al.* 2009). However, there is no definite answer whether these factors are predisposing to periodontitis or not. It rather seems that periodontitis might be caused by cumulative effect of the above gene variants. For example, the polymorphism in IL-1, IL-6 and neutrophil (Fc gamma receptor) showed an effect on inflammatory responses in patients during periodontitis (Kinane *et al.* 2005; Nibali *et al.* 2009).

Treatment options available to patients suffering from periodontitis are dependent on the individual disease pattern, which can include attachment loss, type of disease or (Wirthlin *et al.* 2005) anatomical variations; the aim of any therapy aimed at periodontitis is to stop inflammation and inhibit disease progression. Although, the treatment is predominantly patient dependent, there are two main approaches which are available: (i) anti-infective treatment which is focused on stopping the progression of periodontal attachment loss by removing the aetiological factors; (ii) a regenerative

therapy which includes an anti-infective treatment, and also restoration of the structures destroyed by disease progression (Anon 2001).

1.3.3 Plaque hypotheses of periodontal diseases

Much of our current understanding of periodontal diseases comes from intensive culture-based studies performed in 1970s and early 1980s which revealed some significant differences in the composition of microbiota in oral health and disease (Slots 1977a; Slots 1977b; Socransky 1977; Tanner *et al.* 1979). This led to the development of a “specific plaque” hypothesis by Loesche in 1976 who proposed that only a small number of oral species (specific pathogens) are directly responsible for disease progression (Loesche 1976). Problems with this hypothesis arise, when trying to explain the cases when disease is diagnosed in the absence of the putative species or when pathogens are present but there is no evidence of the disease (Marsh 1994; Marsh 2003). Alternatively, the “non-specific plaque” hypothesis introduced by Theilade (1986) purported that the overall mixture of oral organisms and their interactions with the host instead of only a few pathogens are recognised as the causative agent in development of periodontal diseases. However, if this was entirely true we would not observe the evidence of specificity, i.e. higher abundance of specific species in sites burdened by disease (Marsh 1994; Marsh 2003). To address the arguments surrounding the “specific” and “non-specific” hypotheses, an “ecological plaque” hypothesis was introduced by Marsh (1991) to bridge them and unify the laboratory and clinical findings (Marsh 1989; Marsh 1991; Marsh 2003). This new paradigm stated that key environmental factors trigger a shift in the balance of the oral microbiota to the disease-associated species composition (Marsh 1989; Marsh 1991; Marsh 2003). The presence of potentially putative bacteria as minor constituents of resident community would be consistent with this hypothesis. In health conditions, there is a balance between the host and microorganisms thus these pathogens would be either weakly competitive or suppressed by antagonisms from other oral species. Therefore, they account for a small proportion of a community and lack clinical significance. However, when specific factors such as for example a lack of oral hygiene, aging, genetic factors or immune changes affect the environment, there is an

environmental perturbation that has a direct effect on the resident microbiota, host immune system and plaque composition (Marsh 1989; Marsh 1991; Marsh 2003). Additionally, host susceptibility is one of the factors necessary for the disease initiation as it can strongly affect disease patterns and severity. Therefore, a triad of factors are needed to instigate disease and these include susceptible host, periodontal pathogens and a perturbation in the local environment. Under new, perturbed environmental conditions, the plaque accumulates at gingival margins and instigates an inflammatory response (Marsh 1991; Marsh 2003; Filoche *et al.* 2010). As a result the pH rises and the flow of gingival crevicular fluid (GCF) is elevated which leads to the introduction of new protein rich nutrients. Such a shift has an impact on plaque biomass, metabolism, and virulence of oral bacteria and encourages proliferation of the obligate proteolytic anaerobes associated with periodontal diseases such as (Marsh 1994; Marsh 2003) *F. nucleatum*, *P. intermedia*, *Prevotella nigrescens*, *Prevotella micros*, *Prevotella vincentii*, *Prevotella periodonticum*, *Campylobacter rectus*, *C. gracilis*, *T. denticola*, *P. gingivalis*, and *T. forsythia* (Hajishengallis & Lamont 2012). This process is further detailed in Figure 1.2.

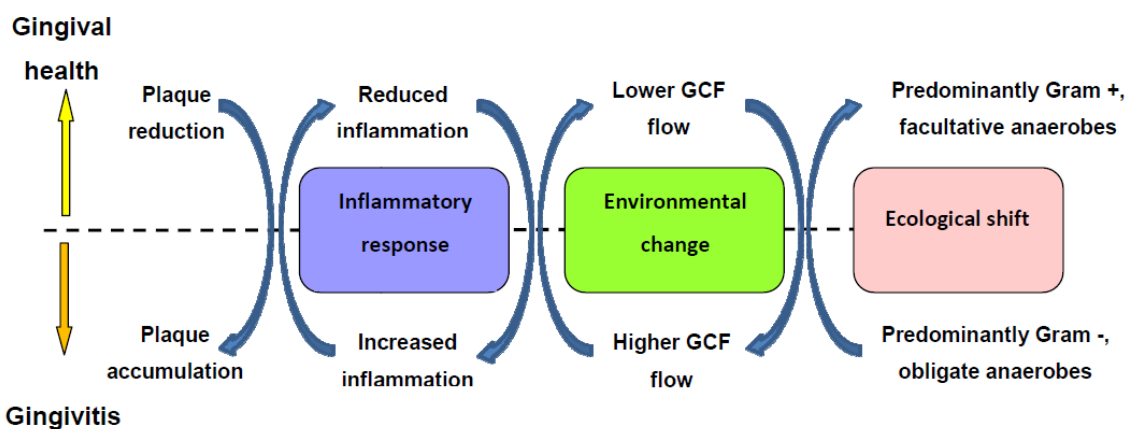


Figure 0.2 Scheme of ecological plaque hypothesis (modified from Marsh 1994)

Further research in this field in the last decade suggests that the aetiology of periodontal diseases is even more complex and multifactorial than previously anticipated. It is dependent on bacteria-bacteria interactions, bacterial-viral co-infections, immunological factors and a combination of genetic variants that alter the response to microbiota and subsequently predispose to disease (Hajishengallis & Lamont 2012; Nath & Raveendran 2013; Nibali *et al.* 2014). Therefore, the

pathogenicity of periodontal diseases can be explained by polymicrobial synergy and dysbiosis (PSD) model that built on previous hypotheses and states that periodontitis is initiated by a dysbiotic microbial community as a whole. According to this hypothesis, the inflammation (host-microbes imbalance) starts with the alteration in relative abundance among the oral bacteria compared to their abundances in health which can change the host-microbial cross-talk (Hajishengallis & Lambris 2012; Hajishengallis & Lamont 2012). The underlying mechanism involves susceptible host, series of microbial events together with predisposing environmental factors and key pathogens (described further below). One of the requirements is that the bacteria present in the community are compatible and can resist the host innate and acquired immune responses while contributing to the inflammation by e.g. the proteolytic activity or cytokine induction. Another requirement is the presence of the key pathogens that express virulence factors (i.e. adhesins, proteases etc) to elevate and remodel the phenotype of the entire community to more virulent. For example, *P. gingivalis* expresses approximately 500 proteins differently when grown in a biofilm community with *F. nucleatum* and *Streptococcus gordonii* (Kuboniwa *et al.* 2009). In this context, the key pathogens (*P. gingivalis*, *T. denticola* etc.) are not directly linked with the disease progression but with reshaping the normal symbiotic community into dysbiotic one that disrupts the homeostatic relationship with the host (Hajishengallis & Lambris 2012; Hajishengallis & Lamont 2012). Other periopathogens, previously underappreciated, include *Falifactor alocis*, *Peptostreptococcus stomatis*, and other species from *Selenomonas*, *Desulfobulbus*, *Prevotella* and *Megasphaera* genera (Lamont & Hajishengallis 2014). Key pathogens and the virulence factors they produce can also modulate the host response, impair immune surveillance, tip the balance from homeostasis to dysbiosis, impair the immune system and subsequently lead to sequence of events explained in the ecological plaque hypothesis; which is the increase of the dysbiotic community leading to GCF flow increase and tissue breakdown products (haemin, degraded proteins) that creates the favourable environment for other disease-provoking microbiota (Nibali *et al.* 2014; Jiao *et al.* 2014; Lamont & Hajishengallis 2014).

1.3.4 Oral microbiome

Comprehensive 16S rDNA high-throughput sequencing analysis performed on the human oral microbiome has revealed that there are 15 bacterial phyla frequently detected in the oral cavity of which 11 are considered as commensals: Actinobacteria, Bacteroidetes, Chloroflexi, Firmicutes, Fusobacteria, Proteobacteria, Spirochaetes, Synergistetes, Tenericutes, SR1 and TM7 (Dewhirst *et al.* 2010; Aagaard *et al.* 2013; Wade 2013). The 6 main phyla including Firmicutes, Actinobacteria, Bacteroidetes, Proteobacteria, Fusobacterium and Spirochaetes represent 96% of all the species present in oral microbiome (Lazarevic *et al.* 2010; Griffen *et al.* 2011; Wade 2013). Griffen and colleagues have showed in their 16S rDNA sequencing study on healthy and periodontitis cohort of subjects that the most predominant genera in the healthy microbiome are *Streptococcus*, *Haemophilus*, *Granitucella*, *Rothia*, *Actinomyces*, *Moraxela*, *Arthrobacter*, *Lautropia*, *Acinetobacter*, and *Gemella* (Griffen *et al.* 2012). A study by Bik and colleagues (Bik *et al.* 2010) listed the most prevalent bacterial species in healthy oral microbiome which included *Streptococcus oralis*, *Haemophilus parainfluenzae*, *Granulicatella adiacens*, *Veillonella parvula*, *Veillonella dispar*, *Rothia aera*, *Actinomyces naeslundii*, *Actinomyces odontolyticus*, *Prevotella melaninogenica*, and *Capnocytophaga gingivalis*. In spite of the relative compositional similarities in oral microbiome shown by the above studies, there are high interpersonal differences among individuals at both the species and strain level (Lazarevic *et al.* 2010; Ursell *et al.* 2012). Some oral communities were mostly dominated by *Streptococcus* while others by *Neisseria*, *Prevotella*, and *Veillonella* species (Bik *et al.* 2010). At the same time, many species are not shared between the subjects and these can include *Fusobacterium*, *Neisseria* and *Corynebacterium* (Bik *et al.* 2010; Ursell *et al.* 2012). Further to this, there was much less difference in the composition of the oral microbiota at different geographical locations than among the individuals (Nasidze *et al.* 2009; Wade 2013). This suggests that diet has little influence on the bacterial composition, especially when taken into account that food is quickly removed from the mouth (Beighton *et al.* 1986).

1.3.4.1 *Gingivitis microbiome*

Identifying species associated with gingivitis is not a simple task as the oral microbiome is a dynamic system influenced by many environmental factors including high-interpersonal differences. Furthermore, many bacterial species are found in either health or disease what even further distorts the distinction (Kistler *et al.* 2013). However, Huang *et al.* stated that the differences between the healthy and diseased microbiome is greater than the interpersonal differences, therefore the differences may be elucidated (Huang *et al.* 2014). Many studies including these based on cultivation or molecular techniques have attempted to determine the healthy and gingivitis microbiome (Zaura *et al.* 2009; Huttenhower *et al.* 2012; Wang *et al.* 2013) and the results of these studies are presented below.

Experimental gingivitis studies have shown that there is an increased taxonomic richness in plaque samples from patients with gingivitis when compared to oral health and also a general shift in prevalence from Gram-positive to Gram-negative species (Slots 1977a; Slots 1977b). Some of the genera and species linked to gingivitis include *Actinobacillus*, *Campylobacter*, *Eikenella*, *Fusobacterium* and *Prevotella* and species such as *P. intermedia*, *P. nigrecens*, *P. oralis*, *F. nucleatum*, *Veillonella parvula*, *A. naeslundii*, *A. odontolyticus* (Slots 1977a; Slots 1977b; Moore *et al.* 1982; Moore *et al.* 1986; Savitt *et al.* 1987; Socransky & Haffajee 1994; Huang *et al.* 2011). Further to this, it has been reported by many that increased numbers of *Actinomyces* spp. are associated with mature dental plaque and gingivitis onset (Ellen 1976; Slots 1977a; Slots 1977b; Syed & Loesche 1978; Moore *et al.* 1984; Tanner *et al.* 1996). Species such as *A. naeslundii* and *A. israelii* were shown to be the dominant cultivable organism in patients with gingivitis (Moore & Moore 1994; Tanner *et al.* 1998) and associated with bleeding gingivitis (Syed & Loesche 1978). Apart from *Actinomyces* spp., certain fusobacteria species were associated with gingivitis progression. These include *F. nucleatum* which was found in increased numbers in gingivitis (Slots 1977a; Slots 1977b) and was reported as a periopathogen that bridges the initial colonisers with late colonisers and also facilitates the attachment of black pigmenting anaerobes (Kolenbrander *et al.* 2002; Kolenbrander *et al.* 2006). Certain species such as *T.*

denticola, *T. vincentii* and *T. socranskii* from *Treponema* genus have also been associated with periodontal diseases. However, their presence is more linked to periodontitis than gingivitis due to their virulence factors (e.g. gingipains etc) that can penetrate epithelial cells and lead to connective tissue loss (Fenno & McBride 1998; Chan & McLaughlin 2000). Other species involved in gingivitis progression belong to *Capnocytophaga* spp. and *Eubacterium* spp. and include e.g. *C. rectus* or *E. corrodens* (Moore *et al.* 1982; Moore *et al.* 1986; Marsh & Martin 1999; Gmur *et al.* 2004).

The emergence of next generation sequencing allowed us to increase our knowledge of healthy and diseased microbiome. To date, most next generation sequencing studies have focused on periodontitis and only a few investigated the composition of gingivitis microbiome in depth. The latter are presented in this paragraph. The pyrosequencing study on 3 healthy and 3 gingivitis patients performed by Huang *et al.* (2011) showed that all the detected sequences were distributed in 11 bacterial phyla with the 6 most predominant including *Firmicutes*, *Proteobacteria*, *Bacteroidetes*, *Actinobacteria*, *Fusobacteria* and *TM7*. Among the above 6 phyla, *Bacteroidetes* and *Actinobacteria* were less abundant in gingivitis, while the remaining 4 were elevated. Further to this, 26 out of 70 genera detected in this study were found to be differently distributed between health and gingivitis. Genera including *Streptococcus*, *Veillonella*, *Prevotella*, *Lautropia* and *Haemophilus* decreased in abundance in gingivitis, while remaining 21 increased (*Leptotrichia*, *Selenomonas*, *Lachnospiraceae*, *Eubacterium*, *Cardiobacterium*, *Peptostreptococcus*, *Tannerella*, *Catonella*, *Synergistes*, *Filifactor*, *Peptococcus*, *Solobacterium*, *SR1*, *Syntrophomonas*, *Johnsonella*, *Chloroflexus*, *Olsenella*, *Propionivibrio*, *Peptoniphilus*, *Desulfomicrobium*, *Pseudoramibacter*) (Huang *et al.* 2011). Another study performed by Huang *et al.* (2014) used the 454 platform to sequence the plaque samples collected from 50 participants that underwent controlled transition from naturally occurring gingivitis to health and then to experimental gingivitis. This study has shown relatively similar results to his previous study. 27 genera were differently expressed in health and gingivitis; 5 of which (*Streptococcus*, *Rothia*, *Actinomyces*, *Haemophilus*, *Lautropia*) were associated with oral health and remaining 22 with gingivitis (*Leptotrichia*, *Prevotella*, *Fusobacterium*, *TM7*, *Porphyromonas*, *Tannerella*, *Selenomonas*, *Lachnospiraceae*, *Comamonadaceae*,

Peptococcus, *Aggregatibacter*, *Catonella*, *Treponema*, *SR1*, *Campylobacter*, *Eubacterium*, *Peptostreptococcus*, *Bacteroidaceae*, *Solobacterium*, *Johnsonella*, *Oribacterium*, *Veillonellaceae*) (Huang *et al.* 2014). Same was reported by Kistler *et al.* who found that species associated with gingivitis include *Tannerella forsythia*, *F. nucleatum*, *P. gingivalis*, *Prevotella* spp., *Filifactor alocis*, *Mogibacterium timidum*, *Dialister pneumosintes*, *Parvimonas micra*, *Peptostreptococcus stomatis*, *Synergistetes* spp., *Eubacterium saburreum*, *Eubacterium saphenum*, *Kingella oralis*, *Selenomonas sputigena*, *Capnocytophaga granulosa*, *Campylobacter gracilis*, and *Leptotrichia* spp. (Kistler *et al.* 2013).

The above studies demonstrated significant differences in species composition between the oral health and gingivitis. However, in neither of the studies mentioned above is there a clear and distinctive boundary between health and gingivitis. It also indicates that periodontal diseases have far more complex aetiology than previously anticipated. Furthermore, all the studies used different methodologies, different subject recruitment procedures or different techniques are applied to analyse either saliva or dental plaque etc. All these lead to differences among the studies and hardship with the comparison. However, the recent findings from high-throughput next generation sequencing presented above helped broaden the existing knowledge on bacterial composition in oral health and disease based on cultivation and molecular methods.

1.3.5 Reductionist approach

For a long time the main approach in understanding the complex oral biofilm was based on a methodological reductionist approach which was aimed at identifying the key pathogens responsible for oral microbial pathogenesis (He & Shi 2009). The reductionist concept assumes that a complex biological system or phenomenon can be understood or explained by a simplified model or analysis of their simpler components. This philosophical idea dates back to 17th century when Bacon proposed that principles derived from specific cases can be used to successfully formulate predictions (Fang & Casadevall 2011). An example of a reductionist approach in oral microbiology can be growing a single- or multi- species biofilm *in vitro* to investigate the aetiology of oral

diseases. This approach enabled microbiologists to understand the complexity of oral biofilms and identify the species involved in oral health and disease. Yet, it still has its methodological limitations which may prevent scientists from recognising the important relationship among organisms in their natural environment (He & Shi 2009; Fang & Casadevall 2011).

1.3.6 Cultivation methods

The principal method of characterising oral microbiota in periodontal diseases has been culture on artificial media; this has allowed determination of the changes in microbial populations associated with health and gingivitis (Aranki *et al.* 1969; Gordon *et al.* 1971; Slots 1977; Tanner *et al.* 1979; Wade 2011; Wade 2013). Many experimental gingivitis studies were solely based on this approach with the initial assessment of the microbial population based on non-selective media such as Columbia Blood Agar (CBA), Fastidious Anaerobe Agar (FAA), Trypticase Soy Agar (TSA) or Nutrient Agar (Syed & Loesche 1978; Moore *et al.* 1982; Moore *et al.* 1983; Moore & Moore 1994). To allow the growth of oral species with more complex nutritional requirements, supplements such as blood, serum, haemin or menadione were added and the environmental conditions during incubation were changed by providing different gas formulations. To enumerate specific species or genera many selective media have been developed. These include Mitis-Salivarius (MS) agar for the isolation of *Streptococcus* spp. (Gold *et al.* 1973), Cadmium Fluoride Acriflavine Tellurite (CFAT) agar for the isolation of *Actinomyces* spp., all of which involve the addition of selective agents such as antibiotics or toxins (Zylber and Jordan 1982). However, this approach is not a simple undertaking as some oral bacteria are typically slow-growing, nutritionally fastidious and many are sensitive to changes in oxygen concentration (Syed & Loesche 1978; Moore *et al.* 1986; Siqueira & Rôças 2013). Therefore, the samples have to be collected carefully, transported in a manner which maintains the viability and then must be cultured promptly; a further problem is the complexity of the cultivable bacterial community. There are approximately 350 cultivable species and the identification process is both time consuming and difficult (Wade 2011; Wade 2013). While these techniques have been an invaluable tool in isolating certain species

responsible for disease progression (Socransky *et al.* 1963; Rosebury & Reynolds 1964; Newman & Socransky 1977; Slots *et al.* 1980) with recent advances in molecular techniques, the current trend in the field of oral microbiology is shifting towards culture-independent techniques that provide information on both cultivable and uncultivable species in the oral microbiome (Wade 2011; Wade 2013).

1.3.7 Culture independent methods

Approximately 40-60% of species of oral bacteria cannot be grown *in vitro* and identified using conventional physiological techniques (Kroes *et al.* 1999; Aas *et al.* 2005; Siqueira & Rôças 2013). Since uncultivable bacteria may play a role in disease progression, methods have been developed for culture-independent analysis of complex bacterial communities. These techniques have primarily been based on the analysis of the small subunit (16S) ribosomal DNA (Paster *et al.* 2001; Kumar *et al.* 2003; Kumar *et al.* 2006; Paster *et al.* 2006;) and are described below.

1.3.7.1 PCR

Polymerase chain reaction (PCR) is a reliable and rapid way of detecting even a small amounts of DNA (Dieffenbach 1993) that was invented by Kary Mullis in 1983 for which he won a Nobel Prize in 1993 (Powledge 2004). It is a very sensitive method and often used for detecting specific bacteria in biological samples based on the 16S rRNA gene which is present in every bacterium. The gene contains conserved, variable and hypervariable regions which, when sequenced, can be used to identify bacterial species. This method is particularly beneficial for detection of bacteria which are not cultivable or easily distinguished in culture (Ashimoto *et al.*, 1996). However, screening large numbers of samples is difficult, time consuming and costly. Its main drawback though is its inability to produce quantitative data on the bacteria present in a sample as it only confirms its presence or absence (Ashimoto *et al.* 1996; Socransky & Haffajee 2005). A few examples of this technique in the field of oral microbiology include the study by Ashimoto *et al.* who used PCR method to determine the prevalence of orange and red complex periodontal pathogens in 50 patients with advanced periodontitis and gingivitis (Ashimoto *et al.* 1996). Meurman *et al.* screened

the samples retrieved from periodontal patients for *T. forsythia*, a bacterial species that is positively correlated with recurrent periodontitis. In his study, *T. forsythia* was successfully cultured in 22 out of 58 periodontitis patients; while PCR confirmed the presence of this bacterium in 52 out of 58 cases (Meurman *et al.* 1997).

1.3.7.2 Quantitative PCR (qPCR)

A modification of end point PCR is a quantitative PCR (qPCR) and this technique has been adopted for a number of studies using the 16S rRNA gene as the target (Pozhitkov *et al.* 2011). It allows the amplification of the low amounts of DNA and a reliable detection of the product generated during each cycle of the PCR reaction, which is directly proportional to the DNA template prior to the start of the PCR reaction (Dieffenbach 1993; Powledge 2004; Ranasinghe & Brown 2005; Saunders 2009; Smith & Osborn 2009). Quantitative PCR has been extensively used in a wide range of microbial applications including the characterisation of the dental plaque and identification of bacterial pathogens associated with gingivitis (Colucci 2000). A qPCR technique was used by Shelburne *at al.* to quantify the amount of *T. forsythia* in samples collected from patients with advanced periodontitis (Shelburne *et al.* 2000). Saygun and colleagues have shown that species including *P. intermedia*, *P. gingivalis*, *T. forsythia*, *F. nucleatum* and *C. rectus* were present in higher numbers in saliva from patient with gingivitis and periodontitis than healthy ones (Saygun *et al.* 2011). Furthermore, Becerik *et al.* used qPCR method to examine the effectiveness of chlorhexidine mouthrinse (CHX) against the untreated gingivitis. This study has proven that the patients treated with CHX mouthwash showed a significant decrease in periodontal pathogens such as *P. gingivalis*, *P. intermedia*, *T. forsythia* and *F. nucleatum* (Becerik *et al.* 2011).

1.3.7.3 Fluorescence In Situ Hybridisation (FISH)

Fluorescent *in situ* hybridisation, in the field of oral microbiology, has been used to determine spatial distribution, microbial diversity and to identify or quantify periodontal pathogens (Gersdorf *et al.* 1993; Ouverney *et al.* 2003). This technique allows the detection of certain species in a mixed community by hybridising

fluorescently labelled DNA probes to a complementary target within the intact cell of a targeted bacterium (Amann *et al.*, 2000). Gersdorf *et al.* (1993) successfully used this technique for direct detection of Gram-negative anaerobes such as *P. gingivalis* and *T. forsythia* in periodontal samples (Gersdorf *et al.* 1993). Ouverney *et al.* (2003) used this technique for detection of uncultivable TM7 species in dental plaque (Ouverney *et al.* 2003). While, Thurnheer *et al.* (2001) focused on identification and enumeration of health associated bacteria and the initial colonisers of dental plaque such as *S. mitis*, *S. anginosus* and *S. sobrinus* (Thurnheer *et al.*, 2001). Studies by Loesche *et al.* (1992) and Savitt *et al.* (1987) on prevalence of periodontal pathogens in dental plaque have also shown that using DNA probes showed higher detection rates and accuracy when compared to culture method (Savitt *et al.* 1987; Loesche *et al.* 1992). Therefore, the DNA probes can be an effective way of bacterial detection in periodontal studies. Despite a few drawbacks which include non-specific labelling, low-throughput, laborious and time consuming probe development (Moter & Göbel 2000; Ouverney *et al.* 2003).

1.3.7.4 DNA – DNA hybridisation checkerboard

The checkerboard DNA-DNA hybridisation technique for oral bacteria was developed by Socransky *et al.* (1994) and was intended to be used for rapid detection of the oral species in periodontal samples (Papapanou *et al.*, 1997). This method uses digoxigenin-labeled whole genomic DNA probes targeted at different oral species and a checkerboard DNA-DNA hybridisation format where probes are fixed in parallel lanes on a nylon membrane that allows detection of 40 species at once on a single membrane (Socransky *et al.* 2004). The technique allows screening of multiple samples for specific pathogens in a relatively inexpensive, specific and rapid manner (Socransky *et al.* 2004; Socransky & Haffajee 2005). This technique has been used in several studies to characterise the oral communities of dental plaque (Siqueira *et al.* 2000; Wall-manning *et al.* 2002; Salvi *et al.* 2005; Dahle & Leonhardt 2006; Nelson-Filho *et al.* 2011). However, one of the main examples mentioned should be the work of Socransky *et al.* (1998) who characterised the periodontal microbial communities and grouped them according to the colour coded classes. Each class had a different level of

correlation to health / gingivitis / periodontitis based on the cluster analysis performed (Socransky *et al.* 1998). The gingivitis and periodontitis associated bacteria were grouped as orange and red complex bacteria and included *P. intermedia*, *P. nigrescens*, *P. micros*, *F. nucleatum*, *P. gingivalis*, *T. forsythis*, and *T. denticola* (Socransky & Haffajee 2005). On the other hand, Teles *et al.* used checkerboard DNA-DNA hybridization to analyse the bacterial succession in supra- and subgingival plaque in healthy and periodontitis patients after professional teeth cleaning. His study confirmed that there is a defined order of succession in biofilm redevelopment with no significant differences between the groups (Teles *et al.* 2012).

1.4 Holistic approaches

Microorganisms are more than just the sum of individual parts; they possess complex cellular processes which are intimately networked with many feedback loops, and complete understanding of these networks certainly presents big challenges (Strange 2005). This realisation has led to systems biology and a more holistic approach which bridges the genotype-to-phenotype gap (Goodacre 2007) by applying a wide range of inter-disciplinary techniques such as proteomics, transcriptomics, genomics and metabolomics, that have given a better understanding of the complex human-microbiota interactions (Grant 2012).

1.4.1 Proteomics

Proteomics is the study of all proteins in a given sample. As a field it was revolutionised with the advancement in mass spectrometry in 1990s that enabled a relatively fast identification of proteins in a given biological sample (Grant 2012). Gingival crevicular fluid (GCF) is a tissue fluid heavy in proteins which include break down products of connective tissues, products derived from host or microbial plaque (Carneiro *et al.* 2014). Thus, the proteomics approach could potentially serve as a novel tool for the identification of potential biomarkers linked to periodontal diseases (Tsuchida *et al.* 2012; Grant *et al.* 2010). For example, Grant and colleagues identified 16 bacterial and 186 human potential protein biomarkers associated with gingivitis (e.g. methylase, glycosyl transferase) when investigating the proteomic patterns of GCF fluid from

gingivitis patients (Grant *et al.* 2010). Conversely, Wu *et al.* used whole unstimulated saliva to investigate the proteomic profiles of healthy and periodontitis patients. This study determined 11 proteins (e.g. serum albumin, immunoglobulin (Ig) α 2 chain C region, zinc- α 2 glycoprotein, salivary α -amylase) which were elevated in periodontitis patients and could potentially serve as biomarkers (Wu *et al.* 2009). Similar studies on whole saliva from healthy and periodontitis patients were performed by Gonçalves (2010) and Salazar (2013). The study by Goncalves revealed that periodontitis patients have increased levels of blood proteins (serum albumin and haemoglobin) and as well as immunoglobulin. Salazar *et al.* identified 20 proteins (e.g. ceruloplasmin, catalase, neutrophil collagenase etc.) that were more abundant in periodontitis patients than in healthy ones and stated that proteomic analysis of whole saliva is a useful tool in differentiation between oral health and periodontitis (Gonçalves *et al.* 2010; Salazar *et al.* 2013)

1.4.2 Transcriptomics

Transcriptomics is the study of complete RNA transcripts (mRNAs, non-coding RNAs and small RNAs) produced by cells in a particular set of conditions. The aim of transcriptomics is to catalogue the RNA transcripts to determine the transcriptional differences and to quantify the change in gene expression levels under certain set of conditions (e.g. disease) (Fábián *et al.* 2008; Grant 2012). Various techniques are available including hybridisation or sequence based approaches. Hybridisation is based on incubating the fluorescently labelled cDNA with microarrays and is still the golden standard in transcriptomics. The most recent technological advances into the field of transcriptomics include the high-throughput RNA sequencing (RNA-seq), also termed as whole transcriptome shotgun sequencing (Wall *et al.* 2009; Chu & Corey 2012). Although it is a relatively novel method under constant development, it shows several advantages over the existing hybridisation method. These include, for example, not being limited to detection of transcripts corresponding to already existing genomic sequences, high reproducibility for either technical or biological replicates and also less amount of sample required (Wang *et al.* 2009). Some examples of transcriptomics in the field of periodontal diseases are presented below.

Jonsson *et al.* investigated the gene expression in gingiva of healthy and gingivitis patients. The study has shown that 373 genes were differently regulated and 184 genes were up-regulated by at least 1.5 fold. Some of the upregulated genes include CXCL13, a CXC chemokine involved in migration of B cells or CXCL6, a granulocyte chemoattractant reported by others to be significantly upregulated in periodontal lesions (Jönsson *et al.* 2011). Jorth *et al.* investigated the gene expression of healthy and periodontal samples at high resolution, i.e. examining the expression of 160,000 genes simultaneously. This study has shown that the diseased periodontal microbiome exhibits distinctively different metabolic gene expression compared to the healthy microbiome and includes increased expression of genes coding for proteins involved in butyrate and pyruvate metabolism (Jorth *et al.* 2014). These studies show the usefulness of transcriptomics in understanding the pathobiology of periodontal diseases.

1.4.3 Genomics

Genomics is the study of the whole genome of a single organism or a whole community (Grant 2012). Since the emergence of next generation sequencing (NGS) in 2005, which offered unprecedented sequencing speed, the field of genomics has grown rapidly and enabled scientists to move from conception to obtaining a full data set in a matter of hours or days (Di Bella *et al.* 2013; Illumina Inc. 2015). In 2007 single sequencing runs were producing approximately one gigabase (Gb) which was followed by nearly a 1000x increase to around one terabase (Tb) by 2011 (Illumina Inc. 2015). Additionally, NGS techniques provide a high degree of flexibility regarding the resolution required. This means that the coverage can be tuned according to the experimental needs, with higher resolution on particular regions of the genome or a more expansive view with lower resolution (Di Bella *et al.* 2013; Grant 2012).

1.4.4 Next generation sequencing

The NGS technologies encompass three different platforms introduced by different companies such as Roche with 454, Life Technologies with the SOLiD platform and Illumina with its MiSeq / HiSeq platform (Shendure & Ji 2008; Metzker 2010; Liu *et al.*

2012). All three platforms allow high-throughput and parallel analysis at reduced cost and led to improvements in the depth and scale of 16S rDNA sequencing studies (Shendure & Ji 2008; Metzker 2010; Liu *et al.* 2012). An overview of the most popular next generation sequencing techniques currently available on the market is presented in table 1.2.

| Sequencer | 454-GS system | FLX | MiSeq v3 | SOLiD v4 |
|----------------------|--|-----|---|---|
| sequencing mechanism | Emulsion PCR + Pyrosequencing | | Bridge Amplification+ Sequencing By Synthesis (SBS) | Emulsion PCR + Ligation and two base coding |
| Read length | 700 bp | | 2x300 bp | 2x35 bp |
| Accuracy | 99.99% | | 98% | 99.99% |
| Time/run | 23 Hours | | ≈56 hours | 8-9 days |
| Advantage | Read length, fast | | high-throughput; fast | accuracy |
| Disadvantage | high error rate in poly-bases longer than 6bp; high cost of reagents | | short read | short read; assembly |

Table 0.1 Mechanism and advantages/disadvantages of NGS sequencers (Claesson *et al.* 2010; Zhang *et al.* 2011; Quail *et al.* 2012; Liu *et al.* 2012; Life Technologies Inc. 2014; Illumina Inc. 2015; Roche Inc. 2015).

1.4.4.1 454 platform using pyrosequencing

The first step in 454 pyrosequencing is emulsion PCR where clonal amplification is performed. In this step an oil-water system is agitated to create an emulsion which consists of aqueous droplets. Each droplet contains PCR reagents, DNA template, primers and magnetic beads. The first primer is complementary to one of the adapter sequences used in the library construction, while the other one is present in the solution. The emulsion amplification yields multiple copies of a unique DNA template on a single bead in each droplet. When the emulsion is broken, the DNA is denatured and transferred to a picotiter plate where the pyrosequencing reaction starts by depositing sequencing reagents into each well. When a single dNTP is being incorporated into ssDNA catalysed by DNA polymerase, a phosphodiester bond is formed and pyrophosphate (PPi) is released. The pyrophosphate is converted to ATP by ATP sulfurylase. ATP production is detected by light which is produced by using ATP to convert luciferin into oxyluciferin. The light detected is directly correlated with the

number of nucleotides incorporated. As one dNTP is incorporated at a time, the strength of the signal seen on the pyrogram determines which nucleotide was incorporated at the given time (Shendure & Ji 2008; Petrosino *et al.* 2009; Claesson *et al.* 2010; Siqueira *et al.* 2012; Liu *et al.* 2012; Harrington *et al.* 2013).

Keijser *et al.* explored the composition of the oral microbiome by sequencing the 16S rRNA hypervariable V6 region of saliva and supragingival plaque samples collected from healthy individuals. The 197,600 sequences generated represented 22 different taxonomic phyla and showed that Firmicutes (*Streptococcus* and *Veillonella* genera) and Bacteroidetes (*Prevotella* genus) were the most predominant phyla in saliva samples. While Firmicutes and Actinobacteria (*Corynebacterium* and *Actinomyces* genera) were the predominant taxa in supragingival plaques (Keijser *et al.* 2008). A study performed by Griffen and colleagues which compared the healthy subgingival community with the one of periodontitis patients using 454 sequencing showed that in general the diversity is higher in the disease state with 123 species being more abundant than in health. These species belonged to the Spirochaetes, Synergistetes and Bacteroidetes phyla, whereas the Proteobacteria were found at higher levels in healthy controls (Griffen *et al.* 2012). Further to that, Abusleme and colleagues showed that the periodontitis community is associated with higher proportion of Synergistetes, Spirochetes, Firmicutes and Chloroflexi when numbers of Actinobacteria were higher in health (Abusleme *et al.* 2013).

1.4.4.2 SOLiD platform based on Ligation

The SOLiD technology uses two-base sequencing based on ligation and is similar to 454 pyrosequencing in respect that it also uses emulsion PCR to clonally amplify the DNA bound to beads before the actual sequencing starts. After the emulsion PCR amplification is broken, the beads with amplified DNA fragments are captured on the glass slide. This allows for high densities of beads per slide so increasing the level of high-throughput sequencing. The SOLiD technology uses fluorescently labelled octamers with di-base complement sequences; the flow cell is flushed with these which compete for ligation to the primer. The annealing sequence is ligated to the primer, fluorescence is detected and then the fluorophore is cleaved. The sequencing

occurs by performing seven cycles of ligation, detection and cleavage; then the second sequencing primer is hybridised to the template. As a result, the 35 base query DNA is sequenced twice to improve the accuracy of the sequencing process. This system is the most complicated sequencing technology and requires complex labelled oligonucleotides and complicated algorithms to analyse and interpret the output data (Liu *et al.* 2012; Di Bella *et al.* 2013).

1.4.4.3 Illumina platform based on sequencing by synthesis

Illumina-based sequencing strategies include MiSeq and HiSeq (version 500, 2500 and X) platforms which are able to generate a large amount of sequence data at a very cost effective price (Caporaso *et al.* 2010; Quail *et al.* 2012; Liu *et al.* 2012). The platforms also vary in their sequencing throughput, with HiSeq X being capable of generating 1.8 Tb using paired 2x150 bp reads (i.e., 3 billion reads per flow cell) and HiSeq 2500 generating up to 1000 Gb using paired 125 bp reads (i.e., 2 billion reads per flow cell). On the other hand, MiSeq, a benchtop sequencer, can generate up to 15 Gb output using paired 300 bp reads (i.e., 25 million reads per flow cell) (Illumina Inc. 2015). Therefore, HiSeq platform has become the standard approach for shotgun metagenomic sequencing because of its increased read depth. However, MiSeq has a greater potential for use with 16S rRNA gene sequence studies, because it generates longer sequence reads, and its performance and cost are tractable to the needs of individual investigators. Until recently, the most significant problem with the Illumina platforms has been the ability to sequence samples with low genetic diversity, such as that commonly found with 16S rRNA gene amplicons. To artificially increase the genetic diversity, it has been common to mix in a control library of genomic DNA from the phage PhiX, such that 50% of the DNA was from PhiX. During the course of this study, Illumina upgraded their image analysis software to overcome this challenge, such that only 5 to 10% PhiX is needed to sufficiently increase the genetic diversity. Another factor that can affect data quality is the amount of DNA loaded onto the flow cell, as this affects the cluster density and the ability of the image analysis software to discriminate between clusters (Caporaso *et al.* 2010; Caporaso, Lauber, Costello, *et al.*

2011; Caporaso *et al.* 2012; Caporaso, Lauber, Walters, *et al.* 2011; Liu *et al.* 2012; Quail *et al.* 2012).

The next generation sequencing typically consists of 3 steps: DNA library preparation, library amplification and sequencing. The library is constructed by amplifying the region of interest of 16S rRNA gene with custom primers that have attached barcode (for identification of individual amplicons) and adapter sequences complimentary to oligonucleotide fragments on the flow cell. Then, the DNA templates are immobilised on a flow cell surface to present the DNA in a manner that facilitates access to enzymes while ensuring high stability of surface-bound template and low non-specific binding of fluorescent labelled nucleotides. The DNA library amplification starts with a bridge amplification, a novel solid phase amplification which creates up to 1,000 identical copies of each single template molecule in close proximity. The amplification starts with dsDNA looping over to form a bridge by binding to oligonucleotide sequence present on the flow cell. The dsDNA is denatured, re-annealed and then the process is repeated. Each cycle of displacement and re-annealing creates clusters of clonal DNA available for sequencing. The sequencing process starts with blocking the free 3' end of the molecules attached to the flow cell. An iterated process of single base extension occurs in which the flow cell is flooded with fluorescently labelled and chemically modified nucleotides able to terminate the DNA chain synthesis. After washing of the flow cell and excitation of the incorporated label, the emitted light is captured as an image identifying which of the four nucleotides have been incorporated. In order to repeat this, the incorporated nucleotide is chemically unblocked and the process is repeated. Thus, by sequentially analysing each cluster, it is possible to derive the sequence of the molecules within the cluster. After the sequencing is finished, the analysis can be directly performed on the MiSeq instrument. MiSeq reporter (MSR), a Illumina's free software, performs a downstream analysis after a run is complete and reports the data down to the species level (Caporaso *et al.* 2010; Caporaso, Lauber, Costello, *et al.* 2011; Caporaso, Lauber, Walters, *et al.* 2011; Caporaso *et al.* 2012; Liu *et al.* 2012; Illumina Inc. 2015). Caporaso *et al.* conducted pioneering work on microbial community identification of environmental bacteria using new Illumina platform (Illumina GAIIx platform) at the

time (Caporaso, *et al.* 2011). This was followed by others, for example, Li *et al.* investigated the bacterial composition of dental plaques from healthy and periodontitis patients using Illumina MiSeq platform. His findings demonstrated a clear difference between health and disease with *Fusobacterium*, *Porphyromonas*, *Treponema*, *Filifactor*, *Tannerella* showing higher relative abundances in periodontitis (Li *et al.* 2014).

1.4.5 Metabolomics

Metabolomics aim to quantify and characterise the metabolites of a living system in a given sample (Nicholson & Lindon 2008). This term was first coined by Nicholson, however, the correlation of certain metabolites with disease dates back to ancient times. Urine charts were used in Middle Ages to predict diseases based on urine smell or colour (Nicholson & Lindon 2008). With the development of high-throughput and powerful techniques such as nuclear magnetic resonance spectroscopy (NMR) and mass spectrometry (MS), this field has started intensively evolving (Xu *et al.* 2014; Mashego *et al.* 2007). Today, it is possible to study the metabolite composition produced by a living system to get an accurate snapshot of its actual physiological state (Grootveld & Silwood 2005; Dunn *et al.* 2005; Xu *et al.* 2014). This approach can complement genomic studies by relating the species abundance to their potential function.

There is a range of techniques available to study metabolite fingerprinting. However, the most widely used ones include nuclear magnetic resonance spectroscopy and mass spectrometry combined with gas or liquid chromatography (GS-MS, LC-MS) (Lenz & Wilson 2007; Goodacre 2007). NMR spectroscopy and MS based platforms gained popularity due to the fact that they offer high sensitivity, simplicity of performance, and fast high-throughput processing (Lenz & Wilson 2007; Goodacre 2007; Barding *et al.* 2013). Additionally, they can be coupled with complex pattern recognition tools such as principal component (PCA) and partial least square (PLS) analyses to enable the pattern recognition identification, non-linear mapping and then the interpretation of the metabolic profiles (Wishart 2008; Fonville *et al.* 2010; Smolinska *et al.* 2012). Consequently, metabolomics has been used for determination of health and disease

(Jenkinson & Lamont 2005) and identification of potential biomarkers associated with periodontal diseases (Sugimoto *et al.* 2012). Barnes and colleagues have successfully used biochemical profiling to analyse the metabolite composition of samples from healthy, gingivitis and periodontitis sites. They have shown significant composition differences among the sites which confirms that metabolite fingerprinting can be a powerful tool for determining periodontal diseases (Barnes *et al.*, 2010; Barnes *et al.*, 2011).

1.4.5.1 ^1H NMR spectroscopy

Nuclear Magnetic Resonance spectroscopy in the field of metabolomics started evolving in the 1980s (Lenz & Wilson 2007). The technique enables detection and structural identification of the organic metabolites simultaneously and non-invasively (Simmler *et al.* 2014). NMR spectroscopy is a study of a physical phenomenon of resonance transition between magnetic energy levels, happening when atomic nuclei are immersed in an external magnetic field. The NMR instrument consists of the magnet, detector, frequency generator, recorder and probe. The magnet is a superconductor which consists of wire coil through which the current passes and generates the electromagnetic field (Dunn *et al.* 2005; Serkova & Niemann 2006; Wishart 2008; Bharti & Roy 2012; Simmler *et al.* 2014). The sample is placed in the magnet and spins around its axis to ensure equal exposure to the electromagnetic field. NMR spectrometry depends on the nuclear spin of the nuclei of the atom; the atoms which act as mini-magnets align themselves with the field or against it. When the electromagnetic radiation is applied, the nuclei with the lower energy state can absorb the energy and jump to the higher energy state. Subsequently we can observe either the absorption of the energy or the subsequent release when the nucleus goes back to the lower energy state. This reemission of energy is recorded, amplified and processed to give an NMR spectrum (Dunn *et al.* 2005; Serkova & Niemann 2006; Wishart 2008; Bharti & Roy 2012; Simmler *et al.* 2014). Today, it is the most often applied platform for structure elucidation of micro- or macro- compounds of unknown natural or synthetic origin (Simmler *et al.* 2014). Its popularity over other metabolomics techniques, despite lower sensitivity, is a simple methodology, virtually

no sample preparation, short analysis time that provides metabolite fingerprinting in both a qualitative and quantitative manner (Dunn *et al.* 2005; Emwas *et al.* 2013). Furthermore, it is a well proven and powerful technique for biofluid profile identification, e.g. saliva, providing comprehensive and highly reproducible data (Grootveld & Silwood 2005; Lenz & Wilson 2007; Fidalgo & Renata 2013; Santone *et al.* 2014). The potential disadvantage of this platform is a requirement for a trained operator and the high cost of apparatus. Though, the costs per sample are relatively low (Dunn *et al.* 2005; Xu *et al.* 2014).

A study by Fidalgo *et al.* on metabolic profiles of saliva obtained from children with and without caries lesions revealed that children with lesions had higher levels of the metabolites n-butyrate, acetate and lactate (Fidalgo & Renata 2013). Aimetti *et al.* (2011) applied ^1H NMR fingerprinting to saliva samples collected from healthy and periodontitis patients and identified that there is an increase in certain biomarkers such as succinate, trimethylamine, butyrate and propionate which are related to host-microbe interactions occurring in the progression of periodontal diseases (Aimetti *et al.* 2011).

1.4.5.2 Mass spectrometry based techniques

1.4.5.2.1 Liquid chromatography – mass spectrometry

Liquid chromatography-mass spectrometry (LC-MS) is a well-known analytical technique that combines the physical and mass separation capabilities of liquid chromatography and mass spectrometry. The main advantages offered by this platform include broader range of molecules that can be analysed when compared to gas chromatography-mass spectrometry, satisfactory range of sensitivity and ability to handle complex compounds and mixtures. Therefore, this technique is often used in the field of metabolomics to identify the metabolite profile of various biological samples (Pitt 2009).

The process of separation starts with a mixture under identification being dissolved in a fluid termed 'mobile phase'. Solvent typically used as mobile phase include e.g. water, methanol and chloroform etc. Next, the sample is forced by the mobile phase

under pressure through the stationary phase. At this stage the sample is separated based on its physical properties, retention in the stationary phase. Different compounds have different retention times, thus they arrive at the mass spectrometer at different times. As the compounds arrive, they are ionised and identified based on their mass-to-charge ratio (Pitt 2009; Wang *et al.* 2011; Gika *et al.* 2014). A periodontal example of using this technique includes the study by Hager *et al.* that investigated the lipid mediator precursors as the potential biomarkers for periodontitis. His study has showed that the ratios of precursors of pro-resolution/pro-inflammatory lipid mediators in GCF fluid of periodontitis patients are lower when compared to healthy individuals (Hager *et al.* 2013).

1.4.5.2.2 Gas chromatography – mass spectrometry (GC - MS)

The GC-MS platform is often a platform of choice for identification of apolar, volatile and semi-volatile analytes of molecular weight lower than 600-700 amu. This is also the major disadvantage of this technique. Especially since it does not provide identification of polar, non-volatile, large or thermolabile compounds without previous derivatisation which is laborious and time consuming. Not only derivatisation, but also extensive sample preparation, low-throughput and long time analysis makes it less favourite than NMR spectroscopy for the metabolomic applications (Dunn *et al.* 2005; Shulaev 2006; Lenz & Wilson 2007).

The major technical difference between the LC/MS and GC/MS platform is that the liquid chromatography is substituted with gas chromatography. This means that the mobile phase is an inert gas such as helium and the stationary phase is a microscopic layer of liquid or polymer. The gaseous compounds interact with the stationary phase, which causes the compound to elute at different time points (different retention time) and then the sample is identified by a mass spectrometer based on its mass-to-charge ratio (Dunn *et al.* 2005; Shulaev 2006; Lenz & Wilson 2007). This technique has been used by Park *et al.* to determine if the edible seaweed *Enteromorpha linza* displays antimicrobial activity against periodontal pathogens such as *P. intermedia*, *P. gingivalis* and *F. nucleatum* (Park *et al.* 2013). Study by Solmaz *et al.* showed that Shitake essential oil is an effective anti-biofilm agent on oral pathogens and can be used as

alternative treatment for periodontal diseases (Solmaz *et al.* 2013). Takada *et al.* used GC-MS platform to characterise the new serotype of periopathogen *A. actinomycetemcomitans* (Takada *et al.* 2010).

1.5 Complex *in vitro* models

The ideal situation for understanding the aetiology of periodontal diseases such as gingivitis is studying the host-biofilm interactions *in vivo*. However, the complexity of the oral environment, ethical issues, limited access and small quantity of samples available for further investigations have led to development of laboratory *in vitro* models (Edlund *et al.* 2013). The idea of complex *in vitro* models is to provide a high degree of flexibility in terms of the experimental conditions to help model and understand the complex biological phenomena. Therefore, these models simulate the oral environment and mimic health and disease associated bacterial shifts (Tang *et al.* 2003; Greenman *et al.* 2005; Lebeaux *et al.* 2013) by enabling the provision of various nutrients, components or gases. Further to this, the apparatus constructed in such a fashion enable real-time biofilm growth, observation at various stages of biofilm formation using various techniques and also provide vital information on disease aetiology, prevention, eradication and management (Kolenbrander *et al.* 2002; Tang *et al.* 2003; Coenye & Nelis 2010; Lebeaux *et al.* 2013).

Various *in vitro* systems have been developed and used to attempt to answer questions of clinical relevance (Sissons *et al.* 1991; Sissons 1997; Guggenheim *et al.* 2001; Guggenheim *et al.* 2004; Guggenheim *et al.* 2009; Shaddox *et al.* 2010). These include simple batch, static systems or fed batch systems which have been used more or less successfully within the field of oral biofilms; but certainly have contributed to the progress within the field of *in vitro* modelling (Sissons 1997; Whiteley *et al.* 1997; Wilson 1999; Donlan *et al.* 2004; Goeres *et al.* 2005; McBain *et al.* 2005). Some drawbacks of these systems include lack of reliability, simplicity or difficulties in maintaining biofilm communities over time (Tang *et al.* 2003; Coenye & Nelis 2010; Lebeaux *et al.* 2013). The review presented below feature currently available complex *in vitro* systems and their contribution to our knowledge of oral diseases.

1.5.1 The Chemostat

The chemostat is ideal for generating steady state cultures and thus has been widely used in studying human oral microbiota (Bradshaw & Marsh 1999; Greenman *et al.* 2005). It gained popularity due to the fact that it is fairly simple to use and provides great control over environmental parameters such as temperature, pH, medium source, or gas regime. This flexibility helps altering the environmental conditions thus aids answering the cause-effect questions (Marsh 1995; Bradshaw & Marsh 1999; Greenman *et al.* 2005). Though the continuous culture approach does not attempt to reproduce or act as a true model of all the physical properties in the oral cavity. The main drawbacks of this system include inability to grow biofilms reliably and control their reproducibility or thickness (as further described below).

The standard chemostat is a single stage reactor limited to bacterial growth in a planktonic form (Bradshaw & Marsh 1999; Greenman *et al.* 2005). Nonetheless, biofilms tend to form on surfaces inserted into the continuous cultures such as glass, hydroxyapatite or acrylic that provides the basis for biofilm investigation (Sissons 1997). This single stage system is characterised by the fact that once perturbed, it is effectively terminated and another chemostat experiment has to be set up. Thus, multi-stage chemostat-based systems were used to aid the downstream treatments on biofilm generated in the first reactor (Marsh 1995; Sissons 1997; Bradshaw & Marsh 1999; Greenman *et al.* 2005). The examples of using this system include Herles *et al.* (1994) who used the chemostat flow-cell system to test anti-plaque agents on oral biofilms generated on hydroxyapatite. Their study has proven that the model is capable of discriminating the bacterial differences in biofilm treated with placebo mouthwash or a mouth rinse containing 0.03% triclosan formulation. Li *et al.*, on the other hand, used this system to characterise the effects of varying pH and fluoride on bacteria or multispecies biofilms formation on hydroxyapatite discs (Li & Bowden 1994; Bradshaw & Marsh 1999). The chemostat system was also widely used in oral microbiology to grow complex oral communities (Mckee *et al.* 1985) and to study the influence of oxygen and inoculum composition (Bradshaw *et al.* 1996) and the pH change on growth of mixed oral bacterial communities (McDermid *et al.* 1986).

1.5.2 The Robbins device

The Robbins device was developed by McCoy and colleagues at the University of Calgary to investigate the biofouling phenomenon occurring in industrial pipelines (McCoy *et al.* 1981). It is a rectangular block usually composed of steel with removable studs (Figure 1.3) placed along its length through which the inoculum and medium flow (McCoy *et al.* 1981; Greenman *et al.* 2005; Coenye & Nelis 2010). The biofilm formed on these studs grows under controlled flow and shear force and can be removed at any time to be investigated by various experimental techniques (McCoy *et al.* 1981; Greenman *et al.* 2005; Coenye & Nelis 2010). This method has been used to study biofilm formation including oral biofilms and their susceptibility to various antimicrobials and antibiotics (Khardori *et al.* 1991; Larsen & Fiehn 1995; Yassien *et al.* 1995; Gristina *et al.* 1987). Further to that, Coenye *et al.* used it to test the efficacy of biofilm removal by the disinfectant NitrAdine and showed it had high activity against oral biofilms (2008).

It's main advantage is growing biofilms under controlled hydrodynamic conditions and it has been proven to be an effective system for biofilm formation investigation (Greenman *et al.* 2005). However, it is not particularly suited for rapid and high-throughput susceptibility testing of various chemicals (Ceri *et al.* 1999; Greenman *et al.* 2005; Coenye & Nelis 2010).

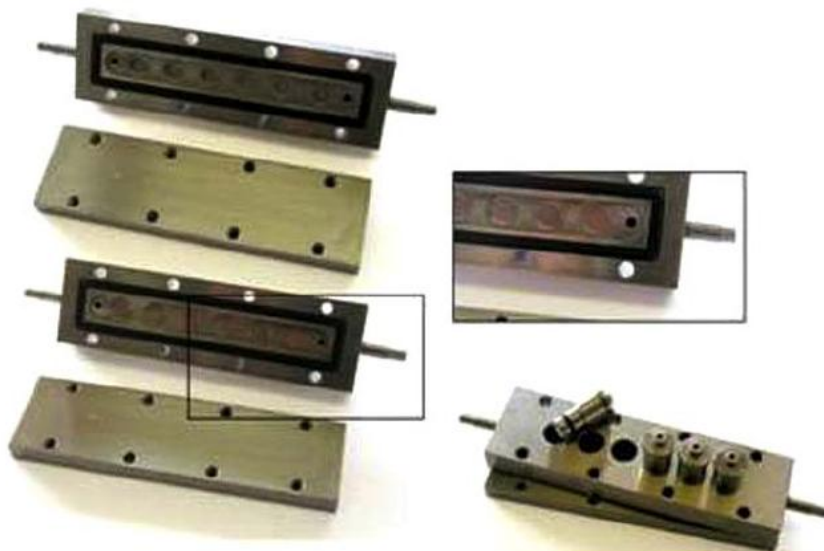


Figure 0.3 Close-up of the Modified Robbins Device (MRD) (adapted from Coenye *et al.* 2011).

1.5.3 Calgary Biofilm Device (CBD)

The Calgary Biofilm Device (CBD) was developed by Ceri *et al.* and now is commercially available at MBEC Biofilms Technology Ltd, Canada (Ceri *et al.* 1999). It consists of a two-part reaction vessel; the top one is a lid with 96 pegs mounted on the inside of its surface designed in a manner that all pegs can be removed at once or individually without opening the vessel. It sits in a standard 96-microtiter plate where each peg is lowered into its well without touching the well surface. The bottom of the microtiter plate allows the medium flow among the pegs and creates an equal and consistent shear among the pegs (Ceri *et al.* 1999; Coenye *et al.* 2011). The CBD is a simple model which is mostly used for high-throughput susceptibility screening of antibiotics (Santopolo *et al.* 2012; Almshawit *et al.* 2014), antimicrobials or metals on biofilms (Ali *et al.* 2006; Harrison *et al.* 2006; Pesciaroli *et al.* 2013). Importantly, it does not require tubing and pumps that makes it easier to use and minimises potential contamination issues. The major limitations of the CBD system are that it does not feature controlled dynamic conditions and biofilm growth is not evenly distributed on the surface of CBD peg (Mcbain 2009). Ciri *et al.* used this system to investigate the antimicrobial susceptibilities of biofilm formed by clinically important species such as *Pseudomonas aeruginosa* and *Staphylococcus aureus* (Ceri *et al.* 1999). A study by Ali *et al.* confirmed the suitability of CBD for assessing the efficacy of disinfectants and antimicrobials on biofilms (Ali *et al.* 2006).

1.5.4 Multiple Sorbarod Device

Multiple Sorbarod Device (MSD) is a fermentor system developed by McBain and colleagues at Manchester University in 2005. MSD was specifically developed to grow perfused oral biofilm of mixed oral microbiota on filters under environmental conditions mimicking the oral cavity. The model enables the control over several key factors such as substrata, oxygen and/or nutrient availability (Mcbain *et al.* 2005; McBain 2009).

The fermentor system consists of two stainless steel plates (top and bottom) and a removable PTFE cylinder placed in between with 5 Sorbarod filters. The Sorbarod

filters are cellulose cylinders which are 10 mm in diameter and 20 mm in length. The inoculation process occurs by removing the top plate of the model and depositing the inoculum directly on the equilibration chamber. The medium is delivered to the model via the medium inlet by a peristaltic pump over the course of the experiment. The equilibration chambers placed above and below the filter cassettes allow medium and perfusate (spent culture fluid) mixing over time. This approach produces relatively large amounts of biomass over time to enable investigation of perfusates by different techniques and monitoring of the population dynamics (Mcbain *et al.* 2005; Mcbain 2009).

This system was mostly used to test various anti-plaque agents. Ledder *et al.* used the MSD and the Constant Depth Film Fermentor (CDFF) model to investigate the anti-plaque properties of various commercially available enzymes such as protease, lipase and amylase (Ledder *et al.* 2009). Another study by Ledder and McBain used the MSD model to compare the antimicrobial efficacy of a triclosan-containing dentifrice with a stannous fluoride and zinc lactate combination. Whilst both formulations reduced plaque accumulation and bacterial viability, the triclosan dentifrice showed higher reductions on biofilm (Ledder & McBain 2012).

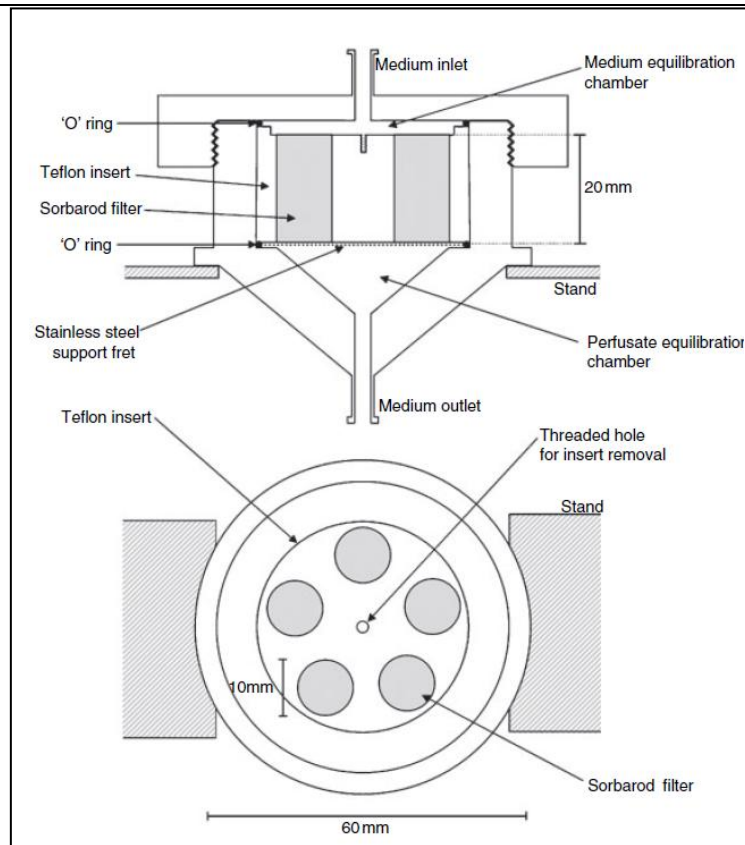


Figure 0.4 Schematic diagram of the multiple Sorbarod Device (adapted from McBain *et al.* 2005).

1.5.5 CDC Biofilm reactor

The CDC Biofilm reactor was developed by Donlan *et al.* in 2002 and is available commercially at BioSurface Technologies, Bozeman, Montana, USA (Donlan *et al.* 2002; Coenye & Nelis 2010). This system consists of a glass vessel with an effluent spout positioned to provide approximately 350 mL operational fluid capacity. The top plate made of polyethylene houses 8 removable polypropylene rods, each with a medium inlet and a gas exchange port and holding three removable coupons on which biofilm grows. Each coupon is a disc of 1.27 cm width and 0.3 cm thickness. All that is enclosed in a glass vessel which is placed on a stir plate to provide constant mixing and shear forces to the biofilm on the coupon surface. In this design the medium and inoculum are provided by the peristaltic pump via the tubing connections. This enables biofilms to be grown on 24 removable coupons simultaneously under moderate to high shear force conditions in a continuous-flow mode. This system allows operation under a wide range of experimental conditions to address various research questions (Donlan *et al.* 2002; Coenye & Nelis 2010).

The studies performed by Goeres *et al.* (2005) and Honraet *et al.* (2005), for example, demonstrated that the CDC reactor can be a reliable tool for the investigation of biofilm formation by various bacterial species. This model was also used for testing of various disinfectants (Buckingham-Meyer *et al.* 2007) and assessment of cleaning procedures (Hadi *et al.* 2010). A study by Parra-Ruiz *et al.* assessed the *in vitro* activities of several antimicrobials alone or in combination against two *S. aureus* isolates (Parra-Ruiz *et al.* 2010). In another study by Lewis *et al.* assessed the antimicrobial activity of the nanocrystalline diamond coating intended to be used on medical implants (Lewis *et al.* 2010).

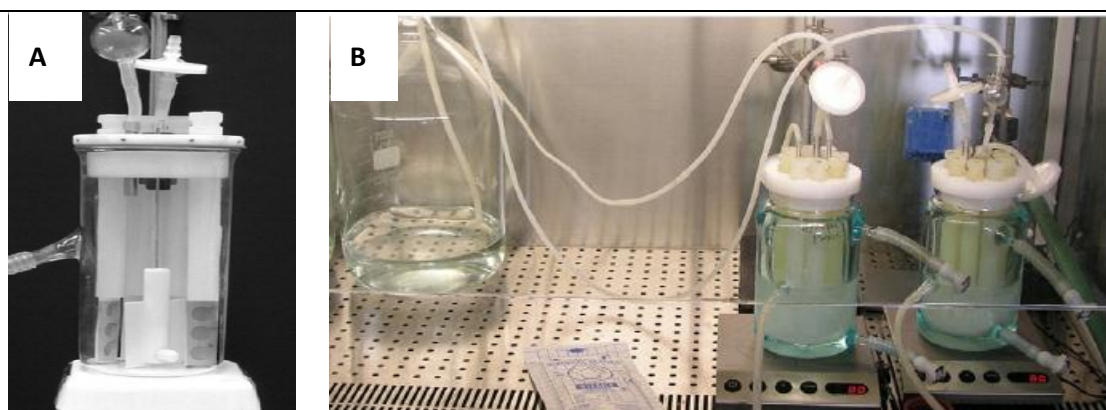


Figure 0.5 The CDC reactor (A) (adapted from Lewis *et al.* 2010) and its experimental set-up (B), where two CDC reactors are coupled with a medium bottle (adapted from Coenye & Nelis 2010).

1.5.6 Constant Depth Film Fermentor (CDFS)

The Constant Depth Film Fermentor was introduced in 1987 by Peters and Wimpenny (Peters & Wimpenny 1987). It is a complex *in vitro* model which provides a closely controlled environment with control over key experimental parameters such as nutrient source, temperature, pH, substrate and the gaseous regime used (Peters & Wimpenny 1987). It has been widely used to study dental plaque formation, the efficacy of antimicrobials and was later established as a representative model for *in vitro* modelling of oral biofilms (Wilson *et al.* 1996; Pratten *et al.* 2003; Leung *et al.* 2005; Dalwai *et al.* 2006; Dalwai 2008).



Figure 0.6 CDFS system (adapted from Wilson 1999).

The CDFS model consists of glass vessel with a stainless steel top and bottom plate. The top plate has the inoculum, medium, gas inlet and a sampling port. Inside, a rotating stainless steel table holds five polytetrafluoroethylene (PTFE) plugs that are recessed to grow biofilms of specific depth and scraper blades that scrap off the excess of media and biofilm produced (Wilson 1999). The system construction enables it to be sterilized and housed in the incubator to obtain better temperature control.

Biofilms are produced in recessed pans, to which inoculum and medium is provided by inputs on the top plate. Both, medium and inoculum drip onto the rotating table where the liquid excess is scrapped off by scraper blades and removed from the model by the waste output. Biofilms that forms on the plugs can be harvested at any point during the experiment via the sampling port (Wimpenny 1987; Dibdin & Wimpenny 1999; Peters & Wilson 1999).

This system essentially allows the development of surface attached biofilms with a predetermined depth by mechanically removing surplus biofilm, simulating the movement of the tongue over the teeth (Peters & Wimpenny 1987; Wilson 1999; Dibdin & Wimpenny 1999). It has been extensively used in the field of oral research. Its applications range from investigating single-, multispecies- biofilm formation, testing various antimicrobials to modelling oral diseases as detailed below. The CDFP has also been successfully used to study the effect of surface properties such as roughness on biofilm formation (Morgan & Wilson 2001) and the effect of different antimicrobial agents, which are either externally added (Pratten, Barnett, & Wilson, 1998; Wilson, Patel, & Noar, 1998) or released internally from the composite tested (Leung *et al.* 2005). Additionally, it has been used to study the formation and the bacterial composition of oral biofilms (Pratten *et al.* 2003) and the effects of sucrose on biofilm formation (Pratten *et al.*, 2000). McBain *et al* (2003) and Hope and Wilson (2004) used the CDFP model to test the efficacy and impact of chlorhexidine digluconate mouthwash on oral microcosm biofilms while Spratt and co-workers at UCL successfully modelled both health and gingivitis associated shifts occurring in gingivitis progression using this system (Dalwai *et al.*, 2007; Dalwai *et al.*, 2008)

1.6 Aims of the project

There is a wide selection of complex and simple *in vitro* models which have been used to answer the scientific questions relating to the biofilm formation or the understanding of bacterial interactions within a biofilm. These models have significantly contributed to the field of oral microbiology and increased our understanding of biofilm formation. However, there is no *in vitro* gingivitis model available that could serve as a direct gingivitis surrogate. One of not many complex models that were successfully used for modelling simple bacterial changes associated with gingivitis progression includes the CDFF model. Therefore, the design of a new triple CDFF model was based on CDFF model.

The research focused on the development of an *in vitro* gingivitis model (triple-CDFF) which could mimic oral health and gingivitis conditions in a reliable and reproducible manner to allow growth of gingivitis associated biofilms. Subsequently, this would allow standardised testing of various dentifrices and antimicrobials as either preventatives or treatments of gingivitis in a cost-effective and relatively high-throughput manner. Therefore, the aim was to construct a model that facilitates the concurrent and reproducible biofilm growth and that was complex enough to enable delivery of various nutrients and gas regimes to simulate the complex environment found in oral cavity. Additionally and at the same time it should be relatively simple to operate by an individual using a standardised operating procedure (SOP) which can be easily followed with the same degree of repeatability at different research institutes.

To fulfil the aims of the project, the research was divided into 3 stages:

- (i) Development, testing and validation of the novel triple CDFF model (Chapter 3).
- (ii) Reproducibility testing of oral biofilms grown in T-CDFF model (Chapter 4).
- (iii) Modelling of the oral health-gingivitis progression *in vitro*. (Chapter 4, Chapter 5 and Chapter 6)

2 CHAPTER

Materials and Methods

2.1 Triple-Constant Depth Film Fermentor model (T-CDFF)

The CDFF model has been extensively used in oral research and is a well-established model (Pratten *et al.* 1998; Wilson 1999; Dalwai *et al.* 2006; Dalwai *et al.* 2007). However, it does not allow concurrent and reproducible antimicrobials testing (Dalwai *et al.* 2006). Therefore, the T-CDFF model has been manufactured to answer these needs and to enable the growth of reproducible oral biofilms that can be treated separately in a controlled but flexible environment that would be of use for dentifrices and antimicrobials testing.

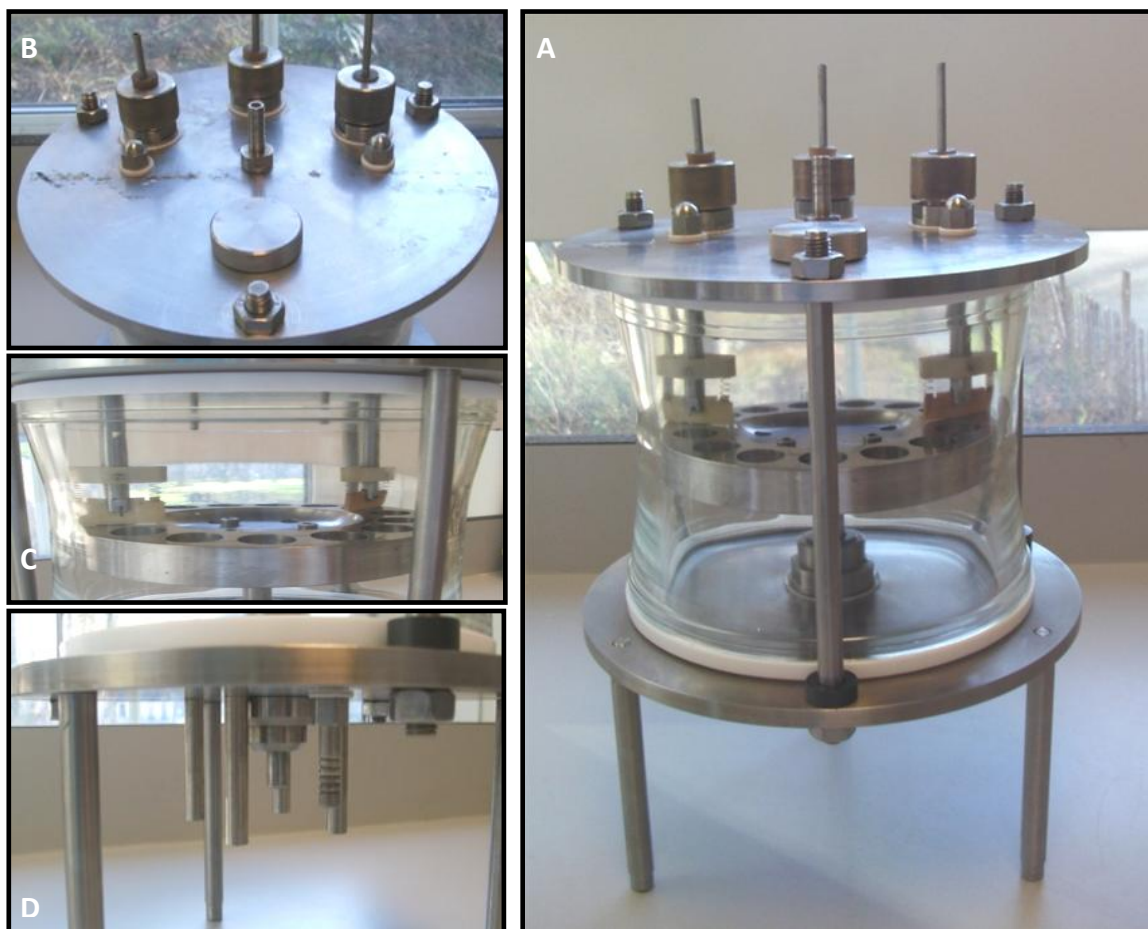


Figure 2.1 A) The standard CDFF - the prototype of T-CDFF, B) Top plate with 3 liquid inlets, gas inlet and sampling port. C) Turntable with 15 gaps for pans. D) Bottom plate with a waste output and a spindle to attach the gear box to.

2.2 Model description

The T-CDFF is a mechanical model that was constructed to simulate gingivitis *in vitro*. It consists of three stainless steel units driven by a single portable motor at a constant speed (Figure 2.1A and 2.2A). Each unit was manufactured in the same manner and consists of a stainless steel base, a glass vessel, and a top plate retained by two polytetrafluoroethylene (PTFE) seals. Each unit's top plate has a sampling port, 3 liquid inlets for inoculum, artificial saliva, artificial gingival crevicular fluid (GCF) and a gaseous inlet enabling us to provide different gas formulations. Each unit houses a turntable with 5 PTFE pans. Each pan houses five PTFE plugs with hydroxyapatite (HA) discs on top (5.0 mm in diameter), each recessed to the depth of 300 μm which replicates the gum pocket size. Two scraper blades are there to smear the inocula and nutrient medium evenly over the discs and remove excess liquids or bacterial waste. Both models are presented in Figure 2.2 for the comparative purposes (Peters & Wimpenny 1987; Wilson 1999).

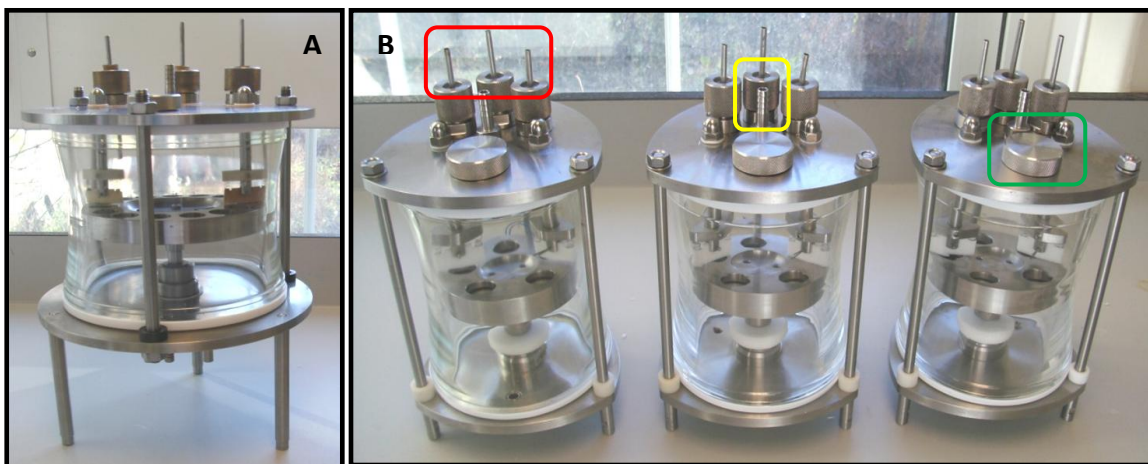


Figure 2.2 The comparison of the two models. A) CDFF model, B) T-CDFF units on the right. Three liquid inlets encircled in red. Gas inlet encircled in yellow and Sampling port encircled in green.

2.2.1 T-CDFF construction

Each T-CDFF unit was constructed in a relatively similar manner to its prototype, the CDFF (Peters & Wimpenny 1987; Wilson 1999). It consists of similar mechanical parts that were either upgraded or adjusted by the manufacturer to answer my experimental needs. Additionally, each T-CDFF unit was scaled down to enable the

running of three separate CDFFs on a single, portable motor in a simultaneous and reproducible manner. Figure 2.3 presents the T-CDFF model sitting on a motor, while Table 2.1 depicts the dimensions of the main mechanical parts of both CDFF and T-CDFF model.



Figure 2.3 shows the T-CDFF model housed on the motor.

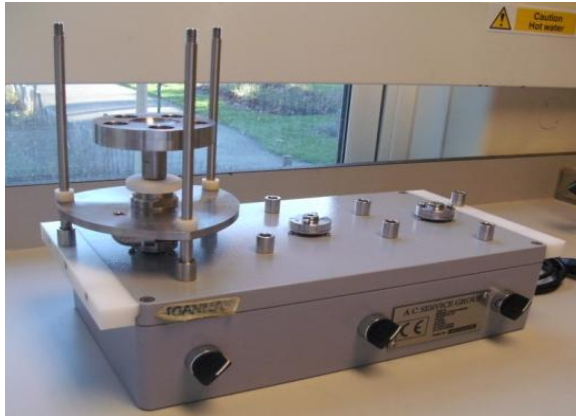
Table 2.1 presents the specification for CDFF and T-CDFF model.

| Parts' diameters | CDFF diameters (mm) | T-CDFF diameter (mm) |
|---|----------------------------|-----------------------------|
| Top & bottom PTFE seal | Ext. 187, Int. 166 | Ext. 135, Int. 115 |
| Glass vessel diameter | Ext. 184.5, Int. 159 | Ext. 133, Int. 105 |
| Glass vessel height | 148 | 149 |
| Glass vessel height with seals | 157 | 158 |
| Top & Bottom plate | 230 | 152 |
| Sampling port width | 26 | 26 |
| Inlet ports width | 3 | 3 |
| Gas port width | 5 | 5 |
| Waste output width | 4.5 | 4.5 |
| Table width | 149 | 94 |
| Pan width | 19 | 19 |
| Screw cap height | 19 | 22.5 |
| Screw cap width | 36 | 63 |
| Turntable-sampling port distance | 81 | 82 |

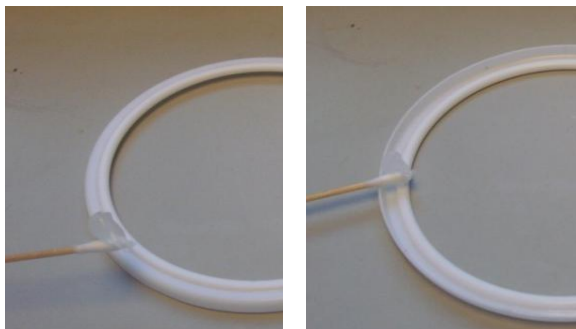
Table 2.1 The specification of CDFF and T-CDFF model.

2.2.2 T-CDFF set-up

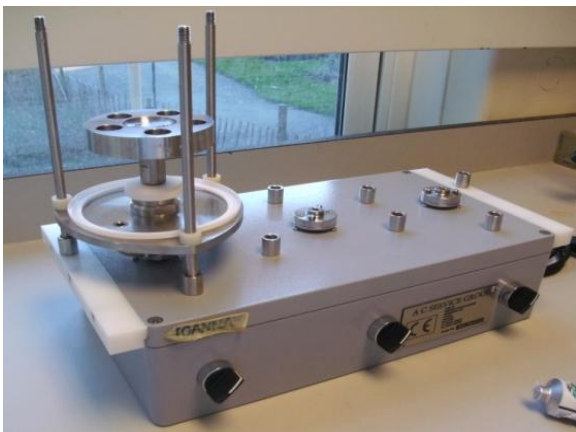
This Section details the experimental set-up of T-CDFF experiments (Figure 2.4).



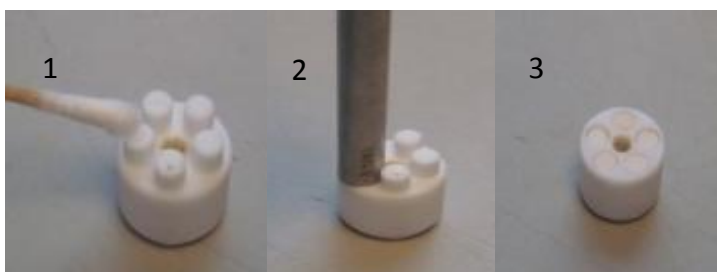
Base of a single unit was placed on the motor.



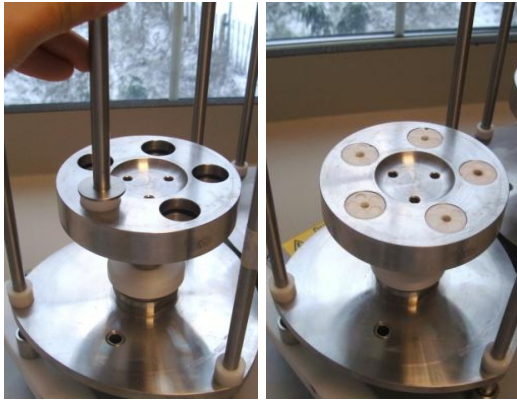
Bottom seal was greased with high vacuum grease on both sides to provide adequate air tightness.



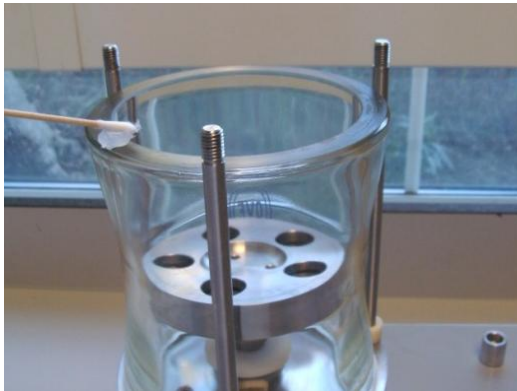
Greased bottom seal was placed firmly on the base of the unit.



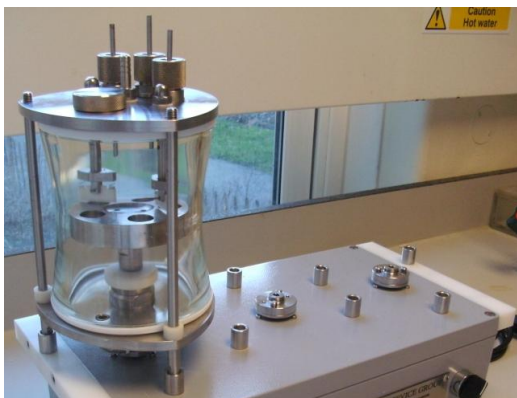
PTFE pans were prepared: **1)** Each pan was fitted with PTFE plugs. Plugs were greased and HA discs were attached to the surface. **2)** Discs were recessed to a depth of 300 μm using a repressing tool. **3)** Pan was ready to be fitted in T-CDFF.



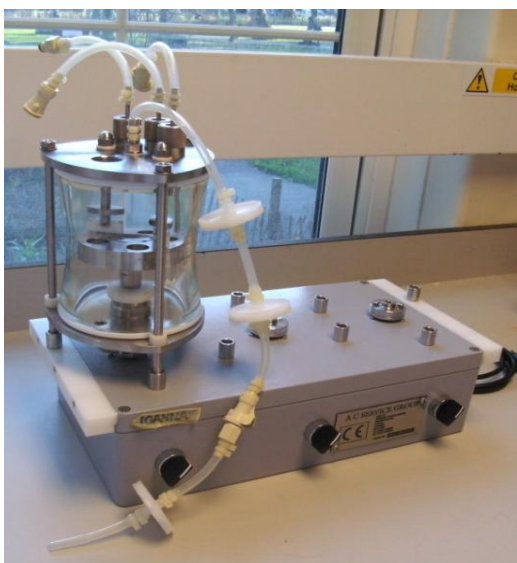
Pans were placed in turntable and recessed by tamping tool.



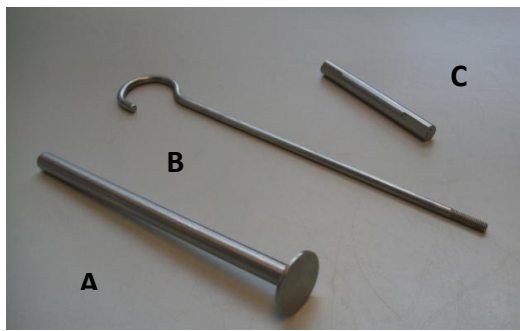
Glass vessel was placed on the top and brim was greased.



Greased seal was placed on the top of the vessel. It was followed by top plate that was screwed in to hold the whole construction firmly in place.



Silicone tubing was attached to all inlets and clamped by autoclaveable cable ties. Then, female and male connectors were attached to finish the tubing connections. Tubing with 0.3 μm hepta-venta filters were attached to gas outlet to provide gaseous exchange.



The same connections were done for the remaining two units. Units were placed on the motor and were ready for the experiment.

Additional tools used with T-CDFD

A) tamping tool

B) sampling tool

C) recessing tool

Figure 2.4 Figures A – I present the CDFD set-up. Figure J presents the tools used with the CDFD set-up and sampling process.

2.2.3 T-CDFD calibration process

The T-CDFD model was designed in a way to provide the highest possible experimental reproducibility among the units. Further to this, several factors that could potentially introduce variability were identified and addressed:

- Reproducible inoculum, artificial saliva and artificial GCF delivery,
- Reproducible delivery of gaseous conditions,

To limit the potential bias, same inoculum was used among separate experiments (Section 2.3.1). To ensure that the same volume of inoculum was delivered to each unit, the same batch of inoculum was used and delivered at a constant flow rate via calibrated peristaltic pumps and tubing connections.

The same formulation of artificial saliva was used throughout all CDFF experiments. To minimise the differences and to enable the same growth pattern among the units, medium was delivered to all units from the same 8 litre saliva batch via calibrated pumps and tubing connections at the same flow rate.

To assure the highest possible reproducibility of environmental conditions, the same gas formulation was delivered to each unit. Gas was supplied to all units from the same gas cylinder via split tubing connections with the flow meters attached to ensure the same gas levels among the units.

2.2.4 T-CDFF scheme of work

The T-CDFF model was designed specifically to grow reproducible oral gingivitis biofilms. Each of the T-CDFF experiments comprised of several stages listed below:

Stage I – preparation process

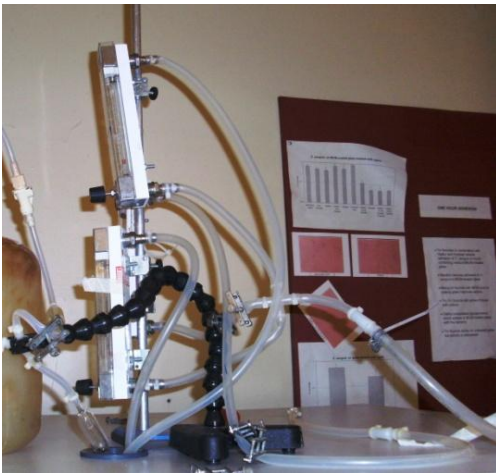
This stage included the preparation of inoculation / artificial saliva / artificial GCF / gaseous and waste output tubing connections. To enable delivery of the above mentioned components, each tubing connection was assembled from 8x11 mm silicone tubing (VWR), 1x3 mm tubing (Fisher), 1.5 mm tubing (Fisher) and 0.8 mm bore pump tubing (Fisher, Watson & Marlow) joined by PTFE connectors (VWR) and then secured by cable ties (VWR) and finished off with the male or female connector (Sigma) (Figure 2.4-2.6). Prepared connections were calibrated with water to ensure that the expected amount of liquid was being delivered to each unit and that there was an absence of leakages within the tubing connections. Next, the tubing connection ends were wrapped up in aluminium foil and secured using autoclave tape for sterilisation prior to commencing the experiment. Due to the extended length and sophistication of all tubing connections, they had to be evenly spread in the autoclave chamber to ensure no pressure built-up during the process and successful sterilisation.



Inoculation flask with the attached inoculum tubing connection.



Two artificial saliva bottles with the tubing connection leading to the T-CDFF units via the opening in the top of incubator.



Gas tubing connection set-up leading from gas cylinder to each unit through the flow meters which regulate the flow rate.



The waste connection with the attached effluent collection bijou bottle. The waste connections lead from the units to a waste collection bottle.

Figure 2.5 presents the experimental set-up of the T-CDFF model

Stage II – experiment launch / inoculation process

All of the sterilised parts were moved to an incubator that was previously sprayed with 70% ethanol. All the connections and parts were aseptically connected in the confined space of the incubator by the operator complying with a set of rules during the experiment launch that included: wearing a mask, protective clean gown and gloves, using 70% ethanol spray and alcohol wipes while setting up the connections. When the set-up was finished, the experiment was started by inoculation to establish a bacterial baseline on the recessed HA discs. The inoculum was delivered via the calibrated tubing connections and was evenly spread over the pans in each unit by smearing it over the surface of the turntable by the two spreaders. After 8 hours of inoculation, the flask was disconnected aseptically and nutrient medium was delivered instead. The experimental set-up is presented in Figure 2.6.

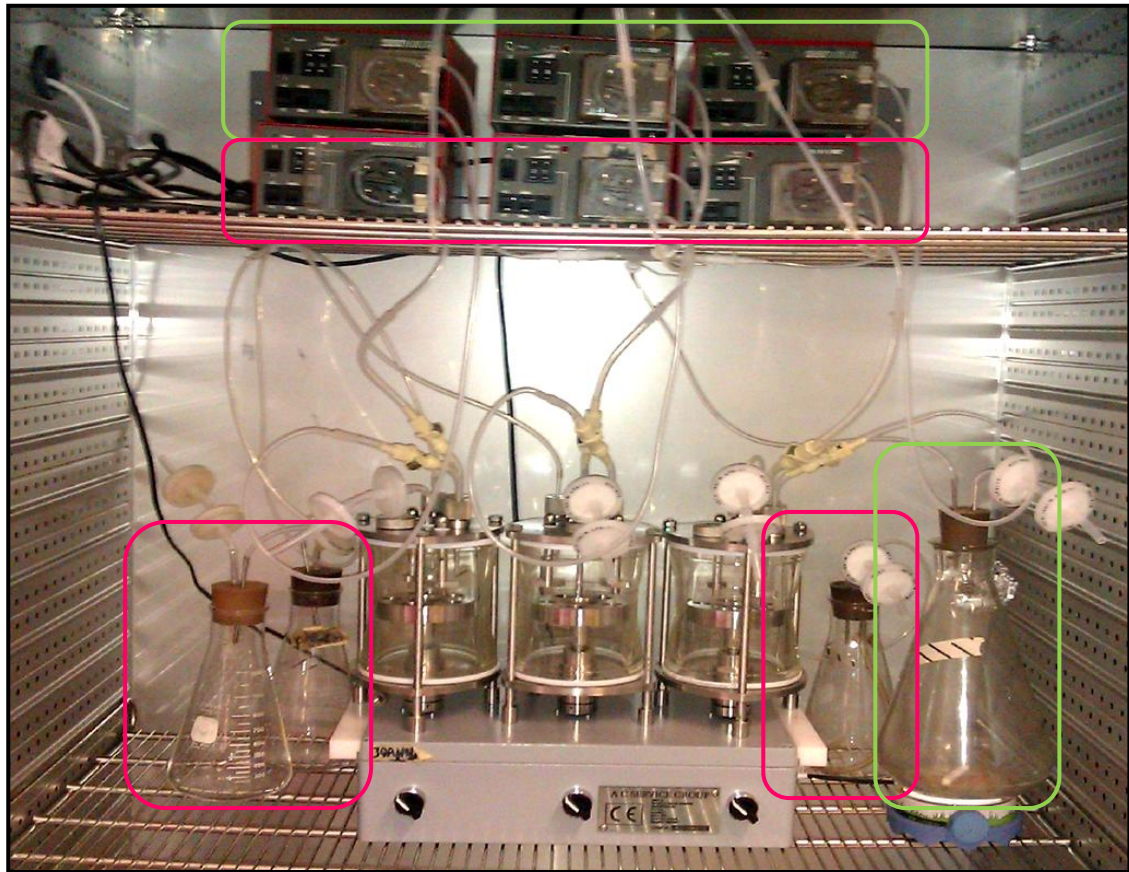


Figure 2.6 presents a simplified T-CDFD set-up. Inoculation flask and pumps for inoculum delivery are encircled in green; the same pumps were re-used for artificial saliva delivery. GCF flasks and pumps are encircled in pink.

Stage III – experimental conditions

At this stage, depending on the exact purpose of the experiment, different experimental conditions can be applied. The generalized T-CDFD experimental conditions are shown in Figure 2.7.

Commonly, the experimental conditions started with the health phase that was followed by the switch to gingivitis (Dalwai *et al.* 2006; Dalwai *et al.* 2007). An artificial saliva formulation is used as a medium source to provide an adequate amount of nutrients to sustain bacterial growth throughout the experiment, either in health or disease. To establish the switch from health to gingivitis conditions, additional components such as artificial GCF were delivered at variable concentrations together with altered gas conditions (Dalwai *et al.* 2006; Dalwai *et al.* 2007).

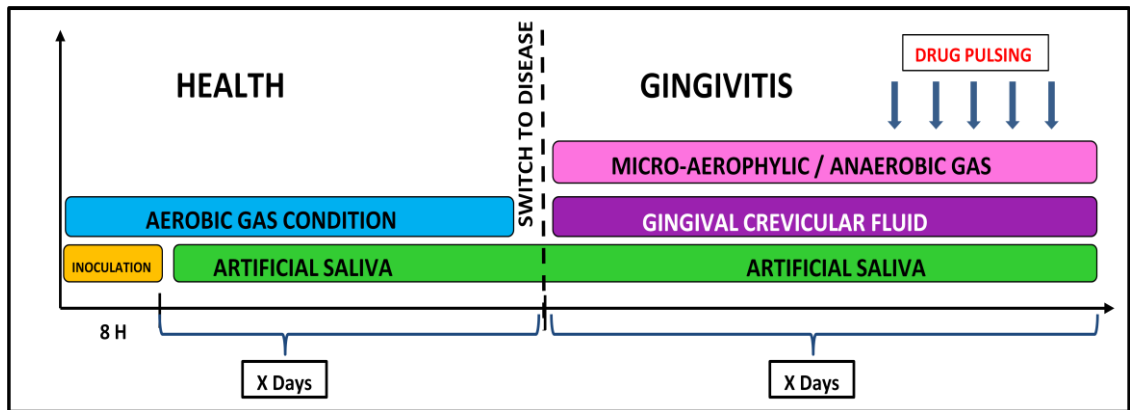


Figure 2.7 Generalised T-CDFF experimental conditions.

Stage IV – experiment complete, sterilisation and clean-up process

At the time point specified in the methodology the experiment was ended and all the tubing connections and flasks were disconnected from T-CDFF and sterilised before cleaning. The T-CDFF was disassembled, removed from the motor and sterilised. After the kill cycle, tubing connections were cleaned by flushing them with a 0.1% acid rinse (Decon Laboratories Limited), followed by water to remove the remaining product residuals. Connections were re-used for the next experiment. After sterilising the model, it was dismantled and washed with 0.1% acid rinse (Decon Laboratories Limited).

2.3 Experimental protocol

2.3.1 Standardized inoculum

2.3.1.1 Dual-species inoculum

Actinomyces naeslundii DSMZ17233 and *Streptococcus sanguinis* NCTC12279 were grown aerobically overnight in brain heart infusion broth (BHI, Oxoid) to a final concentration of approximately 1×10^8 CFU / mL in an orbital shaking incubator (Orbital incubator, Sanyo) at 200 rpm at 37°C. Aliquots of 2.0 mL from each culture was added to 1500 mL of artificial saliva and pumped into the T-CDFF at a continuous rate of 1.0 mL / min for 8 hours using a peristaltic pump (Watson & Marlow, 101 U / R) (Dalwai *et al.* 2006; Dalwai 2008).

2.3.1.2 *Microcosm inoculum*

A microcosm inoculum was obtained by collecting 1.0 mL of whole non-stimulated saliva from each of 21 healthy local research staff volunteers (Ethics ID number: 1364/001). Samples were pooled, mixed well with equal volume of 40% v / v glycerol to obtain a homogenous solution. Thereafter, the solution was split into 1.0 mL aliquots and stored at -80°C. The saliva preparation was performed promptly to limit the cytotoxic effect of oxygen on the anaerobic species. For inoculation, two 1.0 mL aliquots were thawed and used to inoculate 1500 mL of artificial saliva that was pumped through the T-CDFE model at constant a rate of 1.0 mL / min for 8 hours (Dalwai *et al.* 2007; Dalwai 2008).

2.3.2 Artificial saliva

To simulate human saliva, a previously validated standardized artificial saliva formulation was used (Russel and Coulter 1975). One litre of artificial saliva consisted of 1.0 g Lab Lemco (Oxoid), 5.0 g Proteose Peptone (Oxoid), 2.0 g Yeast Extract (Oxoid), 0.35 g NaCl (Oxoid), 0.2 g CaCl₂ (VWR), 0.2 g KCl (VWR), 2.5 g Mucin type III (Sigma), 1.3 mL of 40% w / v Urea (Fisher chemicals). For all CDFE experiments the artificial saliva was pumped at a flow rate of 0.5 mL / min (Pratten *et al.* 1998; Dalwai *et al.* 2006; Dalwai *et al.* 2007; Dalwai 2008).

2.3.3 Conditions to model oral health

To model oral health, dual-species or microcosm biofilms were grown at the temperature of 37 ± 1°C under aerobic conditions, which were maintained by delivering air through sterile 0.3 µm hepta-venta filters. The nutritional source was an artificial saliva delivered continuously to the system at the documented human salivary flow rate of 0.72 L / day (Dalwai 2008; Dalwai *et al.* 2006; Dalwai *et al.* 2007).

2.3.4 Conditions to model gingivitis

Gingivitis conditions were established by providing an artificial GCF, of which 1.0 litre medium consisted of 0.6 L RPMI (Sigma), 0.4 L Horse serum (Sigma), 50 µL Menadione (Sigma), 1.0 mL Heamin (Sigma), to each unit at the flow rate of 50 µL / min or 130 µL /

min for a fixed period of time and altering the gas conditions from aerobic to micro-aerophilic [composition: 2% O₂, 3% CO₂, 95% N, at 200 bar] or anaerobic gas conditions [composition: 5% CO₂, 95% N, at 200 bar]. Micro-aerophilic or anaerobic gas conditions were provided to each unit at the same time and at a constant flow rate of 200 cm³ / min (Goodson 2000). Additionally, artificial saliva was delivered to the system at the flow rate of 0.72 L / day (Wilson 1999; Dalwai *et al.* 2006; Dalwai *et al.* 2007; Dalwai 2008).

2.3.5 T-CDFD sampling and sample processing

2.3.5.1 Biofilm sampling

The sampling process started with a decontamination procedure which included spraying the incubator's interior and then the top plate and sampling port of each unit with 70% ethanol and removing any excess ethanol by wiping the surfaces with 70% ethanol wipes.

Next, the rotating table was switched off to align the appropriate PTFE pan with the sampling port (Wilson 1999). Each sampling port was then opened aseptically by the operator wearing a protective mask, gown and gloves wiped with 70% ethanol. The pan with 5 HA discs was removed from the system by screwing the sterilised sampling tool against the pan and pulling it out from the table. The sampling port was then closed promptly (Wilson 1999). The remaining two units were sampled straight afterwards using the same methodology.

Each pan removed from the T-CDFD system was placed in a separate 50 mL screw cap tube (Fisher); discs were removed from each pan and placed in 2.0 mL cryo-vials with 1.0 mL of phosphate buffered saline (PBS) and 5 glass beads each. Each cryo-vial was vortexed for 1.0 min to disperse the biofilm from the surface of the disc (Wilson 1999). After obtaining a homogenous suspension, bacterial solutions were transferred to a fresh sterile 1.5 mL screw cap tubes (Fisher). Each suspension was designated for different sample analysis techniques such as culturing, quantitative polymerase chain

reaction (qPCR), 16S rRNA gene sequencing, enzymatic assays or ^1H nuclear magnetic resonance (NMR) spectroscopy as described in Sections 2-5.

To ensure a contamination free experiment, the bacterial suspensions retrieved during the biofilm sampling were serially diluted and incubated anaerobically on fastidious anaerobe agar for 3-5 days at 37°C. The experiment was pronounced as contaminated when the community richness on a plate was (i) much lower than 5 morphologically different species and (ii) the contaminant was observed on the agar plates and (iii) also overgrowing the turntable and tubing connections in the model.

2.3.5.2 Effluent sampling

Effluent samples were collected at different time points throughout the T-CDFF. Each effluent sampling event started with clamping the waste output to collect enough waste to sample 5.0 mL of effluent from each unit. Next, the waste connection was unclamped and the effluent was collected in a Bijou bottle attached to the waste tubing. The bijou bottle was then aseptically disconnected and closed to prevent contamination. A new, sterile bijou bottle was aseptically attached to the waste tubing straight after the removal of the previous one. Effluent was collected from each unit at the same time.

The collected effluents were analysed by qPCR, 16S rRNA gene sequencing, ^1H NMR spectroscopy and by culturing. First, 1.0 mL was transferred to a new 1.5 mL Eppendorf and spun down for 10 min at 20,800 x g in a pre-cooled centrifuge to 4°C (Centrifuge 5417R Eppendorf). The supernatant was removed and the pellet was stored at -20°C for qPCR and sequencing analysis (Section 2.5-2.6). In addition, 100 μL of the effluent sample, which had not been centrifuged, was serially diluted and plated on fastidious anaerobe agar (FAA) for total counts of anaerobes (Section 2.4). The remaining \approx 4.0 mL of the effluent was frozen at -20°C and analysed by ^1H NMR spectroscopy (Section 2.7.2).

To ensure a contamination free experiment, the bacterial suspensions retrieved during the effluent sampling were serially diluted and incubated anaerobically on fastidious

anaerobe agar for 3-5 days at 37°C. The experiment was pronounced as contaminated when the community richness on a plate was (i) much lower than 5 morphologically different species and (ii) the contaminant was observed on the agar plates and (iii) also overgrowing the turntable and tubing connections in the model.

2.4 Culture methods

Throughout the T-CDFF experiments, one disc from each unit was aseptically removed and placed in a 1.5 mL crew cap tube (Fisher) containing 1.0 mL of PBS. The discs were vortexed for 1 min to obtain a homogenous suspension. Each equally resuspended biofilm was serially diluted and plated onto fastidious anaerobe agar supplemented with 5% sterile horse blood (Lab M Limited), columbia blood agar supplemented with 5% sterile horse blood (Lab M Limited), cadmium fluoride acriflavine tellurite agar supplemented with 5% blood sterile horse (Oxoid) in duplicate (Table 2.2).

| Medium | Non – selective |
|---|---|
| CBA (columbia blood agar) with 5 % blood | Targeting aerobes. Plates were incubated at 37°C in a 5% CO ₂ incubator (Triple Red Laboratory) for 3-5 days. |
| FAA (fastidious anaerobe agar) with 5 % blood | Targeting anaerobes. Plates were incubated at 37°C in an anaerobic cabinet (MACS-MG-1000-Anaerobic workstation) for 5-7 days. |

| Medium | Selective |
|--|--|
| M-S (mitis-salivarius) agar | M-S is a selective media for <i>Streptococcus</i> spp. Plates were incubated at 37°C in 5% CO ₂ incubator (Triple Red Laboratory) for 3-5 days. |
| CFAT (cadmium, fluoride, acriflavine, tellurite) agar (Zylber and Jordan 1982) | CFAT is a selective media for <i>Actinomyces</i> spp. Plates were incubated at 37°C in 5% CO ₂ incubator (Triple Red Laboratory) for 3-5 days. |

Table 2.2 Selective and non-selective media used for T-CDFF experiments.

2.5 Culture independent molecular methods

2.5.1 DNA extraction - bead beating protocol

Bacterial suspensions obtained from T-CDFF experiments were pelleted by centrifugation at 20,800 x g for 10 min in a pre-cooled centrifuge to 4°C (Centrifuge 5417R Eppendorf). Supernatants were discarded, while bacterial pellets were gently re-suspended in 0.5 mL of cetyltrimethylammonium (CTAB). The suspensions were transferred to 2.0 mL screw cap tubes containing 200 µL of 0.1 mm silica / zirconia beads (Stratech Scientific Ltd.). A 0.5 mL aliquot of Phenol : Chloroform : Isoamyl alcohol (P : C : I – 25 : 24 : 1) was added to the tube and lids were tightened. The cells were disrupted in a Ribolyser Bead-Beater (Hybaid) for 30 seconds at the speed of 5.5 m / s to break the cells. Then, the solutions were centrifuged at 20,800 x g for 20 min in a pre-cooled centrifuge (Centrifuge 5417R Eppendorf) to 4°C. Top aqueous layers were extracted and transferred to the new 1.5 mL Eppendorf. Next, 0.5 mL of Chloroform : Isoamyl alcohol (C : I – 24 : 1) was added to the tubes, and mixed well for a few seconds by vortexing. Subsequently, the solutions were centrifuged at 20,800 x g for 10 min in a pre-cooled centrifuge pre-cooled to 4°C (Centrifuge 5417R Eppendorf). Top aqueous layers were extracted and placed in new tubes. Then, two volumes of polyethylene glycol 6,000 (PEG) (Sigma) were added to precipitate nucleic acids. The solutions were mixed well by vortexing and refrigerated overnight at 4°C to precipitate. After precipitation, the solutions were centrifuged at 20,800 x g for 20 min in a pre-cooled centrifuge (Centrifuge 5417R Eppendorf). The supernatant was removed and the pellet was washed twice with 200 µL of ice cold 70% ethanol to remove impurities. The samples were left on the bench at room temperature to dry. After that, the pellets were re-suspended in 100 µL of Tris - EDTA Buffer with 10 µL / mL RNase. This protocol has previously been proven to be a successful DNA extraction method for communities of mixed Gram-positive and Gram-negative oral bacterial species (Griffiths *et al.* 2000; Ciric *et al.* 2010).

2.5.2 Triplex quantitative Polymerase Chain Reaction (qPCR)

The qPCR Taqman triplexes used for T-CDFE sample analysis were developed by Dr Lena Ciric (Ciric *et al.* 2010). Their design was based on the original sequences reported by Lane for the 16S rRNA gene (Lane 1991). Each primer and probe set was initially optimised to ascertain optimal oligonucleotide concentrations as shown in Table 2.3 (Ciric *et al.* 2010). Then, they were combined into three triplexes and were found to perform at high efficiency when the Mg²⁺ concentration was set to 6 mM. The three triplex reactions were run as FLV (*Fusobacterium nucleatum*, *Lactobacillus casei*, *Veilonella dispar*), NAP (*Neisseria subflava*, *Actinomyces naeslundii*, *Prevotella intermedia*), and SSU (*Streptococcus sanguinis*, *Streptococcus mutans*, Universal) (Ciric *et al.* 2010).

| Organism | | Sequence | | Conc (nM) |
|----------|----------------------|----------|---|-----------|
| FLV | <i>F. nucleatum</i> | F primer | F 5-ACAAATCCGAACTAAGAATAGTTTTTC-3 | 900 |
| | | R primer | R 5-GTCATCATGCCCTTATACG-3 | 900 |
| | | Probe | P 5-6FAM-TCC[+A]CCT[+C][+A][+C]GG[+C]TTT-BHQ1-3 | 50 |
| | <i>L. casei</i> | F primer | F 5-AGAGTTTGATCCTGGCTCAG-3 | 50 |
| | | R primer | R 5-ACTCGTTCCATGTTGAATCTC-3 | 900 |
| | | Probe | P 5-HEX-CGA[+T]CA[+T]CA[+A]CG[+A]G[+A]A[+C]TCG-BHQ1-3 | 50 |
| | <i>V. dispar</i> | F primer | F 5-CTACAATGGGAGTTAATAGACGGAAG-3 | 300 |
| | | R primer | R 5-CAGCCTACGATCCGAACTGAG-3 | 50 |
| | | Probe | P 5-Cy5-AGC[+A]AA[+C]CCGA[+G]AAA[+C][+A]CT-BHQ2-3 | 50 |
| NAP | <i>N. subflava</i> | F primer | F 5-AACGTATTCACCGCAGTATG-3 | 900 |
| | | R primer | R 5-TGGAGCCAATCTCACAAAAC-3 | 300 |
| | | Probe | P 5-HEX-TGAC[+C][+T][+G]CG[+A]TT[+A]CTAGCG-BHQ1-3 | 100 |
| | <i>A. naeslundii</i> | F primer | F 5-GAGCACGCCGCTCTGTA-3 | 900 |
| | | R primer | R 5-ACCTTGCCGCCTCCGAA-3 | 900 |
| | | Probe | P 5-6FAM-CCTCGTCGCCACGGTGGGTCA-BHQ1-3 | 300 |
| | <i>P. intermedia</i> | F primer | F 5-GCCTAATACCGATGTTGTC-3 | 300 |
| | | R primer | R 5-CGCACCAACAAGCTAATCAG-3 | 900 |
| | | Probe | P 5-Cy5-CA[+T][+C]CCC[+A]TCC[+T]CC[+A]CC-BHQ2-3 | 300 |
| SSU | <i>S. sanguinis</i> | F primer | F 5-GTGCATCAATCCCAGAAAAG-3 | 900 |
| | | R primer | R 5-ATTATTGGCTGATGTGGAGTC-3 | 900 |
| | | Probe | P 5-HEX-AGA[+T]GA[+C]CA[+C]CA[+C]CGT-BHQ1-3 | 50 |
| | <i>S. mutans</i> | F primer | F 5-TCACCAGAAAAGACAAAAGTTAC-3 | 900 |
| | | R primer | R 5-AACTACTAACCAAGCCCAAC-3 | 300 |
| | | Probe | P5-Cy5-TA[+G]CC[+G]C[+A]GC[+A]A[+T]CA[+A]TG-BHQ2-3 | 300 |
| | Universal | F primer | F 5-TCCTACGGGAGGCAGCAGT-3 | 900 |
| | | R primer | R 5-GGACTACCAGGGTATCTAATCCTGTT-3 | 300 |
| | | Probe | P 5-6FAM-CGTATTACCGCGGCTGCTGGCAC-BHQ1-3 | 100 |

Table 2.3 FLV, NAP and SSU triplexes consisted of: *F. nucleatum*, *L. casei* and *V. dispar* (FLV); *N. subflava*, *A. naeslundii* and *P. intermedia* (NAP); and *S. sanguinis*, *S. mutans* and Universal (SSU). Bases shown in brackets are locked nucleic acid bases.

All triplex reactions were run in triplicate in a final volume of 25 μ L. SensiMix™ Probe Kit (Bioline) qPCR Master Mix was used and in a Rotor-gene 6500 (QIAGEN) cycler using the green, yellow and red channels for data collection. Each reaction contained the concentrations of the oligonucleotides shown in Table 2.3 and 6 mM Mg²⁺. The reaction conditions were performed with an annealing / extension temperature ranging from 60°C to 64°C as shown in Table 2.4. Data collection took place during the annealing / extension step. Species specific primers and dual-labelled fluorogenic probes shown in Table 2.3 were designed for all organisms using 16S rRNA gene

sequences, with the exception of the *Streptococcus* spp. where the *sodA* gene was used, and *A. naeslundii* where the *ureC* gene was used. Each triplex reaction was shown in one of 3 different fluorescent channels, red, green and yellow. The green channel showed *F. nucleatum*, *A. naeslundii*, Universal. The yellow channel shows *L. casei*, *S. sanguinis*, *N. subflava*. The red channel showed *V. dispar*, *P. intermedia*, *S. mutans*. Data were collected from each channel and quantified using DNA standards (Ciric *et al.* 2010).

| Step | Conditions |
|----------------------------------|---|
| Initialization step: hot – start | 95°C for 10 min |
| Denaturation | 40 cycles: 95°C for 15 s |
| Annealing / Extension step | 40 cycles: x°C for 60 s (60°C for FLV & SSU, 64°C for NAP) |

Table 2.4 Cycling conditions for triplex qPCR.

2.5.2.1 Quantitative Polymerase Chain Reaction (qPCR) standards

In order to produce standard curves for the quantification of eight bacterial species (*F. nucleatum* NCTC 10562, *L. casei* ATCC 334, *V. dispar* NCTC 11831, *N. subflava* DSM 17610, *A. naeslundii* DSM 17233, *P. intermedia* DSM 20706, *S. sanguinis* NCTC 02863 and *S. mutans* ATCC 700610), DNA extractions were performed on organisms previously enumerated using viable counts, making it possible to relate the number of cells to the DNA concentration. A mixture of the above strains' DNA was used as standard DNA in the universal assay. Standard curves consisting of at least four 10-fold dilutions of reference DNA were run in triplex assays. The detection limits for all 8 bacterial strains and the total bacteria were set based on qPCR standards.

2.5.3 Duplex quantitative Polymerase Chain Reaction (qPCR)

The qPCR taqman duplex for detection of *S. sanguinis* and *A. naeslundii* was based on qPCR taqman triplexes developed by Dr Lena Ciric (Ciric *et al.* 2010). The same primers and probes for *A. naeslundii* and *S. sanguinis* used in triplexes were used and each reaction contained the oligonucleotides concentrations shown in Table 2.3 and 6 mM Mg²⁺. Duplex reactions were run in triplicate in a final volume of 15 µL. SensiMix Probe

(Bioline) qPCR mastermix was used in a Rotor-gene 6500 (QIAGEN) cycler using the green and yellow channels for data collection. The reaction conditions were as mentioned in Table 2.5. The green channel showed *A. naeslundii* while the yellow channel showed *S. sanguinis*. Data were collected from each channel and quantified using DNA standards.

| Step | Conditions |
|----------------------------------|----------------------------|
| Initialization step: hot - start | 95°C for 10 min |
| Denaturation | 40 cycles of 95°C for 15 s |
| Annealing / Extension step | 40 cycles of 62°C for 60 s |

Table 2.5 Cycling conditions for duplex qPCR.

2.5.3.1 Quantitative Polymerase Chain Reaction (qPCR) standards

Duplex qPCR standards were performed according to the same methodology as in Section 2.5.2. In order to produce standard curves for the enumeration of *S. sanguinis* and *A. naeslundii*, DNA extractions were performed on organisms that had been enumerated by viable counts making it possible to relate numbers of cells to the amount of DNA. Standard curves consisting of at least four 10-fold dilutions of DNA were run in triplicates. The detection limits for *S. sanguinis* and *A. naeslundii* were set based on the qPCR standards.

2.6 16S rRNA genomics

The 16S rRNA genomic sequencing was performed using dual-index sequencing chemistry on a MiSeq platform with illumina-adapter primers containing Index 1 (i7) and Index 2 (i5). The combination of 12 unique Index 1 sequences with 8 unique sequences of Index 2 allowed cost-effective multiplexing of 96 samples (12x8). The dual-index PCR amplicon library was created by the amplification of the variable region (V5-7) of 16S ribosomal RNA gene present in each community sample. The primers were designed by Dr Tony Brooks (UCL, Institute of Child Health) using the original Kraneveld *et al.* (2012) design where the 454 adapters were replaced with Illumina i5 and i7 adapter. The PCR amplification was carried out in a total volume of 25 μ L using 2 μ L of DNA template, 0.025 μ M MolTaq, 0.4 μ M 785F and 1175R Primers (Sigma), 200 μ M dNTPs (Bioline), 1X Molzym PCR Buffer (VH BIO, Germany) and Moltaq Water. PCR

conditions started with 95°C for 5 min, and then were followed by 25 cycles of 30 sec at 94°C, 60 sec at 40°C, 60 sec at 72°C with the final extension stage at 72°C for 10 min. The presence of the 504 base-pair amplicon was confirmed by electrophoresis on 1% agarose gel and then purified using AMPure XP (Agencourt BioSciences Corporation). Samples were normalised to 10 nM DNA using a Qubit dsDNA BR Assay Kit (Invitrogen) and a Qubit Fluorometer (Invitrogen). Normalized samples were pooled together and supplemented with 5% PhiX to diversify the library. The pooled library was analysed using Bioanalyser (Agilent) to confirm the absence of primer dimers and to confirm the correct amplicon size. Paired-end sequencing (2x251 bp) on the dual-index library was performed by Dr Tony Brooks and Dr Anna Tymon (UCL, Institute of Child Health and UCL Eastman Dental Institute, respectively) using MiSeq Reagent Kit v2 and Illumina MiSeq sequencer. The MiSeq Reporter v2.3 was used to de-multiplex the raw data with its in-built programs to analyse each sample down to the species level. This post-run analysis started with de-multiplexing filtered indexed reads. Data retrieved from the pooled library was based on a mixture of short indices that each respective sample was consigned to. Rarefaction files and summary files of the percentage hits were generated by MiSeq reporter to enable further data analysis. (FASTQ files were generated including the information of each sample's reads and quality scores.) The ClassifyReads algorithm developed by Illumina used the FASTQ files together with a Greengenes Database as a reference to classify each sample at the taxonomic level.

2.7 Metabolomics

2.7.1 Enzymatic assays

2.7.1.1 Acid and alkaline phosphatase assays

Acid and alkaline phosphatase assays were conducted based on modification of the method of Bessey, Lowry and Brock (Bessey *et al.* 1946).

Both Acid and alkaline phosphatase assays started with incubating 0.5 mL of bacterial culture with 0.5 mL of 0.5% w / v; *p*-nitrophenyl disodium orthophosphate (*p*NPP) substrate and 2.0 mL of 0.1 M MES (2-(N-morpholino) ethane sulphonic acid) buffer

adjusted to pH 5.5 for acid phosphatase or 2.0 mL of 0.1 M Bicine (N, N-bis-[2-hydroxyethyl]-glycine) buffer adjusted to pH 9.0 for alkaline phosphatase. The mixture was vigorously mixed and incubated for 120 min at $37 \pm 1^\circ\text{C}$. After 1.0 min incubation, 1.0 mL of the solution was removed and mixed with 2.0 mL of 0.2 M NaOH to stop the reaction. Liberated *p*-nitrophenol (*p*NP) was measured at the wavelength of 405 nm and used as a blank. At particular time intervals (20, 40, 80, 120 min), 1.0 mL of bacterial solution was taken and placed in a test tube with 2.0 mL of 0.2 M NaOH. The measurements were taken at the above mentioned wavelength and recorded as an increase of absorbance per unit of time. The temperature in the laboratory was controlled at $21 \pm 1^\circ\text{C}$.

2.7.1.2 Trypsin – like – protease assay

The Trypsin-like-protease assay was performed based on modified method of Yoshimura *et al.* (Yoshimura *et al.* 1984).

A 100 μL aliquot of bacterial suspension was mixed with 3.6 mL of 0.1 M MOPS buffer adjusted to pH 7.5, 1.0 mL of 0.2 mM $\text{N}\alpha$ -Benzoyl-L-arginine-4-nitroanilide hydrochloride (BAPNA) and 100 μL of 10 mM L-cysteine HCl. The mixture was mixed rapidly and incubated at $37 \pm 1^\circ\text{C}$. The activity was monitored at a wavelength of 410 nm at certain time intervals (2, 7, 11, 20 and 40 min) after blanking the spectrophotometer with the same sterile solution. Measurements were recorded and the increase in absorbance was calculated per unit of time. The temperature in the laboratory was controlled at $21 \pm 1^\circ\text{C}$.

2.7.2 ^1H Nuclear Magnetic Resonance Spectroscopy (NMR)

2.7.2.1 Sample preparation and processing

Bacterial solutions, either from HA discs or effluent samples, were thawed from deep freeze (-20°C) and allowed to defrost. Defrosted samples were transferred to 15 mL screw cap tubes marked with unique identification numbers. All samples were prepared simultaneously to minimise batch-to-batch variability (the temperature in the laboratory was controlled at $21 \pm 1^\circ\text{C}$). The 15 mL screw caps were centrifuged for

30 min at 6654 x g in a pre-cooled centrifuge to 5°C (Centrifuge 5417R Eppendorf). After centrifugation, the supernatant was decanted into appropriately labelled glass screw cap bijoux bottles. The pellets were discarded. A volume of 80 µL of an NMR pyridazine reference standard was pipetted into an Eppendorf tube together with 880 µL of the decanted saliva of each sample. The solutions were mixed and transferred via long glass Pasteur pipette to 5 mm NMR tubes. The freshly prepared samples were placed on a NMR carousel and then in a NMR chamber for analysis (Bruker). The post-experimental analysis was performed by Dr Michael Cannon and included principal component analysis (PCA) and orthogonal partial least square analysis (OPLS).

3 CHAPTER

Development and validation of a Triple-Constant Depth Film Fermentor (T-CDFF)

3.1 Introduction

The existence of multi-species biofilms known as "dental plaque" is the fundamental reason behind the aetiology of oral diseases such as caries, gingivitis or periodontitis. Hence, the understanding of biofilm formation, complexity and its effective eradication is pivotal to the maintenance of oral health and to the prevention of oral diseases. Due to the structural complexity of dental plaque and its formation being dependent on many different factors ranging from the host immune-response to daily diet, it is important to develop a model simulating the oral environment, including its physicochemical and metabolic interactions (Wilson 1999; Guggenheim *et al.* 2001). Several *in vivo* primate and rodent models have been effectively employed, however, for ethical reasons and due to the high purchase and maintenance costs of these models they are much less advantageous than *in vitro* models which offer greater control of environmental factors and allow high-throughput screening (Wilson 1999; Nett *et al.* 2010). Many different *in vitro* models have been proposed for oral disease modelling to date, ranging from simple flow cells, chemostats to more sophisticated models such as Constant Depth Film Fermentor (CDFF) (Guggenheim *et al.* 2001). The CDFF was developed over two decades ago and is currently established as a representative model for modelling diverse microbial populations (Peters & Wimpenny 1987; Pratten *et al.* 1998; McBain *et al.* 2003). Its main advantage is the ability to test many different environmental factors which can affect biofilm growth under controlled and aseptic conditions. All of the above mentioned models contributed to the understanding of biofilm adhesion, formation and kinetics, however, none of the models allowed (i) reproducible and simultaneous testing of oral biofilms under different experimental conditions and (ii) longitudinal screening of multiple products at once and (iii) the dose response measurements at the same time (Pratten *et al.* 1998; Guggenheim *et al.* 2004).

To circumvent the above mentioned problems, a new Triple-Constant Depth Film Fermentor (T-CDFF) has been developed in this project. The T-CDFF's construction is based on the CDFF which underwent a few mechanical alterations (as described in this chapter) to allow for reproducible and simultaneous growth of oral biofilms under different experimental conditions. The study presented in this chapter demonstrates the

development and validation process of this new *in vitro* model with the evaluation of its potential for reproducible disease modelling and antimicrobials testing.

3.2 Materials and Methods

3.2.1 Methodology overview

The experimental set-up of all the CDFF experiments presented in this chapter was performed according to Chapter 2, Section 2.2.2-2.2.4. The methodologies applied throughout the validation process are presented below.

3.2.1.1 Methodology 1

The T-CDFF model was inoculated (Chapter 2, Section 2.2.1) with the dual-species inoculum (Chapter 2, Section 2.3.1.1) and maintained under health conditions for 11 days in the warm-room at 37°C (Chapter 2, Section 2.3.3). The nutrients source for growing *S. sanguinis* and *A. naeslundii* was the artificial saliva provided at the flow rate of 0.5 mL / min (Chapter 2, Section 2.3.2).

3.2.1.2 Methodology 2

The T-CDFF model was inoculated with a microcosm community (Chapter 2, Section 2.3.1.2) and run under health conditions for 11 days in the warm-room at 37°C (Chapter 2, Section 2.3.3) The artificial saliva was used as a nutrient source delivered at the flow rate of 0.5 mL / min (Chapter 2, Section 2.3.2).

3.2.1.3 Methodology 3

Both CDFF and T-CDFF were run simultaneously in separate incubators using the same experimental conditions. The models were inoculated with a microcosm community (Chapter 2, Section 2.3.1.2) and run for 11 days under health conditions (Chapter 2, Section 2.3.3) with artificial saliva as a nutrients source delivered at the flow rate of 0.5 mL / min (Chapter 2, Section 2.3.2).

3.2.1.4 Methodology 4

The last set of experiments was performed using a T-CDFF model inoculated with a microcosm community (Chapter 2, Section 2.3.1.2) and run under health conditions for 12 days in an incubator that fitted the model and its' flasks with tubing connections. The artificial saliva was delivered at a flow rate of 0.5 mL / min (Chapter 2, Section 2.3.2).

Additional mechanical improvements were introduced such as new and tighter top / bottom seal, waste output seal, screw cap seals, and non-domed nuts.

3.2.2 CDFF sampling and data processing

Sampling points for the experiments using methodology 1, 2 and 3 were performed at day 1, 3, 6, 9, and day 11, while samples for experiments using methodology 4 were collected at day 2, 3, 8, 10, and day 12. Biofilm sampling and processing was performed according to the methodology described in Chapter 2, Section 2.3.5. DNA was extracted from biofilms using a bead beating protocol (Chapter 2, Section 2.5.1). The experiments using methodology 1 were analysed by the duplex qPCR with primers for *S. sanguinis* and *A. naeslundii* (Chapter 2, Section 2.5.3), while experiments using methodology 2, 3 and 4 were analysed by triplex qPCR with primer sets for *S. sanguinis*, *S. mutans*, *V. dispar*, *N. subflava*, *L. casei*, *F. nucleatum*, *A. naeslundii*, *P. intermedia* and universal (Chapter 2, Section 2.5.2). To confirm that the experiment was not contaminated, the biofilm community was verified by culturing the bacterial suspensions obtained from each sampling point on fastidious anaerobe agar (explained in Chapter 2, Section 2.3.5).

3.2.3 Statistical analysis

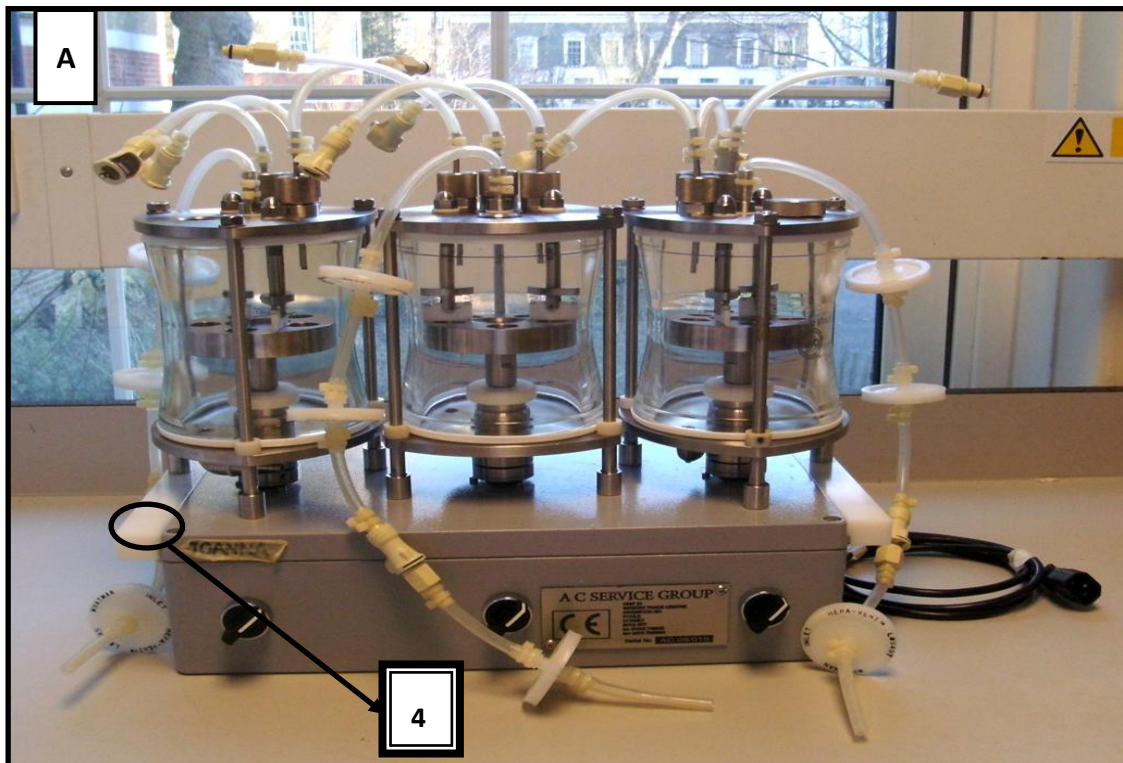
The data are presented as the mean \pm standard deviation. To investigate the growth patterns and the model's repeatability, the qPCR data were subjected to \log_{10} transformation and normal distribution was checked by plotting the histograms. Then the qPCR data were paired according to the bacterial strain and unit, and analysed by Student's t-test with p-value set as 0.05 (IBM SPSS Statistics 22.0).

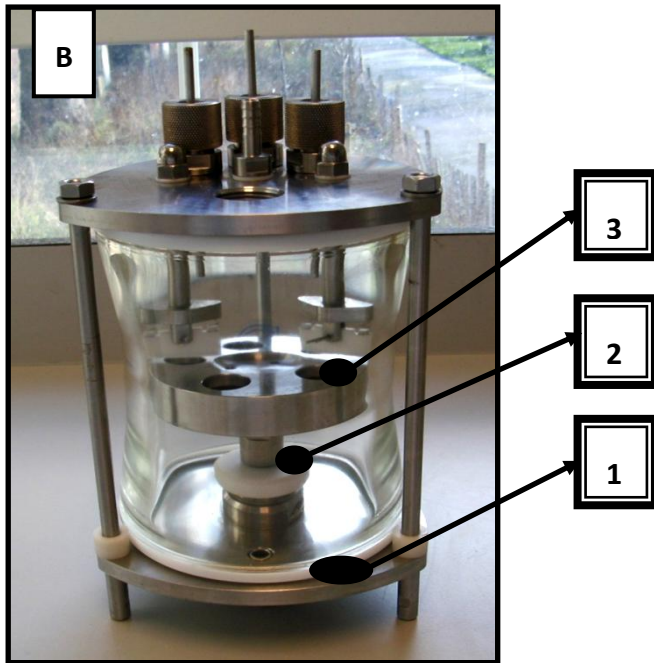
3.3 T-CDFD results

This Section presents the outcomes of the T-CDFD model validation process.

3.3.1 Model development

The T-CDFD model was scaled down in comparison to the CDFD (Chapter 2, Section 2.2) and a few mechanical changes were applied to ease portability and to allow simultaneous biofilm growth as well as testing of dentifrices and antimicrobials. All the adjustments are illustrated in Figure 3.1 and then further described in Table 3.1.





Scaled down units were run simultaneously on a portable motor at a constant speed. All parts such as the stainless steel base, the top plate, the glass vessel, the top and bottom seals were smaller in diameter (see specification in Chapter 2, Table 2.1). The main differences between the models are depicted in the picture on the left and listed in Table 3.1.

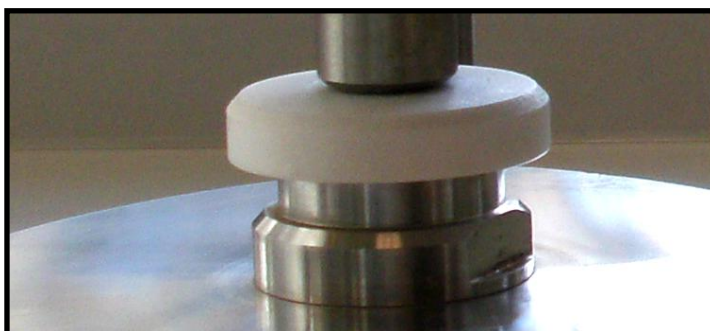
Figure 3.1 The T-CDFF model with the major modifications. A) T-CDFF model with 3 units housed on a single motor housing, B) The enlargement of a single unit with the mechanical modifications highlighted and explained below.

1

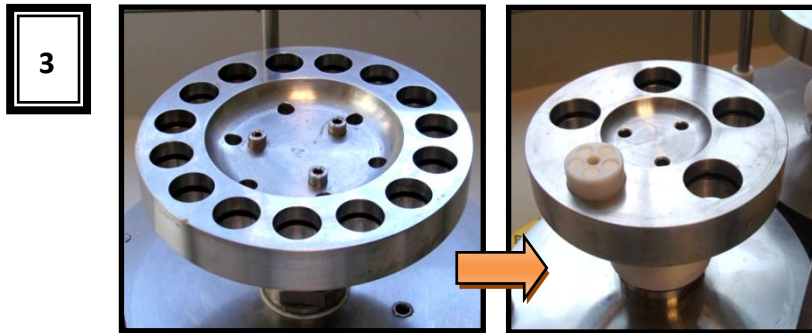


The 'L shape' waste output was implemented instead of 'T shape' to ease tubing attachment and manoeuvring; additional white PTFE seal was added to improve the air-tightness of the joint.

2



A white PTFE cover was placed on the gearbox to prevent gear box damage and extend its bearing life.



The turntable diameter was reduced so that 3 units could be housed on a motor and run in an incubator. Turntable had 5 sampling pans instead of 15.



A single, portable motor with white handles on both sides that ease portability. Three units are driven by the single portable motor housing at the same and non-adjustable speed.

Table 3.1 presents the description of the mechanical modifications applied to the T-CDF model.

The need for the mechanical improvements was either identified by AC Service Ltd or by myself. The implemented changes improved the T-CDF model construction and increased its portability. To verify whether the newly constructed model was working in a reliable manner, we went through the validation process described in the Section below.

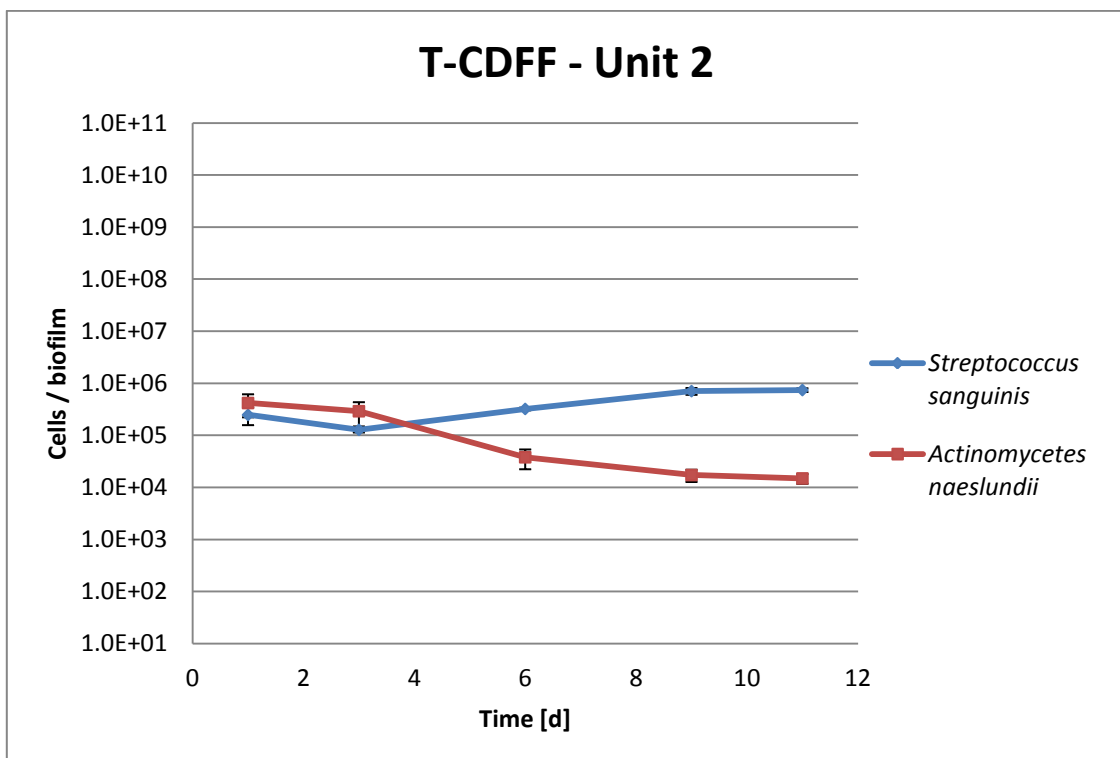
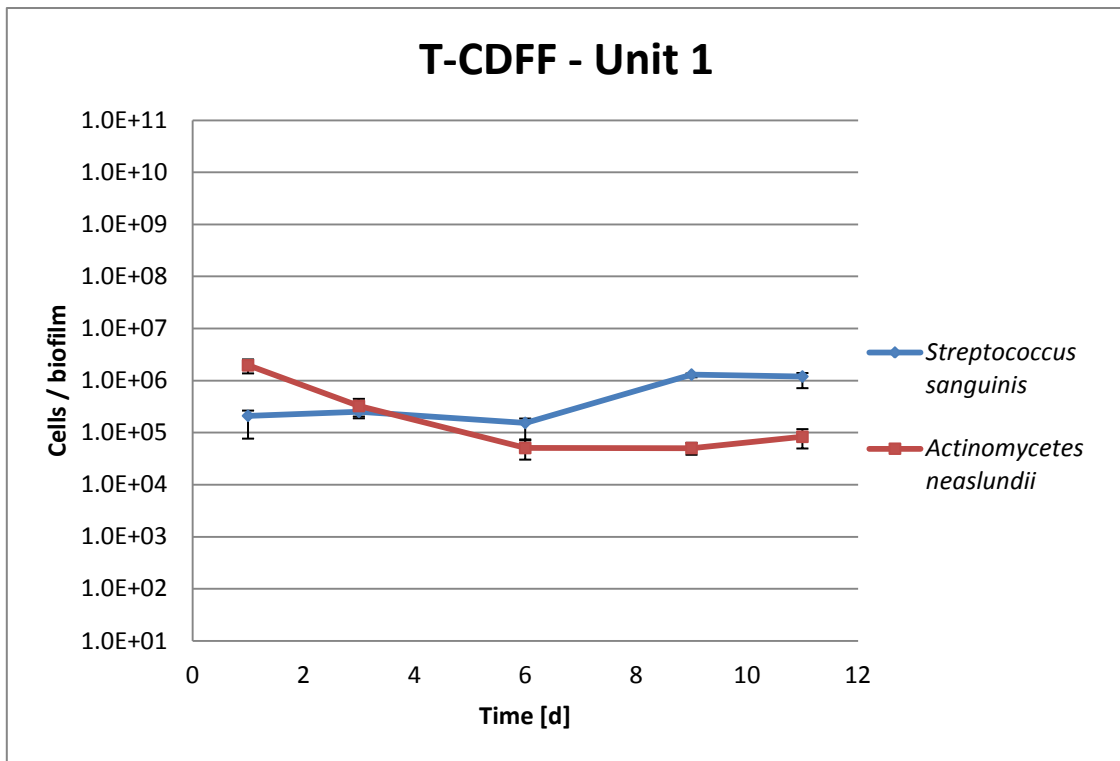
3.4 Model validation

This Section provides information on the validation process of the T-CDF model and broadly fits into four separate development episodes.

3.4.1 Methodology 1

Three unsuccessful T-CDF experiments were conducted using this methodology. All of them were contaminated at the early stage of the experiment by a single species contaminant that outgrew the dual-species community. Regarding the contamination issues, experiments were interrupted and no reliable data generated. The fourth

experiment was partially contaminated, with only unit 3 being affected at the end of the experiment, day 11. Results from this run are presented in Figure 3.2.



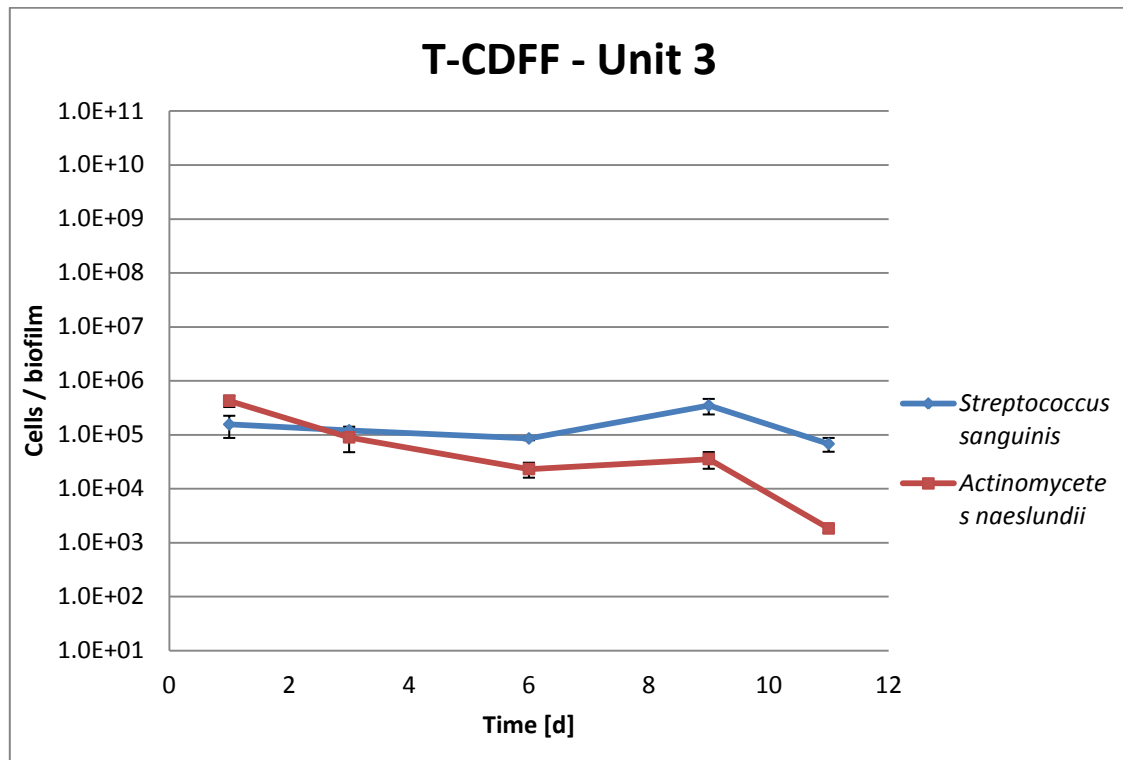


Figure 3.2 The total number of *S. sanguinis* (blue line) and *A. naeslundii* (red line) detected by duplex qPCR primers in each unit of the T-CDFF model. Error bars represent the standard error calculated on $n = 6$. * $n=6$ refers to two biological and three technical replicates

Figure 3.2 presents the total number of *S. sanguinis* and *A. naeslundii* in each unit of the T-CDFF over 11 days of health conditions. Regarding *S. sanguinis*, unit 1, 2 and 3 started with the cell number of 2.10×10^5 , 2.48×10^5 , and 1.55×10^5 cells / biofilm after 24 hours of incubation, respectively. Unit 1 and Unit 2 had a similar growth trend with a significant 0.76 and 0.48 logs increase over time ($p < 0.05$) reaching the number of 1.2×10^6 and 7.43×10^5 cells / biofilm at day 11, respectively. On the contrary, unit 3 did not follow the same growth trend and there was a significant 0.36 log drop of *S. sanguinis* on day 11 ($p = 0.034$).

The numbers of *A. naeslundii* in each of the unit (unit 1-3) after 24 hour incubation reached 1.96×10^6 , 4.19×10^5 and 4.26×10^5 cells / biofilm, respectively and decreased over time. Unit 1 and Unit 2 recorded the same descending pattern with significant bacterial reduction of 1.37 and 1.45 log ($p < 0.05$), respectively. In comparison to unit 1 and 2, unit 3 showed higher reduction of 2.37 log reaching 1.83×10^3 cells / biofilm ($p = 0.003$).

3.4.2 Methodology 2

The experiment conducted using this methodology was contaminated at an early phase of the run. The experiment was stopped and no reliable data were generated.

3.4.3 Methodology 3

The CDFF and a single T-CDFF unit were run simultaneously in separate incubators using the same experimental conditions to investigate the potential experimental differences between the models. Both models were run successfully without contamination and provided a reliable data set presented below. The only difference observed between the models was that bacterial waste clogged the T-CDFF's gearbox and leaked through it damaging the motor. Additionally, a leakage from the waste output occurred via a distorted seal. The above mentioned mechanical problems did not impair the experiment and reliable results were obtained from both models (Table 3.2 and Table 3.3). The problems mentioned above were addressed in Methodology 4. Table 3.2 presents the total number of bacteria over 11 days of health conditions together with the health related bacteria: *S. sanguinis*, *V. dispar* and *N. subflava*.

| MODEL | Time [d] | Total bacteria cells / biofilm | <i>S. sanguinis</i> cells / biofilm | <i>V. dispar</i> cells / biofilm | <i>N. subflava</i> cells / biofilm |
|-------|----------|-----------------------------------|--|-------------------------------------|---------------------------------------|
| CDFF | 1 | 1.3E+07 (5.7E+06) | 1.4E+04 (5.3E+03) | 5.6E+03 (5.7E+02) | 2.1E+02 (1.5E+01) |
| UNIT | 1 | 2.1E+07 (3.9E+06) | 4.9E+03 (1.1E+03) | 7.7E+03 (4.7E+01) | 2.6E+02 (2.2E+01) |
| CDFF | 3 | 7.5E+09 (9.8E+08) | 1.0E+07 (1.7E+06) | 2.9E+08 (5.9E+05) | 6.2E+06 (1.3E+06) |
| UNIT | 3 | 6.5E+09 (2.2E+08) | 1.6E+07 (5.6E+05) | 1.4E+06 (3.8E+03) | 2.7E+07 (1.4E+06) |
| CDFF | 6 | 1.0E+10 (1.1E+09) | 4.5E+07 (1.4E+07) | 3.5E+08 (1.4E+08) | 2.5E+07 (3.7E+06) |
| UNIT | 6 | 1.1E+10 (7.5E+08) | 2.8E+07 (1.5E+06) | 4.9E+08 (2.0E+08) | 1.7E+07 (3.8E+05) |
| CDFF | 9 | 1.0E+10 (3.2E+08) | 3.3E+07 (6.7E+06) | 4.3E+08 (1.7E+08) | 1.1E+07 (1.4E+06) |
| UNIT | 9 | 1.1E+10 (2.1E+09) | 2.2E+07 (1.0E+06) | 4.8E+08 (2.0E+08) | 1.1E+07 (1.6E+06) |
| CDFF | 11 | 5.6E+09 (1.5E+08) | 1.3E+07 (6.4E+05) | 7.1E+08 (5.8E+06) | 7.2E+06 (1.1E+06) |
| UNIT | 11 | 7.3E+09 (5.9E+08) | 2.3E+07 (2.1E+06) | 1.5E+08 (1.3E+06) | 1.6E+07 (4.0E+05) |

S. mutans was not detected

Table 3.2 shows the numbers for the total bacteria and the health associated bacteria detected by triplex qPCR primers in both CDFF and the T-CDFF's unit. The numbers are expressed as cells / biofilm with a standard error presented in brackets (n=6). n=6 refers to two biological and three technical replicates

Table 3.3 presents the numbers of gingivitis associated bacteria i.e. *F. nucleatum*, *A. naeslundii* and *P. intermedia* over the period of 11 days with sampling days at day 1, 3, 6, 9 and day 11. *L. casei* and *S. mutans* were not detected in biofilm samples over time.

| MODEL | Time [d] | <i>F. nucleatum</i> cells / biofilm | <i>A. naeslundii</i> cells / biofilm | <i>P. intermedia</i> cells / biofilm |
|-------|----------|--|---|---|
| CDFF | 1 | 1.7E+02 (7.6E+00) | 5.7E+04 (3.9E+03) | 4.1E+04 (6.7E+03) |
| UNIT | 1 | 1.9E+02 (2.3E+01) | 5.9E+04 (5.1E+03) | 2.4E+04 (6.4E+03) |
| CDFF | 3 | 1.0E+00 (4.1E-01) | 6.4E+04 (5.4E+04) | 4.1E+02 (5.1E+01) |
| UNIT | 3 | 3.0E+01 (4.6E+00) | 5.9E+04 (4.2E+04) | 3.6E+02 (3.0E+01) |
| CDFF | 6 | 7.4E+00 (3.7E+00) | 5.0E+04 (2.6E+03) | 4.3E+02 (4.8E+01) |
| UNIT | 6 | 1.9E+01 (8.5E+00) | 5.6E+04 (2.6E+03) | 2.8E+02 (3.3E+01) |
| CDFF | 9 | 4.4E+01 (1.4E+01) | 5.4E+04 (3.5E+03) | 3.0E+02 (2.6E+01) |
| UNIT | 9 | 1.1E+01 (6.4E+01) | 6.1E+04 (6.4E+04) | 2.6E+02 (2.4E+01) |
| CDFF | 11 | 3.8E+01 (9.0E+00) | 5.5E+04 (2.9E+03) | 2.9E+02 (4.0E+01) |
| UNIT | 11 | 4.1E+01 (7.5E+00) | 5.9E+04 (8.6E+03) | 2.7E+02 (2.1E+01) |

L. casei was not detected

Table 3.3 shows the numbers for the gingivitis associated bacteria detected by triplex qPCR primers in both CDFF and the T-CDFF's unit. The numbers are expressed as cells / biofilm with a standard error presented in brackets (n = 6). n=6 refers to two biological and three technical replicates

The total number of bacteria in both models was detected at around 10^7 cells / biofilm at day 1 and increased by 2.75 log in CDFF and 2.50 log in T-CDFF unit by day 3 ($p < 0.05$). From day 6 onwards, bacteria reached a stable number of 10^{10} cells / biofilm with a slight decrease on the last day and no major difference between the models ($p = 0.304$).

Similar growth trends were seen for the health related bacteria that increased by day 3 and then reached stable numbers from day 6 onwards. The number of *S. sanguinis* was 1.40×10^4 cells / biofilm in the CDFF and 4.90×10^3 cells / biofilm in the T-CDFF's unit at

day 1 and increased by 2.86 log in CDFF and 3.50 log in T-CDFF unit by day 3 ($p < 0.05$). From day 6, *S. sanguinis* reached a stable number of approximately 10^7 cells / biofilm in both models with no differences between them ($p = 0.658$). A similar growth pattern was seen for *N. subflava* and *V. dispar* with no significant difference across the units ($p = 0.426$, $p = 0.374$, respectively).

N. subflava started with 10^2 cells / biofilm in both models at day 1 and increased by 4.48 log in CDFF and 5.02 log in T-CDFF unit at day 3 ($p < 0.05$) and stayed at a constant level of 10^7 cells / biofilm towards the end of the experiment. *V. dispar* reached 5.60×10^3 cells / biofilm and 7.70×10^3 cells / biofilm in the CDFF and the single unit of the T-CDFF respectively after 24 hours incubation with 4.72 log increase in CDFF and 2.27 log increase in T-CDFF unit from day 1 to day 3 ($p < 0.05$) followed by a stable number of 10^8 cells / biofilm from day 6 onwards.

On the contrary, there was no growth increase over time for the gingivitis related bacteria. *F. nucleatum* reached low numbers throughout the experiment in both models. The starting numbers of *A. naeslundii* after 24 hour incubation in both models were 10^4 cells / biofilm. The bacterial numbers remained constant over time with no significant difference in the growth pattern between the models ($p = 0.286$). The number of *P. intermedia* reached 10^4 cells / biofilm at the beginning of the experiment, and then decreased to 10^2 cells / biofilm within 3 days and stayed at this level in both units until the end of experiment ($p = 0.366$).

3.4.4 Methodology 4

This Section presents the results obtained from the T-CDFF experiments with changed parts and optimized methodology. The leakage via the gearbox and from the waste output was addressed by attaching a PTFE cap onto a shaft to protect the gearbox from blockage previously caused by bacterial waste. Additionally, a new tight waste output seal substituted the distorted one. The model's air-tightness was further investigated and improved; a distorted top/bottom seal, waste output seal, screw cap seal were replaced and non-domed nuts were used to enhance the air-tightness.

3.4.4.1 Investigation of the oral community developed in the T-CDFF model

Table 3.4-3.6 presents the bacteria implicated in health and gingivitis over 12 days of health conditions, while being retrieved at different sampling points from the T-CDFF model.

| Time [d] | Total bacteria Average [cells / biofilm] | | | <i>S. sanguinis</i> Average [cells / biofilm] | | |
|----------|---|-------------------------------|-------------------------------|--|-------------------------------|-------------------------------|
| | unit 1 | unit 2 | unit 3 | unit 1 | unit 2 | unit 3 |
| 2 | 5.16E+08 (2.59E+08) | 8.23E+08 (1.42E+08) | 4.19E+08 (1.76E+07) | 1.88E+04 (3.49E+03) | 2.53E+04 (2.17E+03) | 2.39E+05 (9.03E+04) |
| 3 | 3.49E+09 (2.16E+08) | 8.36E+08 (3.57E+08) | 1.12E+09 (7.36E+07) | 2.32E+06 (3.79E+03) | 5.92E+04 (2.48E+04) | 1.80E+05 (4.43E+04) |
| 8 | 2.51E+09 (1.43E+09) | 8.48E+09 (1.03E+09) | 8.31E+09 (4.76E+09) | 2.00E+07 (3.02E+03) | 9.76E+07 (1.43E+07) | 3.23E+07 (1.85E+07) |
| 10 | 7.03E+07 (6.40E+06) | 1.16E+09 (2.94E+08) | 3.61E+09 (4.82E+08) | 7.33E+05 (3.30E+03) | 1.34E+07 (4.91E+06) | 1.13E+07 (8.65E+04) |
| 12 | 7.10E+08 (3.94E+08) | 9.94E+08 (3.39E+08) | 4.14E+09 (2.25E+09) | 7.59E+06 (3.70E+03) | 7.69E+06 (2.36E+06) | 1.83E+07 (9.41E+06) |

Table 3.4 The number of total bacteria and *S. sanguinis* detected by triplex qPCR primers in each unit of the T-CDFF. The amount of bacteria is expressed as cells / biofilm with standard error presented in brackets (n=6). n=6 refers to two biological and three technical replicates

Table 3.5 present the results for *N. subflava* and *V. dispar*. *L. casei* and *S. mutans* were not detected in biofilm samples.

| Time [d] | <i>N. subflava</i> Average [cells / biofilm] | | | <i>V. dispar</i> Average [cells / biofilm] | | |
|----------|---|-------------------------------|-------------------------------|---|-------------------------------|-------------------------------|
| | unit 1 | unit 2 | unit 3 | unit 1 | unit 2 | unit 3 |
| 2 | 7.71E+02 (2.59E+01) | 6.92E+02 (6.88E+01) | 7.92E+02 (5.97E+01) | 1.30E+04 (3.61E+02) | 1.23E+04 (4.34E+02) | 1.19E+04 (1.84E+02) |
| 3 | 6.67E+02 (8.03E+01) | 8.92E+02 (8.31E+01) | 9.83E+02 (1.78E+02) | 1.47E+04 (6.45E+02) | 1.30E+04 (7.13E+02) | 1.33E+04 (4.56E+02) |
| 8 | 6.92E+02 (9.61E+01) | 7.42E+02 (5.69E+01) | 8.33E+02 (7.71E+01) | 1.33E+04 (1.15E+03) | 1.63E+04 (4.84E+02) | 1.41E+04 (1.51E+03) |
| 10 | 5.42E+02 (1.19E+02) | 7.17E+02 (5.73E+01) | 8.42E+02 (9.78E+01) | 1.21E+04 (2.75E+02) | 1.27E+04 (3.76E+02) | 1.56E+04 (4.79E+02) |
| 12 | 7.25E+02 (3.10E+01) | 5.75E+02 (1.34E+02) | 7.50E+02 (5.00E+01) | 1.47E+04 (7.61E+02) | 1.21E+04 (5.54E+02) | 1.32E+04 (6.67E+02) |

S. mutans was not detected

Table 3.5 The number of cells for *N. subflava* and *V. dispar* detected by triplex qPCR primers in each unit of the T-CDFF. The number of bacteria are expressed as cells / biofilm with a standard error presented in brackets (n = 6). *n=6 refers to two biological and three technical replicates

Regarding the health associated bacteria, only *S. sanguinis* recorded a growth increase from 1.88×10^4 , 2.53×10^4 , 2.39×10^5 cells / biofilm (unit 1-3, respectively) at day 2 to 7.59×10^6 , 7.69×10^6 , 1.83×10^7 cells / biofilm at day 12 for all three units, respectively. Due to the air-locked tubing connection, the model was on medium starvation for at least 16 hours before the problem was realised and solved. This resulted in a lower cell number for *S. sanguinis* and the total bacteria on day 10, specifically for unit 1. The remaining health associated bacteria, *N. subflava* and *V. dispar* showed no growth increase over time and lack of significant differences among the units (as shown by the statistical analysis presented in Section 3.4.4.2).

Table 3.6 presents the numbers of the gingivitis associated bacteria over the period of 12 days.

| Time [d] | <i>F. nucleatum</i> Average [cells / biofilm] | | | <i>A. naeslundii</i> Average [cells / biofilm] | | | <i>P. intermedia</i> Average [cells / biofilm] | | |
|----------|--|------------------------------|------------------------------|---|------------------------------|------------------------------|---|------------------------------|------------------------------|
| | unit 1 | unit 2 | unit 3 | unit 1 | unit 2 | unit 3 | unit 1 | unit 2 | unit 3 |
| 2 | 7.50E+01 (1.1E+01) | 9.16E+01 (1.5E+01) | 9.16E+01 (8.3E+00) | 1.43E+04 (5.3E+03) | 1.32E+04 (5.0E+03) | 1.64E+04 (4.6E+03) | 5.63E+04 (8.1E+02) | 5.45E+04 (1.0E+03) | 5.78E+04 (1.1E+03) |
| 3 | 1.16E+02 (1.1E+01) | 7.50E+01 (1.1E+01) | 7.50E+01 (1.7E+01) | 1.19E+04 (3.8E+03) | 1.11E+04 (4.4E+03) | 1.22E+04 (4.8E+03) | 5.74E+04 (8.1E+02) | 5.38E+04 (2.8E+03) | 5.71E+04 (1.7E+03) |
| 8 | 1.0E+02 (1.3E+01) | 1.3E+02 (1.7E+01) | 8.33E+01 (1.7E+01) | 1.12E+04 (3.4E+03) | 1.10E+04 (3.4E+03) | 2.1E+04 (3.9E+03) | 5.75E+04 (2.5E+03) | 5.85E+04 (7.9E+02) | 5.72E+04 (2.0E+03) |
| 10 | 8.33E+01 (1.1E+01) | 9.16E+01 (1.5E+01) | 1.25E+02 (1.1E+01) | 1.12E+04 (4.5E+03) | 1.0E+04 (3.6E+03) | 9.93E+03 (3.7E+03) | 5.23E+04 (8.6E+02) | 5.82E+04 (8.0E+02) | 5.97E+04 (1.8E+03) |
| 12 | 1.08E+02 (8.3E+00) | 7.50E+01 (1.1E+01) | 1.0E+02 (2.2E+01) | 1.03E+04 (4.1E+03) | 1.10E+04 (3.9E+03) | 1.09E+04 (4.7E+03) | 5.98E+04 (4.8E+02) | 5.57E+04 (2.0E+03) | 5.26E+04 (1.3E+03) |

L. casei was not detected

Table 3.6 The number of cells for the gingivitis associated bacteria *F. nucleatum*, *A. naeslundii* and *P. intermedia* detected by triplex qPCR primers in each unit of T-CDFF. The numbers of bacteria are expressed as cells / biofilm with a standard error presented in brackets (n = 6). n=6 refers to two biological and three technical replicates

As health conditions were maintained during the experiment, there was no growth increase over time for the gingivitis related bacteria. *F. nucleatum* reached 7.50×10^1 , 9.16×10^1 and 9.16×10^1 cells / biofilm after 48 hours of incubation for all three units, respectively and remained at this approximate level throughout the whole experiment with no major differences among the units across the sampling points (as shown by the statistical analysis presented in Section 3.4.4.2).

The starting numbers of *A. naeslundii* in all 3 units after 48 hour incubation were 1.43×10^4 , 1.32×10^4 , 1.64×10^4 cells / biofilm, respectively. The number of bacteria remained at this level of 10^4 cells / biofilm over time with no significant difference among the units (presented in Section 3.4.4.2). The number of bacteria for *P. intermedia* reached 5.63×10^4 , 5.45×10^4 , 5.78×10^4 cells / biofilm for all three units, respectively at the beginning of the experiment, and then stayed at this level throughout the whole experiment with no significant disparity among the units (see Section 3.4.4.2).

3.4.4.2 Investigation of the repeatability of the T-CDF model

This Section provides the data on the model's repeatability by applying the statistical analysis to the qPCR data set of 6 strains and the total numbers of bacteria (Table 3.7). The statistical analysis was based on the qPCR data retrieved from T-CDF – methodology 4. The repeatability was tested by applying the Student's t-test to the qPCR data of paired units. The p-value was set as 0.05. The results from the statistical testing are presented in Table 3.7.

| | paired units | p-value | outcome |
|----------------------|--------------|-----------|---------------------------|
| Total bacteria | 1=2 | p = 0.073 | no significant difference |
| | 1=3 | p = 0.018 | significant difference |
| | 2=3 | p = 0.147 | no significant difference |
| <i>S. sanguinis</i> | 1=2 | p = 0.005 | significant difference |
| | 1=3 | p = 0.015 | significant difference |
| | 2=3 | p = 0.051 | no significant difference |
| <i>A. naeslundii</i> | 1=2 | p = 0.865 | no significant difference |
| | 1=3 | p = 0.178 | no significant difference |
| | 2=3 | p = 0.407 | no significant difference |
| <i>P. intermedia</i> | 1=2 | p = 0.646 | no significant difference |
| | 1=3 | p = 0.849 | no significant difference |
| | 2=3 | p = 0.529 | no significant difference |
| <i>N. subflava</i> | 1=2 | p = 0.476 | no significant difference |
| | 1=3 | p = 0.003 | significant difference |
| | 2=3 | p = 0.039 | significant difference |
| <i>F. nucleatum</i> | 1=2 | p = 0.738 | no significant difference |
| | 1=3 | p = 0.856 | no significant difference |
| | 2=3 | p = 0.876 | no significant difference |
| <i>V. dispar</i> | 1=2 | p = 0.597 | no significant difference |
| | 1=3 | p = 0.888 | no significant difference |
| | 2=3 | p = 0.476 | no significant difference |

Table 3.7 Statistical analysis of the data set from the T-CDFE experiment (methodology 4). Abbreviations: 1–Unit 1, 2–Unit 2 and 3–Unit 3.

According to the statistical analysis presented in Table 3.7, there was no significant difference among the units when tested for *F. nucleatum*, *A. naeslundii*, *P. intermedia* and *V. dispar*. However, when data for *N. subflava*, *S. sanguinis* and the total bacteria were paired, at least one pair fail to accepted the null hypothesis which was equivalent to a non-significant difference being observed for this particular pair.

3.5 Discussion

3.5.1 Development process

The multitude of benefits associated with *in vitro* models and their vast contribution to our knowledge and understanding of oral diseases have been widely reported in scientific literature (Guggenheim *et al.* 2001; Baehni & Takeuchi 2003; Silva *et al.* 2012). Not only are they a useful tool for the purpose of disease modeling but there is also a wide spectrum of different *in vitro* models to choose from depending on the research purpose and the experimental sophistication one would like to apply to the study (Guggenheim *et al.* 2004; Greenman *et al.* 2005; Wirthlin *et al.* 2005; Walker & Sedlacek 2007; Sánchez *et al.* 2011). Despite the variety of models available, there has been no report of a satisfactory *in vitro* model for the purpose of reproducible gingivitis modeling and antimicrobial testing, or a complex model which can provide a high-throughput system for testing oral biofilms under varied experimental conditions simultaneously (Dalwai *et al.* 2007; Hope *et al.* 2012).

Until now, the Constant Depth Film Fermentor (CDFF) was the only successfully established *in vitro* model for growing oral biofilms and adequately modeling bacterial shifts associated with gingivitis (Wilson *et al.* 1996; Dalwai *et al.* 2006). Despite the fact, that the CDFF provides high experimental complexity, it does not allow for reproducible concurrent biofilm growth or testing various dentifrices and antimicrobials at the same time (Silva *et al.* 2012; Hope *et al.* 2012).

To deliver a model that enables multiple antimicrobials to be tested in a simultaneous and reproducible manner, a custom made Triple-Constant Depth Film Fermentor (T-CDFF) was manufactured with several mechanical modifications when compared to the standard CDFF. To allow for simultaneous and reproducible biofilm growth and antimicrobials testing, the T-CDFF model was scaled down to allow the running of 3 identical smaller CDFF units at once, side by side within the same incubator. The width of each triple-CDFF is 152 mm with each unit's turntable having a 94 mm diameter width and housing 5 PTFE sampling pans. In comparison, the standard CDFF developed by Peter's and Wimpenny was 230 mm wide and housed a 149 mm turntable with a total of 15 sampling pans (Chapter 2, Section 2.2.1, Table 2.1) (Peters & Wimpenny 1987; Wilson

1999). This reduction allowed for 3 units to be placed in a single incubator to allow simultaneous (parallel use). Additional improvements were identified and applied to increase the comfort of work. The 'L-shape waste' output was used instead of the 'T shape' to ease tubing attachment and maneuvering in the incubator (Section 3.3.1, Table 3.1, 1). An additional PTFE waste output seal was added to increase air-tightness together with a PTFE cap to protect the gearbox from clogging with bacterial waste. To ease the portability of the already bulky model, handles on each side of the motor unit were provided (Section 3.3.1, Table 3.1, 4). The new model was validated to confirm its reliability and to assess its potential for reproducible biofilm growth and oral disease modeling. The findings from the validation process are discussed below.

3.5.2 Validation process

In the work described in this chapter attempts to validate the new *in vitro* T-CDFF model were made. As the T-CDFF was based on the standard CDFF, the experimental set-up and experimental conditions were based upon the knowledge and experience of Fahra Dalwai (a former PhD student at the UCL Eastman Dental Institute) who established a satisfactory *in vitro* gingivitis methodology for the CDFF model (Dalwai *et al.* 2006; Dalwai *et al.* 2007).

Due to the fact that the T-CDFF model is mechanically more complex and thus harder to operate, a simplified CDFF methodology was applied at first to limit the experimental complexity for the operator and to enable easier trouble-shooting (Dalwai *et al.* 2006). **Methodology 1** was limited to a dual-species inoculum, health conditions, and growth for 11 days. This approach enabled focusing on the bacterial interaction between two initial oral colonisers namely *S. sanguinis* and *A. naeslundii* that are involved in gingivitis progression. This was done as it was previously reported that the dual-species inoculum is easier to grow reproducibly (Verkaik *et al.* 2010). As reported in experimental gingivitis studies, *Actinomyces* spp. dominates over *Streptococcus* spp. during gingivitis progression and *vice versa* in health (Syed & Loesche 1978; Dalwai *et al.* 2006). Aerobic conditions were maintained with the inoculum being delivered for 8 hours and followed by provision of a nutrient source in the form of artificial saliva. These conditions were previously

validated and successfully used as an experimental health methodology for CDFE experiments by Dalwai (Dalwai *et al.* 2006).

Three separate T-CDFE experiments were run using the above health methodology. The experiments were performed in an open space warm-room instead of an incubator as the model together with its flasks and extensive tubing connections did not fit in the incubators present within the department at the time (Chapter 2, Section 2.2.4, Figure 2.6). Each of the first 3 experiments was severely contaminated as observed by the naked eye when the turntable and tubing connections were overgrown by biofilm; something not usual for this type of dual-species biofilm. The contamination was confirmed by culturing a sample. In each case, a single species overgrew a dual-species community so the experiments were stopped and data was not collected. The fourth experiment experienced only partial contamination with only unit 3 being affected by the end of the experiment (day 9 / 12). The data were collected and analysed by the duplex qPCR with primers targeting *S. sanguinis* and *A. naeslundii* to investigate the species numbers when affected by the contamination.

The data presented in Figure 3.2 for unit 1 and unit 2 showed the similar growth pattern for both strains with 0.76 and 0.48 log increase for *S. sanguinis* over the time period of the experiment and a log decrease for *A. naeslundii* during the 11 day health condition. As previously reported by Dalwai and colleagues, the numbers of *Streptococcus* spp increased under health conditions at the expense of the gingivitis related *Actinomyces* spp., therefore the results obtained from the T-CDFE validation were satisfactory and followed the trend previously published in the literature (Dalwai *et al.* 2006).

Furthermore, unit 3 had shown a high resemblance to unit 1 and 2 at the beginning of the experiment with the same bacterial numbers and a high potential for reproducibility. However, there was a significant decline recorded for both species from day 6 onwards which was attributed to the presence of the contaminant overgrowing the community.

As the contamination affected growth of the community and hindered the model's reliability it was crucial to investigate the source of contamination. The Wirthlin group observed that improvement in the aseptic work protocol reduced the contamination

issues when validating their Laboratory Model Biofilm Fermentor (Wirthlin *et al.* 2005). As the T-CDFF model is mechanically more sophisticated and much harder to operate, several aseptic-working precautions were introduced such as (i) wearing a clean lab coat, gloves and a face mask, (ii) cleaning model's surfaces with ethanol wipes before sampling and (ii) spraying the surfaces with 70% ethanol when sampling or maintaining tubing connections. Additionally, dual-species inoculum was replaced by a microcosm community which provided a better representation of the oral commensal microbiota. The increased bacterial complexity resulted in more stable community resilient to non-oral contamination (Hope *et al.* 2012). The remaining experimental conditions did not change.

Despite the methodological alterations (**Methodology 2**), the experiment was contaminated at an early stage with all 3 units and the tubing connection being severely overgrown by single species after 24 hours of incubation. The outcome made one reconsider experimental set-up and suspect mechanical malfunction. To address these questions methodology 3 was developed.

Methodology 3 was designed to further investigate the model design, the malfunctioning of any parts, the flaws in the set-up or sampling techniques introduced by the operator. To address these questions, a reliable and well established CDFF model was run at the same time as one of the triple units. Both models were run simultaneously in separate incubators by the same operator. The same conditions as in methodology 2 were applied to both models.

The outcome of this experiment was that models were not only contamination free but also presented the same bacterial growth trend over experimental time period, this confirmed good operational practice and that there were no flaws in the set-up or sampling techniques. Despite the lack of contamination, mechanical problems were observed when running the T-CDFF model. Firstly, bacterial seepage from the waste output seal was observed which despite running several prior T-CDFF experiments was not seen before. Furthermore, the bacterial waste leaked into the gearbox and clogged it which resulted in a dysfunctional turntable and broken motor by the completion of the

experiment. The above-mentioned issues did not impair my experiment and a set of reliable data was obtained from both models.

Following this, my attention focused on the potential lack of air-tightness due to the faultiness of the seals and the malfunctioning of the other parts of the model. These potential issues were addressed in **Methodology 4**. All top / bottom, waste output or screw cap seals were checked for any distortions or faultiness and replaced with new tighter PTFE seals. Furthermore, the screw caps did not have seals or were provided with loose ones that were exchanged for tighter ones (Figure 3.3A). The leakage into the gearbox was addressed by attaching a PTFE cover onto it to protect it from bacterial waste seeping through it and clogging the system (Figure 3.1). The final check-up was to set-up the model and check its air-tightness by filling it up with gas and monitoring for any gas leakages. This allowed us to conclude that the domed nuts did not screw the top plate tight enough against the glass vessel, which in turn compromised the air-tightness. The domed-nuts were replaced with non-domed nuts that had better tightening properties (Figure 3.3B). With all the modifications, the T-CDFE model was run once again in an incubator using the same experimental conditions as mentioned in methodology 3.

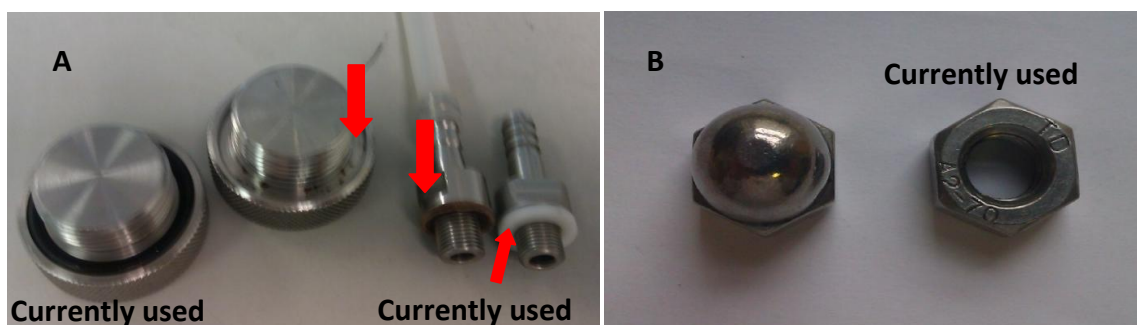


Figure 3.3A) Lack of seals on screw caps and faulty waste output seals were responsible for the lack of air tightness. B) Domed nuts were responsible for the lack of air-tightness of the glass vessel, replaced by the non-domed nuts.

With the mechanical adjustments applied, the T-CDFE experiment did not become contaminated and six bacterial species were detected by triplex qPCR. *L. casei* and *S. mutans* were not detected which may be due to the fact that they are caries associated bacteria and did not have the optimal growth conditions to thrive (Arthur *et al.* 2013). Furthermore, *S. sanguinis* was the only bacterial species that increased in numbers over

the experimental time period and its increase in proportions may have also impaired the growth of *S. mutans* as this phenomenon has been previously reported (Kreth *et al.* 2005; Tamura *et al.* 2009; Arthur *et al.* 2013). The remaining bacterial species *N. subflava*, *V. dispar*, *F. nucleatum*, *P. intermedia* or *A. naeslundii*, regardless of their implications in oral health or gingivitis showed no growth increase over the duration of the experiment.

3.5.3 Investigation of the reproducibility of the model

It is important to stress that the T-CDFF is a highly sophisticated mechanical system for producing a complex biological eco-system prone to bias that can be introduced at any stage of the experiment either by the operator or flawed experimental methodology. As all these factors can directly or indirectly limit the model's reproducibility, the T-CDFF units were manufactured to be identical and run on a single motor housing to limit the mechanical differences between them and to allow for reproducible biofilm growth and antimicrobials testing. Additionally, each T-CDFF experiment was performed with the same standardised inoculum and artificial saliva being delivered to each unit via a calibrated pump and tubing connections. The aim of this was to limit the experimental differences among the units and increase the reproducibility between them.

The level of agreement between the three T-CDFF's units exposed to the same experimental conditions was examined by applying the statistics to the qPCR data of the bacterial strains associated with oral health or gingivitis. The analysis was applied to six bacterial strains detected in biofilms by triplex qPCR. In order to perform the analysis, the data were subjected to \log_{10} transformation and assessed for normal distribution. The data for each strain obtained from each unit were paired accordingly to strain and unit and then analysed by Student's t-test.

Despite the complexity of the model, the statistical analysis failed to reject the null hypothesis ("H0: there is a non-significant difference between the paired units") in most cases which strongly suggested the lack of statistically significant difference between the paired units and thus a high potential for reproducibility. The only significant differences among the units were recorded for *N. subflava*, *S. sanguinis* and the total bacteria. However, this may have been due to the fact that model in question was temporarily starved of medium which may have resulted in lower counts for these particular strains

on day 10 and this skewed the outcome. Ensuring the stable experimental conditions, i.e. the lack of medium starvation, would aid the model's reproducibility in the future.

3.6 Conclusion

In conclusion, this chapter presents a new T-CDFF model designed for growing reproducible oral biofilms. Work within this chapter focused on model validation and testing to establish whether it worked in a reliable and reproducible manner or whether it required any further mechanical modifications.

The contamination problems encountered during the validation process led to the methodological alterations and the identification of mechanical faults. The model's mechanics were improved by providing new and tighter waste output seals, bottom / top and screw caps seals. Additionally, domed caps were replaced with non-domed caps that provided better compressing properties, which in turn allowed the integrity of the air-tight compartment to be maintained. After the mechanical and the methodological improvements, a contamination free *in vitro* T-CDFF model was obtained, this model allowed the growth of oral biofilms with a high potential of reproducibility. Further work has to be performed to investigate the reproducibility of the T-CDFF model and its potential for establishing a health / gingivitis biofilm community *in vitro*. However, this chapter has provided important preliminary findings into the potential future advantages of using the T-CDFF as a tool for mimicking the environments of health and disease for the study of oral biofilms.

4 CHAPTER

Development of an *in vitro* gingivitis model

4.1 Introduction

Gingivitis is a highly prevalent disease that affects around 50-90% of adults nationwide (Brown & Loe 1993; Pihlstrom *et al.* 2005) and if left untreated can lead to periodontitis (Marsh 1994). Although not all cases of periodontitis are preceded by gingivitis, it is thought that gingivitis prevention can help to reduce its incidence (Marsh 1994). In eradication or prevention of any disease, understanding its aetiology and interactions among the pathogens and non-virulent species is very important. After decades of using culture and molecular methods for the purpose of pathogen identification, certain bacteria have been acknowledged as responsible for disease progression: *F. nucleatum* (Kistler *et al.* 2013), *F. alocis* (Kumar *et al.* 2006), *Actinobacillus actinomycetemcomitans*, *Eikenella corrodens* (Darveau *et al.* 1997; Liljemark 2000), *P. intermedia* (Raber-Durlacher *et al.* 1994), *Tannerella forsythia*, *P. nigrescens*, *T. denticola*, *P. gingivalis*, *C. rectus* (Ashimoto *et al.* 1996). Additionally, as observed in experimental gingivitis studies, there is an increase of Gram-negative species (Moore *et al.* 1982) and a dominance of *Actinomyces* spp. over *Streptococcus* spp. during the environmental shift towards gingivitis (Socransky 1963; Syed & Loesche 1978; Moore *et al.* 1982; Moore & Moore 1994).

In vitro models can act as controllable systems that allow for better experimental control than the *in vivo* studies which can be burdened with subjects's compliance and dropout rates. Such models can also help us understand disease progression by allowing to examine the effect of a particular factor/condition change on a bacterial community (Wilson 1999; Pratten *et al.* 2003; Buduneli *et al.* 2004; Greenman *et al.* 2005). Indeed, the complexity of oral biofilms is so great that it is difficult to study them without any recourse to experimental laboratory models (Wilson 1999; Pratten *et al.* 2003; Greenman *et al.* 2005).

Therefore T-CDFF, a complex *in vitro* model, can not only allow for greater control and reproducibility of environmental conditions, but also allow researchers to grow oral communities in health and disease to investigate the interactions between periopathogens and non-virulent species. Additionally, the model can be used to test

various factors such as temperature, nutrient source, oxygen availability, substrata and pH on biofilm development individually (Wilson 1999; Greenman *et al.* 2005; Dalwai *et al.* 2006). Such simplifications can help better understand plaque development. Therefore, modelling the ecological shifts observed in gingivitis onset using such models would be an indispensable tool for understanding plaque formation, testing individual environmental factors', and assessing potential treatments on the developed communities (Baehni & Takeuchi 2003; Dalwai *et al.* 2007).

In Chapter 3, the first results chapter, a new complex *in vitro* model was introduced, and its development and validation process described. The work presented in this chapter is focused on using this model to develop the bacterial shifts associated with the onset of gingivitis and also testing reproducibility. Both of these tasks were evaluated based on culture, molecular and functional studies (as described further).

4.2 T-CDFF Methodology

4.2.1 The experimental set-up

The experimental set-up and scheme of work of all T-CDFF experiments was performed according to the methodology described in Chapter 2, Section 2.2-2.3.

4.2.2 The experimental conditions

All the T-CDFF experimental conditions presented in this chapter were designed according to Figure 4.1.

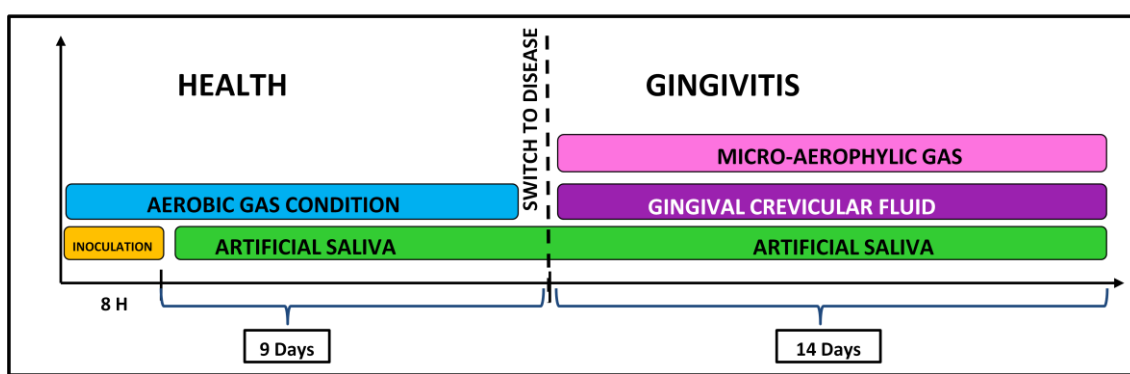


Figure 4.1 The experimental design of T-CDFF experiments. The health conditions were run for 9 days and then switched to 14 days of gingivitis conditions.

Each T-CDFF experiment began with 8 hours of inoculation with a saliva microcosm population (Chapter 2, Section 2.3.1). After the inoculation process, the model was exposed to 9 days of health conditions by providing aerobic conditions and standardized artificial saliva (Chapter 2, Section 2.3.3). The gingivitis conditions were introduced at day 9 and established by providing an additional artificial GCF component and micro-aerophilic gas for 14 days (Chapter 2, Section 2.3.4).

In terms of the experimental set-up, the single peristaltic pumps (Watson & Marlow, 101 U / R) previously used in Chapter 3 for delivering inoculum and artificial saliva were replaced by a multi-channel pump (Watson & Marlow, 205 U). To enable this transition, the silicone 0.8 mm bore tubing (Fisher) was substituted with a special marprene tubing (Marlow & Watson) which was adequate to run with a 205 U multi-channel pump (Watson & Marlow). The artificial GCF, gas and waste output

connections remained unchanged. The modified experimental set-up is shown in Figure 4.2.

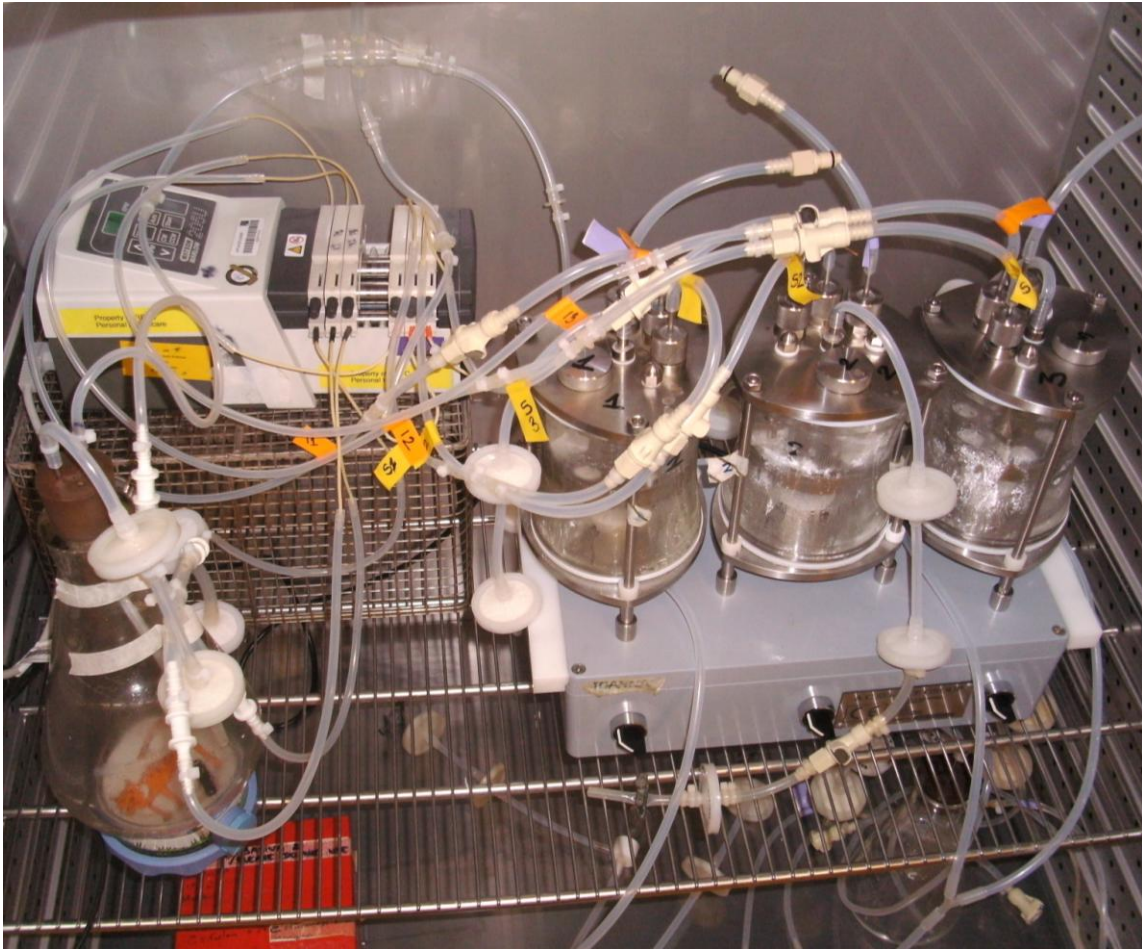
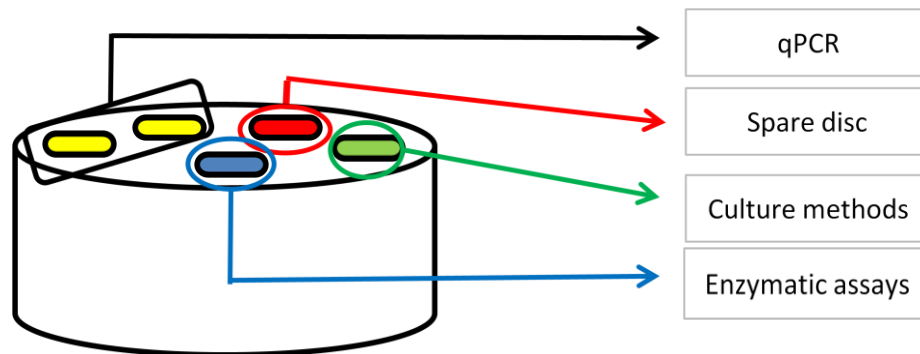


Figure 4.2 shows the experimental set-up with a new multi-channel pump which substituted the single pumps used in delivering the inoculum and the artificial saliva to each T-CDFD unit.

4.2.3 T-CDFD sampling

The T-CDFD experiments presented in this chapter lasted for 23 days, with 9 in health and 14 in gingivitis conditions. Three sampling points were executed in health conditions at day 1, day 5 and day 7, while the remaining two were performed in gingivitis conditions at day 18 and day 23 (9 and 14 days after switching to gingivitis, respectively). Each sampling was performed according to the methodology specified in Chapter 2, Section 2.3.5. During each sampling, one pan was removed from every unit and analysed using different techniques (detailed in Figure 4.3).







| | |
|---|---|
|  | Yellow discs served as two biological replicates for qPCR study. Biofilm from each disc was centrifuged, DNA was extracted according to the bead beating protocol and then analysed by triplex qPCR (Chapter 2, Section 2.5.1-2.5.2). |
|  | Biofilm from green disc was plated out on CBA, FAA, CFAT, M-S (Chapter 2, Section 2.4). |
|  | Biofilm from blue disc was used for the metabolic assays such as trypsin-like-protease and alkaline phosphatase (Chapter 2, Section 2.7.1). |
|  | A spare disc. Biofilm was pelleted down, DNA was extracted according to the bead beating protocol and stored in -20°C (Chapter 2, Section 2.5.1). |

Figure 4.3 shows the T-CDFF sampling pan with 5 discs, each designated for different analysis.

4.2.4 Statistical analysis

The aim of the statistical analysis was to investigate the reproducibility of the T-CDFF model and the differences between the health and disease conditions developed in it.

4.2.4.1 Reproducibility among units

To understand whether bacteria numbers across units differed significantly from each other, univariate ANOVA analysis with post-hoc Bonferroni multiple comparisons correction (IBM SPSS Statistics 22.0) was performed by Aviva Petrie (UCL Eastman Dental Institute). This analysis was conducted on the qPCR data set (total bacteria, *A. naeslundii*, *P. intermedia*, *F. nucleatum*, *S. sanguinis*, *V. dispar* and *N. subflava*) and culture data (total anaerobes and aerobes).

4.2.4.2 Differences between health and disease

To investigate the differences in bacterial numbers across the change in conditions from health to gingivitis in each T-CDF unit, the bacterial numbers retrieved at day 5 and day 7 (health) were averaged, logged and compared with the averaged and logged data from day 18 and day 23 (gingivitis). This was done to both the culture and qPCR data sets. The data from sampling point 1 were excluded from calculating the health averages, as the cell numbers collected at day 1 were usually much lower than for the remaining 4 sampling points collected from mature biofilm.

ANOVA analysis (IBM SPSS Statistics 22.0) was applied to qPCR data set (total bacteria, *A. naeslundii*, *P. intermedia*, *F. nucleatum*, *S. sanguinis*, *V. dispar* and *N. subflava*) and culture data set (total aerobes and anaerobes) to investigate the differences in species numbers across the change from health to gingivitis by comparing the data set obtained from health against the data set from gingivitis.

Data obtained from day 1 were usually different in terms of bacterial numbers (much lower in cell numbers) when compared to days 5 and 7. Because of this, there was a concern that including day 1 might skew the analysis, giving biased results. Therefore, the ANOVA analysis was performed on data with and without sampling point 1 to give more accurate insight into the bacterial changes across the condition change. If statistical analyses with and without the day 1 produced same output (significant/not significant), then the *p*-value from only one analysis is presented. To keep consistency, it was arbitrary decided to report *p*-values from the statistical analysis without day 1.

The Student's t-test (IBM SPSS Statistics 22.0) was used to investigate the differences between the health and disease conditions in the enzymatic data set. The significance level for all hypothesis tests performed in this chapter was chosen to be 0.01.

4.2.5 Functional approach to investigating the gingivitis associated shifts

4.2.5.1 Filter assays

The filter biofilm assay was used to test two different metabolic enzymes, alkaline phosphatase (Bessey *et al.* 1946) and trypsin-like-protease (Yoshimura *et al.* 1984). Nitrocellulose discs of 0.45 cm diameter were cut and placed on fastidious anaerobe agar plates (FAA). Each disc was inoculated with 10 μ L of *Porphyromonas gingivalis* suspension and plates were incubated in the anaerobic cabinet (MACS-MG-1000-Anaerobic workstation) at 37°C. The nitrocellulose discs were removed from the old plates and placed on fresh FAA plates every two days to ensure nutrient availability. The experiment was conducted for 8 days in total, with sampling points on day 1, day 3, day 5 and day 8. At each sampling day, 10 discs were removed from the plate and suspended in 5.0 mL of PBS and then vortexed for 3 min. The bacterial suspension was tested for enzymatic activity using ALPase and TLPase assays (Chapter 2, Section 2.7.1) and then the suspension was cultured to obtain bacterial viable counts so that the metabolic activity could be correlated with the bacterial number.

4.2.5.2 Microcosm biofilm retrieved from T-CDF

The biofilm from a single HA disc was re-suspended in 1.0 mL of PBS by vortexing with 5 glass beads for 1.0 min. The obtained bacterial suspension was used for ALPase (Chapter 2, Section 2.7.1.1) and TLPase assays (Chapter 2, Section 2.7.1.2). The obtained data were presented in a form of a graph depicting the change in metabolic activity and viable counts over time.

4.3 Results

4.3.1 Bacterial shifts from simulated health to gingivitis

4.3.1.1 Culture methods

The composition of modelled supragingival biofilms grown under simulated health and disease conditions in two individual T-CDFE experiments was investigated using non-selective and selective media for the total bacteria and the key genera such as *Streptococcus* spp. and *Actinomyces* spp., respectively as presented in Figure 4.4 and Figure 4.5.

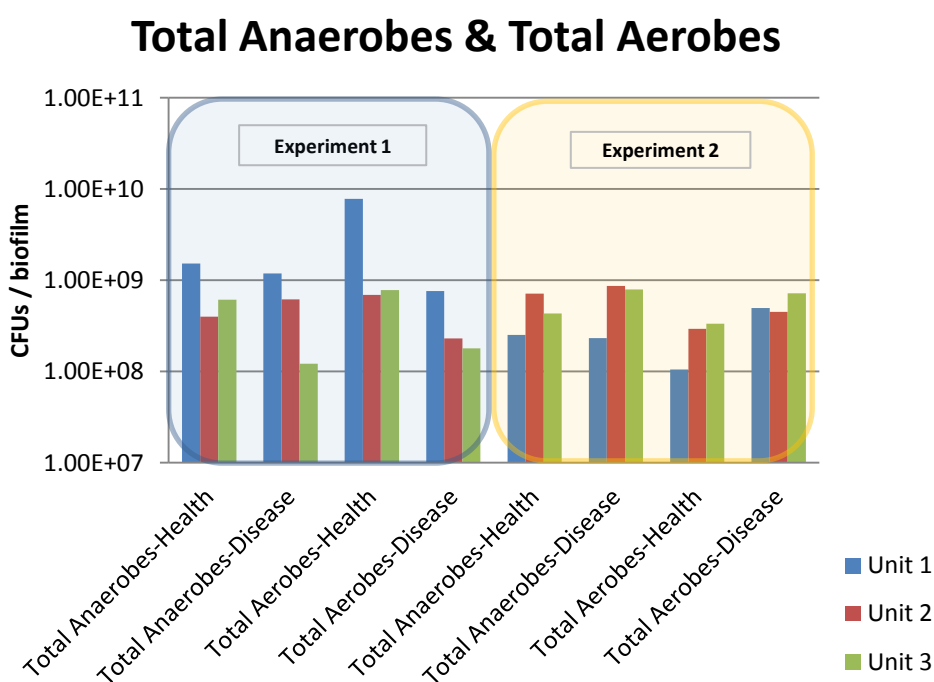


Figure 4.4 presents the viable counts for the total number of anaerobes and aerobes in each T-CDFE unit during two individual experiments across simulated health and disease conditions. The data from two sampling points in health (day 5 and day 7) and two sampling points in disease (day 18 and day 23) were averaged to present the change in viable counts for each unit in time in two T-CDFE experiments (n=2). *n=2 refers to two technical replicates

Figure 4.4 presents the growth trend of the anaerobes and aerobes in T-CDFE experiment 1 and experiment 2. To investigate the differences across the simulated health and gingivitis, the viable counts data from day 5 and 7 were averaged, logged

(health) and compared against the logged average of gingivitis data from day 18 and day 23 (see Section 4.2.4.2).

There was not a uniform growth pattern across the individual experiments. In experiment 1, there was a non-significant decrease in total anaerobes in unit 1 ($p=0.238$) and a significant 0.7 log decrease in unit 3 ($p=0.004$); In unit 2 a non-significant 0.19 log increase ($p=0.856$) was recorded under disease conditions. There was also an overall descending trend for aerobic counts in experiment 1 (unit 1-3: $p=0.020$, $p=0.316$, $p=0.045$) when compared to experiment 2 which recorded an increase from health to gingivitis (unit 1-3: $p=0.067$, $p=0.137$, $p=0.119$). For the total number of anaerobes in experiment 2 across both health and disease, there was no change in counts in unit 1 ($p=0.754$) and 0.1 and 0.3 log increases in units 2 ($p=0.885$) and 3 ($p=0.083$) respectively. However, none of these changes were statistically significant ($p \leq 0.01$).

Figure 4.5 presents the total viable counts for *Actinomyces* spp. and *Streptococcus* spp. detected in two individual T-CDFE experiments across the simulated health and disease conditions. To investigate the differences between health and gingivitis, the viable count data from days 5 and 7 were averaged, logged (health) and compared against the logged average of gingivitis data from day 18 and day 23 (see Section 4.2.4.2).

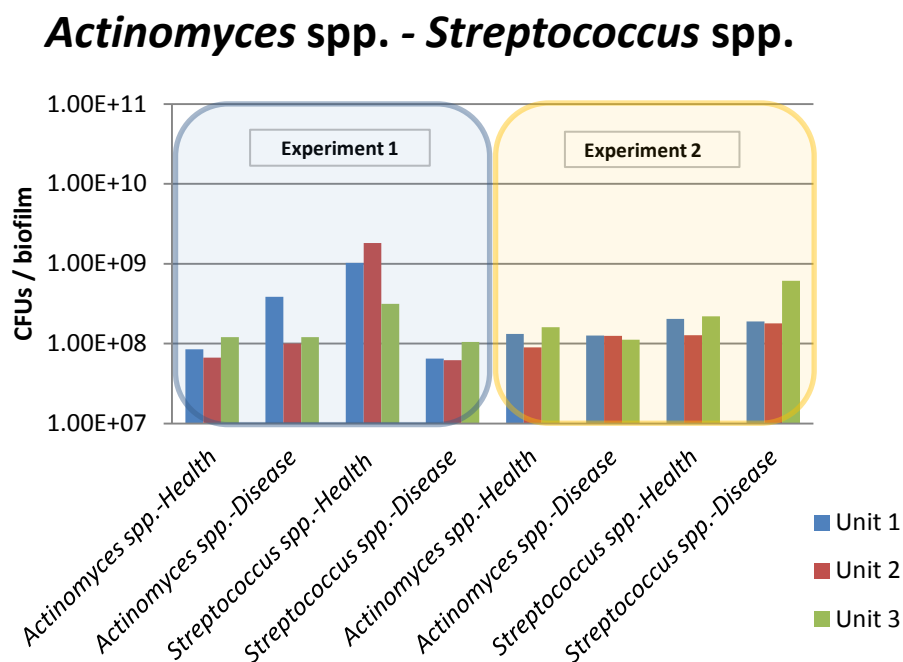


Figure 4.5 presents the viable counts for the total number of *Actinomyces* spp. and *Streptococcus* spp. in each T-CDF unit in two individual experiments across simulated health and disease conditions. The data from two sampling points in health (day 5 and day 7) and two sampling points in disease (day 18 and day 23) were averaged to present the change in viable counts for the total *Actinomyces* spp. and *Streptococcus* spp. for each unit in time for both T-CDF experiments (n=2). *n=2 refers to two technical replicates

In experiment 1 there were 0.65 and 0.17 log increases of *Actinomyces* spp. in units 1 ($p=0.007$) and 2 ($p=0.158$) in simulated disease conditions, respectively. There was no particular growth change across the phases for unit 3 ($p=0.977$). There was an overall decrease in total number of *Streptococcus* spp. with 1.19, 1.46, and 0.47 log decrease in unit 1 ($p=0.004$), unit 2 ($p=0.088$), and unit 3 ($p=0.064$).

In experiment 2, there were no significant changes between the simulated health and disease conditions. There was a 0.1 log increase of *Actinomyces* spp. in unit 2 ($p=0.684$) in comparison to the decrease in counts in units 1 ($p=0.275$) and 3 ($p=0.961$). Similarly, decrease of *Streptococcus* spp. was recorded in unit 1 ($p=0.929$) but a 0.1 log and 0.4 log increase in units 2 ($p=0.535$) and 3 ($p=0.227$).

4.3.1.2 Culture independent methods

Table 4.1 presents the cell number for total bacteria detected by the qPCR in biofilm samples from 6 units (two sets of T-CDFF experiments) throughout time.

| strain | day | Experiment 1 | | | Experiment 2 | | |
|----------------|-----|-------------------------------|-------------------------------|-------------------------------|-------------------------------|-------------------------------|-------------------------------|
| | | Average [cells / biofilm] | | | Average [cells / biofilm] | | |
| | | unit 1 | unit 2 | unit 3 | unit 1 | unit 2 | unit 3 |
| Total bacteria | 1 | 8.09E+06 (2.10E+04) | 1.33E+07 (5.70E+05) | 3.93E+06 (4.46E+04) | 1.18E+07 (3.06E+06) | 1.10E+07 (1.92E+06) | 8.08E+06 (2.39E+06) |
| | 5 | 6.97E+09 (1.24E+07) | 4.10E+09 (1.84E+07) | 4.69E+09 (3.36E+07) | 5.93E+08 (2.52E+08) | 1.16E+09 (4.25E+08) | 2.26E+09 (6.57E+08) |
| | 7 | 2.09E+09 (1.46E+07) | 2.05E+09 (4.59E+06) | 1.09E+09 (4.10E+06) | 4.27E+09 (1.25E+09) | 2.70E+08 (5.17E+07) | 5.64E+08 (8.76E+07) |
| | 18 | 1.02E+09 (1.58E+06) | 9.68E+08 (3.05E+06) | 3.73E+08 (6.89E+05) | 1.38E+09 (2.24E+08) | 8.55E+08 (3.00E+08) | 2.08E+09 (2.38E+08) |
| | 23 | 6.03E+08 (3.77E+06) | 9.83E+08 (5.54E+06) | 5.05E+08 (2.30E+06) | 8.91E+08 (2.32E+08) | 3.28E+09 (1.87E+08) | 5.02E+09 (1.06E+09) |

Table 4.1 shows the cell number for the total bacteria detected by triplex qPCR using universal primers in the biofilm samples collected from each T-CDFF unit over time. The standard error is shown in brackets (n=6). Blue line indicates the introduction of gingivitis conditions at day 9. *n=6 refers to two biological and three technical replicates

The data presented in Table 4.1 shows the total number of bacteria detected in each T-CDFF unit at different time points throughout the 23 days of the experimental conditions. To investigate the growth change across health and gingivitis, the qPCR from day 5 and 7 were averaged, logged (health) and compared against the logged average of the gingivitis data from day 18 and day 23 (see Section 4.2.4.2).

The number of total bacteria after 1 day of incubation reached values between 3.93×10^6 - 1.33×10^7 and 8.08×10^6 - 1.18×10^7 cells / biofilm in experiments 1 and 2, respectively (Table 4.1). After this, there was a 1.7-3.1 log increase in cell numbers across the six T-CDFF units. When the gingivitis conditions were introduced, there was a decrease in total bacteria numbers in experiment 1 (0.69 log, 0.47 log and 0.71 log decrease in units 1-3, respectively). After the data from sampling point 1 were removed (as explained in Section 4.2.4.2), these changes were significant for all units ($p \leq 0.01$).

In experiment 2 there was no significant difference in bacteria numbers across the experimental phases for unit 1 ($p=0.844$) and a significant increase in numbers for

units 2 and 3 ($p \leq 0.01$). This was confirmed by the statistical analysis performed without inclusion of the data from sampling point 1, as explained in Section 4.2.4.2.

Table 4.2 presents the cell numbers for health associated bacteria (*S. sanguinis*, *V. dispar* and *N. subflava*) detected by the qPCR in biofilm samples from 6 units (two sets of T-CDFE experiments).

| strain | day | Experiment 1 | | | Experiment 2 | | |
|---------------------|-----|---|-------------------------------|-------------------------------|-------------------------------|-------------------------------|-------------------------------|
| | | Average [cells / biofilm] | | | Average [cells / biofilm] | | |
| | | unit 1 | unit 2 | unit 3 | unit 1 | unit 2 | unit 3 |
| <i>S. sanguinis</i> | 1 | 1.94E+04 (2.28E+03) | 1.69E+04 (3.73E+03) | 3.72E+03 (6.17E+02) | 1.73E+03 (1.84E+02) | 2.54E+03 (5.28E+03) | 2.43E+03 (1.83E+05) |
| | 5 | 4.45E+07 (6.76E+06) | 2.96E+07 (3.08E+06) | 4.01E+07 (8.31E+06) | 6.51E+05 (6.50E+05) | 2.14E+06 (3.12E+06) | 1.51E+07 (5.20E+06) |
| | 7 | 2.24E+07 (3.98E+06) | 1.81E+07 (2.17E+06) | 1.75E+07 (3.82E+06) | 2.27E+07 (4.55E+06) | 8.67E+05 (1.16E+06) | 5.02E+06 (4.40E+06) |
| | 18 | 2.30E+06 (9.44E+05) | 2.31E+07 (5.13E+06) | 1.14E+07 (4.98E+05) | 2.83E+07 (5.56E+06) | 1.75E+06 (1.15E+07) | 8.47E+07 (1.61E+07) |
| | 23 | 4.30E+06 (1.57E+06) | 1.72E+07 (3.99E+06) | 2.11E+05 (4.52E+04) | 1.18E+07 (2.30E+06) | 2.62E+06 (1.42E+07) | 6.95E+07 (6.64E+06) |
| <i>V. dispar</i> | 1 | 1.77E+04 (4.25E+03) | 5.28E+03 (1.45E+03) | 4.42E+03 (1.47E+03) | 5.23E+03 (1.53E+03) | 5.45E+03 (1.30E+03) | 4.74E+03 (1.32E+03) |
| | 5 | 2.70E+08 (2.77E+07) | 3.31E+07 (1.88E+06) | 2.08E+08 (8.86E+07) | 6.22E+03 (1.39E+03) | 4.51E+07 (2.03E+07) | 1.10E+07 (3.00E+06) |
| | 7 | 1.50E+08 (6.64E+07) | 2.14E+07 (2.22E+06) | 2.39E+07 (1.97E+06) | 1.26E+04 (5.91E+02) | 7.83E+06 (7.35E+05) | 5.54E+07 (2.78E+06) |
| | 18 | 4.08E+07 (1.82E+07) | 3.78E+07 (3.11E+06) | 4.77E+07 (8.85E+06) | 1.06E+04 (8.36E+02) | 3.75E+07 (8.45E+06) | 1.25E+08 (3.34E+07) |
| | 23 | 2.85E+07 (4.35E+06) | 4.17E+07 (7.45E+06) | 4.07E+07 (3.73E+06) | 1.27E+04 (3.28E+02) | 5.33E+07 (4.42E+06) | 1.80E+08 (5.45E+06) |
| <i>N. subflava</i> | 1 | 1.18E+03 (3.74E+02) | 2.53E+03 (8.49E+02) | 6.85E+03 (3.49E+03) | 2.23E+02 (8.85E+01) | 1.45E+02 (8.23E+01) | 1.99E+02 (7.36E+01) |
| | 5 | 3.56E+03 (9.88E+02) | 2.81E+08 (3.26E+07) | 8.58E+07 (3.84E+07) | 7.07E+02 (3.07E+02) | 1.92E+08 (8.19E+07) | 7.44E+07 (3.51E+07) |
| | 7 | 4.26E+07 (1.91E+07) | 4.26E+07 (1.98E+07) | 1.93E+08 (3.14E+07) | 1.55E+06 (6.95E+05) | 1.08E+08 (4.34E+07) | 5.83E+07 (2.15E+07) |
| | 18 | 4.76E+06 (8.21E+05) | 1.64E+07 (1.34E+06) | 3.67E+06 (1.33E+06) | 1.03E+06 (5.28E+05) | 6.84E+06 (2.95E+06) | 3.67E+05 (3.45E+04) |
| | 23 | 2.02E+05 (5.63E+04) | 9.67E+06 (9.98E+05) | 1.85E+06 (7.52E+05) | 6.93E+04 (3.07E+04) | 3.12E+06 (1.36E+06) | 9.51E+05 (3.65E+05) |
| <i>S. mutans</i> | | Not detected throughout the experiments | | | | | |

Table 4.2 presents the total cell number of the health associated bacteria and *S. mutans* detected by triplex qPCR primers in biofilm samples collected from each unit over time. The standard error is shown in brackets (n=6). Blue lines indicate the introduction of gingivitis conditions at day 9. *n=6 refers to two biological and three technical replicates

Table 4.2 presents the growth pattern of 3 health associated species across health and gingivitis conditions in two individual experiments. *S. mutans*, which is a caries

implicated species, was not detected in the T-CDFF experiments. The growth maturation (in terms of cell numbers) in T-CDFF model was established after 5-7 days of incubation. This has been reported before in T-CDFF experiments and is shown in Chapter 3, Section 3.4.3.

For *S. sanguinis*, once the gingivitis conditions were introduced there was a significant 1.0 log and 1.23 log ($p \leq 0.01$) decrease in numbers in units 1 and 3 in experiment 1, and a non-significant 0.07 log increase in unit 2 ($p = 0.188$). Conversely, there were significant 0.68 log, 0.19 log and 0.95 log increases in unit 1, 2 and unit 3 in experiment 2, respectively ($p \leq 0.01$). After excluding the data from sampling point 1 (as explained in Section 4.2.4.2), the bacterial increase in disease conditions in unit 2, experiment 2 was not significant (0.19 log, $p = 0.080$).

V. dispar showed 0.77 and 0.20 log decreases in numbers in units 1 and 3 of experiment 1 ($p = 0.03$ and $p = 0.087$, respectively). There was a non-significant 0.17 log ($p = 0.467$) increase in numbers in unit 2. Despite these large numbers, the differences were not statistically significant due to high levels of variation in the data. In experiment 2, there were 0.12 log ($p = 0.022$), 0.38 log ($p = 0.015$), and 0.78 log ($p < 0.01$) increases in each unit. However, only unit 3 recorded a significant change across the experimental conditions (as explained in Section 4.2.4.2).

There was an overall decrease in *N. subflava* numbers in disease conditions across units in both experiments (except for unit 1 in experiment 1). In experiment 1 there were a 0.93 log ($p < 0.01$) and 1.7 log ($p < 0.01$) decreases in units 2 and 3, as compared with 0.15 log ($p = 0.773$), 1.49 log ($p < 0.01$) and 2.0 log ($p < 0.01$) decreases in experiment 2 in units 1-3, respectively.

Table 4.3 presents the total cell number for 3 bacterial species implicated in gingivitis. Biofilm samples were collected at five sampling events (health conditions: day 1, day 5 and day 7; disease conditions: day 18 and day 23) and analysed by triplex qPCR.

| strain | day | Experiment 1 | | | Experiment 2 | | |
|----------------------|-----|---|-------------------------------|-------------------------------|-------------------------------|-------------------------------|-------------------------------|
| | | Average [cells / biofilm] | | | Average [cells / biofilm] | | |
| | | unit 1 | unit 2 | unit 3 | unit 1 | unit 2 | unit 3 |
| <i>F. nucleatum</i> | 1 | 4.31E+01 (9.74E+00) | 3.69E+01 (7.07E+00) | 6.38E+01 (1.67E+01) | 5.50E+01 (1.40E+01) | 7.57E+01 (1.92E+01) | 6.95E+01 (1.52E+01) |
| | 5 | 4.65E+01 (1.30E+01) | 5.33E+06 (6.01E+04) | 2.82E+06 (1.26E+06) | 8.23E+01 (1.60E+01) | 1.35E+06 (6.12E+05) | 4.97E+05 (4.79E+04) |
| | 7 | 1.49E+06 (6.68E+05) | 3.86E+06 (9.06E+05) | 6.88E+06 (3.49E+05) | 1.35E+02 (1.68E+01) | 9.74E+05 (7.31E+04) | 2.20E+06 (3.13E+05) |
| | 18 | 1.25E+02 (3.18E+01) | 2.71E+06 (1.21E+06) | 9.10E+06 (7.81E+05) | 1.52E+02 (1.91E+01) | 1.44E+06 (2.71E+05) | 5.58E+06 (1.45E+06) |
| | 23 | 2.96E+06 (1.33E+06) | 2.11E+06 (9.58E+05) | 3.74E+06 (1.53E+06) | 1.54E+06 (6.46E+04) | 6.01E+06 (1.48E+06) | 1.09E+07 (4.22E+05) |
| <i>A. naeslundii</i> | 1 | 1.35E+03 (3.35E+02) | 1.46E+03 (3.53E+02) | 1.54E+03 (8.98E+02) | 1.34E+05 (7.95E+04) | 9.45E+04 (6.22E+04) | 1.12E+05 (6.90E+04) |
| | 5 | 1.15E+03 (2.49E+02) | 1.76E+04 (1.56E+04) | 2.22E+05 (1.95E+05) | 1.32E+05 (7.75E+04) | 8.16E+04 (7.52E+04) | 9.13E+04 (4.98E+04) |
| | 7 | 1.39E+04 (8.07E+03) | 2.53E+05 (1.99E+05) | 4.90E+03 (2.62E+03) | 9.09E+04 (4.70E+04) | 2.09E+05 (1.15E+05) | 1.06E+05 (7.67E+04) |
| | 18 | 4.73E+03 (2.21E+03) | 6.45E+03 (1.89E+03) | 5.72E+03 (3.74E+03) | 5.48E+04 (2.46E+04) | 1.15E+05 (5.71E+04) | 1.47E+05 (6.56E+04) |
| | 23 | 8.84E+02 (1.64E+02) | 4.88E+03 (1.31E+03) | 3.03E+03 (2.02E+03) | 1.24E+05 (6.76E+04) | 1.05E+05 (6.27E+04) | 2.74E+04 (1.57E+04) |
| <i>P. intermedia</i> | 1 | 1.61E+04 (9.59E+02) | 1.61E+04 (1.05E+03) | 1.62E+04 (9.54E+02) | 1.79E+04 (9.14E+02) | 1.70E+04 (8.58E+02) | 1.71E+04 (6.74E+02) |
| | 5 | 1.69E+04 (9.13E+02) | 1.47E+04 (1.06E+03) | 1.61E+04 (1.24E+03) | 1.74E+04 (6.09E+02) | 1.50E+04 (5.04E+02) | 1.74E+04 (7.33E+02) |
| | 7 | 1.58E+04 (9.69E+02) | 1.54E+04 (6.76E+02) | 1.45E+04 (3.21E+02) | 1.72E+04 (1.48E+03) | 1.60E+04 (9.69E+02) | 1.95E+04 (6.60E+02) |
| | 18 | 1.66E+04 (7.33E+02) | 1.59E+04 (4.43E+02) | 1.55E+04 (5.23E+02) | 1.79E+04 (4.98E+02) | 1.85E+04 (5.77E+02) | 1.67E+04 (2.37E+02) |
| | 23 | 1.63E+04 (7.83E+02) | 1.60E+04 (4.59E+02) | 1.65E+04 (4.77E+02) | 1.58E+04 (4.22E+02) | 1.69E+04 (1.29E+03) | 1.69E+04 (4.66E+02) |
| <i>L. casei</i> | | Not detected throughout the experiments | | | | | |

Table 4.3 presents the total cell number of the gingivitis associated bacteria detected by triplex qPCR primers in biofilm samples collected from each unit over time. The standard error is shown in brackets (n=6). Blue lines indicate the introduction of gingivitis conditions at day 9. *n=6 refers to two biological and three technical replicates

Table 4.3 presents the gingivitis associated bacteria detected in the biofilm samples over time. *L. casei* was not detected in samples collected from the T-CDFE experiments.

When assessing the average bacterial numbers for health and gingivitis (see Section 4.2.4.2), the numbers of *F. nucleatum* increased 0.3 log ($p=0.758$) and 0.12 log ($p=0.114$) under disease conditions in units 1 and 3, experiment 1, respectively. However, these changes were not statistically significant. Unit 2 recorded a significant 0.28 log ($p=0.006$) decrease in disease condition. In the second T-CDFE experiment, there was a significant increase in the bacterial numbers in unit 1 (2.16 log) and unit 3 (0.87 log), respectively. Unit 2 showed a 0.4 log increase across the health-disease phase which was not significant ($p=0.017$).

With respect to *A. naeslundii*, there was 0.29 log ($p=0.373$), 1.07 log ($p=0.688$), and 0.89 log ($p=0.459$) decrease in disease conditions in units 1-3, experiment 1, respectively. However, none of the above changes were statistically significant. There were also no significant changes across the phases for all units in experiment 2 ($p=0.905$, $p=0.636$, $p=0.842$, units 1-3, respectively).

P. intermedia presented no significant change in numbers across the experimental phases for all units in both T-CDFE experiments ($p=0.829$, $p=0.182$, $p=0.212$, units 1-3, experiment 1; $p=0.394$, $p=0.027$, $p=0.035$, units 1-3, experiment 2).

4.3.2 Investigating the reproducibility of T-CDFF model

The reproducibility of the T-CDFF model was investigated by applying a separate independent univariate ANOVA with a post hoc Bonferroni multiple comparisons correction to the qPCR and culture data. As a pre-processing step here the data were first log-transformed so as to look more Gaussian (as confirmed by histogram plots). Next, a univariate ANOVA analysis was applied using SPSS Statistics 22.0 (IBM, UK) to investigate reproducibility among units run concurrently in individual experiments. To assess validity of the assumptions underpinning ANOVA here, residuals and predicted values were plotted against frequencies. The results are presented below.

Univariate Analysis of Variance performed on the total bacteria detected by the qPCR and presented in Table 4.4 failed to reject the null hypothesis of no significant difference among units within a single experiment ($p=0.374$). The residuals (Table 4.4B) and predicted values (Table 4.4C) were plotted against the frequencies and suggest that the applied model was a reasonable selection for my experimental data set.

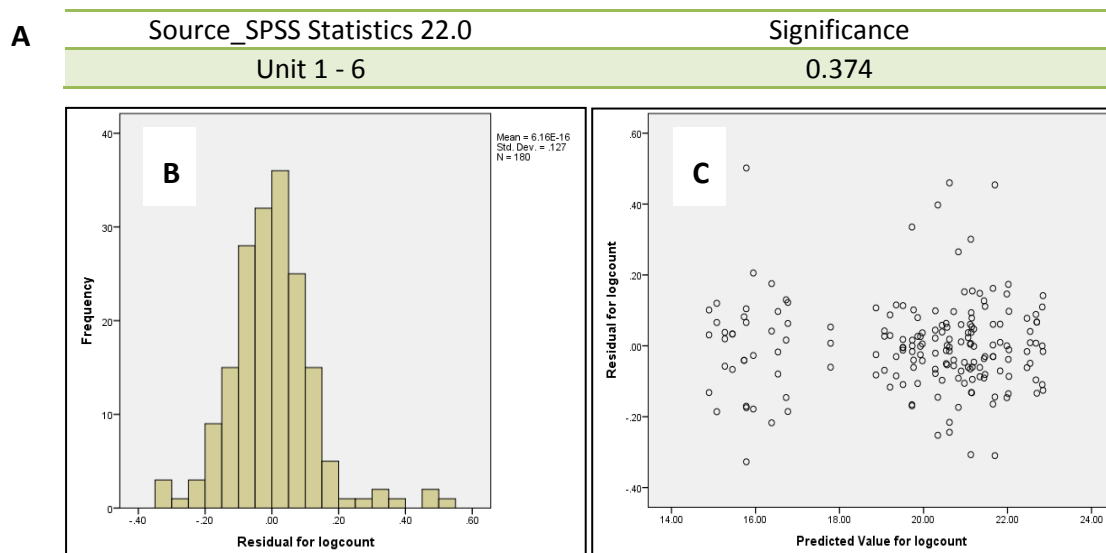


Table 4.4 presents the statistical analysis applied to the qPCR data. A) UNIANOVA output for the analysis performed for 6 T-CDFF units. B) The residuals plotted against the frequency that showed a normal distribution as expected. C) The residuals plotted against the predicted value showed a symmetric distribution.

The statistical analysis performed on the total number of *A. naeslundii* detected in each T-CDFF unit over time showed no significant difference among the units in single

or individual T-CDFF experiments ($p=0.658$) across the experimental phases or sampling events.

Conversely, the data for the total number of *F. nucleatum* showed a significant difference between experiment 1 and 2 ($p\leq 0.01$). When the analysis was performed on these two experiments separately, there were no significant difference observed among the units in experiment 1 ($p=0.019$), while in experiment 2 significant differences existed among units ($p\leq 0.01$).

The analysis performed on *N. subflava* showed significant differences among the units in both T-CDFF experiments ($p\leq 0.01$), but no significant differences were found among the units in single or individual T-CDFF experiments for *P. intermedia* ($p=0.428$). *S. sanguinis* data followed the same trend and showed no significant differences among the units in single or individual T-CDFF experiments ($p=0.693$). The total numbers of *V. dispar* detected in each unit over time showed a significant difference between experiments 1 and 2 ($p=0.001$). When the analysis was performed on these two experiments separately, there was no significant difference observed among the units in experiment 1 ($p=0.910$); while experiment 2 has shown significant differences among the T-CDFF units ($p<0.01$).

A univariate Analysis of Variance was also performed on culture data for total anaerobes and aerobes detected in each unit across the conditions change. The data showed no significant difference for both the total anaerobes ($p=0.291$) and the total aerobes ($p=0.560$) among the T-CDFF units in two individual T-CDFF experiments.

4.3.3 Functional approach to investigate the gingivitis associated shifts

4.3.3.1 Filter assay

The metabolic assays for alkaline phosphatase and trypsin-like-protease activity were tested on single-species biofilm of *P. gingivalis*. Both metabolic assays were tested in two separate filter assays. The results obtained for both assays are shown below in Figure 4.6-4.7.

4.3.3.2 Alkaline phosphatase

Figure 4.6 shows the change in alkaline phosphatase activity (ALPase) over time for the single-species biofilm of *P. gingivalis*.

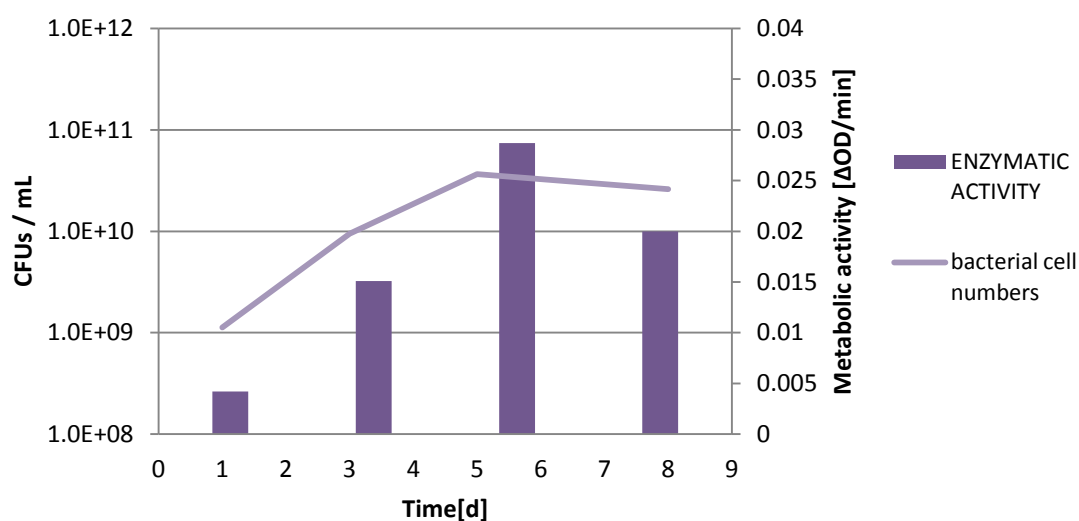


Figure 4.6 shows the alkaline phosphatase activity of *P. gingivalis* over time. The axis on the left shows the total bacterial counts [CFUs / mL]; the right-hand axis shows the optical density change over time that represents the metabolic activity of *P. gingivalis* (n=2). *n=2 refers to two technical replicates

The metabolic activity presented in Figure 4.6 was detectable spectrophotometrically after the 24 hours of the incubation of *P. gingivalis* on the filter discs. The alkaline phosphatase activity increased over time, with its peak activity on day 5 and then decreased on day 8 which was reflected in bacterial viable counts.

4.3.3.3 Trypsin – like – protease

Figure 4.7 illustrates the trypsin-like-protease activity of *P. gingivalis* over time for a single-species biofilm of *P. gingivalis*.

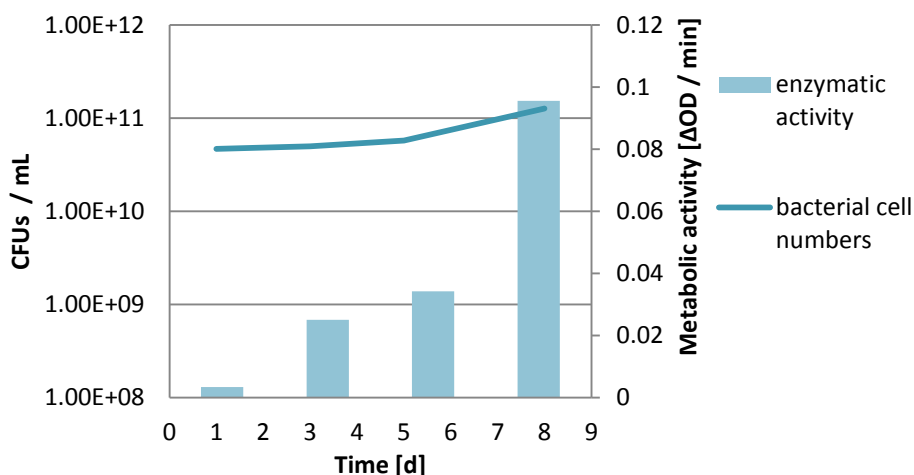


Figure 4.7 shows the trypsin-like-protease activity of *P. gingivalis* over time. The axis on the left shows the total bacterial counts [CFUs / mL]; the right-hand axis shows the optical density change over time that represents the metabolic activity of *P. gingivalis* (n=2). *n=2 refers to two technical replicates

As shown in Figure 4.7, there was an increase in viable counts over time with a relatively steady enzymatic activity increase throughout. The highest enzymatic activity was recorded at day 8 when there was a 2.8 fold increase in enzymatic activity as reflected by 0.3 log increase in counts.

4.3.4 Enzymatic assays on biofilm samples retrieved from T-CDFF

Table 4.5 shown below presents the alkaline phosphatase activity in the biofilms collected from each T-CDFF unit over time. The trypsin-like-protease activity is not presented here, as its activity was not detected in the biofilm samples retrieved from the individual T-CDFF.

| Time [d] | Experiment 1 activity [Δ OD / h] | | | Experiment 2 activity [Δ OD / h] | | |
|----------|---|--------|--------|---|--------|--------|
| | unit 1 | unit 2 | unit 3 | unit 1 | unit 2 | unit 3 |
| 1 | 0.0028 | 0.0 | 0.0034 | 0.00193 | 0.0034 | 0.0 |
| 5 | 0.0252 | 0.0 | 0.0177 | 0.0 | 0.0058 | 0.0 |
| 7 | 0.048 | 0.0 | 0.0366 | 0.0 | 0.0 | 0.601 |
| 18 | 0.0079 | 0.0032 | 0.0143 | 0.538 | 0.132 | 0.14 |
| 23 | 0.0154 | 0.0029 | 0.0079 | 0.277 | 0.007 | 0.343 |

Table 4.5 shows the ALPase activity in biofilms collected from three CDFD units in two separate experiments. The health conditions: day 1, day 5 and day 7; disease conditions: day 18 and day 23. Blue line indicates the introduction of gingivitis conditions at day 9.

Alkaline phosphatase activity was very low and did not show any clear pattern across the sampling points, units or the conditions of change from health to disease. For most units, there was (i) no enzymatic activity detected, (ii) the signal was very weak or (iii) in some instances the signal was stronger at day 5 or 7 than under gingivitis conditions.

4.4 Discussion

4.4.1 Microbial trends in simulated gingivitis onset

The key changes in the microbiota of supragingival plaque as observed by Sockranksy *et al.* and Marsh *et al.* (Marsh 1994; Marsh 1995; Marsh 1999; Marsh 2005; Sockranksy & Haffajee 2005) during the experimental gingivitis studies were two-fold (i) an increase of the anaerobic Gram-negative species belonging to the orange and red complex and (ii) the ascendancy of *Actinomyces* at the expense of the aerobic *Streptococcus* genus (Haffajee & Sockranksy 1994; Marsh 1994; Marsh 1995; Marsh 1999; Marsh 2005; Sockranksy & Haffajee 2005). These changes are a sign of an ecological change occurring in dental plaque during gingivitis progression (Guggenheim *et al.* 2001; Dalwai *et al.* 2007). Dalwai *et al.* reported an increase of anaerobic Gram-negative bacteria during the progression of gingivitis *in vitro* at the expense of the aerobic bacteria present predominantly in health when using the CDFF model. They also reported a predominance of *Actinomyces* spp. at the expense of *Streptococcus* spp. under controlled *in vitro* gingivitis conditions. The research therefore confirmed that these bacterial shifts can be successfully modelled using *in vitro* models (Dalwai *et al.* 2006; Dalwai *et al.* 2007).

To investigate whether I can model the same bacterial changes as mentioned above in T-CDFF model, several techniques were applied to characterise biofilm communities in simulated health and gingivitis. These included culturing methods and qPCR. The first was chosen to assess changes in the total number and proportions of anaerobes and aerobes over time. Selective plating was chosen to focus on determining the total counts of *Actinomyces* spp. and *Streptococcus* spp. and to investigate previously published cross dependence between *Actinomyces* spp. and *Streptococcus* spp. in health-gingivitis progression. This association was further investigated by qPCR targeting *A. naeslundii* and *S. sanguinis*. The qPCR study was further complemented by 3 bacteria implicated in disease (*F. nuclatum*, *P. intermedia*, *L. casei*) and health (*S. sanguinis*, *V. dispar*, *N. subflava*) and 1 oral species implicated in tooth decay (*S. mutans*). Despite the fact that *S. mutans* is not directly associated with gingivitis, its

inclusion broadened the bacterial coverage and potentially my perspective on disease causation.

These two reductionist approaches were complemented by a functional study using enzymatic assays to investigate the biofilm's virulence capacity and the metabolic change during the shift from oral health to gingivitis. It has been previously reported that oral communities possess proteolytic activity; it was beyond my capability at the time to target more than 8 bacterial species, therefore metabolic assays were applied as a surrogate model to track the virulence of the proteolytic enzyme producers associated with gingivitis and belonging to *Phorphyromonas*, *Prevotella*, *Tanarella* or *Capnocytophaga* genera (Soder 1972, Wei 1999).

4.4.2 Culture methods to analyse the gingivitis associated shifts

The aim of using the non-selective and selective plating was to investigate changes in the total anaerobes and aerobes and the *Actinomyces* spp. and *Streptococcus* spp. across the experimental conditions change in the T-CDFF model. The two T-CDFF experiments were run in health conditions for 9 days to establish a mature and healthy biofilm. Then, the conditions were changed to gingivitis and maintained for 14 days.

The data obtained from the T-CDFF experiments showed a relatively high variability and no particular growth trend among units in the two experiments. The total number of anaerobes decreased in gingivitis conditions in experiment 1 (except for unit 2) but an increase was observed in experiment 2 (except for unit 1). A similar trend was observed for the aerobes on the switch from health to disease, where the number of aerobes decreased in experiment 1 but increased in experiment 2. However, these changes were mostly not statistically significant. With regard to the *Actinomyces* spp.-*Streptococcus* spp. relationship, experiment 1 showed an overall decrease in numbers of *Streptococcus* spp. among all units under gingivitis conditions at the expense of *Actinomyces* spp. which increased in numbers (with exception for unit 3). However, again these changes were mostly not statistically significant. Experiment 2 showed much greater variability with no particular growth trend. The statistical analysis

showed no significant difference in bacterial numbers across the health and gingivitis conditions. The *Actinomyces* spp.-*Streptococcus* spp. relationship was further investigated by the culture independent qPCR method with a primer set for *A. naeslundii* and *S. sanguinis*.

As reported by Zee *et al.* in their experimental gingivitis study, there was a significant increase in the proportion of Gram-negative species, up to 47% of the bacterial community in the gingivitis patients (Zee *et al.* 1996). A relatively similar ecological shift was established by Dalwai *et al.* when simulating gingivitis *in vitro* using the CDFF model (Dalwai *et al.* 2006). In terms of the relationship between *Actinomyces* spp. and *Streptococcus* spp., Dalwai and colleagues showed a 50% decrease of *Streptococcus* spp. and 60% increase of *Actinomyces* spp. during the *in vitro* gingivitis conditions using the CDFF model. A similar relationship between *Actinomyces* spp. and *Streptococcus* spp. was reported *in vivo* during the experimental gingivitis trials performed by Zee *et al.* and Moore *et al.* (Moore *et al.* 1982; Zee *et al.* 1996; Dalwai *et al.* 2006). In spite of applying the same experimental gingivitis methodology to T-CDFF experiments (Pratten *et al.* 1998; Dalwai *et al.* 2007), my results did not show a significant increase of anaerobes, which are mostly Gram-negative and gingivitis associated bacteria, under the gingivitis conditions (Section 4.3.1.1, Figure 4.4).

4.4.3 Molecular methods to analyse the gingivitis associated shifts

Molecular techniques are considered a comprehensive, fast and more precise approach in microbial identification than the traditional cultivation techniques as they do not require a microorganism to grow to be detected and can therefore allow for the identification of both the cultivable and non-cultivable fraction (Sánchez *et al.* 2011). The qPCR study presented in this chapter was used to investigate the microcosm population grown in T-CDFF using primers for 8 bacteria associated with either oral health or disease. The selection of these bacteria was based on the fact that they are considered to be the species frequently found in supragingival plaque. This selection also encompasses the early, intermediate and late colonisers belonging to different complexes described by Socransky (Socransky *et al.* 1963; Socransky & Haffajee 1994;

Socransky *et al.* 1998; Socransky *et al.* 2004). Among them, 4 species can be categorised as gingivitis associated (*F. nucleatum*, *P. intermedia*, *A. naeslundii* and *L. casei*), 3 are health associated (*S. sanguinis*, *V. dispar*, *N. subflava*) and 1 species, *S. mutans*, is associated with tooth decay. These 8 bacterial species exemplify a different range of physical and metabolic characteristics, which effectively can represent a wider oral community and help me confirm whether I am dealing with a healthy or a diseased microbiome (Sánchez *et al.* 2011).

The overall total numbers of bacteria detected in the T-CDF model remained in a steady state during the gingivitis conditions whether determined by the culture or qPCR study. This would imply that once the community is established, the total numbers of bacteria are controlled by spatial rather than nutritional limitations. The total bacterial numbers were slightly higher when quantified by qPCR than by culturing; this may be explained by the detection of uncultivable and non-viable species using universal primers. However, this explanation may be too simple as the universal primers are based on the 16S rRNA gene which can be present in multiple copies in certain bacterial species (up to 14 copies per species) (Farrelly *et al.* 1995). Therefore, this may also account for the differences between the traditional cultivation quantification and the qPCR studies.

Kolenbrander *at al.* (2002) stated that the development of a supragingival biofilm is a series of events involving early colonisers bridging the inclusion of the intermittent and secondary colonisers. Therefore, the *Streptococcus* spp. species considered as early colonisers decrease in numbers as *Veilonella* and other intermittent colonisers increase in numbers as the oral biofilm matures (Walker & Sedlacek 2007). In terms of the early colonisers detected in this study, the numbers of *S. sanguinis* showed variation among units in the individual experiments. The results obtained for *V. dispar* from experiment 2 showed an increase in numbers of *V. dispar* in disease among the units with only the change in unit 3 being considered as significant. Experiments 1 showed a non-significant decrease between the health-disease conditions among the units. *S. mutans* was not detected in any of the biofilm samples. This may be explained by the fact that bacteria associated mostly with dental caries require different

nutritional requirements that have not been met in this experimental set-up. It has also been claimed by Marsh *et al.* that mutants streptococci have low adherence properties in the absence of sucrose (Marsh & Martin 1999). With regards to *N. subflava*, there was a descending pattern recorded for all units in both experiments. However, only changes in unit 2 in experiment 1 and 2 were considered as statistically significant.

Despite the fact that previously published and successfully applied gingivitis methodology was followed, there was no clear separation between oral health and disease conditions in terms of the gingivitis associated bacteria such as *F. nucleatum*, *A. neaslundi* and *P. intermedia*. *A. neaslundii* also showed no significant difference in bacterial numbers across the change from health to gingivitis. There was an increase in numbers of *F. nucleatum* in gingivitis conditions for all of the units in both experiments (except unit 2, experiment 1) of which only the changes in units 1 and 3 (experiment 2) were statistically significant. *P. intermedia* was detected in low numbers and there was no significant difference in growth across the health and gingivitis condition in both T-CDFE experiments.

Generally speaking, the data obtained were inconclusive and did not follow the bacterial shifts previously reported by Dalwai *et al.* (Dalwai *et al.* 2006; Dalwai *et al.* 2007). There was no observed ascendancy of *Actinomyces* spp. (i.e. *A. naeslundii*) at the expense of *Streptococcus* spp. (i.e. *S. sanguinis*) under gingivitis condition and Gram-negative bacteria from the orange and red complex such as *F. nucleatum* and *P. intermedia* were found in low numbers. The latter could potentially be improved by extending the experimental duration and allowing longer exposure to gingivitis conditions to allow the biofilm to favour Gram-negative bacteria.

The other possible explanation for the lack of bacterial shifts may include the experimental differences between the results obtained from this study and the results of Dalwai *et al.* (Dalwai *et al.* 2006; Dalwai *et al.* 2007). The main difference between this and the previous work was that the latter used a different experimental *in vitro* model, the standard CDFE. Also, in the study by Dalwai *et al.*, different post-

experimental techniques were used which included Gram-negative selective medium instead of non-selective media targeting anaerobes and aerobes and also different primer chemistry and selection (Dalwai *et al.* 2006; Dalwai *et al.* 2007).

Regarding the T-CDFF *in vitro* model, the conceptual and mechanical operation is identical to the CDFF. However, due to the fact that T-CDFF was designed to run three CDFFs concurrently, it was significantly scaled down and modified to improve the handling and manoeuvrability of the fermentor (see Table 2.1, Chapter 2). Therefore, although the two models have the same cylindrical shape, they have different diameters and this resulted in different volumes, working areas and hydraulic retention times (HRT) as presented in Table 4.6 below.

| Model | CDFF | T - CDFFF |
|------------|------|-----------|
| Volume (V) | | |

Where:

V= Volume.

r=radius

H=height of the cylinder

| Model | CDFF | T - CDFFF |
|-----------------------|------|-----------|
| HRT health conditions | | |

Where:

HRT = hydraulic retention time

Table 4.6 present the volumes and hydraulic retention times calculated for both CDFF and T-CDFF.

These parameters have an unknown influence on the physio-chemical environment created in the model and may have influenced the outcomes and accounted for differences in the data. Additionally, the clearance of delivered substances and metabolic waste products is a function of flow rate and volume (Guggenheim *et al.* 2001). In my case, both models used the same flow rates, but have different volumes and working areas as seen in Table 4.6. This may have directly affected the clearance

of the pulsed substances and then subsequently the biofilm growth. It might be the case that extending the incubation periods or providing a higher volume of artificial GCF would accelerate the process of developing gingivitis *in vitro*.

Another possible difference is that, the ascendancy of *Actinomyces* spp. over *Streptococcus* spp. in gingivitis conditions was modelled by Dalwai and colleagues (Dalwai *et al.* 2006) using different bacterial species, primer sets and different qPCR chemistry. Dalwai *et al.* used the SYBYR green primers for *A. naeslundii* and *Streptococci* and ABI PRISM (PE Applied Biosystems) as the qPCR detection platform (Dalwai *et al.* 2007). In the present study, I used the Taqman qPCR primers for *A. naeslundii* and *S. sanguinis* with a different platform which was Rotor-gene 6500 (QIAGEN) to model the *S. sanguinis* and *A. naeslundii* crossover. The above-mentioned differences may have an indirect influence on my work.

4.4.4 Functional approach to investigate the gingivitis associated shifts

A functional approach was applied to provide additional information about the ecological changes within the microbial community. Two metabolic assays, alkaline phosphatase (ALPase) and trypsin-like-protease (TLPase), were chosen. The activity of these enzymes is positively correlated with periodontal diseases (Shibata *et al.* 1994; Narang *et al.* 2013). Additionally, certain Gram-negative periodontal pathogens have been shown to have high ALPase and TLPase activity using the API ZYM System (Hoover *et al.* 1992; Shibata *et al.* 1994; Narang *et al.* 2013). As trypsin-like enzymes are associated with proteolytic enzyme producers belonging to red complex bacteria (such as *Porphyromonas gingivalis* or *Treponema denticola* and others), the TLPase assay was used to trace their activity and to determine the virulence of the biofilms produced in my models (Waddington & Embery 1994; Sockransky & Haffajee 2005). ALPase is considered a periodontal biomarker as it is correlated with bacterial load increase and gingivae inflammation. A longitudinal study on 8 patients performed by Binder *et al.* showed that bacterial ALPase has a strong correlation with inflammation and can be used as a diagnostic indicator for periodontal diseases (Binder *et al.* 1987).

With regard to the results presented in this chapter, trypsin-like-protease activity was not detected under either health or gingivitis conditions. This suggests that the developed microbial community is either (i) lacking proteolytic periopathogens or (ii) they are too small in proportion to be detected using enzyme assays or (iii) the assay is not sensitive enough to detect the TLPase producers in a complex community. Specifically, as the assays' effectiveness was previously tested using a suspension containing a high concentration of *P. gingivialis* while the T-CDFF biofilm samples are a mixture of diverse bacterial species of a much lower load. ALPase activity has been demonstrated by a range of bacteria including *P. gingivalis*, *P. intermedia*, *P. nigrescens*, *C. ochracea*, *S. sanguinis* and *S. oralis*. However, the enzymatic activity data presented in this chapter were inconclusive as in most cases there was (i) no enzymatic activity detected or (ii) the enzymatic activity was very weak compared with the activity obtained from the ALPase assay performed on a single species biofilm of *P. gingivalis*. Additionally, there was no enzymatic activity pattern among the units and the differences among the health-disease phase were variable and statistically insignificant. Therefore, the enzymatic data showed no repeatability among the units in the individual T-CDFF experiments. The functional approach should be verified by repeating these experiments.

4.4.5 Reproducibility of the bacterial shifts in the T-CDFF model

The experimental T-CDFF methodology was designed so as to maintain the highest reproducibility among the units (Chapter 2, Section 2.2.1). In the set of experiments presented in this chapter, the standardised artificial saliva and a multi-channel pump were used to increase the reproducibility of nutrient delivery and subsequently ensure the most reproducible environment among the units. To investigate the repeatability of the T-CDFF model, complex univariate Analysis of Variance with a post hoc Bonferroni multiple comparisons correction was applied to the qPCR and culture data for total aerobes and anaerobes to verify the repeatability among T-CDFF units across different experimental conditions and sampling events.

Univariate ANOVA analysis applied to the qPCR data showed no significant differences among the units in single or individual experiments in terms of total number of bacteria present. The same results were seen for 3 bacterial species including *A. naeslundii*, *P. intermedia* and *S. sanguinis*. In terms of *F. nucleatum* and *V. dispar*, the T-CDFF units showed repeatability only in experiment 1; while *N. subflava* showed no repeatability among units in either single or separate T-CDFF experiment. The same statistical analysis applied to culture data for total anaerobes and aerobes showed no significant difference among units in either single or individual T-CDFF experiments.

Despite relatively high variation in data collected from different sampling points there was a consistent growth trend across units for most bacterial species. Though, the statistical analysis confirmed no significant difference among units in most cases. Based on this one could postulate that the model shows a degree of repeatability. This assumption can be supported by: (i) there is an actual high degree of repeatability among units or (ii) the statistical analysis could not discriminate the difference among units due to high variability; leading to the statistics showing no significant difference between units. It is also important to mention that biological fermentors such as T-CDFF are prone to high data variability in general; this is because they are complex models which are affected by many factors including experimental, environmental or human errors. Therefore, to obtain a better prediction and to minimise the effect of variability on my data, a greater number of experimental replicates would be required ($n \geq 3$).

Another thing worth mentioning is that reproducibility by definition is termed as 'degree of agreement between the measurements or observations conducted on replicate specimen in different locations by different people' (Adamson *et al.* 2014). Until now only a few models have been reported as reproducible in growing oral biofilms including the Zurich model or CDFF (Sánchez *et al.* 2011). However, even these models, which are (i) less complicated experimentally and (ii) have been extensively used to model oral biofilm, have not been shown to be reproducible as per the definition mentioned above. According to the above mentioned definition, to ultimately confirm the hypothesis that the model enables the growth of the

reproducible oral community under health and gingivitis conditions, the reproducibility of this model would have to be verified by running it under the exact same experimental methodology by different operators and at different facilities.

4.5 Conclusion

In the previous chapter, Chapter 3, the T-CDFF model was validated and proven to work in a satisfactory manner – all three T-CDFF units followed the same growth trend. The current chapter focused on the development of a reproducible *in vitro* gingivitis model. The methodology presented in this chapter was structured to investigate the repeatability of the T-CDFF model and its ability to model ecological shifts associated with gingivitis progression. Although the growth among units in the individual T-CDFF experiments followed similar trends, the degree of variability was relatively high. High variability among the sampling points and low number of repetitions (only 2 individual T-CDFF experiments, n=2) influenced the statistical analysis which mostly showed no significant differences among the units. Thus, the results presented in this chapter are inconclusive and it can not be stated that the model is reproducible. To allow a better prediction and to minimise the effect of variability, a greater number of experiments should be performed. Additionally, there was no clear resolution between the health and gingivitis phases. This might have been caused by applying insensitive/wrong detection tools or by using unsuitable methodology. This approach will be re-validated in chapter 5 by applying the health/gingivitis methodology and testing the health-disease shift by ^1H NMR spectroscopy to fingerprint the metabolites produced in the T-CDFF model over time.

5 CHAPTER

Investigating gingivitis associated
shifts using the metabolomic
approach

5.1 Introduction

According to the Human Oral Microbiome Database (HOMD), the oral microbiome is composed of approximately 600 different species (Siqueira & Rôças 2013). Many of these bacteria are symbiotically present in varying degrees in both health and gingivitis (Huang *et al.* 2011) and there is no clear distinction between health and gingivitis. Despite the technological advances in the field of molecular biology that have allowed cost-effective high-throughput screening of oral biofilms, questions remain regarding the understanding of gingivitis pathogenesis (Goodacre 2007). As oral microorganisms live in a complex biofilm community, they are involved in a vast number of complex host-microbe and microbe-microbe interactions, so when environmental changes occur there is not only a taxonomic shift, but also metabolic and functional shifts (Goodacre 2007; Huang *et al.* 2014). All these changes have a direct effect on biofilm virulence and disease progression. Therefore, metabolic fingerprinting on both healthy and diseased microbiomes and understanding their function might be a way forward in understanding these complex interactions (Mashego *et al.* 2007; Pacchiarotta & Mayboroda 2012).

The major advantage of ^1H NMR metabolic fingerprinting, used in this chapter, is its robust, non-destructive, non-biased processing of multiple samples at once in both a qualitative and a quantitative manner (Serkova & Niemann 2006; Wishart 2008). The only disadvantages when compared with mass spectroscopy are: (i) a relatively lower sensitivity, (ii) higher cost and (iii) addition of deuterated solvents to adjust the pH and maintain the quality of the signal (Constantinou *et al.* 2007). Despite these few drawbacks, NMR has exceptional capacity to handle complex metabolite mixtures and simple sample preparation have made it a popular choice for metabolic profiling studies in the field of oral metabolomics (Cloarec *et al.* 2005; Wishart 2008).

As the ^1H NMR metabolomics approach provides a snapshot of the physiological state of the biological system, it was used in this chapter to determine the metabolites being produced throughout the change in environment. According to the literature search conducted, this is the first study using the ^1H NMR metabolomics to investigate the *in*

vitro gingivitis associated shifts using CDF model. Therefore, it was trialed in this chapter to verify whether this technique is applicable and can provide the desired research answers. A simpler and easier to operate CDF model was used instead of a complex T-CDF to test this technique before implementing it in the T-CDF model. The methodology was structured to combine previously applied techniques such as metabolic assays and quantitative PCR together with ^1H NMR spectroscopy. This approach allowed investigation of the usefulness of metabolomics in studying the physiological status of biofilm in conjunction with more traditional techniques that were used to study gingivitis *in vitro*.

5.2 Materials and Methods

5.2.1 CDF experimental set-up

The experimental set-up and scheme of work of all CDF experiments were performed according to the methodology described in Chapter 2, Section 2.2-2.3.

5.2.2 CDF experimental conditions

All the CDF experiments presented in this chapter were performed according to the description below in Figure 5.1.

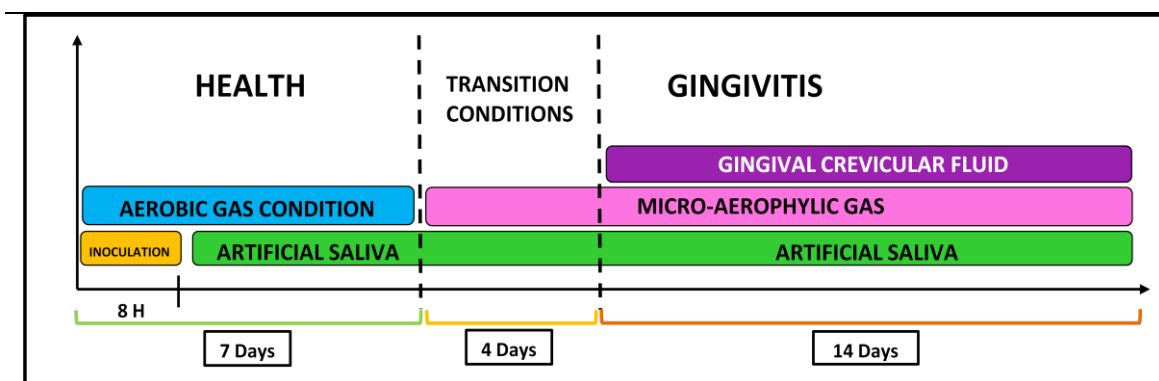


Figure 5.1 shows the experimental design of the CDF experiment.

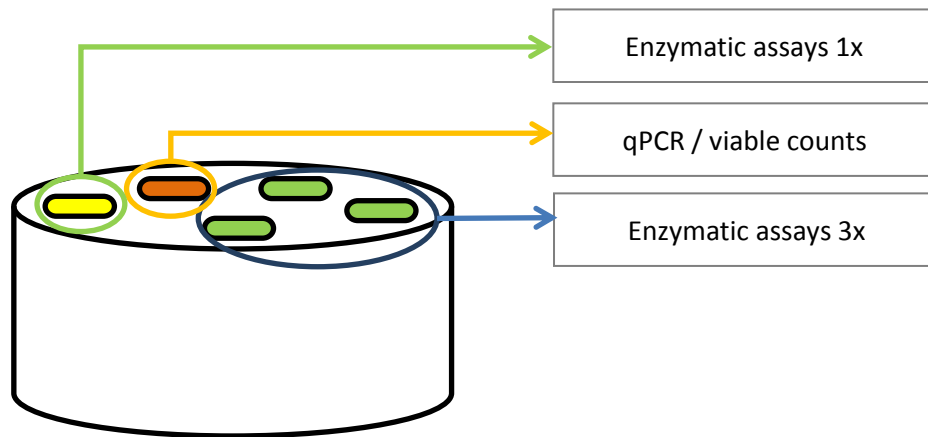
Each CDF experiment started with 8 hours inoculation with the microcosm population (Chapter 2, Section 2.3.1). After the inoculation, the model was exposed to health conditions for 7 days by providing aerobic conditions and the standardised artificial saliva formulation as a nutrient source (Chapter 2, Section 2.3.2). After the 7 days of health conditions, the model was exposed to ‘transition conditions’ that differed from health by providing micro-aerophilic gas [composition: 2% O₂, 3% CO₂, 95% N, at 200 bar] at 200 cm³ / min instead of aerobic gas conditions. After 4 days of transition conditions, the model was exposed to gingivitis conditions by continuing to provide micro-aerophilic gas and artificial saliva and adding the artificial GCF component.

5.3 CDF sampling

5.3.1 Biofilm

Biofilms retrieved from the CDF were sampled at fixed intervals throughout the 25 day experiment. Three biofilm samples were taken in health conditions at days 1, 5

and 7; a further two samples were collected during the gingivitis conditions at day 20 and 25 (Chapter 2, Section 2.3.5). During each biofilm sampling event, one pan was removed and analysed according to the description below (Figure 5.2).






| | |
|---|---|
|  | Biofilm from the yellow disc was resuspended in 1.0 mL of PBS (1x) and used for enzymatic assays such as ALPase and TLPase assay (Chapter 2, Section 2.7.1). |
|  | Biofilm from three discs was pooled and resuspended in 1.0 mL of PBS. Concentrated bacterial suspension (3x) was used for enzymatic assays such as ALPase and TLPase (Chapter 2, Section 2.7.1). |
|  | Biofilm from the orange disc was resuspended in 1.0 mL of PBS. 100 μ L was used for serial dilutions and plating on the FAA medium to determine the lack of contamination in the model (Chapter 2, Section 2.4). The DNA was extracted from the remaining 900 μ L according to the bead beating protocol and then followed by the qPCR analysis (Chapter 2, Section 2.5.1 and 2.5.2). |

Figure 5.2 presents the sampling pan with 5 discs, each designated for different analysis.

Additionally, two pans (10 discs in total) were removed in health (day 5) and disease conditions (day 17) for the metabolomics study using ^1H NMR spectroscopy (Chapter 2, Section 2.7.2). The biofilms obtained from the 10 discs were pooled, resuspended in 5.0 mL of PBS and stored at -20°C for the metabolomics study. The samples were processed according to the methodology described in Chapter 2, Section 2.7.2.

5.3.2 Effluent

The effluent from the CDFF was collected according to the methodology described in Chapter 2, Section 2.3.5. The effluent samples were collected every day and analysed

by the triplex qPCR (Chapter 2, Section 2.5.2) and culture methods to determine the lack of contamination in the model (Chapter 2, Section 2.4). The remaining effluent was analysed by ^1H NMR spectroscopy to investigate the metabolite profile change over time in relation to the microbial changes (Chapter 2, Section 2.7.2).

5.4 Post-experimental data analysis

5.4.1 Differences between health and disease

To investigate the differences in bacterial numbers in biofilm across the change in conditions from health to gingivitis, the qPCR data retrieved at day 5 and day 7 (health) were averaged, logged and compared with the averaged and logged data from day 20 and 25 (gingivitis). The data from sampling point 1 were excluded from the calculation of the health averages, as the cell numbers collected at day 1 were usually much lower than for the remaining 4 sampling points collected from mature biofilm.

To investigate the differences in bacterial numbers in effluent across the health / transition / gingivitis conditions, the qPCR data generated from each phase were averaged, logged and compared.

5.4.2 Statistical analysis

The qPCR and enzymatic data were analysed by the paired Student's t-test with the p - value set to 0.01 to ensure stringent hypothesis testing. The qualitative PCA and PLS analysis on raw NMR data was performed by Dr Michael Cannon (scientist at Procter&Gamble) using the Simca-P programme (UmetricsAB, Sweden). The additional statistical analysis on ^1H NMR data was not performed as only limited data were obtained from Procter & Gamble. Therefore, the results from this study will only give an indication of whether metabolomics can be used successfully for examining the gingivitis related shifts in the model.

5.5 Results

5.5.1 Bacterial shifts

5.5.1.1 Culture independent methods

Figure 5.3 shows the total number of bacteria detected in the biofilm and the effluent samples collected across the experimental phases in the CDFF experiment.

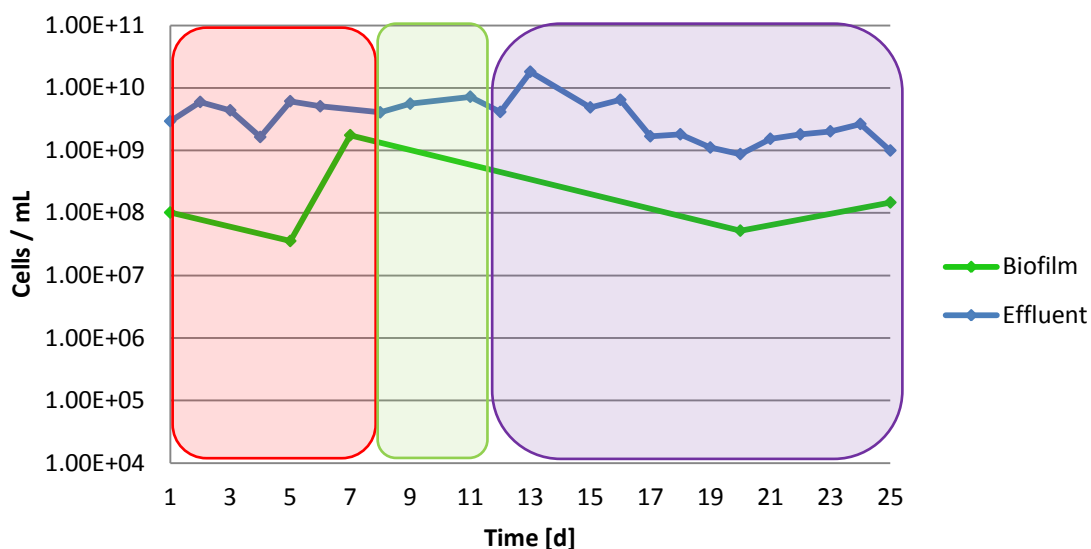


Figure 5.3 The total number of bacteria detected by triplex qPCR primers in the biofilm and the effluent samples collected throughout the health, transition and gingivitis conditions in the CDFF experiment. Health conditions are shown in **red**, transition in **green** and gingivitis in **blue**. **Blue line** shows the total number of cells in the effluent samples; **green line** shows the total number of cells in the biofilm samples ($n = 3$). * $n=3$ refers to three technical replicates

The transition conditions were introduced after 7 days of health and lasted for 4 days. Then gingivitis conditions were introduced for another 14 days. To determine the differences in the total counts across the experimental condition, the data points from each condition were averaged and compared as explained in Section 5.4.1. Following the change in conditions from health to gingivitis states, there was a decrease (approx. 0.40) in total numbers of bacteria in the biofilm samples. In terms of the effluent data, there was no obvious difference between health-transition, transition-gingivitis or health-gingivitis conditions. The variation among the effluent data points was high and

probably related to the problem with collecting a uniformly heterogeneous effluent sample.

5.5.1.2 Bacteria implicated in gingivitis

Figure 5.4 to 5.6 presents the total number of the gingivitis associated species such as *F. nucleatum* (Figure 5.4), *P. intermedia* (Figure 5.5) and *L. casei* (Figure 5.5) in the CDFF experiment.

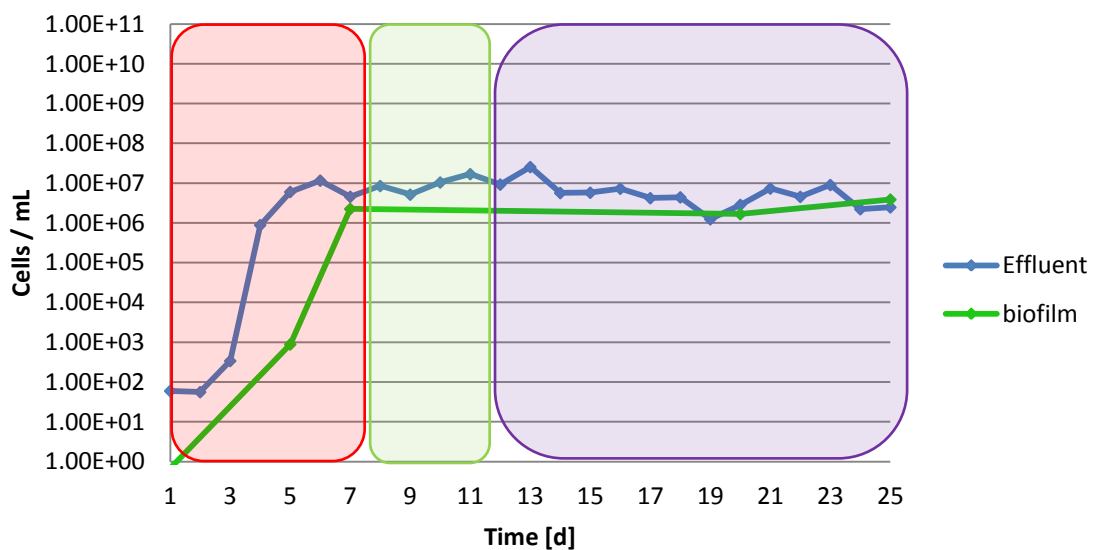


Figure 5.4 shows the total numbers of *F. nucleatum* detected by triplex qPCR primers in the biofilm and the effluent samples collected throughout the health, transition and gingivitis conditions in the CDFF experiment. Health conditions are encircled in red, transition in green and gingivitis in blue. Blue line shows the total number of cells in the effluent samples; green line shows the total number of cells in biofilm samples (n = 3). *n=3 refers to three technical replicates

A logarithmic growth increase was observed in the first 7 days of the experiment for both the biofilm and the effluent samples. After the initial increase and growth maturation, the total numbers of *F. nucleatum* detected in the biofilm and the effluent reached approximately 1.0×10^6 - 1.0×10^7 cells / mL and seemed unaffected by the alteration of the experimental conditions from transition to gingivitis conditions.

Figure 5.5, presents the total number of *P. intermedia* across the health, transition and gingivitis conditions detected both in the biofilm and the effluent samples in the CDFE experiment.

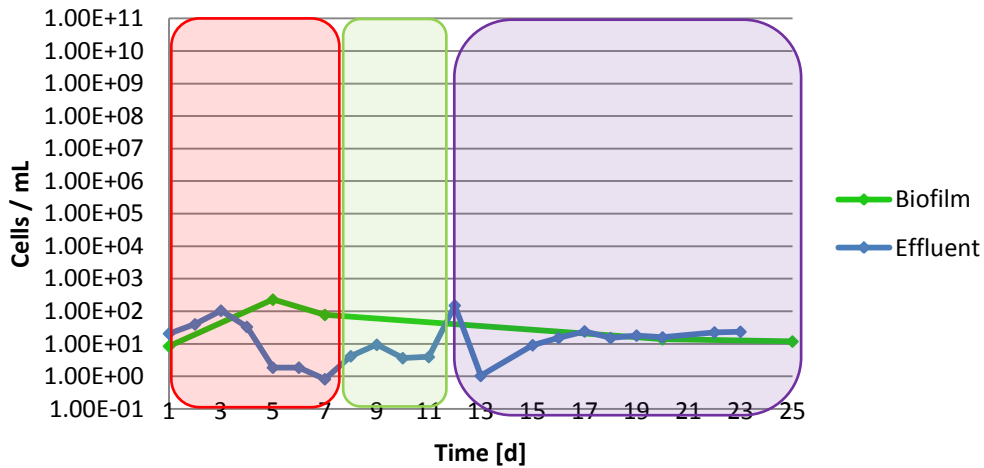


Figure 5.5 shows the total numbers of *P. intermedia* detected by triplex qPCR primers in the biofilm and the effluent samples collected throughout the health, transition and gingivitis conditions in the CDFE experiment. Health conditions are encircled in red, transition in green and gingivitis in blue. Blue line shows the total number of cells in the effluent samples; green line shows the total number of cells in biofilm samples (n = 3). n=3 refers to three technical replicates

The numbers of *P. intermedia* detected in the biofilm and the effluent samples were low and variable across the sampling points with no particular growth trend observed. *P. intermedia* was not detected in the effluent on the last day of the experiment.

Figure 5.6 shows the numbers for *L. casei* detected in both the biofilm and the effluent samples collected from the CDFE experiment.

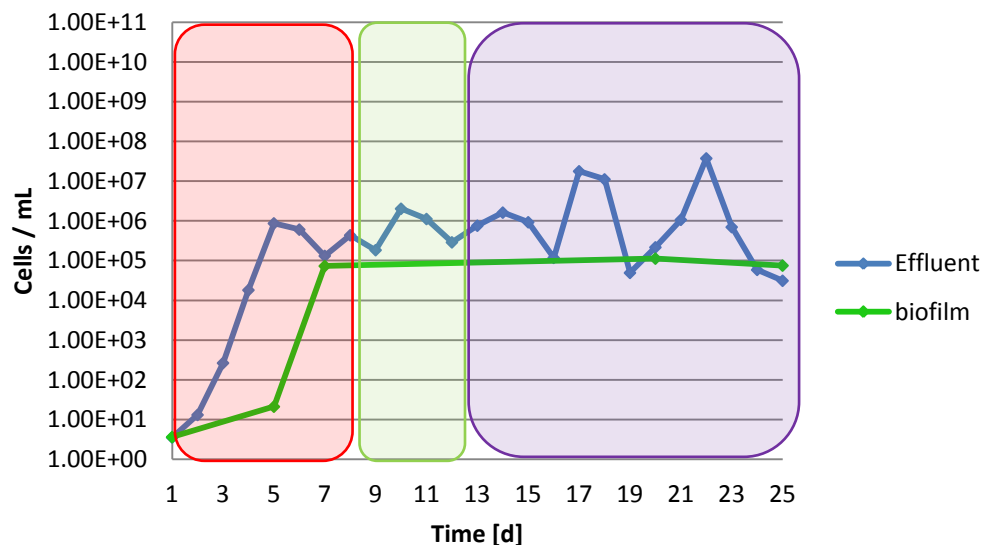


Figure 5.6 shows the total numbers of *L. casei* detected by triplex qPCR primers in the biofilm and the effluent samples collected throughout the health, transition and gingivitis conditions in the CDFE experiment. The health conditions are encircled in **red**, transition in **green** and gingivitis in **blue**. **Blue line** shows the total number of cells in the effluent samples; **green line** shows the total number of cells in the biofilm samples (n = 3). n=3 refers to three technical replicates

L. casei showed a similar growth pattern to *F. nucleatum*; it started with a logarithmic growth increase in cell numbers and was followed by biofilm maturation on day 7. The change in conditions from health to gingivitis did not seem to affect the *L. casei* numbers that stayed at the same level of around 1.0×10^5 cells / mL. The effluent followed a similar growth pattern initially but with much higher variation among the sampling points and no particular growth change across the experimental phases.

5.5.1.3 The *Actinomyces* spp. - *Streptococcus* spp. cross-over

This Section presents the data for *A. naeslundii* and *S. sanguinis* retrieved from the biofilm and the effluent samples throughout the different experimental phases in the CDFE experiment. Figure 5.7 presents the *A. naeslundii* - *S. sanguinis* growth relation observed in the biofilm samples collected at different time points throughout the health, transition and gingivitis conditions.

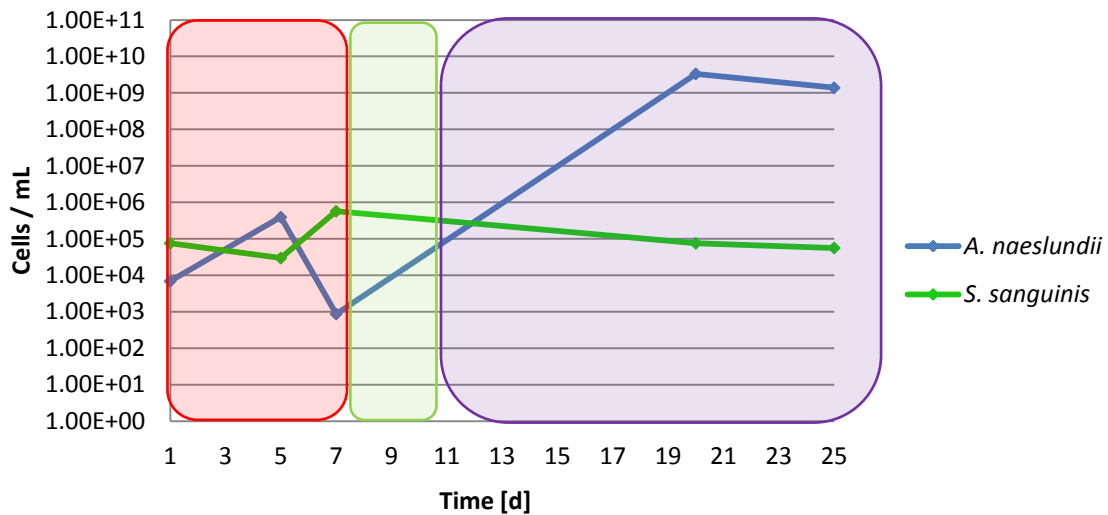


Figure 5.7 presents the cell numbers for *A. naeslundii* (blue line) and *S. sanguinis* (green line) detected by triplex qPCR primers in the biofilm samples collected throughout the health, transition and gingivitis conditions from the CDFF experiment. The health conditions are encircled in red, transition in green and gingivitis in blue. Error bars represent the standard deviations ($n = 3$). $n=3$ refers to three technical replicates

Figure 5.7 presents the cross-over between the *S. sanguinis* and *A. naeslundii* numbers during the change in the experimental conditions. There was approximately a 3.73 log increase in numbers of *A. naeslundii* across the change in conditions versus a relatively stable growth of *S. sanguinis*. However, the variation in cell numbers for both species especially under the health conditions was noticeable.

Figure 5.8 presents the amount of *S. sanguinis* and *A. naeslundii* and the cross-over between these two species in the effluent samples retrieved from the different experimental phases.

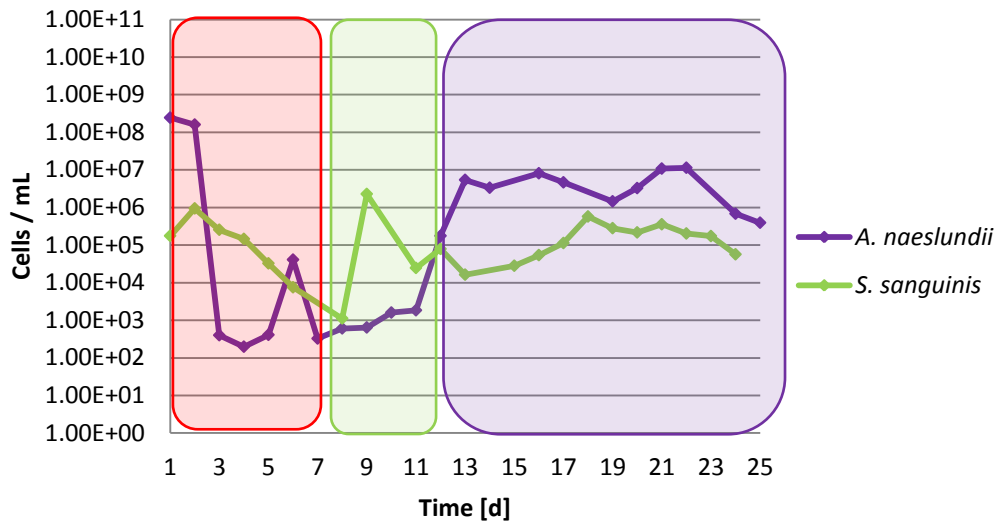


Figure 5.8 presents the cell number for *A. naeslundii* (violet line) and *S. sanguinis* (light green line) detected by triplex qPCR primers in the effluent samples collected throughout the health, transition and gingivitis conditions from the CDFE experiment. The health conditions are encircled in red, transition in green and gingivitis in blue ($n = 3$). $n=3$ refers to three technical replicates

There was a high variation in cell numbers for both species across health and transition conditions. After the introduction of gingivitis conditions, there was an ascendancy of *A. naeslundii* with an average of 1.37 log higher cell numbers in comparison with *S. sanguinis* ($p \leq 0.01$).

5.5.1.4 Bacteria implicated in oral health

Table 5.1 and Table 5.2 show the total numbers for *N. subflava*, *V. dispar*, and *S. mutans* in both the biofilm and the effluent samples at different time intervals throughout the health, transition and gingivitis conditions.

| Strain | <i>N. subflava</i> [cells / biofilm] | <i>V. dispar</i> [cells / biofilm] | <i>S. mutans</i> [cells / biofilm] |
|----------|---|---------------------------------------|---------------------------------------|
| Time [d] | Average | Average | Average |
| 1 | 4.11E+00 | 4.81E+02 | ND |
| 5 | 4.31E+01 | 5.81E+06 | 1.01E+03 |
| 7 | 1.34E+01 | 1.24E+08 | 9.74E+01 |
| 20 | 4.11E+00 | 1.13E+07 | 9.82E+04 |
| 25 | 7.66E+00 | 8.14E+06 | 1.01E+04 |

Table 5.1 The total number of health associated bacteria detected by triplex qPCR primers in the biofilm in the CDFF experiment. The average for each species is calculated based on three technical replicates (n=3). ND - not detected. Blue line indicates the change in conditions. Samples collected at day 1, 5 and 7 were retrieved from health, while samples from day 20 and 25 were retrieved from gingivitis conditions.

N. subflava was detected in very low numbers with no particular growth pattern across the phases. After the initial growth increase of *V. dispar*, there was a 0.45 log decrease in cell numbers in gingivitis conditions. *S. mutans* was not detected at the first sampling point. Its presence was recorded from day 5 onwards with a 2.0 log increase in gingivitis conditions versus the health.

Table 5.2 presents the numbers for health associated bacteria detected in the effluent samples over time.

| Strain | <i>N. subflava</i> | | <i>V. dispar</i> | | <i>S. mutans</i> | |
|----------|--------------------|-------|------------------|-------|------------------|-------|
| | [cells / mL] | | [cells / mL] | | [cells / mL] | |
| Time [d] | Average | Stdev | Average | Stdev | Average | Stdev |
| 1 | 2.24E+03 | | 6.40E+05 | | 1.49E+07 | |
| 2 | 1.89E+05 | | 2.24E+07 | | 1.68E+07 | |
| 3 | 3.86E+04 | | 4.44E+07 | | NDA | |
| 4 | 9.43E+03 | | 3.08E+07 | | NDA | |
| 5 | 2.42E+04 | | 9.61E+07 | | NDA | |
| 6 | 1.13E+04 | | 9.17E+07 | | NDA | |
| 7 | 1.09E+04 | | 3.55E+07 | | 8.98E+07 | |
| 8 | 1.79E+03 | | 1.14E+08 | | 1.08E+06 | |
| 9 | 1.29E+03 | | 4.91E+07 | | 3.21E+07 | |
| 10 | 1.00E+04 | | 4.19E+07 | | 1.69E+08 | |
| 11 | 1.93E+03 | | 3.22E+07 | | 4.26E+07 | |
| 12 | 2.93E+03 | | 2.84E+07 | | 3.66E+07 | |
| 13 | NDA | | 7.50E+07 | | 1.62E+08 | |
| 14 | NDA | | 2.67E+08 | | 9.25E+07 | |
| 15 | NDA | | 4.75E+07 | | 2.13E+08 | |
| 16 | 1.70E+03 | | 7.00E+07 | | 1.49E+06 | |
| 17 | 6.24E+02 | | 2.26E+07 | | 6.58E+07 | |
| 18 | NDA | | 3.15E+07 | | 4.74E+07 | |
| 19 | 1.22E+02 | | 1.97E+07 | | 2.28E+07 | |
| 20 | 2.54E+02 | | 1.96E+07 | | 1.12E+07 | |
| 21 | 9.96E+01 | | 3.21E+07 | | 2.52E+07 | |
| 22 | 2.84E+02 | | 2.77E+07 | | 4.04E+07 | |
| 23 | NDA | | 3.64E+07 | | 1.77E+07 | |
| 24 | 2.47E+02 | | 2.76E+07 | | 8.42E+05 | |
| 25 | 2.41E+01 | | 1.53E+07 | | 6.35E+06 | |

Table 5.2 shows the total number of the health associated bacteria detected by triplex qPCR primers in the effluent samples. The average for each species is calculated based on three technical replicates (n=3). NDA – no data available. Red line indicates the introduction of transition conditions at day 7; Blue line indicates the introduction of gingivitis conditions at day 12.

N. subflava reached a relatively constant growth at day 5-7 of around 1.0×10^4 cells / mL and then generally continued to decrease under the transition and gingivitis conditions (not detected at day 13-15 and days 18, 23) reaching a 1.8 log decrease in comparison with health conditions. *V. dispar* reached high numbers in the CDF experiment with no obvious difference between the health-transition, transition-

gingivitis, health-gingivitis conditions. The cell number for *S. mutans* increased in transition and gingivitis phase versus the health phase.

5.6 *In vitro* gingivitis modelling – a functional approach

5.6.1 Enzymatic assays

ALPase and TLPase metabolic assays were performed on biofilm retrieved from the CDFF experiment at different sampling points. The data for TLPase activity is not shown as no activity was detected in biofilm samples in either single or concentrated biofilm suspension.

Table 5.3 presents the data obtained for alkaline phosphatase activity of a single biofilm suspension (from 1 disc) and a concentrated biofilm suspension (from 3 discs) retrieved at different time points throughout the CDFF experiment.

| Time [d] | Alkaline phosphatase activity [Δ OD / h] | |
|----------|--|-------------|
| | 1x Δ | 3x Δ |
| 1 | 0.048 | 0.06 |
| 5 | 0.06 | 0.12 |
| 7 | 0.18 | 1.02 |
| 20 | 0.06 | 0.06 |
| 25 | 0.0 | 0.06 |

Table 5.3 The ALPase activity in the biofilm collected at different time points. The enzymatic assay was performed on a single (1x) and concentrated biofilm suspension (3x). Δ – delta activity over time (n=2). n=2 refers to two technical replicates

The alkaline phosphatase activity was monitored at each sampling point. The ALPase activity of biofilm samples retrieved from each sampling point was monitored for 120 min. The results [Δ OD / hour of assay duration] showed that the biofilm suspension retrieved from 3 discs had higher enzymatic activity than the single-disc bacterial suspension but the enzymatic activity was very low and showed no particular activity change across the conditions.

5.6.2 ^1H NMR Metabolomics approach

The metabolite fingerprinting study using ^1H NMR spectroscopy was applied to the biofilm and the effluent samples retrieved from the CDFE experiment. A post-experimental qualitative PCA analysis was used to analyse the NMR profiles obtained from health and gingivitis state (Figure 5.9).

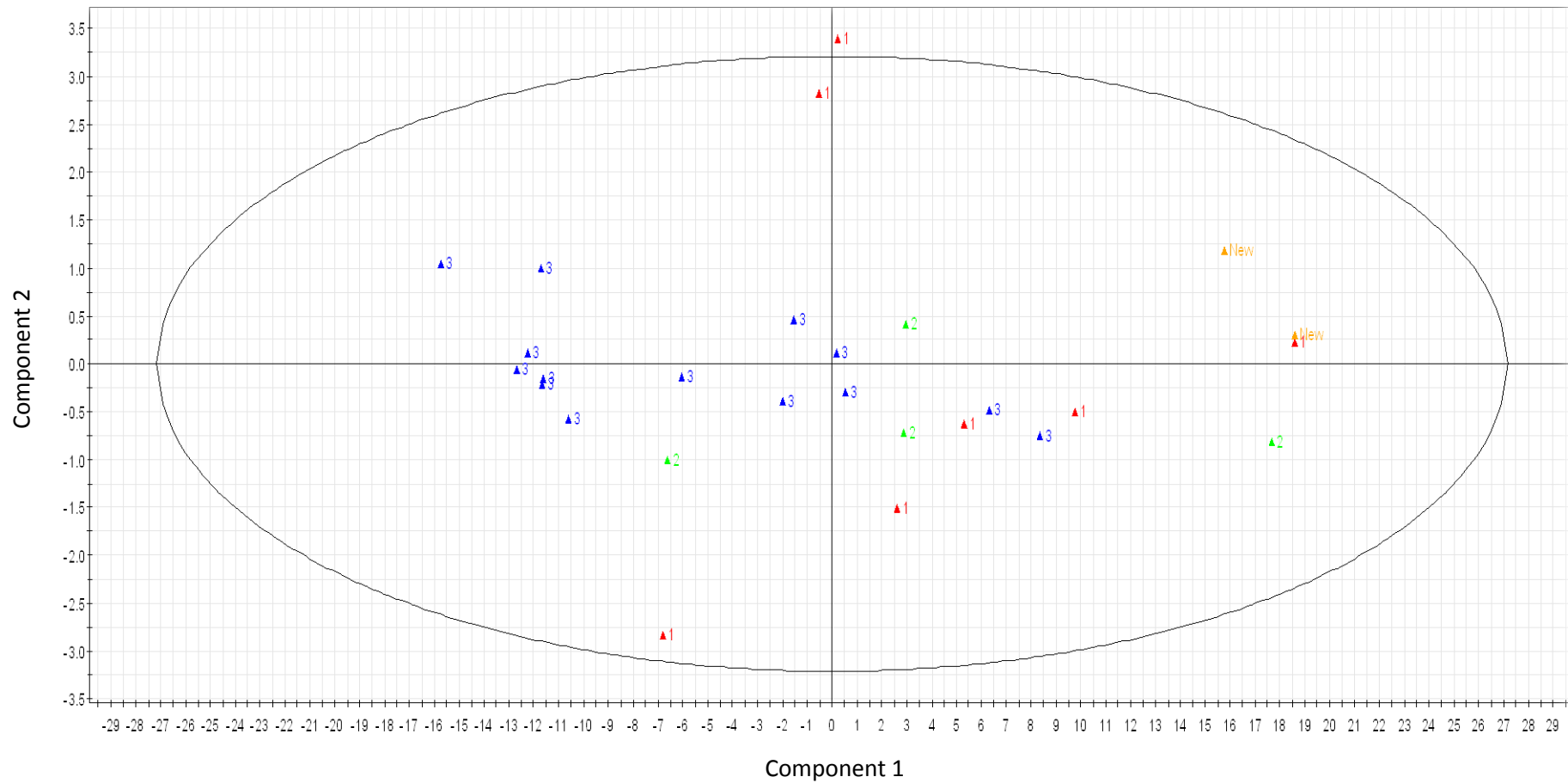


Figure 5.9 shows the PCA analysis applied to the biofilm and the effluent samples. Two biofilm samples (health and disease) are marked as 'New' and highlighted in orange. The effluent samples are highlighted in red, green and blue according to the experiment phase (1-red=health, 2-green=transition, 3-blue=gingivitis). PCA analysis and this Figure were performed by Dr Michael Cannon (Procter & Gamble).

Figure 5.9 presents the post-experimental PCA analysis applied to the NMR data. The biofilm samples, shown in orange, were removed from any further PCA analysis (see Figure 5.10), since (i) they did not follow the effluent distribution, and (ii) their presence skewed the PCA analysis and the separation patterns across the phases.

After the removal of the two biofilm samples, Figure 5.10 showed an improved outcome for the effluent samples as they have shown a higher degree of clustering than previously, as seen in Figure 5.9. The within cluster variation is due to the fact that the change from health to disease takes the form of a gradual change in metabolite levels, rather than a phase transition at a specific time. Thus, the orthogonal PLS analysis performed on this data set showed that the clustering pattern is growth dependent and increases over time throughout the study (Figure 5.11).

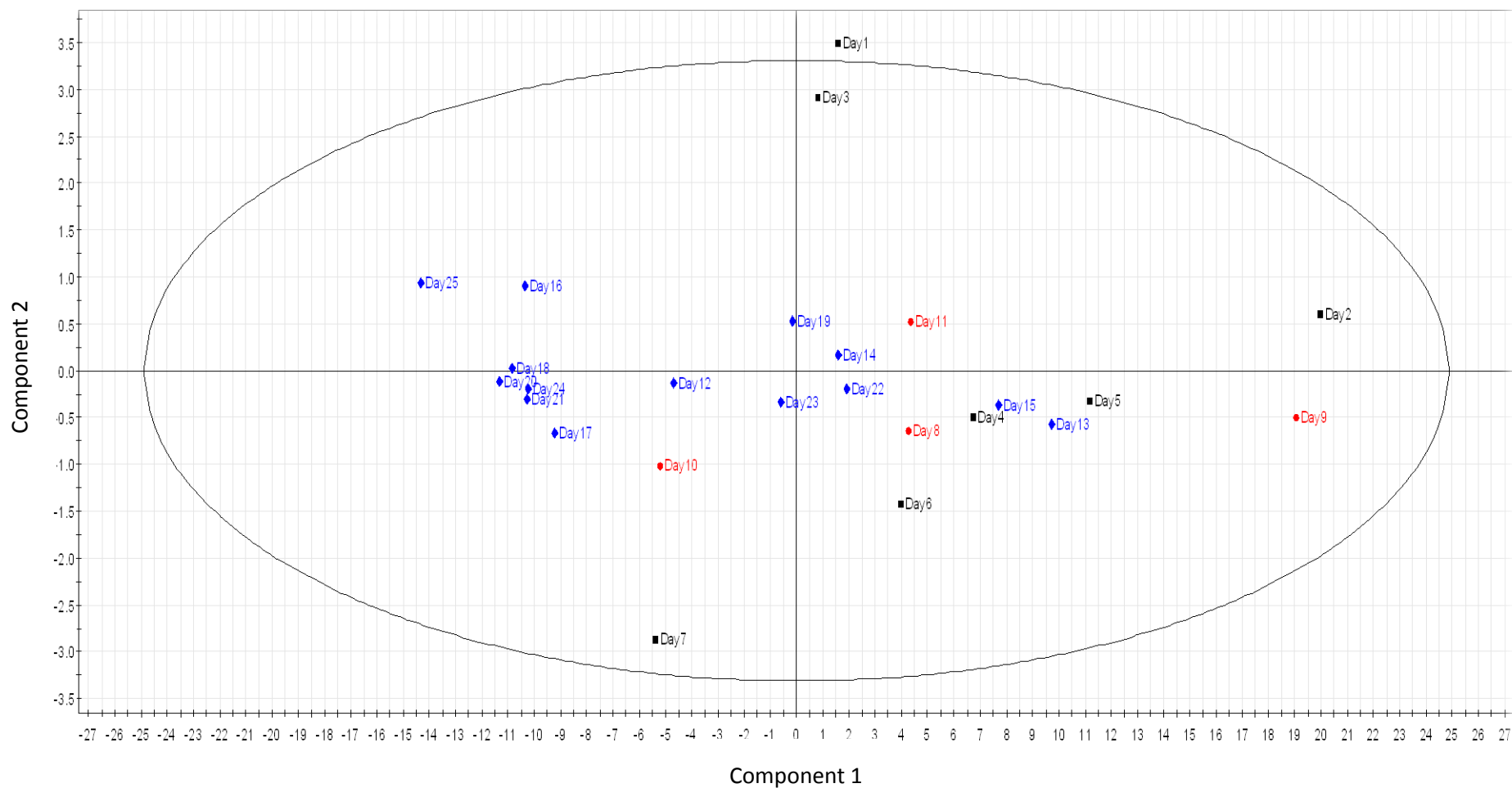


Figure 5.10 shows the PCA analysis applied to the effluent samples only. Samples are highlighted according to the experimental phase (1-black=health, 2-red=transition, 3-blue=gingivitis). PCA analysis and this Figure were performed by Dr Michael Cannon (Procter & Gamble).

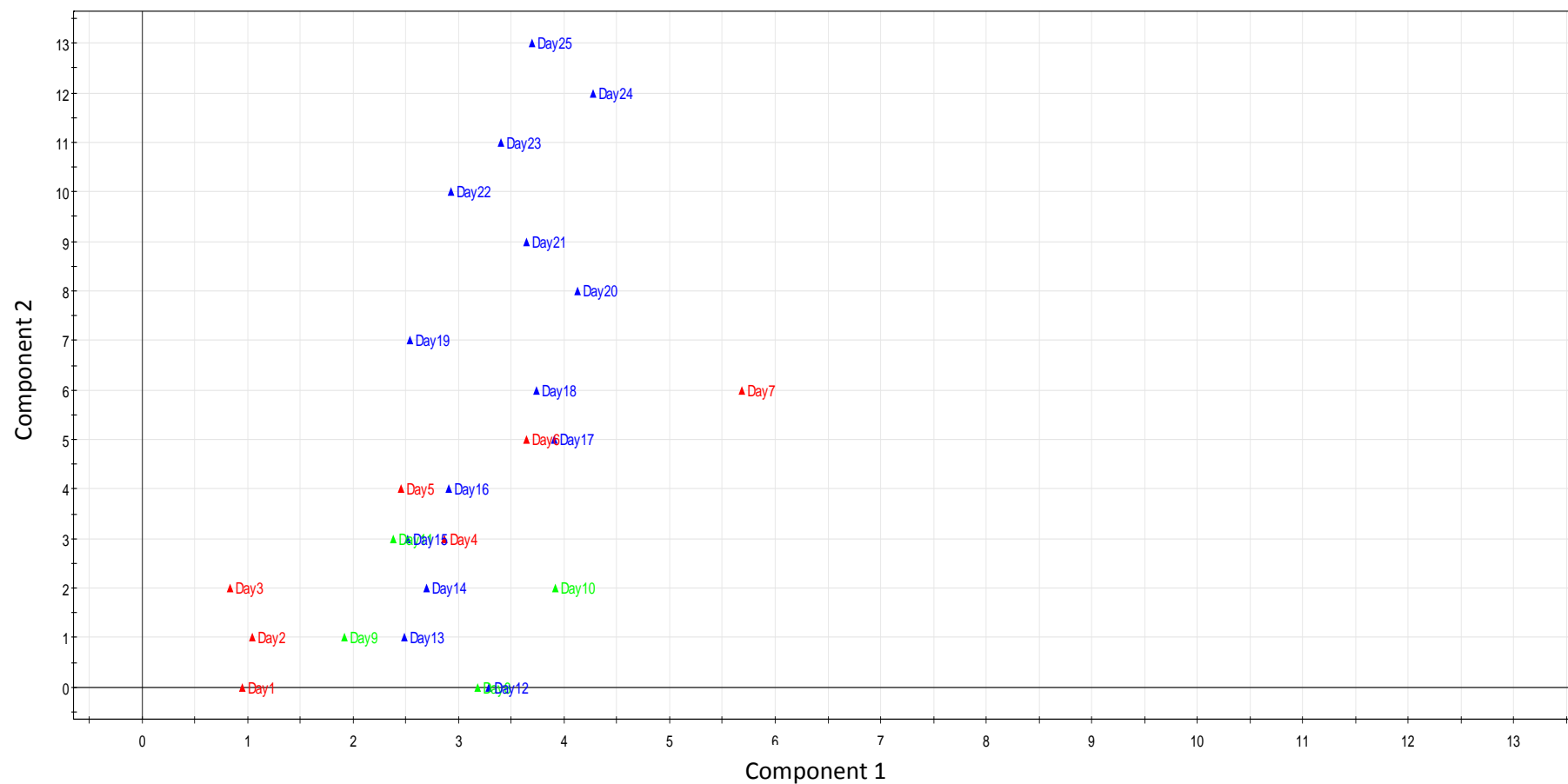


Figure 5.11 shows the orthogonal PLS analysis applied to the effluent samples and how the analysis is growth dependent. Samples are highlighted according to the experimental phase (1-red=health, 2-green=transition, 3-blue=gingivitis). OPLS analysis and this Figure were performed by Dr Michael Cannon (Procter & Gamble).

The orthogonal PLS composition analysis applied to the effluent samples showed that the clustering is growth dependent and that the components discriminating the health-transition-gingivitis phases included propionate and butyrate, and ethanol. There was an increase in propionate and butyrate as opposed to a decrease in ethanol levels in disease conditions.

Figures 5.12-5.14 presented below, show the change in propionate (Figure 5.12), butyrate (Figure 5.13) and ethanol levels (Figure 5.14) throughout the health-transition-gingivitis conditions.

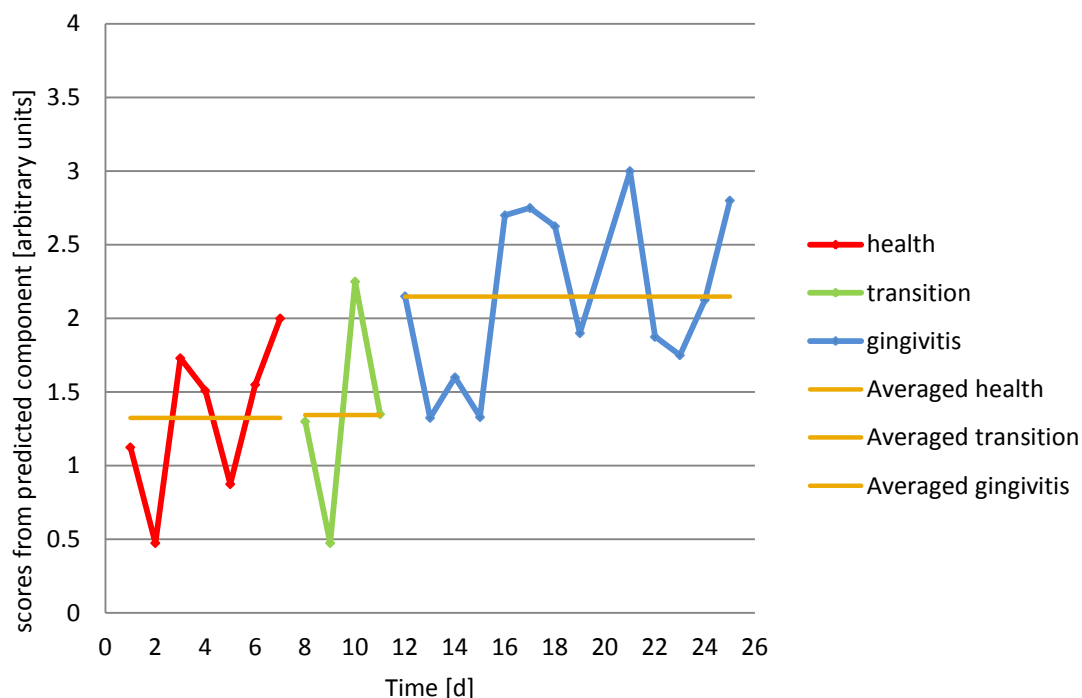


Figure 5.12 presents the change in propionate levels across the experimental phases. Health conditions – **red line**, transition conditions – **green line**, gingivitis conditions – **blue line**. The averaged health, transition and gingivitis lines represent the differences among the conditions.

The qualitative data presented in Figure 5.12 showed an increase in the levels of propionate throughout the course of the experimental conditions with the highest propionate levels in gingivitis conditions. The transition phase showed similar propionate levels to those seen in health conditions and the introduction of micro-aerophilic gas at day 7 had no noticeable effect on the levels of this metabolite.

Figure 5.13 presents the butyrate levels across the health-transition-gingivitis phases.

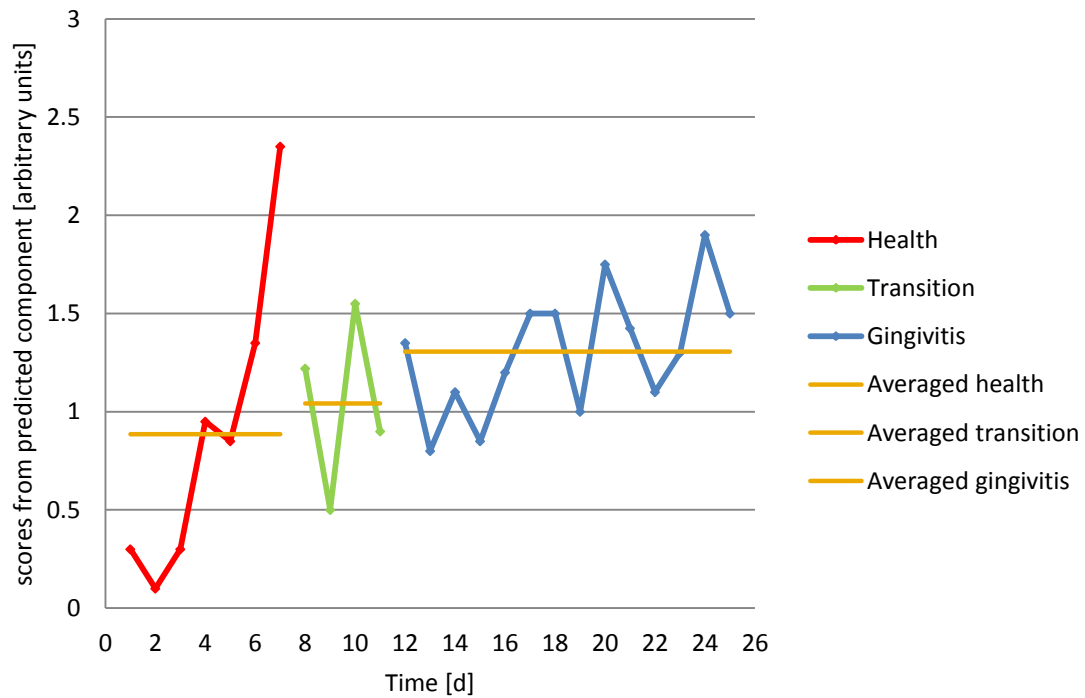


Figure 5.13 presents the change in butyrate levels across the experimental phases. Health conditions – **red line**, transition conditions – **green line**, gingivitis conditions – **blue line**. The averaged health, transition and gingivitis lines represent the differences among the conditions.

With the except of day 7 which seems to be an outlier with extraordinarily high butyric levels when compared to other sampling points in health, transition or gingivitis, on average there was an increase in butyrate levels in gingivitis conditions.

Figure 5.14 shows the levels of ethanol across the health-transition-gingivitis phases.

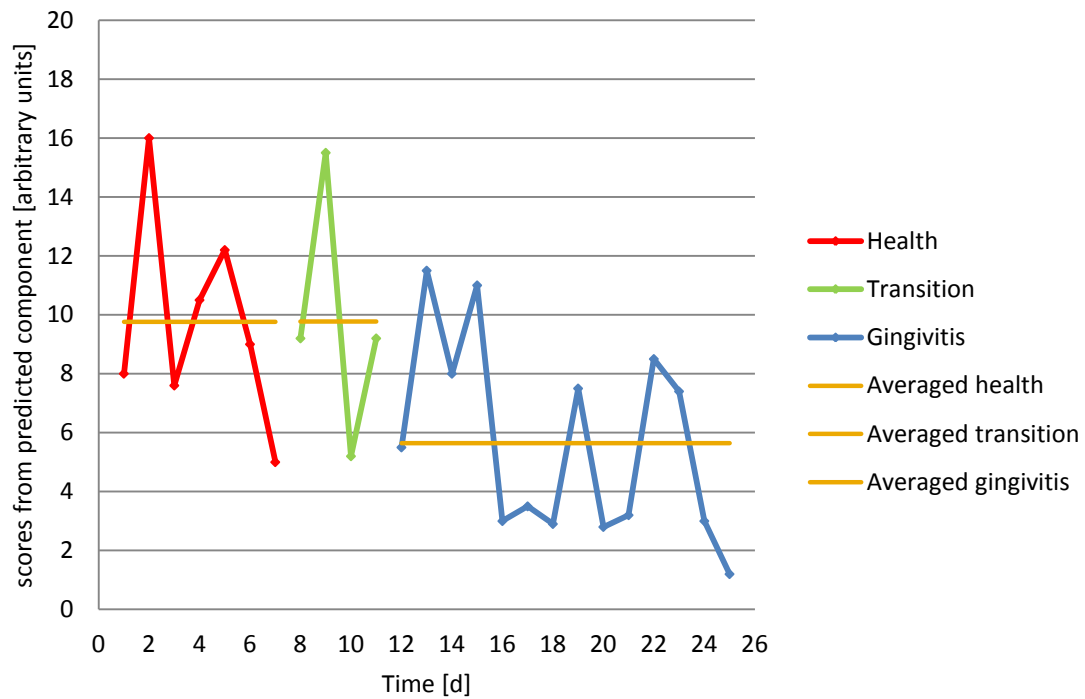


Figure 5.14 presents the change in ethanol levels across the experimental phases. Health conditions - **red line**, transition conditions - **green line**, gingivitis conditions - **blue line**. The averaged health, transition and gingivitis lines represent the differences among the conditions.

Throughout the course of 25 days of health, transition and gingivitis conditions, the ethanol levels fell constantly.

5.7 Discussion

Our current understanding of gingivitis aetiology derives mostly from extensive culture based characterisation performed on dental microbiota in the 1970s and 1980s (Slots 1977a; Slots 1977b; Socransky 1977; Tanner *et al.* 1979; Moore *et al.* 1982; Moore *et al.* 1983). These studies have shown major structural and compositional differences between the healthy and diseased microbiome (Moore *et al.* 1983). This led to identification of periodontal pathogens and classification of them into a colour coded system where orange and red complex bacteria were considered as strongly associated with gingivitis development. These two groups included e.g. *P. intermedia*, *F. nucleatum*, *P. gingivalis*, *T. denticola* and *T. forsythia* (Socransky & Haffajee 2005). As the concept of red, orange and other colour coded bacteria is still widely accepted, my study was based on these findings and included a primer selection for bacterial biomarkers classified as orange type bacteria (*F. nucleatum* and *P. intermedia* – gingivitis associated bacteria) (Hajishengallis & Lamont 2012). Additional biomarkers included *S. sanguinis* and *A. naeslundii* which are reported to have a cross depended relation across the health and gingivitis conditions and are indicative of gingivitis onset (Syed & Loesche 1978). Due to time and funding limitations, I was unable to develop primer sets for the red complex bacteria and other proteolytic bacteria associated with gingivitis. Therefore, the TLPase assay was introduced, as a surrogate for proteolytic producing bacteria (*P. gingivalis*, *T. denticola*, *A. actinomycetemcomitans*), to trace them and provide further information about the virulence of developed biofilms (Waddington & Embery 1994; Potempa & Travis 1996; Kamaguchi 2003). Additionally, the ALPase assay was introduced as it is considered a good periodontal biomarker for gingivae inflammation (Chapple *et al.* 1996).

The emergence of sequencing in the field of oral microbiology confirmed not only that the aetiology of gingivitis is highly complex (Caporaso *et al.* 2011; Caporaso *et al.* 2012; Huang *et al.* 2014) but also showed that (i) gingivitis associated bacteria can be found in both health and disease (Huang *et al.* 2011; Hajishengallis & Lamont 2012; Huang *et al.* 2014) and (ii) that the oral microbiota are more heterogeneous and diverse than previously anticipated (around 700 different species) (Dewhirst *et al.* 2010;

Hajishengallis & Lamont 2012), and (iii) that many newly recognised Gram-positive bacteria such as *Filifactor alocis* or *Peptostreptococcus stomatis* are showing a strong correlation with disease (Paster *et al.* 2001; Kumar *et al.* 2003; Kumar *et al.* 2006; Griffen *et al.* 2012). As I was not able to perform the NGS study at the time mainly due to funding constraints; it was decided to focus not only on the bacterial composition but also on the physiological status of the microbiome as a complementary study to the qPCR analysis. The question I wanted to answer was “What is the microbiome doing?” and how is it influencing the virulence of dental plaque (Nicholson & Lindon 2008b). Especially that pathogenicity is related to the metabolic activity of oral bacteria. Having a better understanding of the metabolic characteristics of the oral ecosystem can increase the knowledge in this area (Takahashi 2005). To enable this to happen, I have performed a ^1H -NMR metabolomic study to determine the metabolite fingerprint profile in both health and gingivitis conditions in my biofilm model.

Metabolomics is a relatively new technique to oral microbiology and has not been extensively exploited in gingivitis studies. It has been mostly limited to *in vivo* studies where metabolomics have been applied for diagnostic purposes and also a few studies focused on finding disease associated biomarkers (Aimetti *et al.* 2011; Barnes *et al.* 2011). Aimetti and colleagues (2011) demonstrated the power of ^1H NMR metabolic pattern recognition in discriminating the profiles of healthy and gingivitis patients. They have reported that periodontal diseases can be characterised by higher levels of propionate, butyrate, acetate, succinate, trimethylamine, propionate and valine as compared to health. The metabolomic studies performed by Barnes *et al.* (Barnes *et al.* 2009; Barnes *et al.* 2010; Barnes *et al.* 2011) on GCF samples confirmed that metabolomics can be a useful tool in discriminating periodontal health and disease and they have identified 4 potential gingivitis associated biomarkers inosine, lysine, putrescine and xanthine and a link between the purine degradation metabolites and periodontal diseases. Other oral metabolomic studies performed on either whole saliva or GCF include the work of Takeda *et al.* (2009), Sugimoto *et al.* (2012), and Santone *et al.* (2014).

These examples show that metabolomics is a fast growing field in oral microbiology and can provide useful information about gingivitis progression and aetiology. However, according to the literature review performed to date, little attention has been paid to *in vitro* gingivitis studies and using metabolomics as a tool for validation and comparison purposes with the *in vivo* experimental gingivitis studies. Therefore, the work described in this chapter is a novel approach where metabolomics were used to correlate the *in vitro* metabolite profiles with the *in vivo* gingivitis pattern.

¹H-NMR spectroscopy together with complex pattern recognition of NMR spectra including two multivariate methods such as principal component analysis (PCA) and partial least squares regression (PLS) analysis was kindly performed by Dr Michael Cannon, Procter & Gamble. As PCA and PLS are powerful pattern recognition techniques in investigating NMR metabolic profiles, they seem suitable for answering the research questions of this nature (Fonville *et al.* 2010; Aimetti *et al.* 2011). It was also decided not to perform a culture study which was previously used in chapters 3 and 4 (except for contamination testing), as it was very time consuming, expensive and did not bring much insight into the bacterial shifts occurring in the model over the change in experimental conditions.

5.7.1 Microbial trends in simulated gingivitis onset

The microbial composition in biofilm samples across the experimental phases was monitored using culture independent methods, triplex qPCR. The transition conditions were introduced for the first time in the gingivitis methodology and were applied to investigate whether the gas regime change from aerobic to micro-aerophilic conditions alone had a significant influence on the community composition. The qPCR study performed on the effluent data targeting 8 bacterial species showed that in most cases there was no significant difference between the health-transition conditions. The functional approach coupled with PCA and PLS confirmed that there was no difference between the health and transition conditions which indicate that gas regime alone does not invoke the desired environmental change (detectable change) and that additional nutrients such as artificial GCF are needed. The findings of this chapter corroborate the previous *in vitro* gingivitis studies performed by Guggenheim *et al.*

(2009) and Dalwai *et al.* (2006). These studies reported that changes in nutritional composition result in quantitatively different bacterial biofilm composition and that increase of the serum concentration at the expense of saliva lead to an increase in the number of Gram-negative bacteria.

The total bacterial cell number presented in Figure 5.3, Section 5.5.1 showed no statistical difference throughout the health, transition and gingivitis conditions in both the biofilm and effluent samples, respectively. In terms of the bacterial response to the ecological shift, there was no increase of the gingivitis associated orange complex species such as *F. nucleatum* or *P. intermedia* in the gingivitis conditions. *P. intermedia* was detected in extremely low numbers, while *F. nucleatum* reached a stable growth of approximately 10^6 - 10^7 cells / mL after 7 days of cultivation. There was also no change in numbers for the *L. casei* after the introduction of transition and gingivitis conditions.

Despite the lack of a substantial increase in the numbers of orange complex bacteria, there was an ascendancy of *A. naeslundii* in disease conditions over the *S. sanguinis*; this ecological shift is correlated with the onset of gingivitis which was previously reported in a similar *in vitro* study performed by Dalwai *et al.* (2006). *Streptococcus* spp. and *Actinomyces* spp. are both saccharolytic bacterial genera that utilise carbohydrates derived from saliva to form lactate, formate, acetate and succinate. Therefore they may change the ecological conditions which could allow colonisation by orange and red complex bacteria (Takahashi 2005); interestingly, the above mentioned metabolic end products were not identified in my ^1H NMR metabolite fingerprinting study (Section 5.6.2).

The overall lack of detection of microbial change in the model, specifically from orange complex bacteria, might have been due to focusing on a very limited bacterial selection and missing the bigger picture. Given that there are a large number of taxa present perhaps other candidate taxa increased in numbers but were not detected because I did not have primers for them. Thus, additional tools that provide a more

holistic approach and more information about the microbiome's metabolic / virulence status were applied.

5.7.2 Functional approach

The TLPase assay has been used to investigate biofilm virulence indirectly by tracing the proteolytic enzyme producers associated with gingivitis. The bacterial ALPase activity is associated with certain species e.g. *P. gingivalis*, *P. intermedia*, *C. ochracea*, and *A. actinomycetemcomitans* and thus is correlated with gingivae inflammation (Chapple *et al.* 1996). Both assays have been previously used in Chapter 4. However neither of these enzyme markers gave statistically significant changes in the gingivitis model (Chapter 4, Section 4.3.4). The main concern raised in chapter 4 was that the amount of biofilm used for TLPase assay was not adequate to give a strong signal and a clear separation across the health-disease phases. To address this issue, the methodology in chapter 5 addressed the problem by repeating both assays and using a single biofilm suspension in conjunction with a biofilm suspension from 3 discs (higher bacterial concentration per mL) to verify the usefulness of this method in modelling gingivitis *in vitro*. The data obtained in chapter 5 followed the same trend as previously observed in Chapter 4, Section 4.3.4 which showed no TLPase activity and low ALPase activity in either health or gingivitis conditions. This could potentially be explained by the fact that I either could not establish the health-disease transition (orange and red complex bacteria not present) or they were present in very low numbers (not detectable) or the selection of these two assays was not ideal due to low sensitivity.

^1H -NMR is a sensitive and holistic approach to understanding the metabolic changes occurring in a healthy or diseased microbiome. It was applied to both biofilm and effluent samples to determine whether the biofilm or effluent samples were more suitable for monitoring the changes which occur when shifting conditions from health to gingivitis *in vitro*. The ^1H NMR data for the biofilms showed that biofilms are not suitable for metabolomic studies on *in vitro* gingivitis (as explained below). The biofilm samples when analysed by ^1H NMR spectroscopy, first did not cluster as the remaining effluent samples did. Second, the analysis yielded a better separation when the biofilm samples were removed and more importantly no end-product metabolites were

recorded on increase/decrease in the biofilm samples. One potential explanation for this is that the collected biofilm samples (10 discs collected in health and another 10 in disease) are much lower in volume and metabolite concentration than the effluent samples and were even further diluted by re-suspending them in 5.0 mL of PBS to enable $^1\text{H-NMR}$ analysis. Additionally, the gingivitis associated end-products might have been flushed out from the pans (on which biofilm grew) by constant provision of medium and removal of excess waste by scrapper blades.

Despite the lack of detection of *P. intermedia* or other gingivitis associated species in the effluent samples, the PCA and PLS performed on T-CDFF samples from health- gingivitis phases showed: (i) a separation between the phases and (ii) an increase of propionate and butyrate together with (iii) a decrease in the levels of ethanol. Propionate and butyrate are the main end-products of gingivitis associated bacteria such as *Prevotella* spp., *Porphyromonas* spp., *Capnocytophaga* spp. and *Treponema* spp. These species are frequently found in the active sites of gingivitis or periodontitis. Moore *et al.* reported the butyrate producing bacteria to be correlated with gingivitis (Moore *et al.* 1981). Furthermore, similar metabolite changes were reported by Aimetti *et al.* in an *in vivo* study on healthy and periodontal patients including gingivitis patients. These authors showed that diseased samples can be differentiated from health samples by the elevated levels of propionate, butyrate and also other metabolitic end products such as succinate, trimethylamine, and acetate etc (Aimetti *et al.* 2011). My findings suggest that I might have developed a gingivitis associated community shift. Lack of detection of the bacterial species responsible for the production of the above mentioned metabolites might be explained by applying techniques which did not have a high degree of sensitivity or provided only a limited insight into the community.

The metabolomic study presented in this chapter was limited to a qualitative analysis only which was not followed by a statistical investigation as limited data was available / obtained from Procter & Gamble. Therefore, this study is only indicative in terms of the metabolite changes in health and gingivitis and the potential benefits of using metabolomics in the *in vitro* gingivitis model. Metabolomics will be used in the future

T-CDFE experiments as it has shown the potential in modelling gingivitis associated bacterial shifts and samples can be easily quantified without the need for time consuming extractions and purifications (Harada *et al.* 1987). Furthermore, this technique provides data that can be comparable with *in vivo* gingivitis studies for verification purposes.

5.8 Conclusion

As described in Chapter 4 the culture dependent and qPCR study may not have been satisfactory to detect the health-disease shifts as they are focused on a limited number of genera or species, respectively. The work in this chapter describes the use of an alternative method to monitor population shifts between health and disease, namely I applied ^1H NMR metabolomics to study the shift from health to gingivitis *in vitro*.

The ^1H NMR metabolomics has shown potential in monitoring the health-gingivitis associated changes. The data presented in this chapter have shown that an increase in gingivitis associated metabolites was detected in the shift from health to gingivitis conditions. Conversely, the molecular qPCR approach failed to distinguish between the health-gingivitis phases confirming the findings from the previous chapter, chapter 4. As the metabolomics approach proved to be useful in detecting the health / gingivitis associated changes, this technique will be used in future T-CDFF experiments.

6 CHAPTER

In vitro gingivitis model - Investigating
gingivitis associated shifts using
metabolomic and genomic approaches

6.1 Introduction

Gingivitis affects between 50-90% of the adult population worldwide (Stamm 1986), yet it is still poorly understood (Olsen, 2006; Paster, 2006). As the most critical point in the eradication of any disease is the understanding of its aetiology, gingivitis has been extensively studied for over 4 decades using culture and molecular techniques (Rosebury & Reynolds, 1964; Newman & Sockransky, 1977; Slots, 1977; Moore *et al.*, 1984; Brinig *et al.*, 2003; Huang *et al.*, 2014). The last 10 years have brought a profound technological shift towards 'omics' techniques, genomic or metabolomic, which present new holistic approaches to understanding the complexity of biofilm mediated diseases such as gingivitis. Genomic approach in a form of 16S rRNA gene next generation sequencing (NGS) is a high-throughput technology used for identifying the microbial phylotypes present within biofilms (Zaura *et al.* 2009; Zaura 2012; Schmidt *et al.* 2013). Due to the recent advances in sequencing technology and bioinformatics it is possible to reveal the previously undiscovered biodiversity of oral biofilms at much faster and cheaper rate (Caporaso, Lauber, Walters, *et al.* 2011). However, to get a real understanding of the aetiology and changes which occur during disease progression, it is important to bridge the genotype-to-phenotype gap (Barnes *et al.* 2009; Barnes *et al.* 2011). A method to achieve this can be $^1\text{H-NMR}$ metabolite fingerprinting. This technique has been proven to be a useful tool in metabolites identification and providing an overall physiological profile of a biological system (Serkova & Niemann 2006).

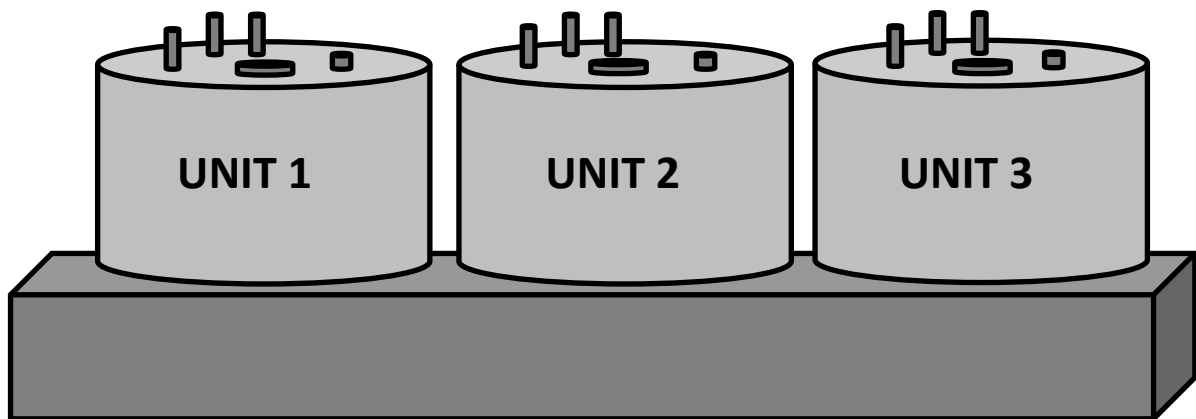
The previous chapter, Chapter 5, focused on validation of $^1\text{H-NMR}$ spectroscopy in studying the metabolome in gingivitis *in vitro*. This study confirmed that a metabolomic approach was useful in determining the differences between the health and disease conditions established in T-CDF model. As the cultivation and molecular techniques presented in Chapters 4 and 5 provided only a limited insight into microbial complexity, a sequencing study was introduced in this chapter to give a better understanding of the microbial shifts occurring during the progression from health to gingivitis *in vitro*. The work presented in this chapter describes a study were 16S rRNA gene sequencing based

on the Illumina platform was combined with ^1H -NMR fingerprinting to understand the complexness of the healthy and diseased oral biofilms.

6.2 Methodology

6.2.1 The experimental set-up and conditions

The experimental methodology and set-up of all T-CDFF experiments presented in this chapter was detailed in Figure 6.1 and Chapter 2, Section 2.2.2-2.2.4.



| UNIT 1 | UNIT 2 | UNIT 3 |
|--|---|---|
| CONTROL | GINGIVITIS + | GINGIVITIS ++ |
| 30 days of health conditions: artificial saliva: 1.0 mL / min aerobic conditions | 9 days health conditions: artificial saliva: 1.0 mL / min 21 days of gingivitis conditions: anaerobic gas conditions GCF at 50 μL / min | 9 days health conditions: artificial saliva: 1.0 mL / min 21 days of gingivitis conditions: anaerobic gas condition GCF at 130 μL / min |

Figure 6.1 presents the experimental conditions for each of the T-CDFF units. Unit 1 served as control and underwent the health conditions for 30 days. Unit 2 was run under health conditions for 9 days and then under enhanced gingivitis conditions (gingivitis+) by providing anaerobic gas conditions (instead of micro-aerophilic gas condition used in chapter 4 and 5 - Chapter 2, Section 2.3.4 & Chapter 4, Section 4.2.2). Unit 3 was run under health conditions for 9 days and then under 'gingivitis++' methodology that was defined by higher levels of the artificial GCF (130 μL / min) and anaerobic gas conditions (Chapter 2, Section 2.3.4).

Each T-CDFF unit started with 8 hours of inoculation with saliva microcosm population (Chapter 2, Section 2.3.1). After the inoculation, each unit was run under health conditions for 9 days. The health conditions in unit 1 were extended for another 21 days (extended health) and this unit served as a control group. The remaining two units, unit 2 and unit 3, were run for 21 days under 'gingivitis+' and 'gingivitis++' with methodology detailed in Chapter 2, Section 2.3.3 and 2.3.4, respectively.

6.2.2 CDFF sampling

6.2.2.1 *Biofilm*

Two biofilm samples were collected from each T-CDFF experiment at day 5, 7, 18, 23 and day 30 (Chapter 2, Section 2.3.5). The samples retrieved from each unit at each sampling point were analysed by culture independent methods: triplex qPCR (Chapter 2, Section 2.5) and comparative 16S rRNA gene sequencing (Chapter 2, Section 2.6). The genomic data are presented as the phylum composition at each sampling point and also as the species composition across the experimental phases. Non-selective culture methods were used to confirm the absence of contamination in the model (Chapter 2, Section 2.3.5 and 2.4).

6.2.2.2 *Effluent*

The effluent samples were collected according to the methodology detailed in Chapter 2, Section 2.3.5. During the first T-CDFF experiment 18 effluent samples were taken out from each unit, while 15 effluent samples were collected from the second T-CDFF experiment. Out of 18 samples, 5 were collected in health and 13 samples in either extended health (unit 1) or gingivitis (unit 2 and 3). In experiment 2, four samples were collected in health while remaining 11 were collected in extended health (unit 1) or gingivitis conditions (unit 2 and 3).

All the effluent samples were analysed by ^1H NMR spectroscopy and triplex qPCR (Chapter 2, Section 2.5-2.7). Due to funding constraints, only a selection of the effluent samples collected at day 5, 7, 21, 23, and day 30 were analysed by comparative 16S rRNA gene sequencing to determine if there was a correlation between the effluent and the biofilm genomic data. The genomic study determined the phylum composition at each sampling point and the species composition across the health, extended health and gingivitis conditions (Chapter 2, Section 2.6). Non-selective culture methods were used to confirm the absence of contamination in the model (Chapter 2, Section 2.3.5 and 2.4).

6.2.3 Statistical analysis

The qPCR data obtained from the biofilm samples in health (day 5, and 7), extended health (day 18, day 23 and day 30) and gingivitis (day 18, day 23 and 30) were logged and averaged to compare the differences across the health-extended health and health-gingivitis conditions. Furthermore, a paired Student's t-test was applied to the qPCR data to determine whether the differences between the phases were significant. The significance level for all hypothesis tests was chosen to be 0.01.

Same as above was applied to the effluent data. The qPCR data from samples collected in health, extended health, and gingivitis were logged and averaged to compare the differences across the health-extended health and health-gingivitis conditions. Student's t-test was applied to determine whether the differences between the phases were significant. The value was set as 0.01 to ensure a stringent hypothesis testing.

The raw ^1H NMR data were analysed by Michael Cannon (scientist at Procter & Gamble) by applying the principal component analysis coupled with the orthogonal partial least square analysis to determine the principle components discriminative across the health-extended health and health-gingivitis conditions in each T-CDFF experiment. A paired Student's t-test was applied to determine whether the differences in metabolite production were significant. The significance level for the hypothesis tests was chosen to be 0.05.

6.3 Results

Unit 2 broke down in the early stage of experiment 2 due to bacterial waste that leaked through the shaft and the gearbox damaging them. As this fault was not rectifiable at the time, unit 2 was stopped and not included in any further analysis. For comparison purposes i.e. to compare the same data sets from two individual T-CDFF experiments, the data retrieved from unit 2 in experiment 1 were also excluded from the analysis and are not shown in this chapter.

6.3.1 Real-time PCR study to investigate the gingivitis associated shifts

Quantitative PCR analysis was performed on the biofilm and the effluent samples collected from two individual T-CDFF experiments. The qPCR data for the biofilm samples are shown in Figure 6.2 and Table 6.1. The data for the effluent samples are shown in Figure 6.3.

6.3.2 Biofilm

The qPCR data retrieved from biofilm samples collected from two individual T-CDFF experiments are shown in Figure 6.2 and Table 6.1.

Figure 6.2 presents *S. sanguinis* and the total cell number of bacteria detected in the biofilm samples retrieved from T-CFFF experiment 1 and experiment 2, units 1 and 3.

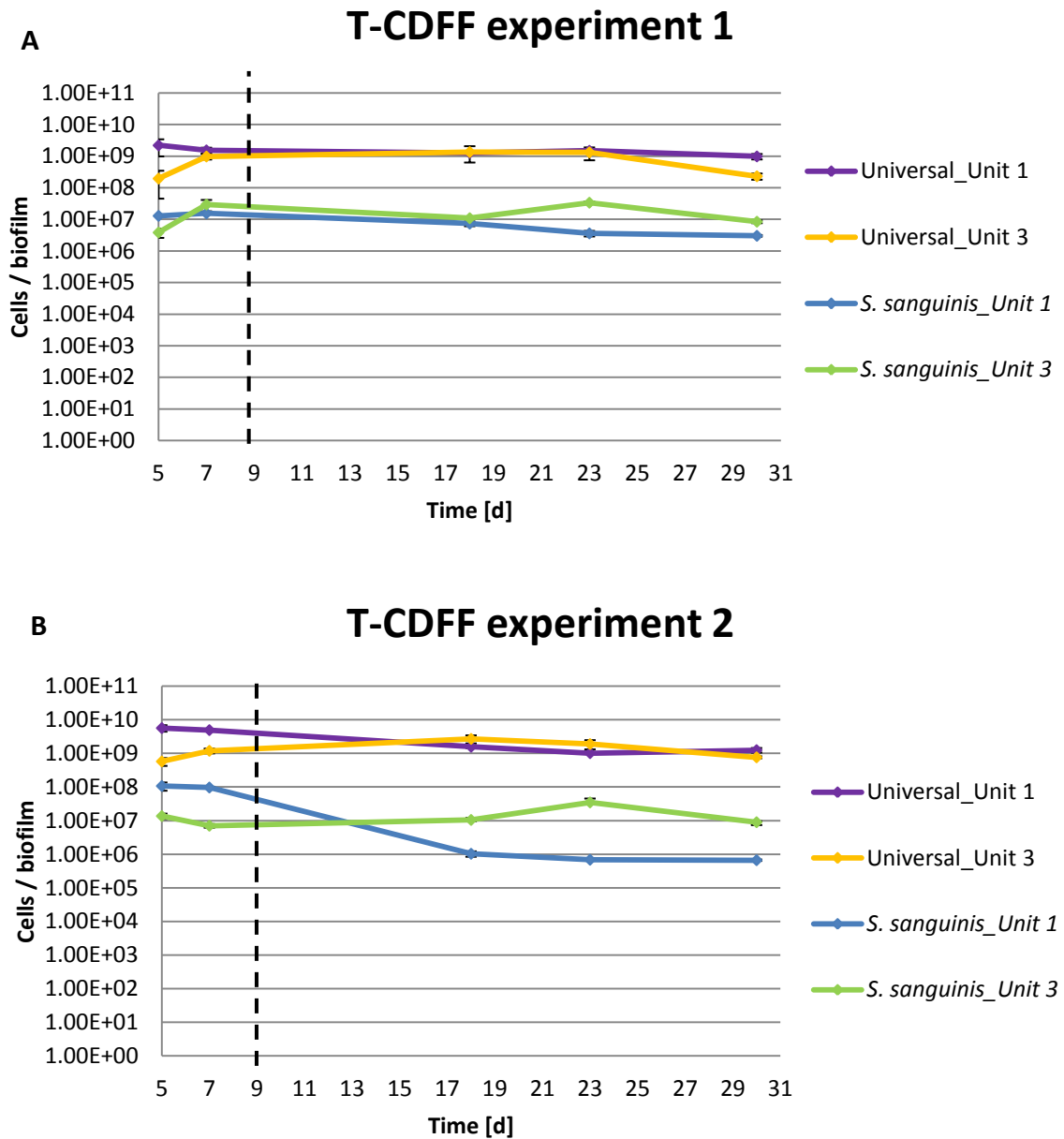


Figure 6.2 A) presents the data for the total bacteria and the total cell number of *S. sanguinis* detected in the biofilm samples collected over time in T-CDFD experiment 1 and B) experiment 2. The violet line (Universal) represents the total bacteria detected in unit 1; the yellow line (Universal) represents the total bacteria in unit 3. The blue line represents the total amount of *S. sanguinis* detected in unit 1; green line represents the amount of *S. sanguinis* in unit 3. Dotted line represents the conditions change from health to extended health or gingivitis introduced at day 9*. Standard errors are presented as error bars (n=6); n=6 refers to two biological and three technical replicates.

The total cell numbers in unit 1, experiment 1 started off with 2.21×10^9 cells / biofilm and no significant differences between the health and extended health phases ($p=0.018$). Conversely, there was a significant 0.22 log increase in cell numbers across the health – gingivitis phases in unit 3 (as further explained in Section 6.2.3). In

experiment 2, there was a significant 0.62 log decrease in total bacteria numbers in extended health in unit 1. On the other hand, unit 3 recorded a non-significant 0.31 log increase in disease conditions ($p=0.017$).

The cell numbers of *S. sanguinis* in unit 1, experiment 1 reached 1.30×10^7 cells / biofilm at day 5 and fluctuated at around 3.03×10^6 - 1.55×10^7 cells / biofilm throughout the experiment. When the health data (1.42×10^7 cells / biofilm) were compared with the extended health data (4.67×10^6 cells / biofilm), there was a significant 0.48 log decrease in cell numbers (as further explained in Section 6.2.3). On the other hand, there was not a significant difference between the health (1.68×10^7 cells / biofilm) and the gingivitis conditions (1.77×10^7 cells / biofilm) in unit 3, experiment 1 ($p=0.442$). In experiment 2, there was a significant 2.1 log decrease across the health-extended health conditions in unit 1 and a non-significant 0.24 log increase in gingivitis conditions in unit 3 ($p=0.102$).

Table 6.1 presents the total amount of *S. mutans*, *N. subflava*, and *A. naeslundii* detected in biofilm in experiment 1 and experiment 2 across unit 1 and unit 3. *F. nucleatum*, *P. intermedia*, *L. casei*, and *V. dispar* were not detected in any of these experiments.

| strain | day | Experiment 1 Average [cells / biofilm] | | Experiment 2 Average [cells / biofilm] | |
|----------------------|-----|---|-------------------------------|---|-------------------------------|
| | | unit 1 | unit 3 | unit 1 | unit 3 |
| <i>S. mutans</i> | 5 | 3.99E+04 (1.81E+04) | 1.45E+02 (8.94E+01) | 1.23E+05 (1.13E+05) | 7.87E+05 (3.49E+05) |
| | 7 | 1.61E+05 (1.00E+05) | 1.64E+05 (1.63E+05) | 1.88E+05 (1.83E+05) | 1.65E+05 (6.86E+04) |
| | 18 | 2.90E+01 (1.28E+01) | 2.27E+04 (1.94E+04) | 2.82E+04 (2.11E+04) | 1.17E+06 (9.06E+05) |
| | 23 | 8.39E+03 (5.43E+03) | 2.96E+03 (1.70E+03) | 1.03E+05 (6.65E+04) | 6.96E+05 (6.33E+05) |
| | 30 | 7.42E+02 (6.86E+02) | 7.32E+05 (4.78E+05) | 4.95E+03 (4.57E+03) | 4.34E+03 (3.77E+03) |
| <i>N. subflava</i> | 5 | 2.13E+01 (1.36E+01) | ND | 3.50E+07 (1.44E+07) | 3.38E+01 (1.54E+01) |
| | 7 | 4.26E+01 (2.38E+01) | 4.57E+01 (2.19E+01) | 7.99E+07 (1.16E+07) | 1.18E+03 (5.23E+02) |
| | 18 | 4.53E+01 (3.23E+01) | 1.02E+02 (5.47E+01) | 7.47E+05 (2.38E+05) | 4.05E+04 (1.83E+04) |
| | 23 | 1.40E+01 (8.90E+00) | 1.02E+02 (3.31E+01) | 1.15E+05 (1.40E+04) | 3.05E+01 (6.98E+00) |
| | 30 | 5.06E+01 (3.20E+01) | 4.96E+01 (1.64E+01) | 5.69E+05 (5.18E+04) | 4.39E+03 (3.41E+02) |
| <i>A. naeslundii</i> | 5 | 7.62E+02 (3.18E+02) | ND | 6.02E+01 (3.63E+01) | ND |
| | 7 | 1.74E+02 (9.72E+01) | 1.79E+02 (8.65E+01) | 2.88E+02 (1.46E+02) | ND |
| | 18 | 1.86E+02 (1.32E+02) | 4.11E+02 (2.17E+02) | 1.31E+01 (8.25E+00) | 4.17E+00 (4.16E+00) |
| | 23 | 5.69E+01 (3.62E+01) | 4.18E+02 (1.37E+02) | 5.96E+00 (3.21E+00) | 2.29E+01 (1.48E+01) |
| | 30 | 2.12E+02 (1.34E+02) | 1.53E+02 (6.25E+01) | 1.09E+06 (4.86E+05) | 3.18E+05 (1.42E+05) |

Table 6.1 presents the total cell numbers for *S. mutans*, *N. subflava*, *A. naeslundii* detected in the biofilm samples collected from unit 1 and unit 3 in the T-CDFF experiment 1 and 2. Unit 1 was maintained in the health conditions throughout the time; unit 3 was exposed to the health conditions for 9 days and then the conditions were changed to gingivitis and maintained for 21 days. *V. dispar*, *F. nucleatum*, *P. intermedia* and *L. casei* were not detected in the biofilm samples and thus are not presented in this table. Blue line indicates the introduction of extended health /gingivitis conditions at day 9. ND - not detected. The standard error is shown in brackets (n=6). n=6 refers to two biological and three technical replicates

When the data for *S. mutans* were compared across the phases (as explained in Section 6.2.3); there was a decrease in cell numbers in extended health and an

increase in gingivitis condition in both T-CDFE experiment but these changes were not significant ($p \geq 0.01$).

The numbers for *N. subflava* in experiment 1 (both units) were very low with no detection at day 5 for unit 3. Conversely, the numbers of *N. subflava* in both units in experiment 2 were much higher. The average cell number in health conditions (day 5 and 7) in unit 1, experiment 2 was 5.74×10^7 cells / mL and decreased significantly ($p \leq 0.01$) by approximately 2.1 logs in extended health conditions to 4.77×10^5 cells / mL (see Section 6.2.3). On the other hand, there was no particular growth trend in unit 3, experiment 2. When the health and gingivitis data were compared, there was a non-significant increase in cell numbers in gingivitis conditions ($p \geq 0.01$; see Section 6.2.3).

The numbers of *A. naeslundii* detected in both experiments were low (exception for the last day of experiment 2) with no significant differences between the health-extended health or health-gingivitis conditions ($p \geq 0.01$).

6.3.3 Effluent data

This Section presents the qPCR analysis of the effluent samples collected from two individual T-CDFE experiments. The data for the total number of bacteria and *S. sanguinis* in experiments 1 and 2, in unit 1 and unit 3 are presented in Figure 6.3.

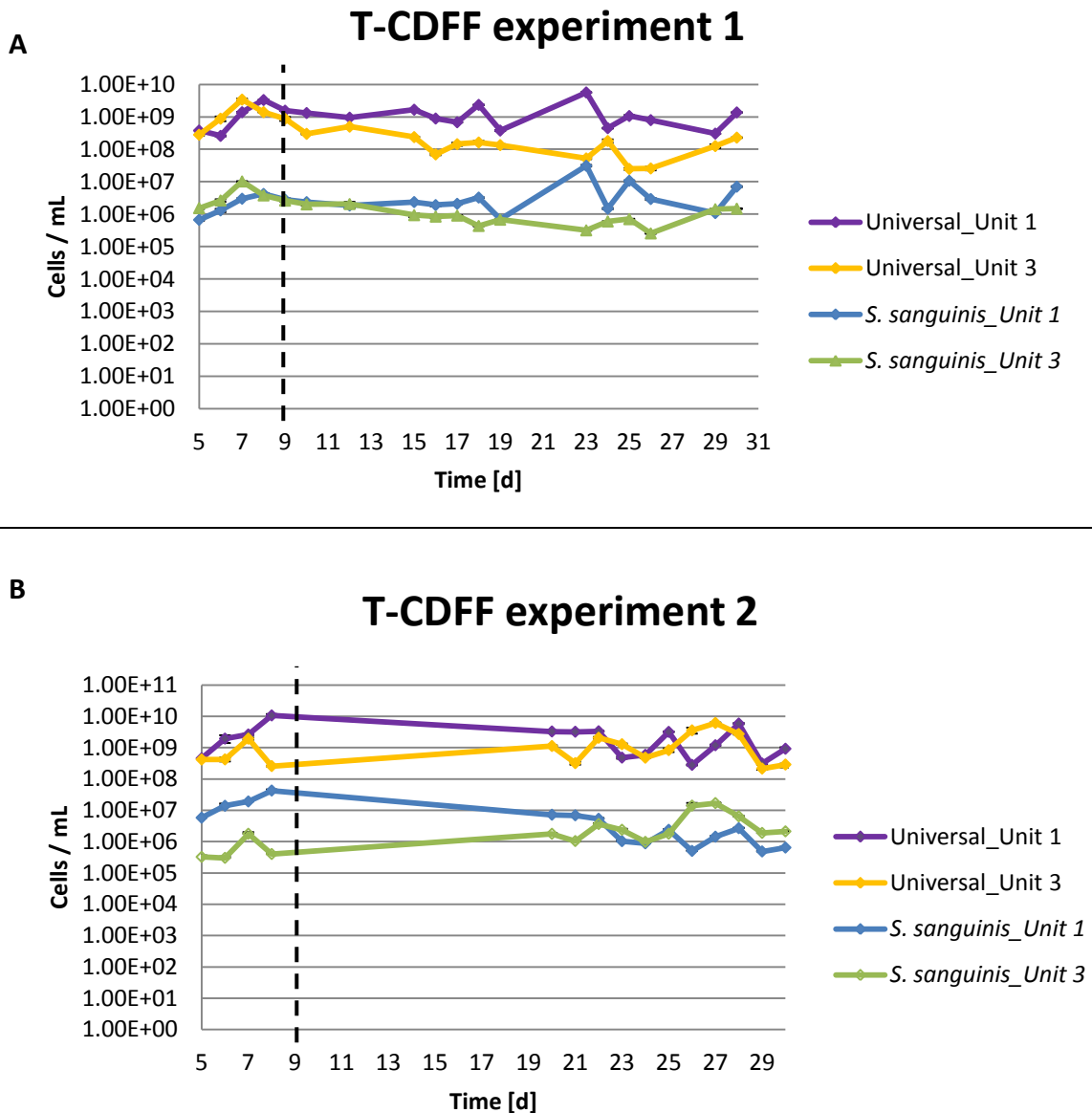


Figure 6.3 A) presents the data for total bacteria and the total cell number of *S. sanguinis* detected in the effluent samples collected over time in T-CDFE experiment 1 and B) experiment 2. The violet line (Universal) represents the total bacteria detected in unit 1; the yellow line (Universal) represents the total bacteria in unit 3. The blue line represents the total amount of *S. sanguinis* detected in unit 1; green line represents the amount of *S. sanguinis* in unit 3. Dotted line represents the conditions change from health to extended health or gingivitis introduced at day 9*. Standard errors are presented as error bars ($n=6$); $n=6$ refers to two biological and three technical replicates.

To investigate the growth change across the health-extended health or health-gingivitis phases in the two individual T-CDFE experiments, the qPCR data retrieved from each experimental phase were logged, averaged and compared (as explained in Section 6.2.3). The average cell number in health conditions in experiment 1, unit 1 was 1.39×10^9 cells / mL and showed no significant difference from the extended health conditions which had an average of 1.38×10^9 cells / mL ($p=0.410$). The average cell number in health conditions in experiment 1, unit 3 reached 1.38×10^9 cells / mL and was significantly higher (0.91 log) when compared to the average cell number in gingivitis conditions that was 1.69×10^8 cells / mL ($p=0.002$). The average cell number in health conditions in unit 1, experiment 2 reached 3.91×10^9 cells / mL and decreased significantly by 0.71 log in the extended health conditions reaching 7.54×10^8 cells / mL ($p \leq 0.01$). Unit 3 reached the average of 2.16×10^9 cells / mL in health conditions and showed no significant decrease in gingivitis conditions (average of 1.87×10^9 cells / mL; $p=0.238$).

The average cell number for *S. sanguinis* in health conditions in unit 1, experiment 1 was 2.40×10^6 cells / mL and increased by 0.34 log in the extended health conditions but it was not statistically significant ($p=0.482$). The average cell number in health conditions in unit 3, experiment 1 reached 4.17×10^6 cells / mL and decreased significantly by 0.63 log to 9.72×10^5 cells / mL under gingivitis conditions ($p=0.009$). The average cell number in health condition in unit 1, experiment 2 reached 2.03×10^7 cells / mL and decreased significantly by 0.85 log to 2.87×10^6 cells / mL in extended health conditions ($p \leq 0.01$). Unit 3 recorded an average cell number of 7.54×10^8 cells / mL in health conditions that significantly increased by 0.39 log to 1.87×10^9 cells / mL in gingivitis condition ($p \leq 0.01$).

F. nucleatum, *L. casei* and *P. intermedia* were not detected in experiment 1 and experiment 2. *S. mutans*, *N. subflava*, and *A. naeslundii* were detected but either (i) in very low numbers or (ii) showed no particular growth trend across the experimental phases so the data were not presented in this chapter as they did not bring any additional insight into this project.

6.3.4 Genomic approach to investigate the gingivitis associated shifts

This Section presents the comparative 16S rRNA gene sequencing data obtained from the biofilm and the effluent samples collected from T-CDFF experiment 1 and 2. The sequencing data for the biofilm samples collected from the experiment 1 and 2 are presented in the Figure 6.4-6.5 and Table 6.2. The sequencing data for the effluent samples collected from the experiment 1 and 2 are presented in the Figure 6.6-6.7 and Table 6.3.

6.3.4.1 Biofilm data

The 16S rRNA gene sequencing data for the biofilm samples collected from unit 1 and 3 from two individual T-CDFF experiments are presented in Figure 6.4-6.5 and Table 6.2. Figure 6.4-6.5 show the phyla composition of the biofilm samples retrieved from experiment 1 and experiment 2, unit 1 and unit 3, while Table 6.2 presents the species composition across the experimental conditions in each T-CDFF experiment.

6.3.4.1.1 Phyla composition

The Section below presents the phyla composition of the samples collected across different experimental conditions from individual T-CDFF experiments. Figure 6.4A presents the phyla composition of the biofilm samples collected from the T-CDFF experiment 1, health-extended health conditions (unit 1), while Figure 6.4B presents the phyla composition of the samples collected across health-gingivitis conditions (unit 3).

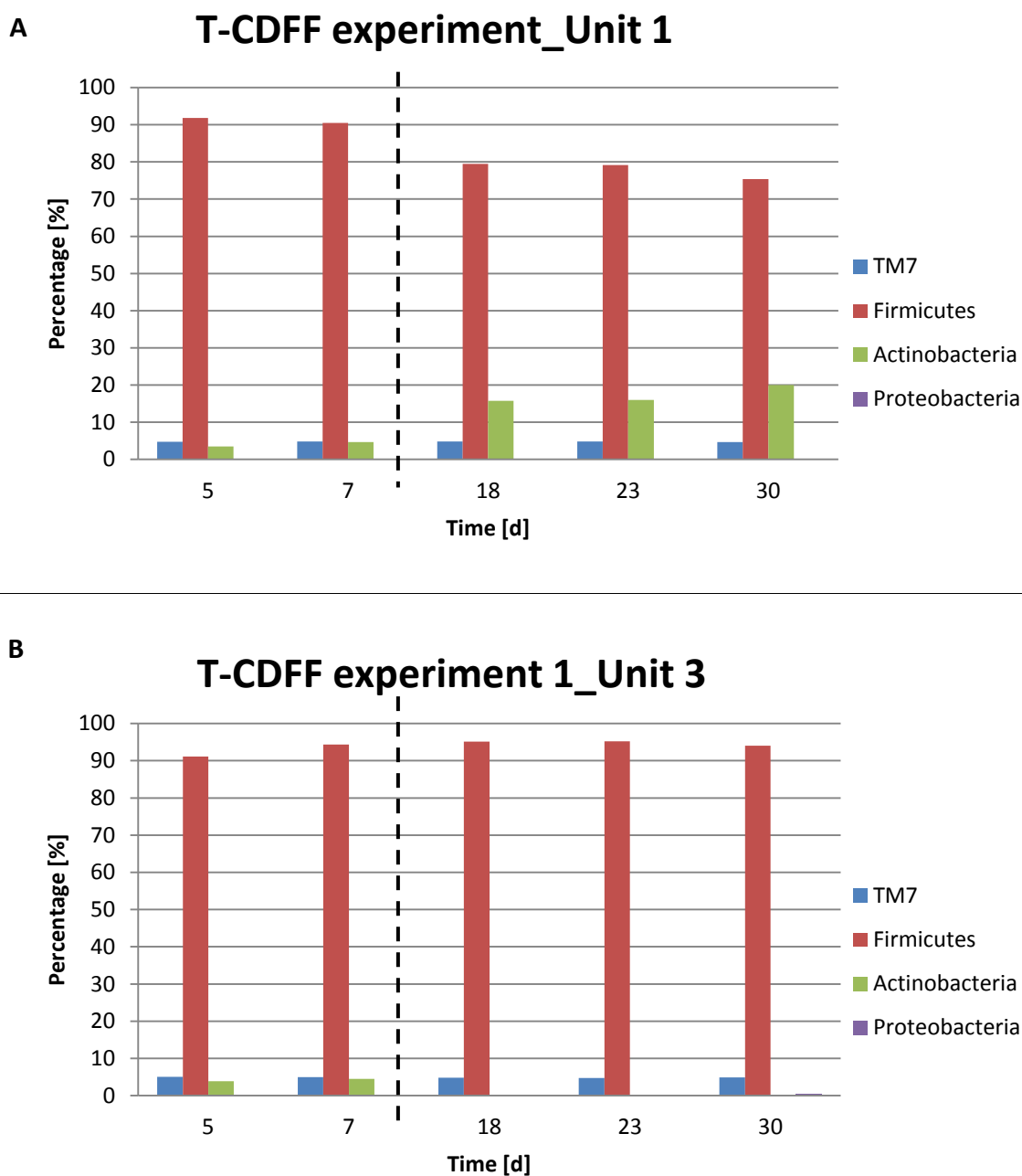
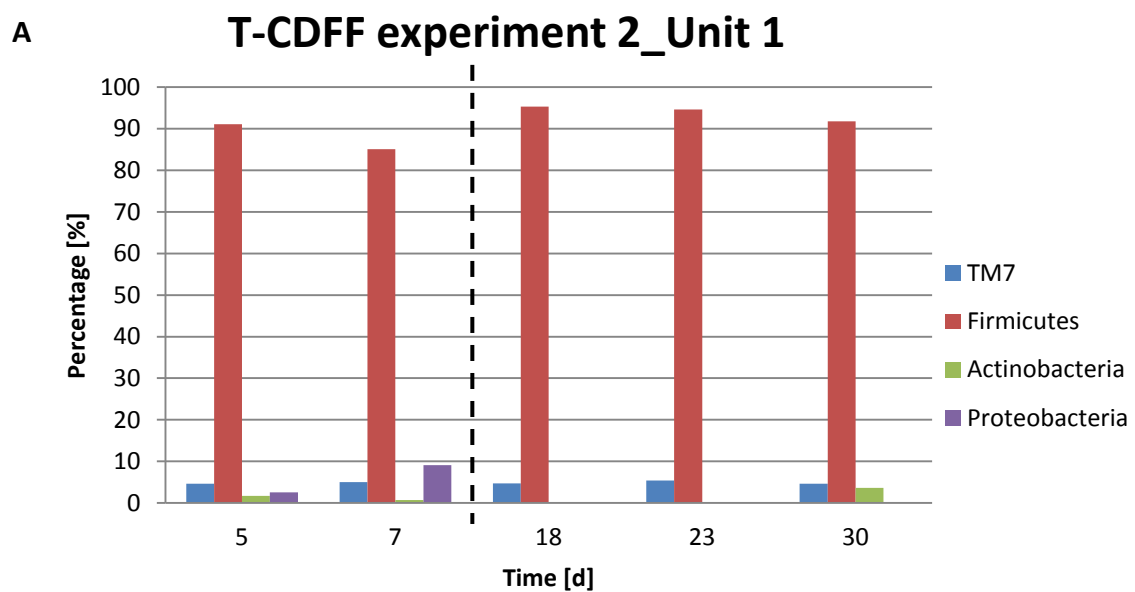


Figure 6.4 presents the phyla composition of the biofilm samples retrieved from T-CDFF experiment 1, unit 1 and unit 3. Figure 6.4 A) presents the data from experiment 1, unit 1 across the health and the extended health conditions. Figure 6.4 B) presents the data from experiment 1, unit 3 across the health and gingivitis conditions. Blue represents the TM7, red represents the Firmicutes, green represents the Actinobacteria and violet the Proteobacteria. Dotted line represents the change in conditions from the health to the extended health or gingivitis conditions introduced at day 9. N=1 refers to one biological replicate.

Only 3 phyla out of 13 present in oral cavity (Dewhirst *et al.* 2010) were detected in samples collected throughout the time across the health-extended health and health-gingivitis conditions in experiment 1. These included TM7, Firmicutes and

Actinobacteria. Figure 6.4A shows a gradual increase in Actinobacteria from 5% to 30% throughout the experiment at the expense of Firmicutes that decreased from 90% to 75%. TM7 amounted to 5% of the community and stayed at this level throughout the time. Proteobacteria were not detected in any of the collected samples. Figure 6.4B presents the phyla composition in experiment 1, unit 3. The TM7 group amounted to 5% of the community across the sampling points. Actinobacteria were only detected in health and at a low percentage (<5%). Firmicutes maintained a steady percentage of the community that was greater than 90% throughout the course of the whole experiment.

Figure 6.5 presents the phyla composition of the biofilm samples collected across the health-extended health and health-gingivitis conditions in experiment 2.



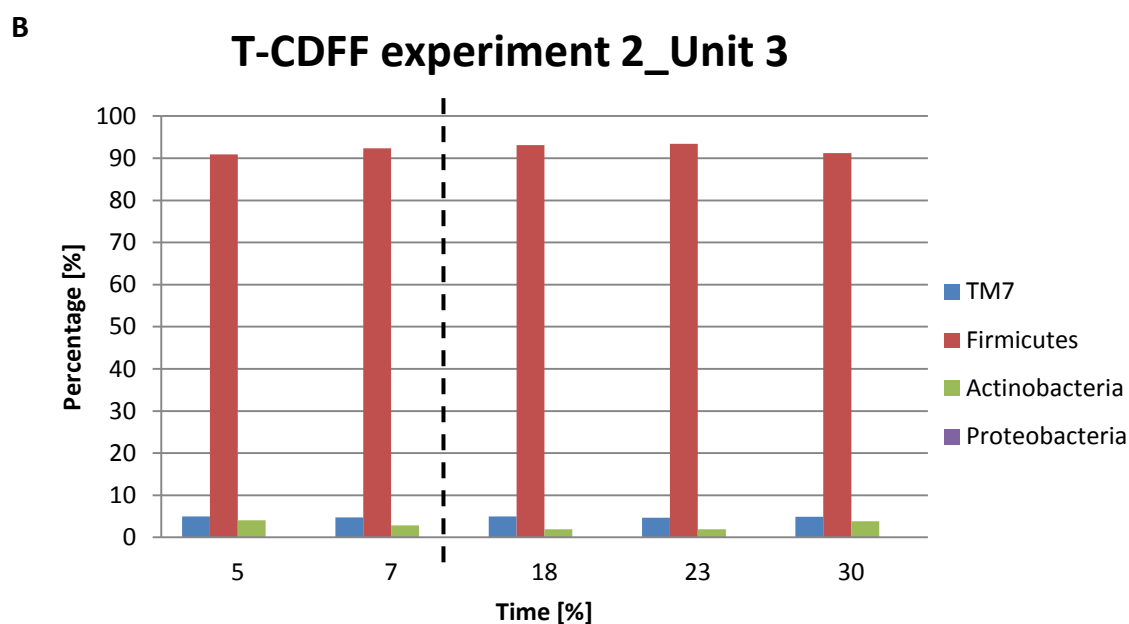


Figure 6.5 presents the phyla composition of the biofilm samples retrieved from T-CDFF experiment 2, unit 1 and unit 3. Figure 6.5 A) presents the data from experiment 2, unit 1 across the health and the extended health conditions. Figure 6.5 B) presents the data from experiment 2, unit 3 across the health and gingivitis conditions. Blue represents the TM7, red represents the Firmicutes, green represents the Actinobacteria and violet the Proteobacteria. Dotted line represents the change in conditions from the health to the extended health or gingivitis conditions introduced at day 9. N=1 refers to one biological replicate.

Figure 6.5A presents the phyla composition of the samples in experiment 2, unit 1. The Firmicutes amounted to more than 80% of the population at each sampling point. The TM7 genera stayed at the constant level of 5% throughout the whole experiment. The Actinobacteria were detected in low percentages at day 5, 7 and 30, while Proteobacteria were detected only in the beginning of the experiment at day 5 and day 7 with the percentages below 5% and 8%, respectively. Figure 6.5B presents the phyla composition of the biofilm samples collected in experiment 2, unit 3. The Firmicutes represented $\leq 90\%$ of the biofilm community at each sampling point collected across the health-gingivitis conditions. The amount of TM7 stayed at the constant level of 5% throughout the time. Further to this, there was a low percentage of Actinobacteria ($\leq 5\%$) detected in each biofilm samples throughout the time, while Proteobacteria were not detected.

6.3.4.1.2 Genus and species composition

The Section below presents the genus and species composition of the biofilm samples collected from unit 1 and unit 3 from two individual T-CDFF experiments across the health, extended health and gingivitis conditions.

The genus composition of the samples retrieved from health conditions in experiment 1, unit 1 consisted of 51.6% *Streptococcus*, 27.8% *Enterococcus*, 7.4% *Rothia*, 6.5% *Granulicatella*, 4.7% TM7 and 2.1% *Gemella*. When the health conditions were extended for another 21 days, the genus composition shifted. There was a decrease in the proportions of *Streptococcus* spp. from 51.6% to 37.6%; an increase of *Rothia* to 17.8%; a decrease of *Enterococcus* to 13.7% and an increase of *Granulicatella* to 10.2%. *Gemella* increased from 2.1% to 5.5%; *Lactobacillus* was detected only in extended health and amounted to 5.3% while TM7 stayed at the same level of 4.7% throughout the condition change from health to extended health.

Unit 3, on the other hand, underwent 9 days of health and then a shift to gingivitis conditions. The genus composition in health conditions consisted of 71.3% of *Streptococcus*, 11.7% of *Granulicatella*, 5.4% of *Lactobacillus*, 5.0% of TM7, 4.2% of *Rothia*, 2.2% of *Gemella* and 1.4% of *Enterococcus*. After the introduction of the gingivitis conditions, *Streptococcus* decreased from 71.3% to 62.4%, *Gemella* increased up to 17.1% and *Enterococcus* increased up to 15.2%. TM7 amounted to 4.8%, while *Granulicatella* decreased to 3.2% and *Rothia* reached 0.7%.

The genus composition of the samples retrieved from health in unit 1, experiment 2 consisted of 71.7% *Streptococcus*, 7.9% *Granulicatella*, 7.7% *Gemella*, 6.5% *Neisseria*, 4.8% TM7, 1.6% *Rothia* and 0.6% *Enterococcus*. When the health conditions were extended for another 21 days, the genus composition has changed with a decrease in the proportions of *Streptococcus* to 68.4%, *Granulicatella* increased up to 17.9%, *Enterococcus* increased up to 1.1%, *Gemella* recorded a small decrease in proportions and reached 7.4%, TM7 reached 4.9% and two additional genera were detected, *Actinomyces* 3.6% and *Lactobacillus* 0.7%.

The genus composition of samples retrieved from health conditions in unit 3, experiment 2 consisted of 76.2% *Streptococcus*, 13.2% *Granulicatella*, 4.8% TM7, 3.8% *Gemella*, 3.4% *Rothia* and 0.8% *Enterococcus*. When the gingivitis conditions were introduced at day 9, the genus composition has shifted. The *Rothia* was not detected, *Streptococcus*, *Granulicatella*, and *Enterococcus* decreased in proportions to 73.8%, 8.3% and 0.7%, respectively. *Gemella* increased to 10.1%, *Actinomyces* to 3.1% and *Lactobacillus* only detected in disease conditions amounted to 0.5%.

The species composition of the biofilm samples collected from health, extended health and gingivitis conditions across two individual T-CDFF experiments is presented in Table 6.2.

| bacterial strain | Experiment 1 | | | | Experiment 2 | | | |
|---------------------------------------|--------------|------|------------|------|--------------|------|------------|------|
| | Unit 1 [%] | | Unit 3 [%] | | Unit 1 [%] | | Unit 3 [%] | |
| | H | EH | H | G | H | EH | H | G |
| Unclassified | 4.8 | 4.7 | 5.0 | 4.8 | 4.9 | 4.9 | 4.9 | 4.8 |
| <i>Streptococcus mitis</i> group | | | | | | | | |
| <i>S. pseudopneumoniae</i> | 29.9 | 11.7 | 35.9 | 27.1 | 33.8 | 13.7 | 21.2 | 19.1 |
| <i>S. australis</i> | 3.4 | 1.3 | 3.9 | 3.0 | 3.0 | 1.0 | 1.7 | 2.7 |
| <i>S. parasanguinis</i> | | | | | | 1.5 | | 1.6 |
| <i>S. infantis</i> | 1.5 | | 2.6 | 0.7 | 1.4 | | 0.9 | |
| <i>S. anginosus</i> | | | | 3.8 | | 32.8 | 2.0 | 21.2 |
| <i>S. sanguinis</i> | 0.6 | 0.9 | 1.3 | 1.5 | 2.2 | | 1.4 | 0.8 |
| <i>S. gordonii</i> | 0.6 | 6.5 | 2.3 | 4.8 | 1.9 | 5.7 | 23.7 | 8.4 |
| <i>Streptococcus anginosus</i> group | | | | | | | | |
| <i>S. intermedius</i> | | 7.6 | | 2.8 | | 0.7 | | 0.6 |
| <i>Streptococcus salivarius</i> group | | | | | | | | |
| <i>S. vestibularis</i> | | | | | | | 1.5 | |
| <i>S. thermophilus</i> | | | | | | | 1.1 | |
| <i>Streptococcus pyogenic</i> group | | | | | | | | |
| <i>S. fryi</i> | 2.7 | 0.7 | 3.5 | 1.7 | 2.5 | 1.3 | 1.7 | 1.8 |
| <i>S. urinalis</i> | | | | | | | 0.7 | 0.4 |
| <i>S. gallinaceus</i> | | | | 0.8 | | | | 0.4 |
| <i>Streptococcus bovis</i> group | | | | | | | | |
| <i>S. bovis</i> | 3.2 | 2.0 | 5.1 | 3.8 | 5.7 | 1.9 | 4.8 | 3.5 |
| <i>Vagococcus teuberi</i> | 6.2 | 4.3 | 1.4 | 2.9 | 0.6 | 1.1 | 0.8 | 0.7 |
| <i>Enterococcus faecalis</i> | 16.9 | 9.3 | | 8.2 | | | | |
| <i>Enterococcus italicus</i> | 1.3 | 0.5 | | 0.4 | | | | |
| <i>E. casseliflavus</i> | 0.6 | 1.7 | | 1.7 | | | | |
| <i>Granulicatella adiacens</i> | 0.9 | 0.9 | 1.6 | 0.4 | 0.9 | 1.9 | 1.4 | 1.1 |
| <i>Gamella sanguinis</i> | | | | | | 0.9 | | |
| <i>Gemella cunicula</i> | | 0.7 | | | 0.9 | 0.9 | 0.5 | 1.2 |
| <i>Gemella haemolysans</i> | 0.8 | 2.1 | 1.1 | 6.9 | 3.0 | 2.3 | 1.5 | 4.0 |
| <i>Lactobacillus rhamnosus</i> | | | | | | | | 0.5 |
| <i>Lactobacillus fermentum</i> | | 5.3 | 5.1 | | | | | |
| <i>A. odontolyticus</i> | | | | | | | | 0.4 |
| <i>Rothia dentocariosa</i> | 0.6 | 0.9 | | | 0.7 | | 0.6 | |
| <i>Rothia mucilaginosus</i> | 4.7 | 12.8 | 3.0 | 0.7 | 0.9 | | 2.2 | |
| <i>Neisseria subflava</i> | | | | | 2.2 | | | |
| <i>Neisseria mucosa</i> | | | | | 3.1 | | | |

Table 6.2 presents the phylogenetic composition of biofilm collected from experiments 1 and 2, units 1 and 3 in health (H), extended health (EH) and gingivitis conditions (G). The biofilm samples collected from health/extended health/gingivitis were averaged to compare the

species proportions between the H-EH and H-G phases. The numbers highlighted in yellow indicate that specific species was not present in all the samples used to calculate an average.

In total only 29 bacterial species were detected and identified down to species level in the biofilm samples retrieved from the experiments 1 and 2. The majority of species, 24 out of 29, belonged to Firmicutes phyla, 3 species belonged to Actinobacteria phyla, and 2 to Proteobacteria phyla. In general, the abundance was very low with no visible trend across the experimental conditions.

6.3.4.2 Effluent data

This Section presents the genomic data obtained for the effluent samples collected from two individual T-CDFF experiments, unit 1 and unit 3, collected across the health, extended health and the gingivitis conditions.

Figure 6.6 and 6.7 presents the phyla composition of the effluent samples collected from the T-CDFF experiment 1 and experiment 2 across unit 1 (health-extended health) and unit 3 (health-gingivitis). Table 6.3 present the species composition of the effluent samples collected from each unit in two individual T-CDFF experiments.

6.3.4.2.1 Phyla composition

Figure 6.6 presents the phyla composition of the effluent samples collected from health, extended health and gingivitis conditions from unit 1 and unit 3 in experiment 1. Figure 6.6A presents the phyla composition of samples collected across health-extended health conditions, while Figure 6.6B presents the phyla composition of samples collected across health-gingivitis conditions.

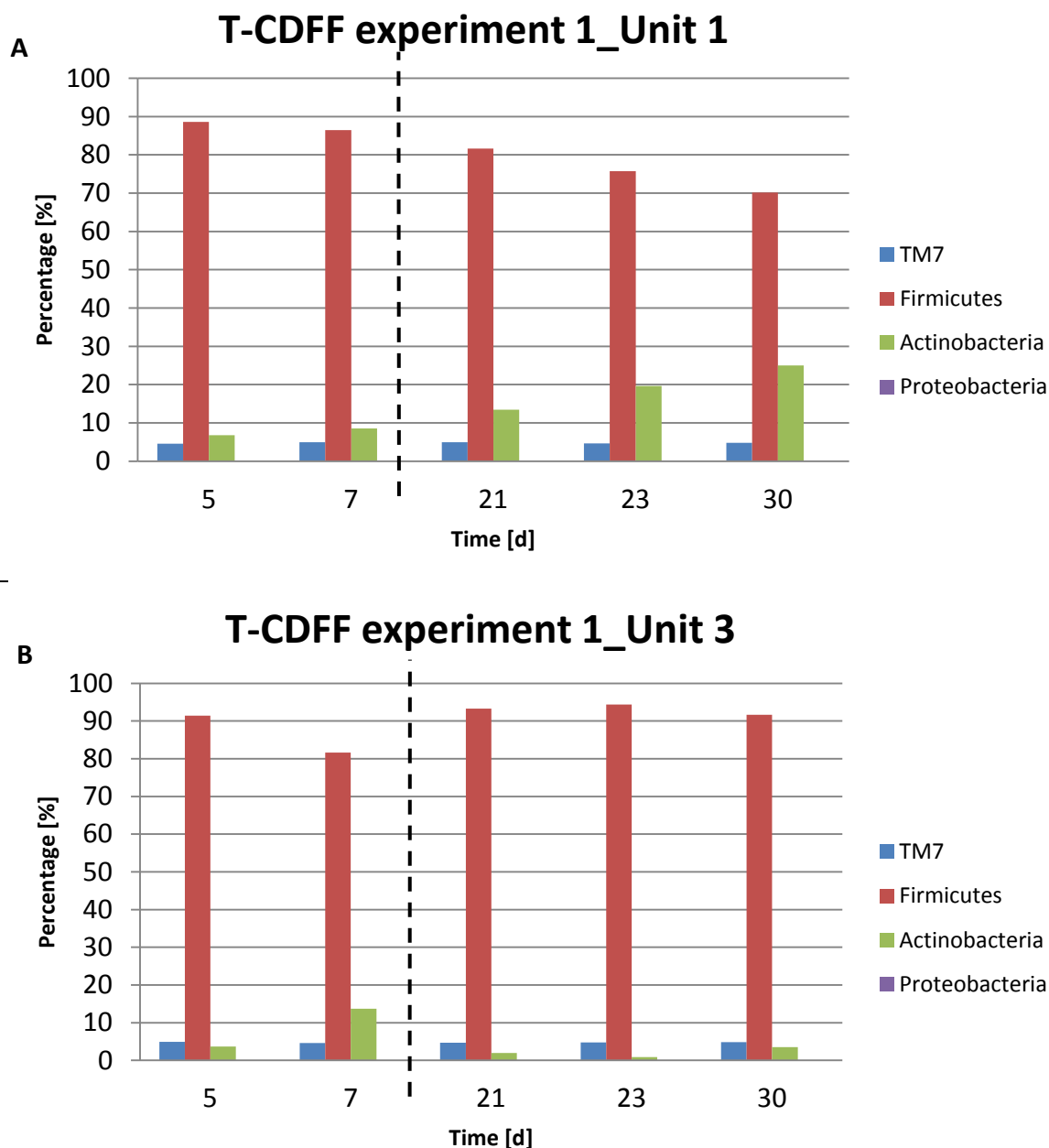


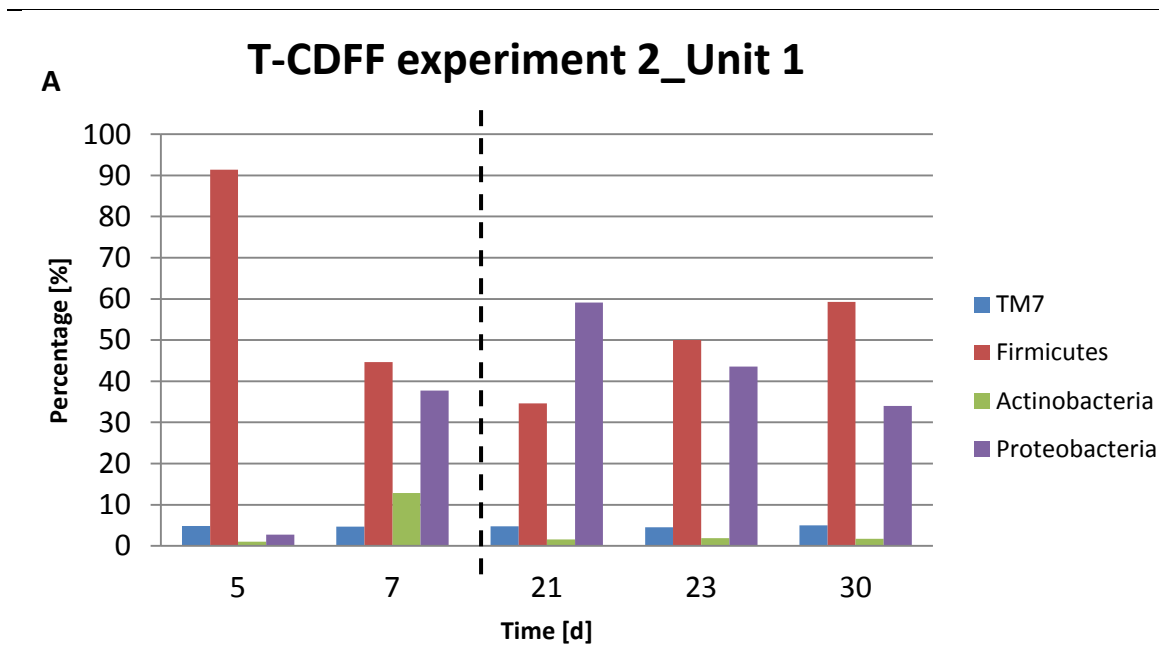
Figure 6.6 presents the phyla composition of the effluent samples retrieved from T-CDFE experiment 1, unit 1 and unit 3. Figure 6.6 A) presents the data from experiment 1, unit 1 across the health and the extended health conditions. Figure 6.6 B) presents the data from experiment 1, unit 3 across the health and gingivitis conditions. Blue represents the TM7, red represents the Firmicutes, green represents the Actinobacteria and violet the Proteobacteria. Dotted line represents the change in conditions from the health to the extended health or gingivitis conditions introduced at day 9.

Figure 6.6 presents the phyla detected in the effluent samples across the health, extended health and gingivitis conditions in unit 1 and unit 3, experiment 1. In total 3 phyla were detected across the health-extended health conditions in unit 1, experiment 1 including TM7, Firmicutes, and Actinobacteria (Figure 6.6A). The TM7

represented 5% of the community and stayed at this level throughout the phases. Firmicutes gradually decreased over time from around 90% at day 5 to 70% on the last day of the experiment, while the Actinobacteria phylum increased in proportions from 6% to 25% on the last sampling day.

Figure 6.6B presents the phyla detected in the effluent samples collected from unit 3, experiment 1 under health-gingivitis conditions. The phyla detected included TM7, Firmicutes and Actinobacteria. The TM7 genera reached 5% of the effluent community across the experimental phases. Firmicutes decreased from 91% to 81% under health conditions but then increased back to <90% in the gingivitis conditions. The Proteobacteria phyla was not detected in the effluent samples retrieved from experiment 1 as opposed to the biofilm samples collected from experiment 2, unit 1 or the effluent samples collected from experiment 2, unit 1 and unit 3.

Figure 6.7 presents the phyla composition of the effluent samples collected from health, extended health and gingivitis conditions in experiment 2, unit 1 and 3. Figure 6.7A presents the phyla composition of samples collected across health-extended health, while Figure 6.7B presents the phyla composition across the health-gingivitis conditions.



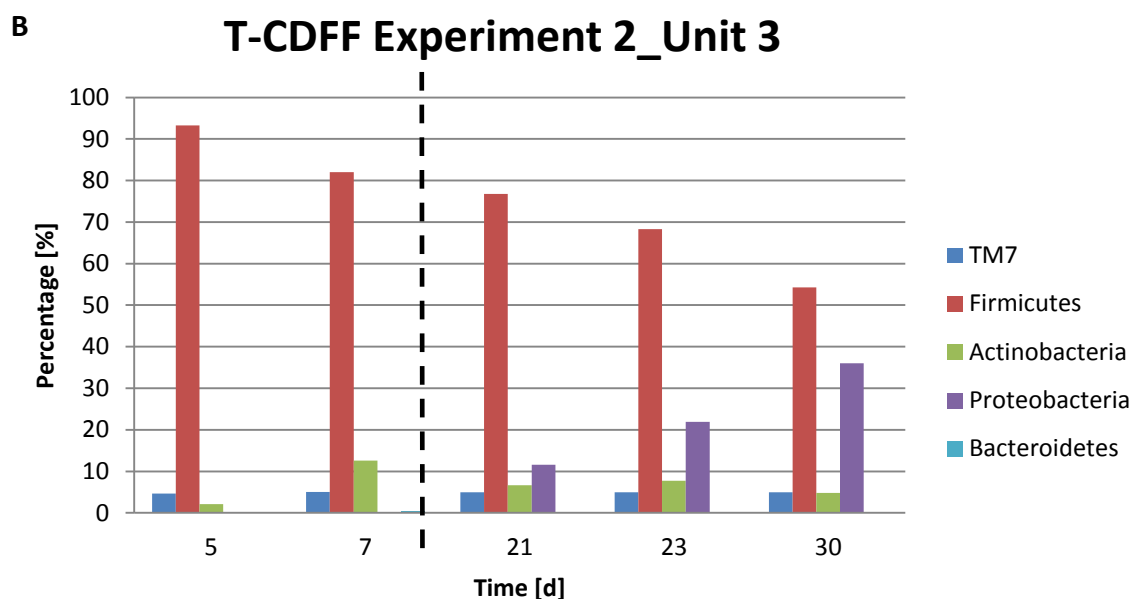


Figure 6.7 presents the phyla composition of the effluent samples retrieved from T-CDFE experiment 2, unit 1 and unit 3. Figure 6.7 A) presents the data from experiment 2, unit 1 across the health and the extended health conditions. Figure 6.7 B) presents the data from experiment 1, unit 3 across the health and gingivitis conditions. Blue represents the TM7, red represents the Firmicutes, green represents the Actinobacteria, violet represents Proteobacteria and light blue the Bacteroidetes. Dotted line represents the change in conditions from the health to the extended health or gingivitis conditions introduced at day 9.

Figure 6.7 presents the phyla composition of the effluent samples retrieved from unit 1 and unit 3, experiment 2. The phyla composition of the samples retrieved from experiment 2, unit 1 (health-extended health) consisted of 5% TM7 that stayed at this level throughout the time (Figure 6.7A). Firmicutes represented over 90% of the population at day 5 and declined to 40% on day 7 with a recovery to approximately 60% on day 30. There was an increase in Proteobacteria from day 5 to day 21 where it reached the highest proportion of approximately 60% at day 21 and then decreased to 35% at day 30.

Figure 6.7B presents the phyla composition of the samples collected from unit 3, experiment 2 (health-gingivitis). Firmicutes amounted to $\leq 90\%$ of the community at day 5 and were a dominating phylum. From day 5 onwards, there was a gradual decline in Firmicutes to just over 50% at the last day of the experiment. The Proteobacteria recorded a steady increase from day 7 onwards and reached approximately 35% of the community by the end of the experiment. Firmicutes, on the

other hand, recorded a gradual decrease in percentage over time from 93% to 54%. The TM7 maintained a steady percentage of the effluent population at around 5%. The Actinobacteria amounted to less than 10% of the effluent population throughout the time with the exception of day 7 when the percentage of Actinobacteria reached more than 10% of the effluent community.

6.3.4.2.2 Genus and species composition

The Section below presents the genus and species composition of the effluent samples collected from unit 1 and unit 3 from two individual T-CDFF experiments across the health, extended health and gingivitis conditions.

The genus composition of the effluent samples retrieved from experiment 1, unit 1 (health-extended health conditions) consisted of 60.5% *Streptococcus*, 16.8% *Enterococcus*, 8.5% *Granulicatella*, 7.7% *Rothia*, 4.8% TM7 and 2.3% *Lactobacillus*. When the health conditions were extended for another 21 days, the *Enterococcus*, *Rothia*, *Gemella* and *Lactobacillus* increased in proportions to 21.3%, 19.8%, 6.1% and 3.5%, respectively at expense of *Streptococcus* and *Granulicatella* that decreased in proportions to 39% and 6.0%, respectively. TM7 stayed at the same level of 4.8% of the effluent community. In unit 3, experiment 1 that underwent health-gingivitis conditions, the genus composition in health consisted of 64.1% of *Streptococcus*, 10.1% *Enterococcus*, 9.4% *Rothia*, 8.0% *Granulicatella*, 4.8% TM7, 3.1% *Lactobacillus* and 0.4% *Gemella*. When the gingivitis conditions were introduced at day 9, *Streptococcus* decreased to 50.6%; this was followed by a decrease of *Rothia* and *Granulicatella* down to 3.12% and 0.8%, respectively. *Enterococcus*, *Gemella* increased in proportions up to 22.2% and 3.4%, respectively. *Bacillus* which was not detected in health reached 12.7% in gingivitis conditions while TM7 stayed at the same level of 4.8%.

In unit 1, experiment 2 that underwent health-extended health conditions, the genus composition of the effluent samples in health consisted of 61.5% *Streptococcus*, 17.5% *Neisseria*, 6.9% *Granulicatella*, 6.8% *Rothia*, 4.8% TM7, 1.6% *Gemella* and 0.6% *Enterococcus*. When the health conditions were extended for another 21 days, the

composition shifted towards *Neisseria* (45.5%) at expense of *Streptococcus* that decreased to 31.0% of the community. Further to this, *Granulicatella* and *Gemella* increased in proportions up to 7.4% and 2.1%, respectively. On the other hand, *Enterococcus*, *Rothia* decreased in numbers to 0.4% and 0.8%, respectively. Genera previously not detected in health included *Lactobacillus* (1.06%), *Bacillus* (0.53%), *Actinomyces* (0.9%) and *Lysinibacillus* (5.3%).

In experiment 2, unit 3 that underwent the health-gingivitis conditions, the genus composition of samples collected from health consisted of 75.1% *Streptococcus*, 9.3% *Granulicatella*, 7.3% *Rothia*, 4.8% TM7, 1.8% *Actinomyces*, 1.1% *Lactobacillus* and 0.4% *Porphyromonas*. When the gingivitis conditions were introduced the proportions of *Streptococcus*, *Rothia*, *Granulicatella*, *Lactobacillus* decreased to 50.7%, 2.7%, 4.9%, and 0.6%, respectively. Genera previously not detected in health included *Enterococcus*, *Gemella* and *Actinomyces* with proportions of 0.6%, 7.8% and 4.0%, respectively.

Table 6.3 presents the taxonomic composition of the effluent samples collected from unit 1 and 3 in two individual T-CDFF experiments.

| strain | Experiment 1 | | | | Experiment 2 | | | |
|--|--------------|------|------------|------|--------------|------|------------|------|
| | Unit 1 [%] | | Unit 3 [%] | | Unit 1 [%] | | Unit 3 [%] | |
| | H | EH | H | G | H | EH | H | G |
| Unclassified | 4.8 | 4.8 | 4.8 | 4.8 | 4.8 | 4.8 | 4.8 | 4.9 |
| <i>Streptococcus mitis</i> group | | | | | | | | |
| <i>S. pseudopneumoniae</i> | 30.5 | 17.1 | 33.4 | 23.9 | 29.9 | 9.5 | 26.4 | 20.7 |
| <i>S. australis</i> | 2.4 | 2.2 | 3.4 | 2.1 | 2.3 | | 2.5 | 2.3 |
| <i>S. parasanguinis</i> | | | | | | 1.0 | 1.1 | 1.6 |
| <i>S. infantis</i> | 3.2 | 2.0 | 3.5 | 6.9 | 1.0 | 2.2 | 2.3 | 1.2 |
| <i>S. sanguinis</i> | | 0.5 | | | 0.7 | | | 0.2 |
| <i>S. gordonii</i> | | 1.0 | 3.6 | 0.8 | 3.7 | 0.6 | 9.2 | 2.1 |
| <i>Streptococcus anginosus</i> group | | | | | | | | |
| <i>S. intermedius</i> | | 1.6 | | 0.6 | | | | |
| <i>S. anginosus</i> | 5.6 | 4.6 | 1.6 | 3.2 | 6.3 | 11.0 | 9.3 | 11.0 |
| <i>Streptococcus salivarius</i> group | | | | | | | | |
| <i>S. vestibularis</i> | | | 1.3 | | 0.7 | | 4.6 | |
| <i>S. thermophilus</i> | | | 1.0 | | 0.5 | | 3.7 | |
| <i>Streptococcus pyogenes</i> group | | | | | | | | |
| <i>S. fryi</i> | 2.2 | 1.7 | 3.3 | 3.3 | 2.3 | 1.2 | 2.1 | 1.9 |
| <i>S. gallinaceus</i> | | | | | | | | 0.2 |
| <i>Streptococcus bovis</i> group | | | | | | | | |
| <i>S. bovis</i> | 3.3 | 2.6 | 3.3 | 2.6 | 3.8 | 1.7 | 4.0 | 3.1 |
| <i>Vagococcus teuberi</i> | 3.5 | 6.3 | 3.4 | 5.7 | 0.7 | 0.4 | 0.6 | 0.6 |
| <i>Enterococcus faecalis</i> | 10.2 | 11.1 | 5.3 | 10.8 | | | | |
| <i>Enterococcus italicus</i> | | 1.0 | 0.4 | 1.0 | | | | |
| <i>Enterococcus casseliflavus</i> | 1.2 | 3.0 | 1.4 | 3.0 | | | | |
| <i>Granulicatella adiacens</i> | 1.3 | 0.9 | 1.0 | 0.8 | 0.9 | 1.3 | 1.2 | 0.8 |
| <i>Gemella cunicula</i> | | 1.0 | | 1.1 | | | | 0.9 |
| <i>Gemella haemolysans</i> | | 2.4 | | 2.2 | 0.6 | 0.9 | 0.6 | 3.1 |
| <i>Lactobacillus rhamnosus</i> | | 2.4 | | | | 1.1 | | 0.5 |
| <i>Lactobacillus fermentum</i> | 2.3 | 1.1 | 3.1 | | | | 1.1 | 0.4 |
| <i>Actinomyces turicensis</i> | | | | | | | | 0.2 |
| <i>Actinomyces odontolyticus</i> | | | | | | | | 0.4 |
| <i>Arthrobacter psychrochitiniphilus</i> | | 0.7 | | | | | | |

| | | | | | | | | |
|--------------------------------------|-----|-----|-----|-----|------|------|-----|------|
| <i>Arthrobacter stackebrandtii</i> | | 0.5 | | | | | | |
| <i>Rothia dentocariosa</i> | | 5.0 | 1.4 | 0.4 | 2.4 | | 1.6 | 0.6 |
| <i>Rothia mucilaginosa</i> | 5.8 | 9.9 | 5.9 | 1.6 | 4.4 | 0.8 | 3.9 | 2.1 |
| <i>Bacillus horneckiae</i> | | | | 1.4 | | | | |
| <i>Bacillus cereus</i> | | | | 2.4 | | | | |
| <i>Lysinibacillus boronitolerans</i> | | | | | | 7.3 | | |
| <i>Atopobium rimae</i> | | | | | | | | 0.2 |
| <i>P. gingivalis</i> | | | | | | | 0.4 | |
| <i>Neisseria subflava</i> | | | | | 7.4 | 16.4 | | 16.9 |
| <i>Neisseria cinerea</i> | | | | | | | | 0.5 |
| <i>Neisseria mucosa</i> | | | | | 10.1 | 22.0 | | 2.3 |

Table 6.3 presents the phylogenetic composition of effluent samples from experiments 1 and 2, units 1 and 3 in health (H), extended health (EH) and gingivitis conditions (G). The effluent samples collected from health/extended health/gingivitis phases were averaged to compare the species proportions between the H-EH and H-G phases. The numbers highlighted in yellow indicate that specific species was not present in all the samples used to calculate an average.

Altogether, there were 36 bacterial species detected in total in the effluent samples in two individual T-CDFF experiments. The 22 species out of 36 detected belonged to the Firmicutes, 10 to Actinobacteria, 3 species belonged to Proteobacteria and 1 to Bacteroidetes phylum. Despite the fact, that a slightly higher number of species was detected in the effluent samples than in biofilm, there was no visible pattern across the experimental phases and abundance was still low when compared to oral microbiome which was reported to comprise of around 11-13 phyla, many genera and hundreds of species (Aas *et al.* 2005; Dewhirst *et al.* 2010; Huttenhower *et al.* 2012; Griffen *et al.* 2012;).

6.3.5 Functional approach to investigate the health-gingivitis associated shifts

6.3.6 Qualitative Analysis

This Section presents the qualitative analysis performed on the effluent NMR data retrieved from experiments 1 and 2. The Principal Component Analysis (PCA) and Orthogonal Partial Least Square (OPLS) analysis were performed by Michael Cannon (scientist at Procter & Gamble).

6.3.6.1 Experiment 1 unit 1 (simulated health conditions only)

When the OPLS analysis with one component was forced on the raw NMR data from unit 1, the standard deviations were higher than the signal measured (Figure 6.8); therefore there were no metabolites discriminating between the health and extended health conditions.

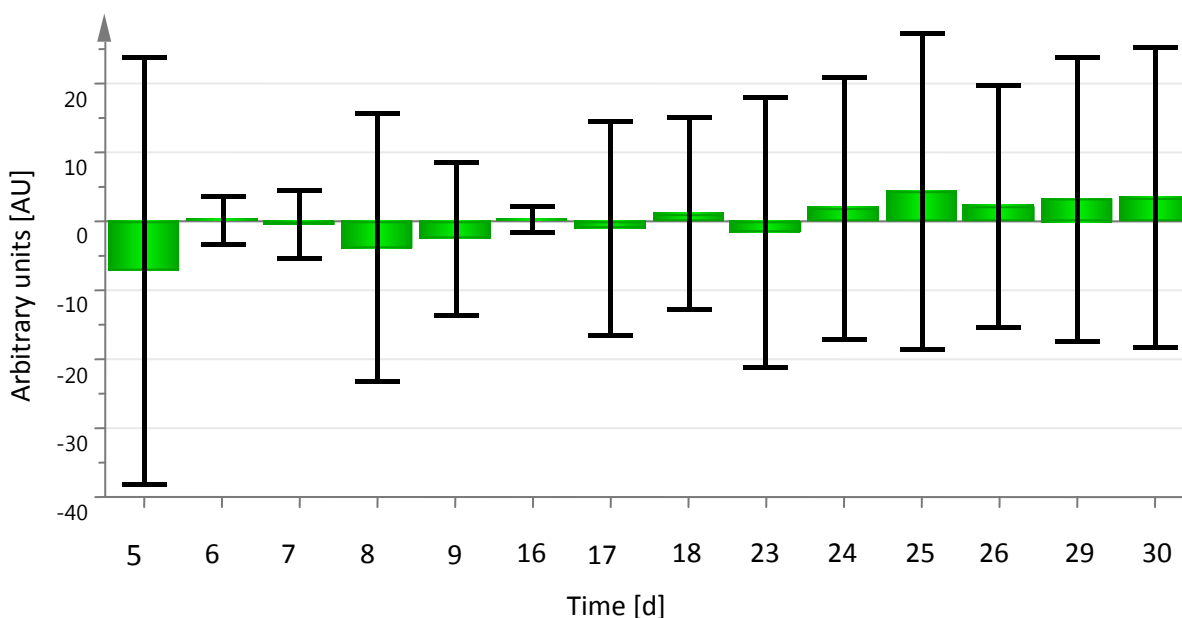


Figure 6.8 presents the results of the OPLS analysis on NMR data retrieved from unit 1, experiment 1.

6.3.6.2 Experiment 1 unit 3 (health – gingivitis conditions)

Figure 6.9 presents the OPLS analysis performed on the effluent samples retrieved from unit 3, experiment 1.

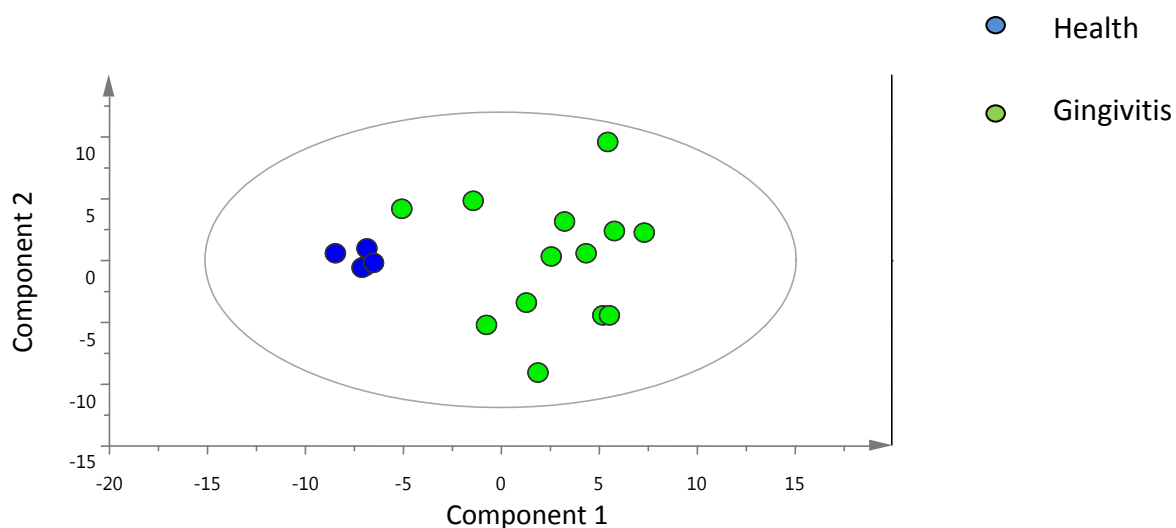


Figure 6.9 presents the OPLS analysis performed on the effluent samples retrieved from the health and gingivitis conditions in unit 3, experiment 1. Health is represented as blue; gingivitis is represented as green. Sample collected at day 7 was an outlier and was removed from the analysis.

Figure 6.9 shows the OPLS analysis performed on the effluent data retrieved from unit 3, experiment 1 (health and gingivitis conditions). When the OPLS analysis was applied to a batch of samples retrieved from unit 3, experiment 1 across the health-gingivitis conditions, the health associated samples (blue) clustered together. The gingivitis associated samples (green) were more sporadic and spread out but still distinctively different from the health cluster. The metabolites that were discriminative between the two phases included trimethylamine, pyruvate, propionate, butyrate, formate, alanine, lactate and ethanol: these are shown in Figures 6.10-6.14.

Figure 6.10 presents the first four OPLS components that were discriminative across the health and disease clusters in experiment 1, unit 3.

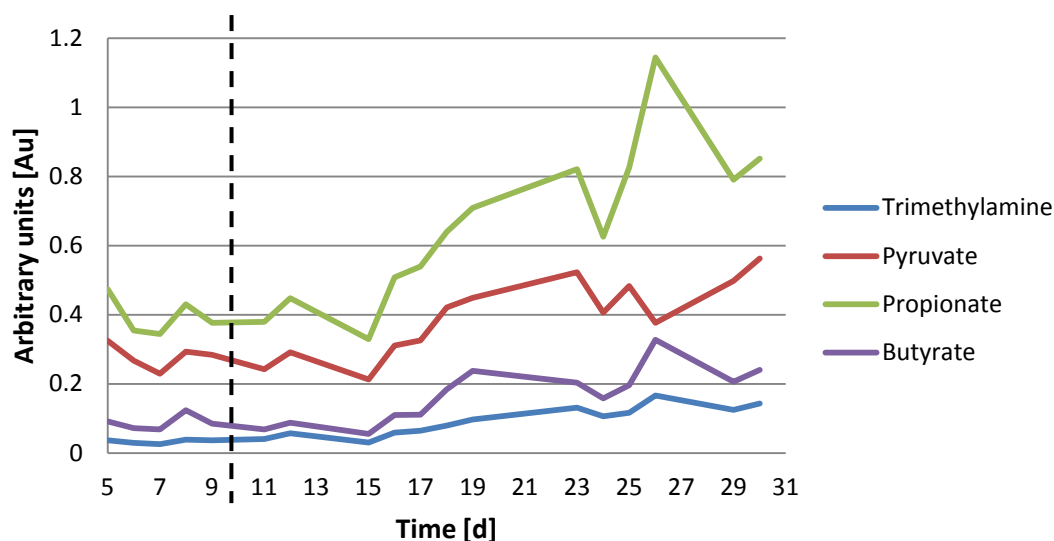


Figure 6.10 presents the components discriminating between the health and gingivitis clusters. Trimethylamine is presented in blue; Pyruvate in red; Propionate in green and Butyrate in violet. Dotted line represents the change in conditions from the health to the gingivitis conditions introduced at day 9.

Figure 6.11 presents the data for the levels of formate that were discriminative across the health and gingivitis conditions in unit 3, experiment 1.

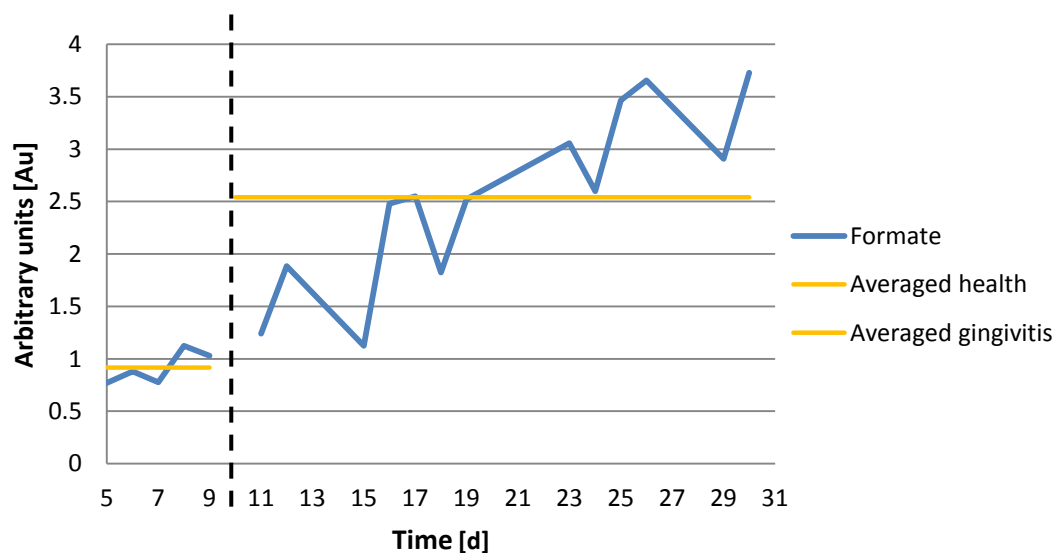


Figure 6.11 presents the levels of formate that were discriminating across the health-disease phase. Dotted line represents the change in conditions from the health to the gingivitis conditions introduced at day 9. Yellow lines represent the averaged data across the health and gingivitis conditions.

Figure 6.12 presents the data for the levels of alanine that were discriminative across the health - gingivitis phases in unit 3, experiment 1.

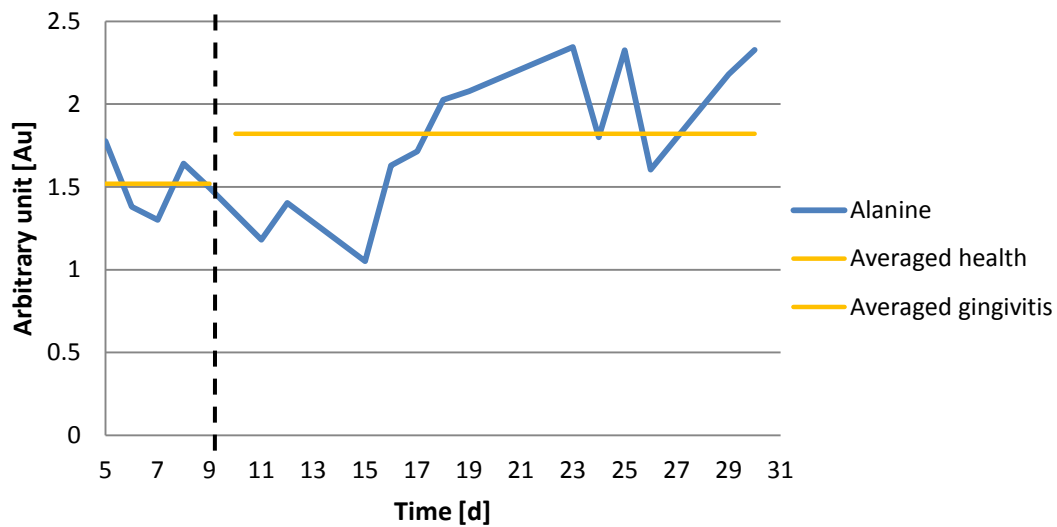


Figure 6.12 presents the levels of alanine that were discriminating across the health-disease phase. Dotted line represents the change in conditions from the health to the gingivitis conditions introduced at day 9. Yellow lines represent the averaged data across the health and gingivitis conditions.

Figure 6.13 presents the data for the levels of lactate that were discriminative across the health - gingivitis phases in unit 3, experiment 1.

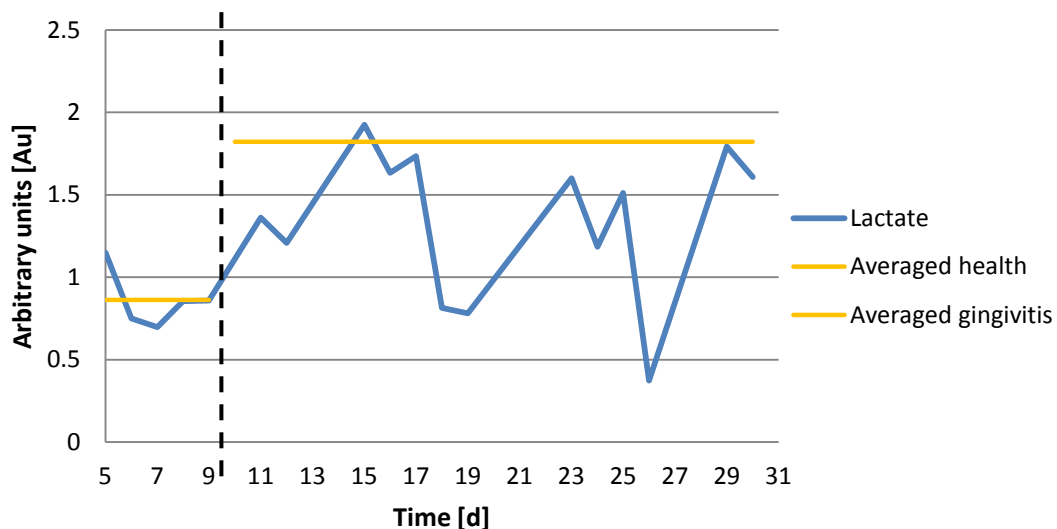


Figure 6.13 presents the levels of lactate that were discriminating across the health-disease phase. Dotted line represents the change in conditions from the health to the gingivitis conditions introduced at day 9. Yellow lines represent the averaged data across the health and gingivitis conditions.

Figure 6.14 presents the data for the levels of ethanol that were discriminative across the health - gingivitis phases in unit 3, experiment 1.

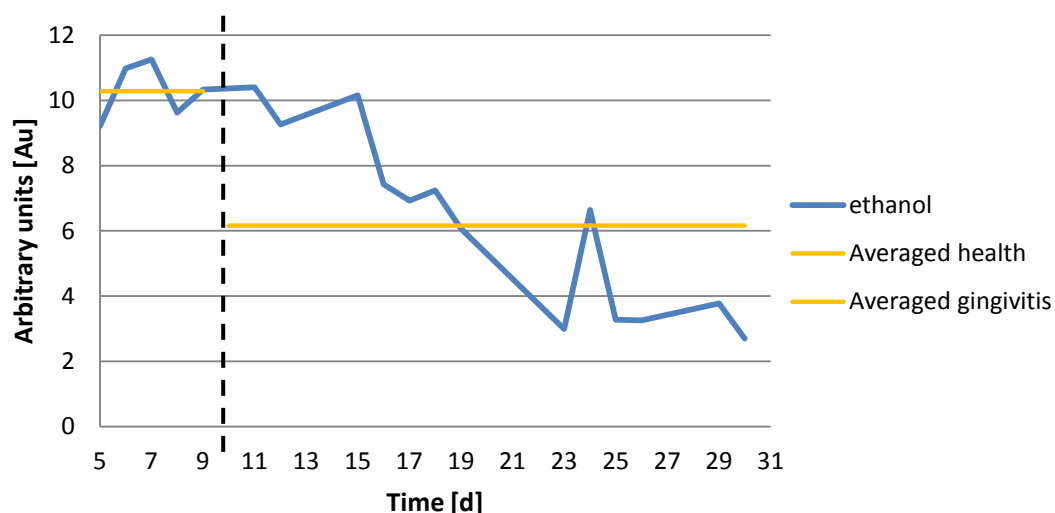


Figure 6.14 presents the levels of ethanol that were discriminating across the health-disease phase. Dotted line represents the change in conditions from the health to the gingivitis conditions introduced at day 9. Yellow lines represent the averaged data across the health and gingivitis conditions.

Figures 6.10-6.14 present data for 8 metabolites which were discriminative between the health and disease phases in experiment 1. The health data were averaged and compared with the averaged gingivitis data to investigate the fold change across the experimental conditions. Analysis of the first four metabolites (Figure 6.10) showed a 2.79 fold increase of trimethylamine, 1.40 fold increase of pyruvate, 1.67 fold increase of propionate and 1.91 fold increase of butyrate in gingivitis conditions. Figures 6.11-6.14 present the data for the remaining metabolites which showed a 2.76 fold increase for formate, 1.20 fold increase for alanine, 1.56 fold increase for lactate and 0.60 fold decrease of ethanol under gingivitis conditions. The Student's t-test applied to the above data confirmed that only formate ($p=0.016$), trimethylamine ($p=0.038$) and lactate ($p=0.015$) recorded a significant increase in gingivitis conditions

6.3.6.3 Experiment 2 unit 1 (simulated health conditions only)

When the OPLS analysis was forced on samples collected from health-extended health conditions in unit 1, experiment 2, they did not cluster and there were no discriminative components across the phases.

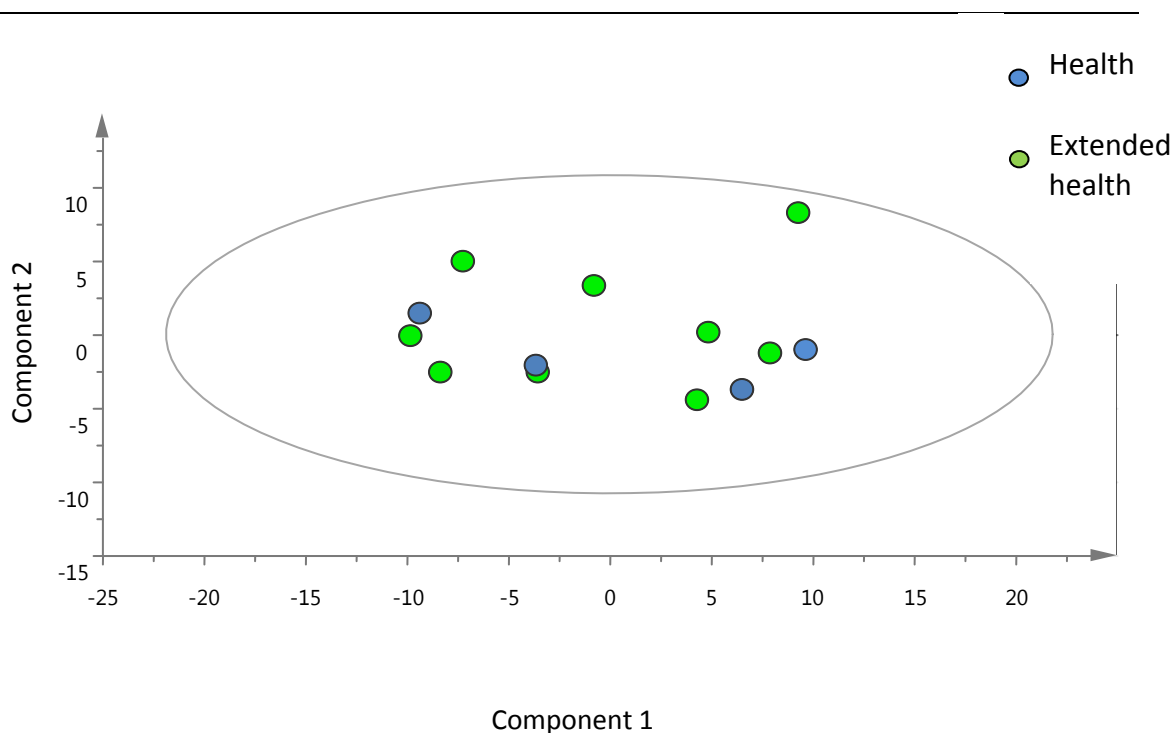


Figure 6.15 presents the OPLS analysis equivalent to the one performed on the NMR data from unit 3, experiment 1 shown in Figure 6.9 and unit 3, experiment 2 shown in Figure 6.16. Samples retrieved from health conditions are represented in blue and samples from the extended health are represented in green.

As depicted in Figure 6.15 samples were randomly distributed with no particular pattern across the health and the extended health conditions. This suggests that there was no particular difference between the health and the extended health conditions in unit 1, experiment 2.

6.3.6.4 Experiment 2 unit 3 (health – gingivitis conditions)

This Section presents the results from the qualitative OPLS study performed on the raw effluent NMR data retrieved from the health and gingivitis conditions from unit 3, experiment 2 and shown in Figure 6.16.

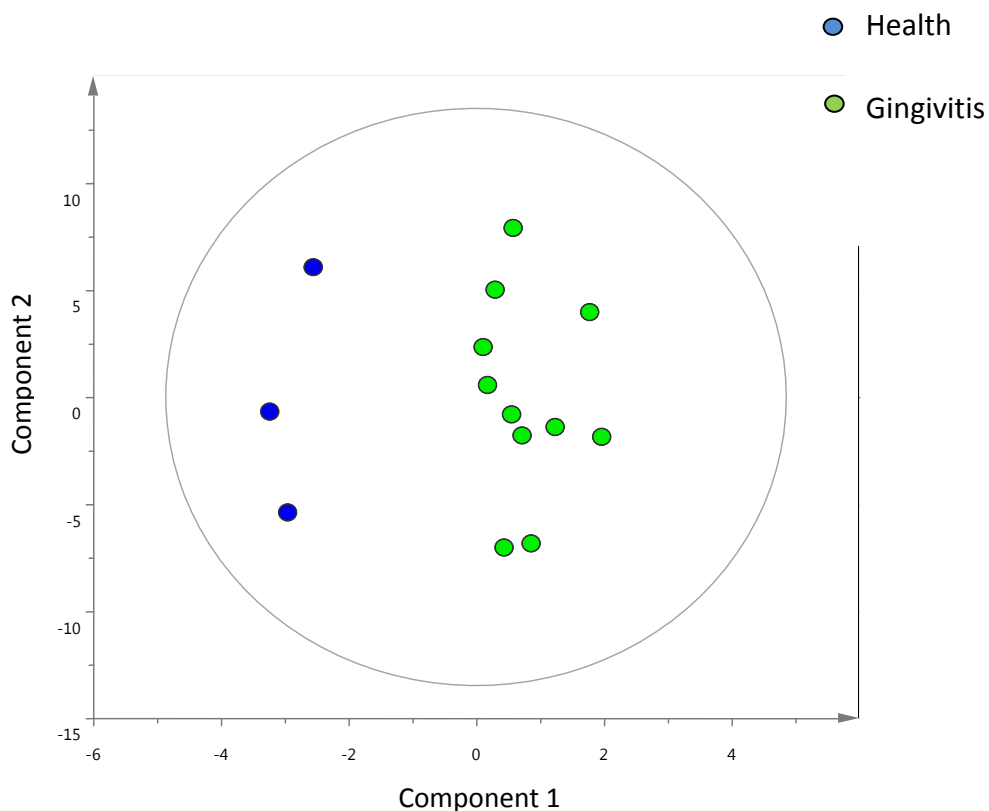


Figure 6.16 presents the OPLS analysis performed on the effluent samples retrieved from the health and the gingivitis conditions in unit 3, experiment 2. Health is represented as blue; gingivitis is represented as green. This figure is equivalent to Figure 6.9 (unit 3, experiment 1).

Figure 6.16 presents the data for effluent samples retrieved from unit 3, experiment 2 across the health and gingivitis conditions. The PCA showed that there is a clear difference between the health and gingivitis samples as they cluster across the phases. The metabolites that were discriminative between the phases included succinate, trimethylamine, formate, and acetate and are shown in Figure 6.17 and 6.19.

Figure 6.17 presents the data for the levels of succinate that were discriminative across the health-gingivitis phases in unit 3, experiment 2.

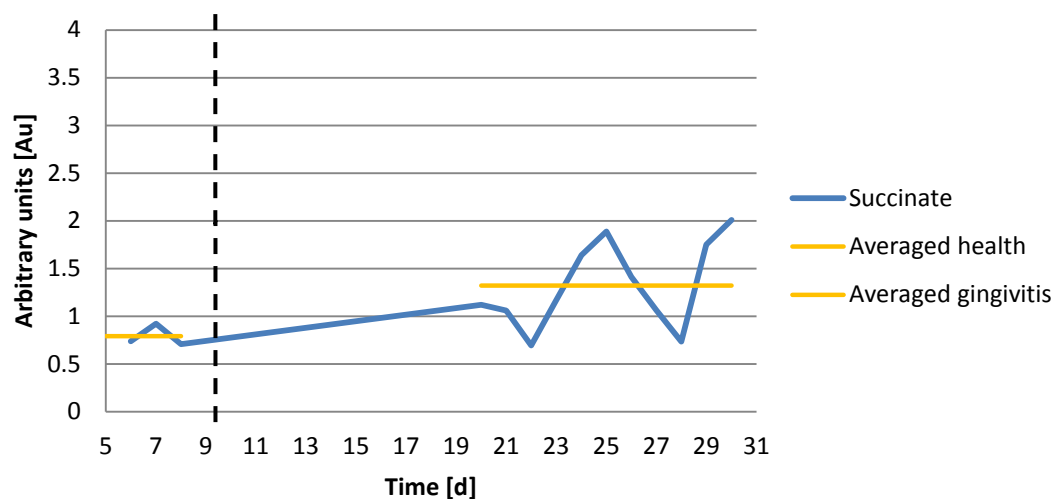


Figure 6.17 presents the levels of succinate that were discriminating across the health-disease phase. Dotted line represents the change in conditions from the health to the gingivitis conditions introduced at day 9. Yellow lines represent the averaged data across the health and gingivitis conditions.

The qualitative OPLS analysis showed an increase of succinate over time across the health and diseases phases. The health data was averaged and compared to the averaged gingivitis data to investigate the fold change across the experimental conditions. This approach was applied to succinate and the three other metabolites trimethylamine, formate and acetate. The average amount of succinate in health amounted to 0.79 Au and increased to 1.3 Au in gingivitis conditions that was a 1.67 fold increase ($p=0.281$). However the change was not significant when the Student's t-test was applied.

Figure 6.18 presents the data for the levels of trimethylamine that were discriminative across the health - gingivitis phases in unit 3, experiment 2.

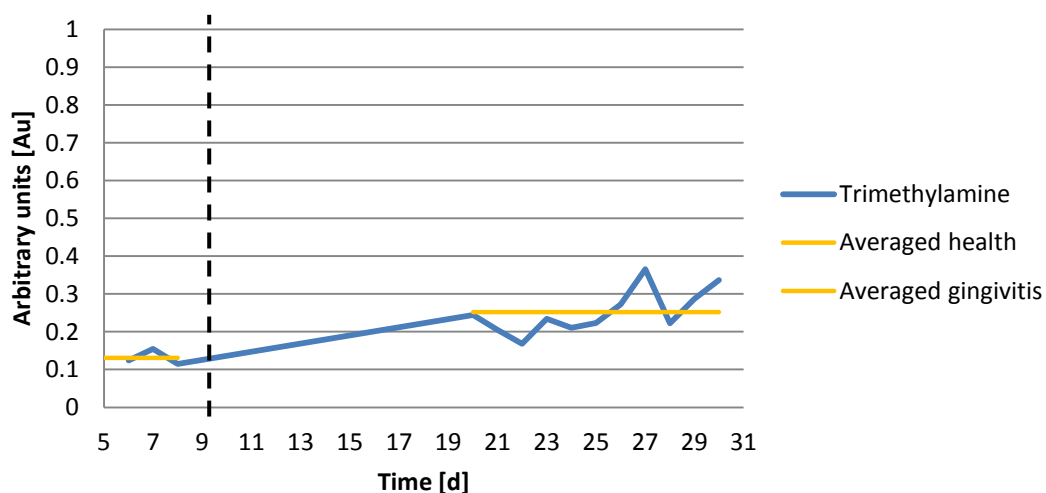


Figure 6.18 presents the trimethylamine the OPLS component discriminating across the health-disease phase. Dotted line represents the change in conditions from the health to the gingivitis conditions introduced at day 9. Yellow lines represent the averaged data across the health and gingivitis conditions.

Figure 6.18 presents the qualitative OPLS analysis that showed an increase of trimethylamine by 1.92 fold across the phases ($p=0.063$). However, the change was not significant when analysed using a paired Student's t-test.

Figure 6.19 presents the data for the levels of formate that were discriminative across the health - gingivitis phases in unit 3, experiment 2.

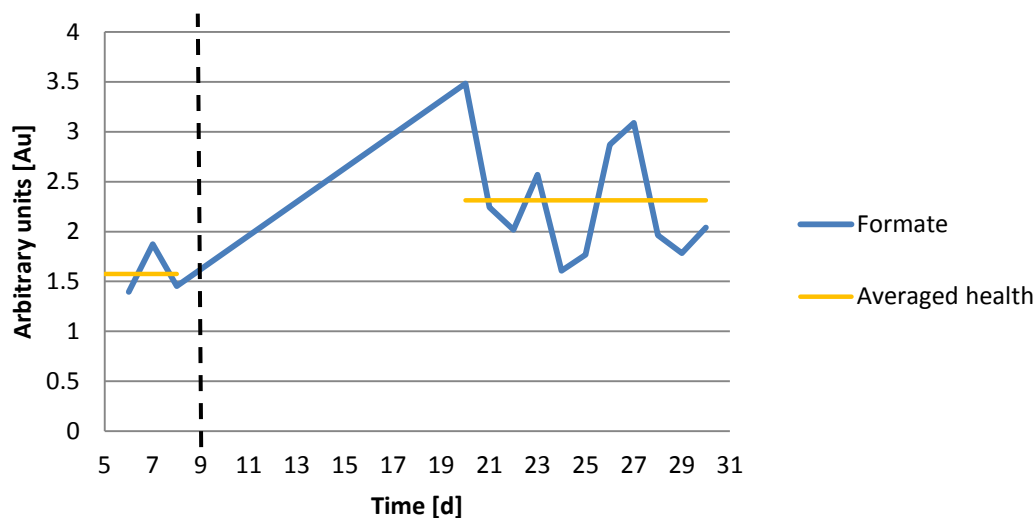


Figure 6.19 presents the formate the OPLS component discriminating across the health-disease phases. Dotted line represents the change in conditions from the health to the gingivitis conditions introduced at day 9. Yellow lines represent the averaged data across the health and gingivitis conditions.

Figure 6.19 presents the data obtained from the qualitative OPLS analysis for the levels of formate that were discriminative across the health - gingivitis phases in unit 3, experiment 2. When the average health was compared to the average gingivitis data, there was a 1.47 fold increase of formate in gingivitis conditions as shown in Figure 6.19. However, the change was not significant when analysed using a Student's t-test ($p=0.208$).

Figure 6.20 presents the data for the levels of acetate that were discriminative across the health - gingivitis phases in unit 3, experiment 2.

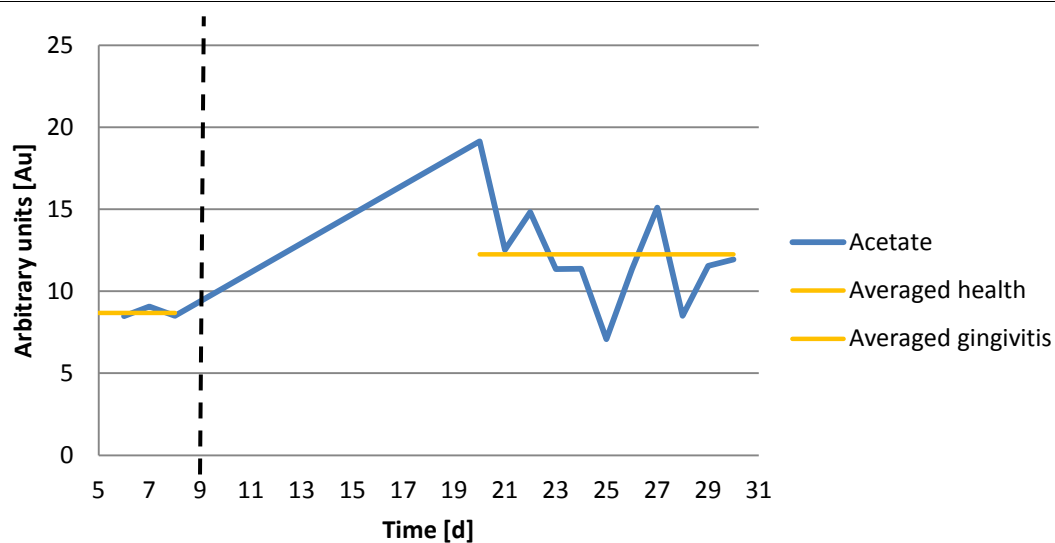


Figure 6.20 presents the acetate levels across the health and disease conditions. Dotted line represents the change in conditions from the health to the gingivitis conditions introduced at day 9. Yellow lines represent the averaged data across the health and gingivitis conditions.

There was high variability in the level of acetate in gingivitis conditions when compared to health. When the average health was compared to the average acetate level in gingivitis conditions, there was a 1.41 fold increase in gingivitis conditions. However, the change was not significant when analysed using a Student's t-test ($p=0.058$).

6.4 Discussion

With the today's technological advances it is possible to look into the oral microbiome in depth. The richness of the human oral cavity was estimated to be over 700 species, of which more than a half is still uncultivable. Identifying specific bacteria provides a good indication of disease progression, however it does not explain the disease aetiology, nor does it provide adequate knowledge for complete disease eradication. Thus holistic approaches which have the prospect of bringing a comprehensive understanding of disease are gaining in popularity. The availability of cost-effective sequencing, allowing high-throughput and fast sample-to-data turnover has opened a new chapter of 'omics' techniques in the field of oral microbiology which allows one to take a more holistic approach to understanding pathogenicity.

6.4.1 Methodology choice

The methodology presented in this chapter was designed to determine whether the absence of the bacterial changes across the experimental conditions presented in chapter 4 and 5 was due to a limited focus on only 8 bacterial species or due to inadequate gingivitis methodology (provision of an appropriate environment) which might have led to lack of the ecological shift. To address these questions, two different *in vitro* gingivitis methodologies were aimed to be tested in this chapter (gingivitis+ in unit 2, gingivitis++ in unit 3). However, due to the fact that unit 2 was broken at early stage of experiment 2, the gingivitis+ methodology was not tested in this chapter. My investigation focused on gingivitis++ methodology only and the use of two 'omics' techniques. 16S rRNA gene sequencing and ¹HNMR metabolite fingerprinting were applied to obtain a greater understanding of the complex biofilm interactions and the bacterial composition across the experimental phases.

The data obtained from chapter 5 showed that there was no increase in *F. nucleatum* and *P. intermedia* which are associated with gingivitis, despite the detection of increased levels of gingivitis associated metabolites which are mainly produced by the gingivitis associated Gram-negative bacteria (Fukushima & Ochiai 1995). To explore this phenomenon further and to get a better insight into bacterial shifts occurring across the

health-disease and health-extended health, 16S rRNA gene sequencing was introduced in this chapter to determine the species composition over time and across the different experimental conditions. This was combined with ^1H NMR metabolomic study which had been previously validated in chapter 5 and proved to be a useful technique in gingivitis modelling *in vitro*. It provides useful information about the function of the microbiome that can be linked with its virulence (Emwas *et al.*, 2013; Xu *et al.*, 2014). A combination of these two techniques can potentially bring an explicit understanding regarding the microbial composition and the physiological status of the collected samples. Despite the fact, that qPCR study was focused on a limited number of species (8 bacteria associated with health/gingivitis) and provides only a limited insight into community changes, it was included in this chapter to enable a direct comparison with the qPCR data obtained from previous chapters.

6.4.2 Methodology optimisation

Alterations of the gingivitis methodology included applying different experimental conditions to each of three T-CDFF units.

- Unit 1 was run under health conditions for 30 days and served as a control group for the remaining two units.
- Unit 2 was run for 9 days under health conditions and then the gingivitis conditions were introduced for the remaining 21 days ('gingivitis+').
- Unit 3 followed a similar experimental pattern with the difference being that the 'gingivitis++' methodology was applied instead; this included delivering artificial GCF at a higher flow rate of 130 μL / min.

The approach of applying two different gingivitis methodologies was aimed at elucidating whether the absence of a significant increase in the numbers of Gram-negative bacteria was related to a possibly inadequate gingivitis methodology applied in the past. The 16S rRNA gene sequencing study was used to investigate the species composition and then to correlate the metabolites with the bacterial producers detected by the genomic study. For the comparison purposes, the biofilm and the effluent sampling points in two individual T-CDFF experiments were arranged in the same manner. The biofilm analyses

were performed at day 5, 7, 18, 23 and day 30. The effluent collection from experiments 1 and 2 was aimed to be performed at the same time intervals, however, due to technical constraints and operator's sickness the sampling schedule was affected. Subsequently, 18 effluent samples were collected from experiment 1 and 15 from experiment 2.

6.4.3 Experimental problems encountered

Throughout the set of two T-CDFF experiments performed in this chapter, a few mechanical issues were encountered which required solving. On a few occasions the gearbox broke down in different units; this was due to bacterial seepage through the shaft, causing the mechanism to cease up and stop in the middle of the experiment. This issue was resolved without much difficulty by substituting the broken gearbox with a new one. As it was fixed immediately, it did not affect the experiment or any further data collection or analysis.

The majority of mechanical issues encountered were due to excessive waste leakage. As each T-CDFF experiment is run for 30 days, the model is continuously exposed to waste material that can leak through and block the shaft and turntable. This situation occurred on several occasions in the past and was resolved by attaching an additional PTFE cover to protect the shaft (Chapter 3, Section 3.3.1, Figure 3.1B2). This solution proved satisfactory for most experiments with the exception of the last T-CDFF experiment, experiment 2. During this last experiment, the waste seeped through the PTFE cover and blocked the shaft and turntable. Unfortunately, I was not able to substitute this unit with another one to revive the experiment. The mechanical fault was quite severe, and there was no option of repairing it without fully dismantling it and sending it off to the manufacturing company (AC Service group). This unit therefore was excluded from the study and a new solution to the problem was sought. After the consultation with AC Service group, the PTFE cover protection was substituted with a newly designed shaft which was made of stainless steel and embedded into the model's construction. This new design was applied to all three units but was not tested due to time constraints of this project. To compare the two data sets obtained from these two individual T-CDFF experiments, the data retrieved from the T-CDFF experiment 1, unit 2 were also excluded from further analysis and are not presented in this chapter.

6.4.4 Real-time PCR study to investigate the health-gingivitis associated shifts

Real-time PCR was initially chosen as it is a fast, reliable and cost effective method for identifying and quantifying bacteria associated with gingivitis onset. Additionally, this method permits a reliable quantitative analysis on the bacterial shift across the experimental conditions' change. To enable this happen, the biofilm and the effluent samples collected throughout the experiment duration were screened for the 8 bacteria associated with oral health and gingivitis. The data for the total bacteria presented in Figure 6.2 showed no major differences across the phases with the exception for unit 1 in experiments 2 that recorded a 0.62 log decrease in extended health. One may hypothesise that while the total number of bacteria remained relatively constant over time, the proportions of certain gingivitis associated species across the phases might have changed due to the experimental conditions applied over time. This was further investigated by analysing the qPCR data obtained for the remaining 8 species.

There were 3 health associated bacteria (*S. sanguinis*, *S. mutans*, *N. subflava*) detected in biofilm samples collected from T-CDFE experiments 1 and 2. *V. dispar*, *F. nucleatum* and *P. intermedia*, and *L. casei* were not detected in either experiment 1 or 2. The lack of detection of these 3 pathogenic species (*F. nucleatum* and *P. intermedia*, and *L. casei*) may suggest that the experimental gingivitis methodology applied in this chapter was not suitable to invoke a gingivitis associated community *in vitro* or that the species selection was too narrow to reflect the diverse oral population.

The same pattern was observed for the effluent samples collected from the T-CDFE experiments. These four bacteria associated with gingivitis (*F. nucleatum* and *P. intermedia*, *A. naeslundii* and *L. casei*) were either not detected or detected in very low numbers. The lack of detection or increase of the gingivitis associated bacteria may suggest that (i) the *in vitro* gingivitis conditions were not established in the model or (ii) that focusing on only 4 gingivitis associated bacterial species may have given a very limited understanding of what was happening throughout the health-extended health and health-gingivitis transition.

These findings do not corroborate with the data published by Dalwai (2007, 2006). Dalwai and colleagues modelled gingivitis associated shifts *in vitro* using CDFF model and similar gingivitis methodology. They have established that the change from health to *in vitro* gingivitis invokes an ecological shift which results in a significant increase of *Actinomyces* spp. at the expense of *Streptococcus* spp. under gingivitis conditions (2006). Further to this, there is an increase in numbers of *Prevotella* spp., *Fusobacterium* spp. and Gram-negative spp. (2007). Similar findings were presented in other studies (Syed & Loesche 1978; Moore *et al.* 1984; Moore & Moore 1994). On the contrary, the qPCR study presented in this chapter showed no detection of *F. nucleatum*, *P. intermedia*, detection of low numbers of *A. naeslundii* and also lack of significant change for *S. sanguinis* across the simulated health-gingivitis conditions. To provide a better understanding of the oral community composition developed in T-CDFF model, 16S rRNA gene sequencing was applied to both the biofilm and the effluent samples to investigate the compositional differences across the conditions' change.

6.4.5 Genomic approach to investigate the health-gingivitis associated shifts

The taxonomic composition of the biofilm and effluent samples retrieved from unit 1 and 3 in experiments 1 and 2 is presented in Table 6.2 and Table 6.3. The comparison of the health-disease genomic data (unit 3) with the control data (unit 1) allowed us to determine whether or not the *in vitro* model reflected the *in vivo* oral health and gingivitis. A set of genomic data obtained from the biofilm samples presented in Figure 6.4, 6.5 and Table 6.2 showed low taxonomic abundance in health, extended health or gingivitis conditions in two individual T-CDFF experiments and no detection of gingivitis associated species. The phyla detected in the biofilm retrieved from unit 1 and 3 in experiment 1 included Firmicutes, Actinobacteria, Proteobacteria and TM7. Out of the 11 phyla found in oral cavity, the most predominant 6 include Firmicutes, Proteobacteria, Bacteroidetes, Actinobacteria, Fusobacteria and TM7 (Huang *et al.* 2011). My data agree with these findings as Firmicutes were the most abundant phylum found in my samples followed by TM7 and Actinobacteria. However, the data do not reflect the abundance of oral cavity where around 11 phyla and hundreds of species are found (Dewhirst *et al.*,

2010; Wade *et al.*, 2011). Additionally, there was a disparity in terms of phyla composition between the units in individual experiments and no particular pattern observed across the switch from health to extended health / gingivitis.

Figure 6.6-6.7 presents the phyla composition of the effluent samples collected from unit 1 and 3 in two T-CDFF experiments. The taxonomic data for the effluent samples showed low abundance as only 5 phyla were detected (Firmicutes, Actinobacteria, Proteobacteria, Bacteroidetes and TM7). The major difference between the biofilm and the effluent phyla composition was that the effluent data recorded a high percentage of Proteobacteria in both units in experiment 2. Importantly to mention is that the Bacteroidetes phylum which consists of the gingivitis associated genera such as *Prevotella*, *Porphyromonas*, *Tannerella* and *Capnocytophaga* was only detected in health conditions in experiment 2, unit 3. As shown by Huang *et al* (2014) in his experimental gingivitis study and confirmed by others (Wade 2011; Abusleme *et al.* 2013; Wang *et al.* 2013), out of 6 most abundant phyla in oral cavity Firmicutes and Actinobacteria are associated with oral health while Bacteroidetes, Fusobacterium and TM7 are associated with gingivitis. My data, retrieved from both effluent and biofilm samples, showed a steady level of TM7 throughout the conditions' change and overall lack of detection of Bacteroidetes and Fusobacterium. This would suggest that the bacterial composition of the samples collected from T-CDFF consisted of the health associated bacteria mostly. This is consistent with the qPCR study as *P. intermedia* (Bacteroidetes) and *F. nucleatum* (Fusobacteria), two species associated with gingivitis progression, were not detected in either biofilm or effluent samples. However, it is important to mention that I screened for only 4 gingivitis and 3 health associated bacteria, so the comparison between the data sets is limited.

The phylogenetic data presented in Table 6.2 and 6.3 showed a total of 29 bacterial species detected in biofilm and 36 in the effluent samples collected from two individual T-CDFF experiments. Generally speaking, a lower abundance was expected due to the fact that I was simulating the oral conditions in an *in vitro* system with has a limited ability to provide the complex biofilm-host interactions and sophisticated nutrient sources which are seen *in vivo* (Siqueira & Rôças 2013). However, the above mentioned

abundances were still lower than anticipated. Further to this, the species detected in the biofilm and effluent across different experimental conditions (presented in Table 6.2 and Table 6.3) belonged to health associated genera with the exception for Bacteroidetes, *Porphyromonas gingivalis* which was detected in unit 3, experiment 2 (health conditions only).

Most of the species detected (i.e. *Streptococcus* or *Lactobacillus* genera) are the major lactate producers thus contributed to a significant rise in lactate across the health-gingivitis phases. Other metabolites that increased across the health-gingivitis conditions, but the change was not significant, included for example butyrate, acetate, and propionate. Although the species detected in the genomic study could not be directly linked with the above mentioned metabolites. The exact reason for the discrepancy between the metabolomic and genomic study in terms of lack of detection of Gram-negative species (mainly from *Prevotella*, *Fusobacterium* or *Porphyromonas* genera) responsible for the production of butyrate, acetate and propionate is unknown. In the Section below I hypothesise what might be the most likely reason for this situation.

In my 16S rRNA gene sequencing study I had a limited number of reads available per sample. Thus, if the samples contained high numbers of *Streptococcus* spp. and other health associated genera compared to relatively low numbers of Gram-negative gingivitis associated bacteria, they might have not been covered. It is hypothesised here that the proportion of Gram-negative bacteria associated with the butyrate, propionate and acetate production was much lower than the overwhelming numbers of *Streptococcus* spp. plus they might have been further underrepresented by bias introduced during the sample processing that resulted in losing them from genomic study. This may include the choice of the DNA extraction protocol method which can introduce bias into diversity studies. DNA extraction is based on cell lysis to remove the cell membrane and other components. If the extraction conditions including physical and chemical conditions are too harsh it might lead to underrepresentation of Gram-negative bacteria which are more susceptible to lysis than Gram-positive bacteria. The bead-beating DNA extraction protocol, which is a harsh chemical method, was previously validated and confirmed by Lena Ciric (Griffiths *et al.*, 2000; Ciric *et al.*, 2010) to work effectively against both the

Gram-negative and positive species. Therefore, it seems more probable that bias could have been accumulatively gained throughout the sample processing (e.g. library preparation).

Another one may include poor DNA quality that have resulted from prolonged DNA storage (-20 °C for \geq year) and often thawing. This might have also led to degradation of DNA that was already present in lower amounts (Anchordoquy & Molina 2007).

At the time of sample processing, the Illumina MiSeq v2 had been just recently launched. It was chosen for the purposes of this project due to its relative low cost and long-read lengths in comparison to other platforms. Despite all that, Illumina's sequence by synthesis sequencing is a second generation NGS which still requires library preparation that can introduce bias into diversity studies (van Dijk *et al.*, 2014). There are several stages in library preparations that can influence the evaluation of community composition. PCR is recognised as the major factor contributing to biased identification of microorganisms due to uneven amplification efficiency - loss of specific DNA fragments when others are more efficiently amplified (van Dijk *et al.*, 2014). More importantly, however, next generation sequencing platforms require a clean DNA product that is free from inhibitors and do not interfere with the sequencing reaction. The AmPure XP Magnetic Bead method used in this study works by binding the DNA on magnetic beads and creating a DNA pellet on one side of the cuvette by applying the magnet. Pelleted DNA is washed with ethanol to remove the contaminants. Then the beads are rinsed with PCR-grade water and eluted by removing the magnet. This method provided a good clean-up strategy but is burdened with DNA losses which might be particularly problematic if dealing with low concentration of DNA that can be eventually lost.

Cleaned-up samples are quantified and pooled to create a library. At this stage the sample DNA is even further diluted what might results in loss of the DNA that was present in very low quantities when compared to overrepresentation of other species (e.g. *Streptococcus* genus). Last but not least, the post-processing stage might have also added to the problem. For example, the quality step that involves data de-noising and

removing low abundance reads, might have further led to removal of OTUs present in low quantities.

It is hard to get a full understanding of phenomenon discussed in this chapter based on one genomic and metabolomic study performed. If the time constraints were not in place, more T-CDFE experiments and sequencing runs on the data gathered would be done ($n \geq 3$).

6.4.6 Functional approach to investigate the health-gingivitis associated shifts

Metabolomics is a relatively new technique which brings detailed information about the physiological status of the biological system. It was introduced in the previous chapter, chapter 5, to validate its usefulness in modelling gingivitis associated shifts *in vitro*. As verified in chapter 5, metabolite fingerprinting using the $^1\text{H-NMR}$ spectroscopy provides information about the metabolic end products which can be then directly related to pathogenicity (Aimetti, 2011).

The metabolomic analysis was introduced in this chapter to investigate the metabolite fingerprint profile of the effluent samples collected from different experimental conditions throughout the duration of the experiment. The qualitative analysis was performed on raw NMR spectra obtained from each unit using the PCA and OPLS analysis performed by Michael Cannon using Simca-P v 22 (scientist at Procter & Gamble). The PCA and PLS analysis performed on the control data from unit 1 in both T-CDFE experiments showed no clustering across the health and the extended health conditions (Figure 6.8 and Figure 6.15). These results indicate that there was no differentiation across the health and the extended health conditions in both T-CDFE experiments. When the same qualitative analysis was applied to unit 3 (experiments 1 and 2) exposed to health - gingivitis conditions, there was a clear clustering across the experimental phases. Figure 6.9 and Figure 6.16 present a clear differentiation across the health-disease conditions in both experiments. The PCA and OPLS analysis applied to the raw NMR data from unit3 showed that the components discriminative across the health-gingivitis conditions include trimethylamine, pyruvate, propionate, butyrate, formate, alanine,

lactate and ethanol in experiment 1 and succinate, trimethylamine, formate and acetate in experiment 2.

The T-CDFF experiment 1 showed an increase of trimethylamine, pyruvate, propionate, butyrate, formate, alanine and lactate under gingivitis conditions with the exception of ethanol which decreased over time. However, only changes recorded for formate, trimethylamine and lactate were considered as statistically significant. Experiment 2 showed an increase in succinate, trimethylamine, formate and acetate under gingivitis conditions, with none of the changes statistically significant. The species composition detected across the health-gingivitis conditions in unit 3 in two individual T-CDFF experiments consisted mostly of health associated bacteria. These belonged mostly to *Streptococcus* genus that is the major lactate producer and contributed to high levels of lactate. The major producers of other metabolites detected in this study (propionate, butyrate, acetate and succinate) belong to *Porphyromonas* spp., *Fusobacterium* spp., *Prevotella* spp., *Actinomyces* spp. but were not detected in either qPCR or genomic study.

Aimetti and colleagues (2011) investigated a healthy cohort of patients versus gingivitis patients using ¹H-NMR metabolomics and reported that gingivitis patients are characterised by elevated levels of acetate, butyrate, trimethylamine, succinate and propionate which are strongly correlated with gingival inflammation. In their study, they propose that the healthy patients can be distinguished from the gingivitis patients by a 1 fold increase of acetate, >2 fold increase of trimethylamine and approximately 4 fold increase of succinate (Aimetti *et al.*, 2011). My qualitative PCA and PLS analysis performed on data from experiment 1 showed 2.79 fold increase of trimethylamine, 1.4 fold increase of pyruvate, 1.67 fold increase of propionate, 1.91 fold increase of butyrate across the health-gingivitis conditions. Experiment showed 1.41 fold increase of acetate, 1.47 fold increase of formate, 1.92 fold increase of trimethylamine and 1.67 fold increase of succinate under gingivitis conditions. My findings show similar fold increases (in spite of being mostly borderline insignificant), what would suggest that there might have been a shift towards the Gram-negative species which are the main producers of the above mentioned metabolites. However, further testing and optimisation is needed to confirm these findings.

6.5 Conclusion

The qPCR study was a satisfactory approach in validating and determining model's reproducibility as presented in chapter 4. However, in terms of the investigation of the community shifts across the experimental conditions' change it has given a very limited insight into community composition. The 16S rRNA gene sequencing study was introduced to investigate the community composition across the conditions' change and to correlate it with the metabolites being produced. The genomic study showed a low bacterial abundance and a lack of detection of the gingivitis associated bacteria. This did not corroborate with data obtained from the metabolomic study. The metabolite fingerprinting showed a separation between the simulated health and gingivitis conditions with the components discriminating between the phases including formate, acetate, succinate or trimethylamine etc. These metabolites are correlated with gingivitis and their main producers include the Gram-negative gingivitis associated bacteria (*Prevotella* spp, *Fusobacterium* spp, or *Porphyromonas* spp. etc) that were not detected in my model. The results presented in this chapter were inconclusive and further investigation would be needed. That should involve increasing the number of repetitions to minimise the experimental bias and also optimising the experimental methodology to mimic the *in vivo* situation reliably.

7 Final Discussion

7.1 Project background

Periodontal diseases affect populations all over the world and are amongst the most prevalent human illnesses on our planet (Brown *et al.* 2000). Gingivitis in particular affects approximately 32% of adults in the USA (approximately 33 million people) every year (Brown *et al.* 2000). In a review from 1999 it was estimated that around \$14.3 billion per visit is spent on periodontal preventive procedures in the U.S. (Brown *et al.* 2000). In another study from 2005 it was estimated that the treatment of patients with a primary diagnosis for periodontal diseases admitted to Emergency Units in the U.S. cost close to \$33.3 million with a mean hospital charge of \$456 per visit (Elangovan *et al.* 2011). As another example, the National Health Service in the United Kingdom spends around 1.6 billion on dental services per year (Marsh 2003).

Periodontal diseases (e.g. gingivitis) may affect the quality of life and well-being of those affected. It is also hypothesised that they might have a link with chronic diseases such as diabetes (Petersen *et al.* 2005) and can lead to indirect costs to the country's economy such as days lost at work (treatments or dentist's visit) (Elangovan *et al.* 2011). Gingivitis, for example, is a prevalent disease affecting most of us throughout our lifetime. Having this in mind, it is important to understand the aetiology of its progression, to either treat or eradicate this disease (Brown *et al.* 2000). *In vitro* models are useful tools in addressing these needs as they allow us to (i) gain an understanding of the disease progression mechanism, (ii) screen or test compounds with anti-gingivitis properties and (iii) predict the *in vivo* outcomes (Greenman *et al.* 2005). The utility of *in vitro* models is that they mimic the phenomenon observed in real life (e.g. plaque formation, gingivitis onset) and offer both explanatory and predictive capabilities. As the aetiology of gingivitis is complex, we need laboratory models to investigate disease development with more flexibility than is possible in *in vivo* studies, which are usually limited by patients' compliance and the amount of perturbations that can be done on oral biofilms in mouth. Therefore, it is easier to

study gingivitis onset in a confined laboratory system that provides greater control and flexible manipulation of experimental conditions. The ability to perturb biofilms with a wide range of experimental factors at an operator's will and in a precise manner also helps to investigate the cause-effect relationship (Greenman *et al.* 2005).

To date, the standard methods of gingivitis prevention or treatment are mechanical and chemical plaque control means (Baehni & Takeuchi 2003). Antimicrobial approaches represent an invaluable tool additional to mechanical plaque control and can be used both as prevention and/or treatment (Lamster 2006; Moran 2008). The products currently available on the market are based on chemical actives such as triclosan, essential oils or chlorhexidine and provide satisfactory means of prevention and gingivitis treatment (Allaker & Douglas 2009). Essential Oils (EO) are clinically proven to inhibit supragingival plaque up to 56% and gingivitis by up to 36% as reported by Loe and Schiott. The chlorhexidine based products decrease plaque by up to 61% and reduce gingivitis by up to 80% (Loe & Schiott 1970; Santos 2003; Allaker & Douglas 2009; Gunsolley 2010; Becerik *et al.* 2011). To prove the efficacy of any novel antimicrobial technique and to ascertain unwanted side effects, a large amount of testing needs to be performed before reaching the expensive phase of clinical trials. Therefore, the use of *in vitro* models such as the one presented in this study can also be used for the standardised testing of novel dentifrices and antimicrobial agents. Such models allow for longitudinal approach, and hence a long-term assessment of antimicrobial efficacy on microbial populations by reliable and cost effective means. Furthermore, the ability to reproducibly grow oral biofilms associated with gingivitis is not only useful for antimicrobial testing, but also for understanding the aetiology of gingivitis, as mentioned above.

7.2 Summary of main findings

Chapter 3 (the first results chapter – “Development and validation of a Triple-Constant Depth Film Fermentor”) focused on testing and optimisation of the model’s parts and the experimental methodology. A simplified methodology, using only simulated oral health conditions and a shorter experimental duration, was used to test model reliability. At this stage I was facing constant contamination issues and biofilm growth did not seem reliable. Similar problems were encountered by Wirthlin *et al.* when developing their Laboratory Model Biofilm Fermentor model. Their issues were improved when a better aseptic working procedure was introduced (Wirthlin *et al.* 2005). A similar strategy was applied here by implementing a stringent aseptic working procedure and replacing faulty parts with new, more reliable ones (new PTFE seals, non-domed nuts etc). Additionally, several improvements were introduced to increase model reliability and manoeuvrability. Specifically, an L-shaped waste output was added to increase portability, a PTFE cover was placed on the gearbox to prevent bacterial leakage and handles were added on both sides of the motor to increase portability. The air-tightness issues were addressed by providing new PTFE seals and using non-domed nuts instead of domed ones (further explanation is given in Chapter 3). After implementing these changes, the model was able to grow oral biofilms in a reliable way without contamination issues.

Planktonic cells are known to have higher susceptibility to antimicrobials than those grown in biofilm. In recognition of these differing susceptibilities, antimicrobial agents should be characterised not only by MIC (minimum inhibitory concentration) and MBC (minimum bacteriocidal concentration) but also by BEC (biofilm eliminating concentration) to provide a better measure of the characteristics of test antimicrobial agents. An *in vitro* model which is able to mimic gingivitis associated biofilms in a reliable and reproducible manner could be an invaluable tool in the initial testing stage of antimicrobials (Wilson 1996). Therefore, a reproducibility study of oral biofilms grown in T-CDFF was carried out, and summarised in Chapter 4. This chapter focused on (i) reproducibility testing of the oral biofilms and also (ii) on mimicking the gingivitis associated bacterial shifts which occur during the progression of a health associated

biofilm to a gingivitis associated one. The reproducibility study broadly showed a lack of significant differences among the units in single or individual experiments. As this might be indicative of having a reproducible *in vitro* model, these findings were questioned as the data set retrieved from each experiment was burdened with high variability (high standard deviation) that limited the conclusiveness of the statistical analysis. Similar problems with high variability and reproducibility of developed biofilms were encountered by others using complex *in vitro* systems (Kinniment *et al.* 1996; Pratten *et al.* 1998; Wirthlin *et al.* 2005).

Kinniment and Pratten used CDFs, the closest model to the current system, to grow single- and multi-species biofilms and demonstrated some major variations between the experiments in terms of bacterial numbers or community composition (Kinniment *et al.* 1996; Pratten *et al.* 1998). This confirms that growing reproducible oral biofilms in a complex *in vitro* system is not easy and can be affected by many experimental factors, including slight differences in relative proportions of bacteria in inoculum, varied flow rates etc (Kinniment *et al.* 1996; Pratten *et al.* 1998). Even small differences in inoculum composition can lead to differences in community composition which can be further magnified by slight differences in conditions in the initial phase of biofilm formation (Hope *et al.* 2012). Additionally, small mutations take place in any growing cell populations and can affect the variability among units despite, in theory, having same experimental conditions (Powell 1958). Therefore, further optimisation of the experimental design and investigation of artificial saliva and inoculum composition and its handling over time would be beneficial to this study. In addition, to increase the power of the statistical analysis, it would be necessary to increase the number of experiments ($n \geq 3$) to obtain a larger data set.

The second part of the research presented in Chapter 4 focused on establishing the bacterial shifts associated with gingivitis progression. The aim was to establish (i) an increase in the proportion of total anaerobes and decrease in that of total aerobes, (ii) an increase in orange complex bacteria (*F. nucleatum*, *P. intermedia*), and (iii) an increase in red complex bacteria, and (iv) the dominance of *A. naeslundii* over *S. sanguinis* after the transition from health to gingivitis. This attempt was unsuccessful

as none of the changes were observed despite using the same experimental methodology and similar experimental set-up as previously reported by Dalwai *et al* (Dalwai *et al.* 2006; Dalwai *et al.* 2007).

Dalwai and colleagues used CDFFs to model gingivitis *in vitro*. They observed an increase in Gram-negative bacteria *Fusobacteria* spp. and *Prevotella* spp. as well as the ascendancy of *Actinomyces* spp. over *Streptococcus* spp. under simulated gingivitis conditions. The disparities between the current study and the two studies by Dalwai (Dalwai *et al.* 2006; Dalwai *et al.* 2007) led to the conclusion that either simulated gingivitis conditions might have not been established in the T-CDFF model or the post-analysis techniques used were not best suited to determining the differences. This seems strange, as the techniques used here were more refined than those used in the Dalwai study. Therefore, it was decided to apply more holistic approach (^1H NMR metabolomics) to investigate the physiological status of biofilms and the metabolites produced under oral health and disease. Chapter 5 investigated whether ^1H NMR metabolomics was suitable for the purposes of this study and whether it could provide enough resolution when analysing biofilm and effluent samples. A simple to operate CDFF model was run under the health and gingivitis methodology and the analysis of the raw NMR data set showed an increase of propionic and butyric acid in gingivitis conditions. These metabolites have been reported by Aimettii *et al.* to be associated with periodontitis (Aimetti *et al.* 2011). Therefore, this technique was not only proven to work in a reliable manner when applied to the effluent samples, but also to be sensitive enough to discriminate between the experimental conditions.

The ^1H NMR metabolomic study was used together with comparative 16S rRNA gene sequencing in Chapter 6 to correlate the bacteria with the metabolites produced. The effluent samples retrieved from these two T-CDFF experiments were analysed by ^1H NMR metabolomics, 16S rRNA gene genomics and qPCR. The metabolomic study showed an increase in metabolites associated with gingivitis progression (trimethylamine, formate, pyruvate, propionate etc) as reported by Aimetti *et al.* (Aimetti *et al.* 2011). However, the 16S rRNA gene sequencing study did not reflect it as there was not any Gram-negative gingivitis associated bacteria detected (apart from

P. gingivalis detected only in health in unit 3, experiment 2) responsible for the productions of these metabolites. This indicates that there may have been problems with sample processing. These potential problems including DNA extraction and sample processing during the 16S rDNA sequencing study (mentioned in chapter 6) were the biggest limitation to the study and should be further investigated. Due to many pre-processing steps (e.g. library preparation, PCR amplification etc) this technique can introduce significant bias to diversity studies and is less reliable than ¹H NMR metabolomic studies which work on raw (unprocessed) biological samples. Concluding, I could not say with a high degree of certainty that the shifts developed in the model are gingivitis related. Because of this, additional T-CDFE experiments would have to be performed together with further optimisation and testing of both the experimental design/methodology and the post-experimental techniques to verify the nature of the shifts and to improve the reproducibility.

7.3 Conclusions and future work

This study presents a new model which at the moment can be used to grow oral biofilms in a reliable manner. It appears that the model has the potential to mimic gingivitis associated shifts *in vitro* in a reproducible manner, and if further optimised it could likely be used for standardised testing of antimicrobials in either gingivitis prevention or treatment. Therefore, the scope of future work should focus on optimising the experimental methodology and validating the post experimental techniques. This could include (i) using newer next generation sequencing technologies that give longer read lengths and do not require a PCR amplification stage, (ii) comparing different 16S rRNA gene regions in terms of their ability to identify different bacterial taxa, and (iii) investigating DNA extraction methods that are less laborious than the one applied in this project and can be representative for both Gram negative and Gram-positive species.

In terms of the experimental design and methodology, it would be beneficial to investigate how inoculum composition influences biofilm growth and how to standardise it to increase reproducibility of the runs. Additionally, it would be important to further improve the experimental set up (tubing connections, pump choice or set-up etc) to increase the reproducibility of the runs. It might also be interesting to investigate whether an extended experimental duration and longer exposure to artificial GCF would have a significant impact on the bacterial shifts and the metabolite production over time etc.

The triple-CDFF can also be used to facilitate the investigation of efficacy of novel therapies such as phage therapy, probiotics, prebiotics or the use of nanoparticles (Allaker & Douglas, 2009). Silver nanoparticles show antimicrobial and antiviral activity and have been already used in a wide range of medical applications including dental resin composites and burn dressings (Shameli *et al.*, 2011).

The systems biology approach with 'omics' techniques present a potential benefit for investigating the health/gingivitis associated changes in oral microbiome. The use of

various 'omics' techniques in health/gingivitis modelling in either *in vitro* or *in vivo* opens a new field of research into identification of the potential biomarkers of gingivitis. Combining genomics, metabolomics, transcriptomics and proteomics approaches together to document the biomarkers can give a strong association with the early detection of disease, disease presence or absence and the prediction of treatment outcomes.

8 References

- Aagaard, K. *et al.*, 2013. The Human Microbiome Project strategy for comprehensive sampling of the human microbiome and why it matters. *FASEB Journal*, 27(3), pp.1012–22.
- Aas, J.A. *et al.*, 2005. Defining the normal bacterial flora of the oral cavity. *Journal of Clinical Microbiology*, 43(11), pp.5721–5732.
- Abusleme, L. *et al.*, 2013. The subgingival microbiome in health and periodontitis and its relationship with community biomass and inflammation. *The ISME Journal*, 7(5), pp.1016–25.
- Adamson, J. *et al.*, 2014. An inter-machine comparison of tobacco smoke particle deposition *in vitro* from six independent smoke exposure systems. *Toxicology in vitro: an International Journal published in association with BIBRA*, 28(7), pp.1320–8.
- Aimetti, M. *et al.*, 2011. Metabonomic analysis of saliva reveals generalized chronic periodontitis signature. *Metabolomics*, 8(3), pp.465–474.
- Ali, L. *et al.*, 2006. Investigating the suitability of the Calgary Biofilm Device for assessing the antimicrobial efficacy of new agents. *Bioresource Technology*, 97(15), pp.1887–93.
- Allaker, R.P. *et al.*, 2009. Novel anti-microbial therapies for dental plaque-related diseases. *International Journal of Antimicrobial Agents*, 33(1), pp.8–13.
- Almshawit, H. *et al.*, 2014. A simple and inexpensive device for biofilm analysis. *Journal of Microbiological Methods*, 98, pp.59–63.
- Amann, R.L., 1995. Phylogenetic identification and in situ detection of individual microbial cells without cultivation. *Microbiological Reviews*, 59(1), pp.143–69.
- Anchordoquy, T.J. *et al.*, 2007. Preservation of DNA. *Cell Preservation Technology*, 5(4), pp.180–188.
- Academy report submitted by Research, Science and Therapy Committee of the American Academy of Periodontology, 2001. Treatment of plaque-induced gingivitis, chronic periodontitis, and other clinical conditions. *Journal of Periodontology*, 72(12), pp.1790–1800.
- Aranki, A. *et al.*, 1969. Isolation of anaerobic bacteria from human gingiva and mouse cecum by means of a simplified glove box procedure. *Applied Environmental Microbiology*, 17(4), pp.568–576.

- Armitage, G.C., 2003. Diagnosis of periodontal diseases. *Journal of Periodontology*, 74, pp.1237–1247.
- Arthur, R. A. *et al.*, 2013. A defined-multispecies microbial model for studying enamel caries development. *Caries Research*, 47(4), pp.318–24.
- Ashimoto, A. *et al.*, 1996. Polymerase chain reaction detection of 8 putative periodontal pathogens in subgingival plaque of gingivitis and advanced periodontitis lesions. *Oral Microbiology and Immunology*, 11(4), pp.266–73.
- Baehni, P.C. *et al.*, 2003. Anti-plaque agents in the prevention of biofilm-associated oral diseases. *Oral Diseases*, 9 (Suppl 1), pp.9-23.
- Barding, G. A. *et al.*, 2013. VIZR-an automated chemometric technique for metabolic profiling. *Analytical and Bioanalytical Chemistry*, 405(26), pp.8409–17.
- Barnes, V.M. *et al.*, 2009. Acceleration of purine degradation by periodontal diseases. *Journal of Dental Research*, 88(9), pp.851–5.
- Barnes, V.M. *et al.*, 2010. Assessment of the effects of dentifrice on periodontal disease biomarkers in gingival crevicular fluid. *Journal of Periodontology*, 81(9), pp.1273–9.
- Barnes, V.M. *et al.*, 2011. Metabolomics reveals elevated macromolecular degradation in periodontal disease. *Journal of Dental Research*, 90(11), pp.1293–7.
- Becerik, S. *et al.*, 2011. Antimicrobial effect of adjunctive use of chlorhexidine mouthrinse in untreated gingivitis: a randomized, placebo-controlled study. *APMIS: Acta Pathologica, Microbiologica, et Immunologica Scandinavica*, 119(6), pp.364–72.
- Beighton, D. *et al.*, 1986. The growth of bacteria and the production of exoglycosidic enzymes in the dental plaque of macaque monkeys. *Archives of Oral Biology*, 31(1), pp.829–835.
- Di Bella, J.M. *et al.*, 2013. High throughput sequencing methods and analysis for microbiome research. *Journal of Microbiological Methods*, 95(3), pp.401–414.
- Bennick, A., 1982. Salivary proline-rich proteins. *Molecular and Cellular Biochemistry*, 99(6), pp.83–99.
- Bessey, O.A. *et al.*, 1946. A method for the rapid determination of alkaline phosphatase with 5 cubic milliliters of serum. *Journal Biological Chemistry*, 164(1), pp.321–329.
- Bharti, S.K. *et al.*, 2012. Quantitative H NMR spectroscopy. *Trends in Analytical Chemistry*, 35, pp.5–26.

- Bik, E.M. *et al.*, 2010. Bacterial diversity in the oral cavity of 10 healthy individuals. *The ISME Journal*, 4(8), pp.962–74.
- Binder, T. *et al.*, 1987. Gingival fluid levels of acid and alkaline phosphatase. *Journal of Periodontal Research*, 22, pp.14–19.
- Bowen, W.H. *et al.*, 2011. Biology of *Streptococcus mutans*-derived glucosyltransferases: role in extracellular matrix formation of cariogenic biofilms. *Caries Research*, 45(1), pp.69–86.
- Bradshaw, D. & Marsh, P., 1999. Use of continuous flow techniques in modeling dental plaque biofilms. *Methods in Enzymology*, 310(1991).
- Bradshaw, D.J. *et al.*, 1996. Effect of oxygen, inoculum composition and flow rate on development of mixed-culture oral biofilms. *Microbiology*, (1996), pp.623–629.
- Bradshaw, D.J. & Marsh, P.D., 1999. Use of continuous flow techniques in modeling dental plaque biofilms. *Methods in Enzymology*, 310, pp.279–296.
- Brinig, M.M. *et al.*, 2003. Prevalence of bacteria of division TM7 in human subgingival plaque and their association with disease. *Applied and Environmental Microbiology*, 69(3), 1687-1694.
- Brown, J. *et al.*, 2000. The economics of periodontal diseases. *Periodontology 2000*, 29(1), pp.223–234.
- Brown, L.J. & Loe, H., 1993. Prevalence, extent, severity and progression of periodontal disease. *Periodontology 2000*, (2), pp.57–71.
- Buckingham-Meyer, K. *et al.*, 2007. Comparative evaluation of biofilm disinfectant efficacy tests. *Journal of Microbiological Methods*, 70(2), pp.236–44.
- Buduneli, E. *et al.*, 2004. Accuracy and reproducibility of two manual periodontal probes. *Journal of Clinical Periodontology*, 31, pp.815–819.
- Caporaso, J.G. *et al.*, 2011. Global patterns of 16S rRNA diversity at a depth of millions of sequences per sample. *PNAS*, 108, pp.4516–4522.
- Caporaso, J.G. *et al.*, 2011. Moving pictures of the human microbiome. *Genome Biology*, 12(5), p.R50.
- Caporaso, J.G. *et al.*, 2010. QIIME allows analysis of high-throughput community sequencing data. *Nature Methods*, 7(5), pp.335–336.
- Caporaso, J.G. *et al.*, 2012. Ultra-high-throughput microbial community analysis on the Illumina HiSeq and MiSeq platforms. *The ISME Journal*, 6(8), pp.1621–4.

- Carneiro, L.G. *et al.*, 2014. Quantitative gingival crevicular fluid proteome in health and periodontal disease using stable isotope chemistries and mass spectrometry. *Journal of Clinical Periodontology*, 41(8), pp.733–47.
- Ten Cate, J.M., 2006. Biofilms, a new approach to the microbiology of dental plaque. *Odontology*, 94(1), pp.1–9.
- Ceri, H. *et al.*, 1999. The Calgary Biofilm Device: new technology for rapid determination of antibiotic susceptibilities of bacterial biofilms. *Journal of Clinical Microbiology*, 37(6), p.1771.
- Chan, E.C.S. & McLaughlin, R., 2000. Taxonomy and virulence of oral spirochetes. *Oral Microbiology and Immunology*, 15(1), pp.1–9.
- Chapple, I. *et al.*, 1996. Chemiluminescent assay of alkaline phosphatase in human gingival crevicular fluid: investigations with an experimental gingivitis model and studies on the sources of the enzyme within crevicular fluid. *Journal of Clinical Periodontology*, pp.587–594.
- Chu, Y. *et al.*, 2012. RNA sequencing: platform selection, experimental design, and data interpretation. *Nucleic Acid Therapeutics*, 22(4), pp.271–4.
- Ciric, L. *et al.*, 2010. Development of a novel multi-triplex qPCR method for the assessment of bacterial community structure. *Environmental Microbiology Reports*, 2(6), 770–774.
- Claesson, M.J. *et al.*, 2010. Comparison of two next-generation sequencing technologies for resolving highly complex microbiota composition using tandem variable 16S rRNA gene regions. *Nucleic Acids Research*, 38(22), pp.1–13.
- Cloarec, O. *et al.*, 2005. Statistical total correlation spectroscopy: an exploratory approach for latent biomarker identification from metabolic ¹H NMR data sets. *Analytical Chemistry*, 77(5), pp.1282–1289.
- Coenye, T. *et al.*, 2011. Prevention of *Candida albicans* biofilm formation. *The Open Mycology Journal*, 5, pp.9–20.
- Coenye, T. *et al.*, 2008. Use of the modified Robbins device to study the *in vitro* biofilm removal efficacy of NitrAdine, a novel disinfecting formula for the maintenance of oral medical devices. *Journal of Applied Microbiology*, 105(3), pp.733–40.
- Coenye, T. *et al.*, 2010. *In vitro* and *in vivo* model systems to study microbial biofilm formation. *Journal of Microbiological Methods*, 83(2), pp.89–105.
- Colucci, G., 2000. New technologies and applications of PCR in clinical diagnosis. *International Journal of Microbial Agents*, 16, pp.499–500.

- Constantinou, M.A. *et al.*, 2007. ¹H NMR monitoring of the canine metabolic profile after oral administration of xenobiotics using multivariate statistics. *Molecular Pharmaceutics*, 4(2), pp.258–268.
- Costerton, W. *et al.*, 2003. The application of biofilm science to the study and control of chronic bacterial infections. *Journal of Clinical Investigation*, 112(10), pp.1466–1477.
- Dahle, G. *et al.*, 2006. A new checkerboard panel for testing bacterial markers in periodontal disease. *Oral Microbiology and Immunology*, 21, pp.6–11.
- Dalwai, F., 2008. *In vitro modeling of bacterial populaion shifts in oral biofilms*. Published PhD thesis. University College London.
- Dalwai, F. *et al.*, 2007. Use of quantitative PCR and culture methods to characterize ecological flux in bacterial biofilms. *Journal of Clinical Microbiology*, 45(9), pp.3072–6.
- Dalwai, F. *et al.*, 2006. Modeling shifts in microbial populations associated with health or disease. *Applied and Environmental Microbiology*, 72(5), pp.3678–3684.
- Darveau, R.P. *et al.*, 1997. The microbial challange in periodontitis. *Periodontology 2000*, (14), pp.12–32.
- Dewhirst, F.E. *et al.*, 2010. The human oral microbiome. *Journal of Bacteriology*, 192(19), pp.5002–17.
- Dibdin, G. & Wimpenny, J., 1999. Steady-state biofilm: practical and theoretical models. *Methods in Enzymology*, 310, pp.296–322.
- Dieffenbach, C.W. *et al.*, 1993. General concepts for PCR primer design. *PCR Methods and Applications*, pp. 530-7.
- Van Dijk, E.L. *et al.*, 2014. Library preparation methods for next-generation sequencing: tone down the bias. *Experimental Cell Research*, 322(1), pp.12–20.
- Dominguez-Bello, M.G. *et al.*, 2010. Delivery mode shapes the acquisition and structure of the initial microbiota across multiple body habitats in newborns. *PNAS*, 107(26), pp.11971–5.
- Donlan, R. *et al.*, 2002. Monochloramine disinfection of biofilm-associated *Legionella pneumophila* in a portable water model system. *ASM press*, pp.406-10.
- Donlan, R.M. *et al.*, 2004. Model system for growing and quantifying *Streptococcus pneumoniae* biofilms in situ and in real time. *Applied and Environmental Microbiology*, 70(8), pp.4980–4988.

- Dunn, W.B. *et al.*, 2005. Measuring the metabolome: current analytical technologies. *The Analyst*, 130(5), pp.606–25.
- Edlund, A. *et al.*, 2013. An *in vitro* biofilm model system maintaining a highly reproducible species and metabolic diversity approaching that of the human oral microbiome. *Microbiome*, 1(25), pp.1-17.
- Elangovan, S. *et al.*, 2011. Outcomes in patients visiting hospital emergency departments in the United States because of periodontal conditions. *Journal of Periodontology*, 82(6), pp.809–19.
- Ellen, R.P., 1976. Establishment and distribution of *Actinomyces viscosus* and *Actinomyces naeslundii* in the human oral cavity. *Infection and Immunity*, 14(5), pp.1119–1124.
- Emwas, A. H. M. *et al.*, 2013. NMR-based metabolomics in human disease diagnosis: applications, limitations, and recommendations. *Metabolomics*, 9(5), pp.1048–1072.
- Fábián, T.K. *et al.*, 2008. Salivary genomics, transcriptomics and proteomics: the emerging concept of the oral ecosystem and their use in the early diagnosis of cancer and other diseases. *Current Genomics*, 9(1), pp.11–21.
- Fang, F.C. & Casadevall, A., 2011. Reductionistic and holistic science. *Infection and Immunity*, 79(4), pp.1401–4.
- Farrelly, V. *et al.*, 1995. Effect of genome size and rrn gene copy number on PCR amplification of 16S rRNA genes from a mixture of bacterial species. *Applied Environmental Microbiology*, 61(7), pp.2798–2801.
- Fenno, J.C. & McBride, B.C., 1998. Virulence factors of oral Treponemes. *Anaerobe*, 4(1), pp.1–17.
- Fidalgo, T.K.S. & Renata, L.B.F., 2013. Salivary metabolite signatures of children with and without dental caries lesions. *Metabolomics*, pp.657–666.
- Filoche, S. *et al.*, 2010. Oral biofilms: emerging concepts in microbial ecology. *Journal of Dental Research*, 89(1), pp.8–18.
- Fonville, J.M. *et al.*, 2010. The evolution of partial least squares models and related chemometric approaches in metabonomics and metabolic phenotyping. *Journal of Chemometrics*, 24(11-12), pp.636–649.
- Fukushima, K. & Ochiai, K., 1995. Volatile fatty acids, metabolic by-products of periodontopathic bacteria, inhibit lymphocyte proliferation and cytokine production. *Journal of Dental Resource*, 74(7), pp.1367–1373.

- Genco, R.J., 1996. Current view of risk factors for periodontal diseases. *Journal of Periodontology*, 67(10 Suppl), pp.1041–9.
- Gersdorf, H. *et al.*, 1993. Fluorescence in situ hybridization for direct visualization of gram-negative anaerobes in subgingival plaque samples. *FEMS Immunology and Medical Microbiology*, 6(2-3), pp.109–14.
- Gika, H.G. *et al.*, 2014. Current practice of liquid chromatography-mass spectrometry in metabolomics and metabonomics. *Journal of Pharmaceutical and Biomedical Analysis*, 87, pp.12–25.
- Gilbert, P. *et al.*, 2002. Biofilms *in vitro* and *in vivo*: do singular mechanisms imply cross-resistance? *Journal of Applied Microbiology*, 92, pp.98–110.
- Gmur, R. *et al.*, 2004. Gingival crevice microbiota from Chinese patients with gingivitis or necrotising ulcerative gingivitis. *European Journal of Oral Sciences*, 112(1), pp.33–41.
- Goeres, D.M. *et al.*, 2005. Statistical assessment of a laboratory method for growing biofilms. *Microbiology*, 151, pp.757–762.
- Gold, O.G. *et al.*, 1973. A selective medium for *Streptococcus mutans*. *Archives of Oral Biology*, 18(11), 1357-1364.
- Gonçalves, L.D.R. *et al.*, 2010. Comparative proteomic analysis of whole saliva from chronic periodontitis patients. *Journal of Proteomics*, 73(7), pp.1334–41.
- Goodacre, R., 2007. Metabolomics of a superorganism. *The Journal of Nutrition*, 137(1 Suppl), p.259S–266S.
- Goodson, J.M., 2000. Gingival crevice fluid flow. *Journal of Periodontology*, 31, pp.43–54.
- Goodson, J.M. *et al.*, 2000. Gingival bleeding accentuated by plaque in healthy IL-1(+) genotype subjects. *Journal of Dental Research*, 79(221) Abstract, pp.171.
- Gordon, D.F. *et al.*, 1971. Improved isolation of anaerobic bacteria from the gingival crevice area of man. *Applied Microbiology*, 21(6), pp.1046–1050.
- Grant, M.M. *et al.*, 2010. Proteomic analysis of a noninvasive human model of acute inflammation and its resolution: the twenty-one day gingivitis model. *Journal of Proteome*, 9(9), pp.4732–4744.
- Grant, M.M., 2012. What do omic technologies have to offer periodontal clinical practice in the future? *Journal of Periodontal Research*, 47(1), pp.2–14.

- Greenman, J. *et al.*, 2005. *In vitro* models for oral malodor. *Oral Diseases*, 11 (Suppl 1), pp.14–23.
- Griffen, A.L. *et al.*, 2011. CORE: a phylogenetically-curated 16S rDNA database of the core oral microbiome. *PLoS one*, 6(4), pp.1-10.
- Griffen, A.L. *et al.*, 2012. Distinct and complex bacterial profiles in human periodontitis and health revealed by 16S pyrosequencing. *The ISME Journal*, 6(6), pp.1176–85.
- Griffiths, R.I. *et al.*, 2000. Rapid method for coextraction of DNA and RNA from natural environments for analysis of ribosomal DNA- and rRNA-based microbial community composition. *Journal of Applied Environmental Microbiology*, 66, pp.5488–5491.
- Gristina, A.G. *et al.*, 1987. Adhesive colonization of biomaterials and antibiotic resistance. *Biomaterials*, 8, pp.16–19.
- Grootveld, M. & Silwood, C.J.L., 2005. ¹H NMR analysis as a diagnostic probe for human saliva. *Biochemical and Biophysical Research Communications*, 329(1), pp.1–5.
- Guggenheim, B. *et al.*, 2004. Application of the Zürich biofilm model to problems of cariology. *Caries Research*, 38(3), pp.212–22.
- Guggenheim, B. *et al.*, 2009. *In vitro* modeling of host-parasite interactions: the “subgingival” biofilm challenge of primary human epithelial cells. *BMC Microbiology*, 9(280), pp.1-12.
- Guggenheim, B. *et al.*, 2001. Validation of an *in vitro* biofilm model of supragingival plaque. *Journal of Dental Research*, 80(1), pp.363–70.
- Gunsolley, J.C., 2010. Clinical efficacy of antimicrobial mouthrinses. *Journal of Dentistry*, 38, pp.6–10.
- Haber, J. *et al.*, 1993. Evidence for cigarette smoking as a major risk factor for periodontitis. *Journal of Periodontology*, 64(1), pp.16–23.
- Hadi, R. *et al.*, 2010. Biofilm removal by medical device cleaners: comparison of two bioreactor detection assays. *The Journal of Hospital Infection*, 74(2), pp.160–7.
- Haffajee, A.D. & Socransky, S.S., 1994. Evidence of bacterial etiology: a historical perspective. *Periodontology 2000*, 5, pp.7–25.
- Hager, R. *et al.*, 2013. Ratio of pro-resolving and pro-inflammatory lipid mediator precursors as potential markers for aggressive periodontitis. *PLoS one*, 8(8), pp. 1-13.

- Hajishengallis, G. & Lambris, J.D., 2012. Complement and dysbiosis in periodontal disease. *Immunobiology*, 217, pp.1111–1116.
- Hajishengallis, G. & Lamont, R.J., 2012. Beyond the red complex and into more complexity: the polymicrobial synergy and dysbiosis (PSD) model of periodontal disease etiology. *Molecular Oral Microbiology*, 27(6), pp.409–419.
- Hall-Stoodley, L. *et al.*, 2004. Bacterial biofilms: from the natural environment to infectious diseases. *Nature Reviews Microbiology*, 2(2), pp.95–108.
- Harada, H. *et al.*, 1987. ¹H-NMR of human saliva. An application of NMR spectroscopy in forensic science. *Forensic Science International*, 34, pp.189–195.
- Harrington, C.T. *et al.*, 2013. Fundamentals of pyrosequencing. *Archives of Pathology & Laboratory Medicine*, 137(9), pp.1296–303.
- Harrison, J.J. *et al.*, 2006. The use of microscopy and three-dimensional visualization to evaluate the structure of microbial biofilms cultivated in the Calgary Biofilm Device. *Biological Procedures Online*, 8(1), pp.194–215.
- He, X. & Shi, W., 2009. Oral microbiology: past, present and future. *Oral Microbiology*, 1(2), pp.47–58.
- Hentzer, M. *et al.*, 2003. Attenuation of *Pseudomonas aeruginosa* virulence by quorum sensing inhibitors. *The EMBO Journal*, 22(15), pp.3803–3815.
- Herles, S. *et al.*, 1994. Chemostat flow cell system: an *in vitro* model for the evaluation of antiplaque agents. *Journal of Dental Research*, 73(11), pp.1748–1755.
- Holla, L.I. *et al.*, 2008. Association of interleukin-6 (IL-6) haplotypes with plaque-induced gingivitis in children. *Acta Odontologica Scandinavica*, 66, pp.105–12.
- Honraet, K. *et al.*, 2005. Comparison of three assays for the quantification of *Candida* biomass in suspension and CDC reactor grown biofilms. *Journal of Microbiological Methods*, 63(3), pp.287–95.
- Hoover, C.I. *et al.*, 1992. Correlation of hemagglutination activity with trypsin-like-protease activity of *Porphyromonas*. *Archives of Oral Biology*, 31(1), pp.515–520.
- Hope, C.K. *et al.*, 2012. Reducing the variability between constant-depth film fermenter experiments when modelling oral biofilm. *Journal of Applied Microbiology*, 113(3), pp.601–8.
- Hope, C.K. & Wilson, M., 2004. Analysis of the effects of chlorhexidine on oral biofilm vitality and structure based on viability profiling and an indicator of membrane integrity. *Antimicrobial Agents and Chemotherapy*, 48(5), pp.1461–1468.

- Huang, S. *et al.*, 2014. Predictive modeling of gingivitis severity and susceptibility via oral microbiota. *The ISME Journal*, pp.1–13.
- Huang, S. *et al.*, 2011. Preliminary characterization of the oral microbiota of Chinese adults with and without gingivitis. *BMC Oral Health*, 11(1), p.33.
- Huttenhower, C. *et al.*, 2012. Structure, function and diversity of the healthy human microbiome. *Nature*, 486(7402), pp.207–14.
- Illumina Inc., 2015. Overview: NGS for Microbiology. [Online] Available at: www.illumina.com. [Accessed October 30, 2014].
- Jefferson, K.K., 2004. What drives bacteria to produce a biofilm? *FEMS Microbiology Letters*, 236(2), pp.163–73.
- Jenkinson, H.F. & Lamont, R.J., 2005. Oral microbial communities in sickness and in health. *Trends in Microbiology*, 13(12), pp.589–95.
- Jiao, Y. *et al.*, 2014. The role of oral pathobionts in dysbiosis during periodontitis development. *Journal of Dental Research*, 93(6), pp.539–547.
- Jönsson, D. *et al.*, 2011. Gingival tissue transcriptomes in experimental gingivitis. *Journal of Clinical Periodontology*, 38(7), pp.599–611.
- Jorth, P. *et al.*, 2014. Metatranscriptomics of the human oral microbiome during health. *ASM Journal*, 5(2), pp.1-10.
- Kamaguchi, A., 2003. Adhesins encoded by the gingipain genes of *Porphyromonas gingivalis* are responsible for co-aggregation with *Prevotella intermedia*. *Microbiology*, 149(5), pp.1257–1264.
- Kebschull, M. *et al.*, 2009. Granulocyte chemotactic complements interleukin-8 in periodontal disease. *Journal of Periodontal Research*, 44(4), pp.465–471.
- Keijser, B.J.F. *et al.*, 2008. Pyrosequencing analysis of the oral microflora of healthy adults. *Journal of Dental Research*, 87(11), pp.1016–1020.
- Khardori, N. *et al.*, 1991. Effect of subinhibitory concentrations of Clindamycin and Trospectomycin on the adherence of *Staphylococcus epidermidis* in an *in vitro* model of vascular catheter colonization. *Infectious Diseases*, 164(1), pp.108-113.
- Kinane, D.F. *et al.*, 2005. The genetic basis of periodontitis. *Periodontology 2000*, 39, pp.91-117.
- Kinane, D.F. *et al.*, 2006. Gingival epithelial cells heterozygous for Toll-like-receptor 4 polymorphism Asp299Gly and Thr399Ile are hypo-responsive to *Porphyromonas gingivalis*. *Genes & Immunity*, 7, pp.190-200.

- Kinniment, S.L. *et al.*, 1996. Development of a steady-state oral microbial biofilm community using the constant-depth film fermenter. *Microbiology*, 142, pp.631–638.
- Kistler, J.O. *et al.*, 2013. Bacterial community development in experimental gingivitis. *PloS one*, 8(8), pp.1-13.
- Kohler, B. & Andreen, I., 1994. Influence of caries-preventive measures in mothers on cariogenic and caries experience in their children. *Archives of Oral Biology*, 39, pp.907–911.
- Kolenbrander, P.E. *et al.*, 2006. Bacterial interactions and successions during plaque development. *Periodontology 2000*, 42(5), pp.47–79.
- Kolenbrander, P.E. *et al.*, 2002. Communication among oral bacteria. *Microbiology and Molecular Biology Reviews*, 66(3), pp.486–505.
- Kranevel, E.A. *et al.*, 2012. The relation between oral *Candida* load and bacterial microbiome profiles in Dutch older adults. *PloS one*, 7(8), pp.1–8.
- Kreth, J. *et al.*, 2005. Competition and coexistence between *Streptococcus mutans* and *Streptococcus sanguinis* in the dental biofilm. *Journal of Bacteriology*, 187(21), pp.7193–7203.
- Kroes, I. *et al.*, 1999. Bacterial diversity within the human subgingival crevice. *PNAS*, 96(25), pp.14547-14552.
- Kuboniwa, M. *et al.*, 2009. Proteomics of *Porphyromonas gingivalis* within a model oral microbial community. *BMC Microbiology*, 9(98), pp.1-14.
- Kuboniwa, M. & Lamont, R.J., 2010. Subgingival biofilm formation. *Periodontology 2000*, 52(1), pp.38–52.
- Kumar, P.S. *et al.*, 2006. Changes in periodontal health status are associated with bacterial community shifts as assessed by quantitative 16S cloning and sequencing. *Journal of Clinical Microbiology*, 44(10), pp.3665–73.
- Kumar, P.S. *et al.*, 2003. New bacterial species associated with chronic periodontitis. *Journal of Dental Research*, 82(5), pp.338–345.
- Lamont, R.J. & Hajishengallis, G., 2014. Polymicrobial synergy and dysbiosis in inflammatory disease. *Trends in Molecular Medicine*, 21(3), pp.1–12.
- Lamster, I.B., 2006. Antimicrobial mouthrinses and the management of periodontal diseases. *American Dental Association*, 137(3), pp.5–9.

- Lane, D.J., 1991. 16S/23S rRNA sequencing. In *Nucleic Acid Techniques in Bacterial Systematics*, John Wiley & Sons, pp.115–147.
- Larsen, T. & Fiehn, N., 1995. Development of a flow method for susceptibility testing of oral biofilms *in vitro*. *Microbiologica et Immunologica Scandinavica*, 103(1-6), pp.339-44.
- Lazarevic, V. *et al.*, 2010. Study of inter- and intra-individual variations in the salivary microbiota. *BMC Genomics*, 11, pp.523–534.
- Lebeaux, D. *et al.*, 2013. From *in vitro* to *in vivo* models of bacterial biofilm-related infections. *Pathogens*, 2(2), pp.288–356.
- Ledder, R.G. *et al.*, 2009. An *in vitro* evaluation of hydrolytic enzymes as dental plaque control agents. *Journal of Medical Microbiology*, 58, pp.482–491.
- Ledder, R.G. & McBain, A.J., 2012. An *in vitro* comparison of dentifrice formulations in three distinct oral microbiotas. *Archives of Oral Biology*, 57(2), pp.139–47.
- Lenz, E.M. & Wilson, I.D., 2007. Analytical strategies in metabonomics. *Journal of Proteome*, 6, pp.443–458.
- Leung, D. *et al.*, 2005. Chlorhexidine-releasing methacrylate dental composite materials. *Biomaterials*, 26(34), pp.7145–53.
- Lewis, J.S. *et al.*, 2010. Assessment of microbial biofilm growth on nanocrystalline diamond in a continuous perfusion environment. *ASME Journal*, 132(3), pp.1-7.
- Li, Y. *et al.*, 2014. Phylogenetic and functional gene structure shifts of the oral microbiomes in periodontitis patients. *The ISME Journal*, 8(9), pp.1879–1891.
- Li, Y.H. & Bowden, G.H., 1994. Characteristics of accumulation of oral gram-positive bacteria on mucin-conditioned glass surfaces in a model system. *Oral Microbiology and Immunology*, 1(32), pp.1-11.
- Life Technologies Inc., 2014. SOLiD® next generation sequencing. [Online] Available at: www.appliedbiosystems.com. [Accessed October 30, 2014].
- Liljemark, W.F., 2000. Microbial ecology of marginal gingivitis. *Microbial Ecology in Health and Disease*, 12(3), pp.149–159.
- Liu, L. *et al.*, 2012. Comparison of next-generation sequencing systems. *Journal of Biomedicine & Biotechnology*, 2012, pp.1-11.
- Loe, H. & Schiott, R., 1970. The effect of mouthrinses and topical application of chlorhexidine on the development of dental plaque and gingivitis in man. *Journal of Periodontal Research*, 5(2), pp.79–83.

- Loe, H. & Silness, J., 1963. Periodontal disease in pregnancy: prevalence and severity. *Acta Odontologica Scandinavica*, 21(6), pp.533–551.
- Loesche, W.J., 1976. Chemotherapy of dental plaque infections. *Oral Science Research*, 9, pp.65–107.
- Loesche, W.J. *et al.*, 1992. Comparison of various detection methods for periodontopathic bacteria: can culture be considered the primary reference standard? *Journal of Clinical Periodontology*, 30(2), pp.418-26.
- Loesche, W.J. & Grossman, N.S., 2001. Periodontal disease as a specific, albeit chronic, infection: diagnosis and treatment. *Clinical Microbiology Reviews*, 14(4), pp.727–752.
- Loos, B.G. *et al.*, 2005. Identification of genetic risk factors for periodontitis and possible mechanisms of action. *Journal of Clinical Periodontology*, 32 (Suppl 6), pp.159–79.
- Marsh, P. *et al.*, 2011. Dental plaque biofilms: communities, conflict and control. *Periodontology 2000*, 55(90), pp.16–35.
- Marsh, P.D., 2003. Are dental diseases examples of ecological catastrophes? *Microbiology*, 149(2), pp.279–294.
- Marsh, P.D., 2004. Dental plaque as a microbial biofilm. *Caries Research*, 38(3), pp.204–11.
- Marsh, P.D., 1989. Host defenses and microbial homeostasis: role of microbial interactions. *Journal of Dental Research*, 68, pp.1567–1575.
- Marsh, P.D., 1994. Microbial ecology of dental plaque and its significance in health and disease. *Advanced Dental Research*, 8(2), pp.263–272.
- Marsh, P.D., 1991. Sugar, fluoride, pH and microbial homeostasis in dental plaque. *Proceedings of the Finnish Dental Society*, 87(4), pp.515–525.
- Marsh, P.D. *et al.*, 1983. The influence of growth rate and nutrient limitation on the microbial composition and biochemical properties of a mixed culture of oral bacteria grown in a chemostat. *Journal of General Microbiology*, 129, pp.755–770.
- Marsh, P.D., 1995. The role of continuous culture in modelling the human microflora. *Chemical Technology and Biotechnology*, 64(1), pp.1–9.
- Marsh, P.D. & Martin, M. V., 1999. *Oral microbiology*. Wright, Oxford, United Kingdom.
- Marsh, P.D., 2005. Dental plaque: biological significance of a biofilm and community life-style. *Journal of Clinical Periodontology*, 32(6), pp.7–15.

- Mashego, M.R. *et al.*, 2007. Microbial metabolomics: past, present and future methodologies. *Biotechnology letters*, 29(1), pp.1–16.
- McBain, a J. *et al.*, 2003. Growth and molecular characterization of dental plaque microcosms. *Journal of Applied Microbiology*, 94(4), pp.655–64.
- McBain, A.J., 2009. Chapter 4 *in vitro* biofilm models: an overview. *Advances in Applied Microbiology*, 69, pp.99–132.
- McBain, A.J. *et al.*, 2005. Development and characterization of a simple perfused oral microcosm. *Journal of Applied Microbiology*, 98(3), pp.624–634.
- McBain, A.J. *et al.*, 2003. Effects of a chlorhexidine gluconate-containing mouthwash on the vitality and antimicrobial susceptibility of *in vitro* oral bacterial ecosystems. *Applied and Environmental Microbiology*, 69(8), pp.4770–4776.
- McCoy, W.F. *et al.*, 1981. Observations of fouling biofilm formation. *Canadian Journal of Microbiology*, 27(9), pp.910-917.
- McDermid, A. *et al.*, 1986. The effect of lowering the pH on the composition and metabolism of a community of nine oral bacteria grown in a chemostat. *Journal of General Microbiology*, 132(5), pp.1205–1214.
- Mckee, A.S. *et al.*, 1985. The establishment of reproducible, complex communities of oral bacteria in the chemostat using defined inocula. *Journal of Applied Bacteriology*, 59(3), pp.263–275.
- Metzker, M.L., 2010. Sequencing technologies - the next generation. *Nature Reviews Genetics*, 11(1), pp.31–46.
- Meurman, J.H. *et al.*, 1997. Identification of *Bacteroides forsythus* in subgingival dental plaque with the aid of a rapid PCR method. *Journal of Dental Research*, 76(7), pp.1376–80.
- Miller, W.D., 1891. The human mouth as a focus of infection. *The Lancet*, 138(3546), pp.340–342.
- Moore, L.V.H. *et al.*, 1986. Bacteriology of human gingivitis. *Journal of Dental Research*, 66(5), pp.989–995.
- Moore, W.E. *et al.*, 1984. Bacteriology of experimental gingivitis in children. *Infection and Immunity*, 46(1), pp.1–6.
- Moore, W.E. *et al.*, 1982. Bacteriology of experimental gingivitis in young adult humans. *Infection and Immunity*, 38(3), pp.1137–1148.

- Moore, W.E. & Moore, L.V., 1994. The bacteria of periodontal diseases. *Periodontology 2000*, 5(1), pp.66–77.
- Moore, W.E. *et al.*, 1981. Butyric acid bacteria in periodontal disease. *Journal of Dental Research*, 60, pp.414.
- Moore, W.E. *et al.*, 1983. Bacteriology of moderate (chronic) periodontitis in mature adult humans. *Infection and Immunity*, 42(2), pp.510-515.
- Moore, W.E. *et al.*, 1982. Bacteriology of severe periodontitis in young adult humans. *Infection and Immunity*, 38(3), pp.1137–1148.
- Moran, J., 2008. Home-use oral hygiene products: mouthrinses. *Periodontology 2000*, 48(1), pp.42–53.
- Moreira, P.R. *et al.*, 2007. Interleukin-6 expression and gene polymorphism are associated with severity of periodontal disease in a sample of Brazilian individuals. *Clinical & Experimental Immunology*, 148, pp.119-26.
- Morgan, T.D. & Wilson, M., 2001. The effects of surface roughness and type of denture acrylic on biofilm formation by *Streptococcus oralis* in a constant depth film fermentor. *Journal of Applied Microbiology*, 91, pp.47–53.
- Moter, A. & Göbel, U.B., 2000. Fluorescence in situ hybridization (FISH) for direct visualization of microorganisms. *Journal of Microbiological Methods*, 41(2), pp.85–112.
- Narang, R. *et al.*, 2013. Salivary biomarkers for periodontal diseases-a review. *Bangladesh Journal of Medical Science*, 12(3), pp.244–249.
- Nasidze, I. *et al.*, 2009. Global diversity in the human salivary microbiome. *Genome research*, 19(4), pp.636–43.
- Nath, S.G. & Raveendran, R., 2013. Microbial dysbiosis in periodontitis. *Journal of Indian Society of Periodontology*, 17(4), pp.2011–2014.
- Nelson-Filho, P. *et al.*, 2011. Use of the checkerboard DNA-DNA hybridisation technique for *in vivo* detection of cariogenic microorganisms on metallic brackets, with or without use of an antimicrobial agent. *Journal of Dentistry*, 39(7), pp.513–7.
- Nett, J.E. *et al.*, 2010. Development and validation of an *in vivo* *Candida albicans* biofilm denture model. *Infection and Immunity*, 78(9), pp.3650–9.
- Newman, M.G. & Socransky, S.S., 1977. Predominant cultivable microbiota in periodontosis. *Journal of Periodontal Research*, 12(2), pp.120–128.

- Nibali, L. *et al.*, 2009. Periodontal infectogenomics. *Journal of Medical Microbiology*, 58, pp.1269-74.
- Nibali, L. *et al.*, 2014. Genetic dysbiosis: the role of microbial insults in chronic inflammatory diseases. *Journal of Oral Microbiology*, 6, pp.1–10.
- Nicholson, J.K. & Lindon, J.C., 2008. Systems biology: metabonomics. *Nature*, 455, pp.1054–1056.
- Olsen, I., 2006. New principles in ecological regulation – features from the oral cavity. *Microbial Ecology in Health and Disease*, 18(1), pp.26–31.
- Ouverney, C.C. *et al.*, 2003. Single-cell enumeration of an uncultivated TM7 subgroup in the human subgingival crevice. *Applied and Environmental Microbiology*, 69(10), pp.1–6.
- Pacchiarotta, T. & Mayboroda, O.A., 2012. Metabolomic investigations of human infections. *Bioanalysis*, 4(8), pp.919–925.
- Papapanou, P.N. *et al.*, 1997. “Checkerboard” versus culture: a comparison between two methods for identification of subgingival microbiota. *European Journal of Oral Sciences*, 105(1), pp.389–96.
- Park, N.H. *et al.*, 2013. Antimicrobial activities of stearidonic and gamma-linolenic acids from the green seaweed *Enteromorpha linza* against several oral pathogenic bacteria. *Botanical Studies*, 54(39), pp.1-9.
- Parra-Ruiz, J. *et al.*, 2010. Activities of high-dose daptomycin, vancomycin, and moxifloxacin alone or in combination with clarithromycin or rifampin in a novel *in vitro* model of *Staphylococcus aureus* biofilm. *Antimicrobial Agents and Chemotherapy*, 54(10), pp.4329–34.
- Paster, B.J. *et al.*, 2001. Bacterial diversity in human subgingival plaque. *Journal of Bacteriology*, 183(12), pp.3770-3783.
- Paster, B.J. *et al.*, 2006. The breadth of bacterial diversity in the human periodontal pocket and other oral sites. *Periodontology 2000*, 42(1), pp.80–7.
- Pesciaroli, L. *et al.*, 2013. Characterization of *Pleurotus ostreatus* biofilms by using the calgary biofilm device. *Applied and Environmental Microbiology*, 79(19), pp.6083–92.
- Peters, A.C. & Wimpenny, J.W.T., 1987. A constant-depth laboratory model film fermentor. *Biotechnology and Bioengineering*, 32(3), pp.263–270.
- Petersen, P.E. *et al.*, 2005. The global burden of oral diseases and risks to oral health. *Bulletin of World Health Organisation*, 83(9), pp.661–669.

- Petrosino, J.F. *et al.*, 2009. Metagenomic pyrosequencing and microbial identification. *Clinical Chemistry*, 55(5), pp.856–866.
- Pihlstrom, B.L. *et al.*, 2005. Periodontal diseases. *Lancet*, 366(9499), pp.1809–1820.
- Pitt, J.J., 2009. Principles and applications of liquid chromatography-mass spectrometry in clinical biochemistry. *Clinical Biochemistry*, 30(1), pp.19–34.
- Potempa, J. *et al.*, 1996. *Porphyromonas gingivalis* proteinases in periodontitis, a review. *Acta Biochimica Polonica*, 43(3), pp.455–466.
- Powell, E., 1958. Criteria for the growth of contaminants and mutants in continuous culture. *Journal of General Microbiology*, 18, pp.259–268.
- Powledge, T.M., 2004. The polymerase chain reaction. *Advances in Physiology Education*, 28(2), pp.44–50.
- Pozhitkov, A. *et al.*, 2011. High-throughput methods for analysis of the human oral microbiome. *Periodontology*, 55(1), pp.70–86.
- Pratten, J. *et al.*, 2000. Structural studies of microcosm dental plaques grown under different nutritional conditions. *FEMS Microbiology Letters*, 189, pp.215–218.
- Pratten, J. *et al.*, 1998. Composition and susceptibility to chlorhexidine of multispecies biofilms of oral bacteria. *Applied and Environmental Microbiology*, 64(9), pp.3515–9.
- Pratten, J. *et al.*, 2003. Characterization of *in vitro* oral bacterial biofilms by traditional and molecular methods. *Journal of Oral Microbiology and Immunology*, 18(1), pp.45–49.
- Quail, M. a *et al.*, 2012. A tale of three next generation sequencing platforms: comparison of Ion Torrent, Pacific Biosciences and Illumina MiSeq sequencers. *BMC Genomics*, 13(341), pp.1-13.
- Raber-Durlacher, J.E. *et al.*, 1994. Experimental gingivitis during pregnancy and post-partum: clinical, endocrinological, and microbiological aspects. *Journal of Clinical Periodontology*, 21(8), pp.549–58.
- Ranasinghe, R.T. & Brown, T., 2005. Fluorescence based strategies for genetic analysis. *Chemical Communications*, 44, pp.5487–5502.
- Roche Inc., 2015. Metagenomics: products, long read advantage, methods, analysis software, publications. [Online] Available at: www.my454.com. [Accessed October 30, 2014].

- Rölla, G. *et al.*, 1983. Identification of IgA, IgG, lysozyme, albumin, alpha-amylase and glucosyltransferase in the protein layer adsorbed to hydroxyapatite from whole saliva. *Oral Sciences*, 91(3), pp.186–190.
- Rosebury, T. & Reynolds, J.B., 1964. Continuous anaerobiosis for cultivation of spirochetes. *Experimental Biology and Medicine*, 117(3), pp.813–815.
- Russel, C. & Coulter, W.A., 1975. Continuous monitoring of pH and Eh in bacterial plaque grown on a tooth in an artificial mouth. *Applied Microbiology*, 29(2), pp.141–144.
- Rykke, M. *et al.*, 1990. Interindividual and longitudinal studies of amino acid composition of pellicle collected *in vivo*. *Oral Sciences*, 98(2), pp.129–34.
- Salazar, M.G. *et al.*, 2013. Identification of periodontitis associated changes in the proteome of whole human saliva by mass spectrometric analysis. *Journal of Clinical Periodontology*, 40(9), pp.825–32.
- Salvi, G.E. *et al.*, 2005. Experimental gingivitis in cigarette smokers: a clinical and microbiological study. *Journal of Clinical Periodontology*, 32(5), pp.441–7.
- Samaranayake, L.P., 2002. *Essential microbiology for dentistry*. Churchill Livingstone, New York.
- Sánchez, M.C. *et al.*, 2011. Structure, viability and bacterial kinetics of an *in vitro* biofilm model using six bacteria from the subgingival microbiota. *Journal of Periodontal Research*, 46(2), pp.252–60.
- Santone, C. *et al.*, 2014. Saliva metabolomics by NMR for the evaluation of sport performance. *Journal of Pharmaceutical and Biomedical analysis*, 88, pp.441–6.
- Santopolo, L. *et al.*, 2012. A novel approach combining the Calgary Biofilm Device and Phenotype MicroArray for the characterization of the chemical sensitivity of bacterial biofilms. *Biofouling*, 28(9), pp.1023–32.
- Santos, A., 2003. Evidence-based control of plaque and gingivitis. *Journal of Clinical Periodontology*, 30, pp.13–16.
- Saunders, N.A., 2009. *Quantitative Real-Time PCR*. Caister Academic Press, Saffron Walden, Essex, United Kingdom.
- Savage, A. *et al.*, 2009. A systematic review of definitions of periodontitis and methods that have been used to identify this disease. *Journal of Clinical Periodontology*, 36(6), pp.458–67.
- Savitt, E.D. *et al.*, 1987. Comparison of cultural methods and DNA probe analyses for the detection of *Actinobacillus actinomycetemcomitans*, *Bacteroides gingivalis*,

- and *Bacteroides intermedius* in subgingival plaque samples. *Journal of Periodontology*, 59(7), pp.431–438.
- Saygun, I. *et al.*, 2011. Salivary infectious agents and periodontal disease status. *Journal of Periodontal Research*, 46(2), pp.235–9.
- Scannapieco, F. A., 2013. The oral microbiome: Its role in health and in oral and systemic infections. *Clinical Microbiology Newsletter*, 35(20), pp.163–169.
- Scapoli, C. *et al.*, 2007. Role of IL-6, TNF-A and LT-A variants in the modulation of the clinical expression of plaque-induced gingivitis. *Journal of Clinical Periodontology*, 34, pp.1031-8.
- Schmidt, P.A. *et al.*, 2013. Illumina metabarcoding of a soil fungal community. *Soil Biology and Biochemistry*, 65, pp.128–132.
- Serkova, N.J. & Niemann, C.U., 2006. Pattern recognition and biomarker validation using quantitative ¹H-NMR-based metabolomics. *Future Drugs*, 6(5), pp.717–731.
- Shaddox, L.M. *et al.*, 2010. Perpetuation of subgingival biofilms in an *in vitro* model. *Molecular Oral Microbiology*, 25(1998), pp.81–87.
- Shameli, K. *et al.*, 2011. Fabrication of silver nanoparticles doped in the zeolite framework and antibacterial activity. *International Journal of Nanomedicine*, 6, pp.331–341.
- Shao, H. & Dermuth, D., 2010. Quorum sensing regulation of biofilm growth and gene expression by oral bacteria and periodontal pathogens. *Periodontology 2000*, 52(1), pp.53–67.
- Shelburne, C.E. *et al.*, 2000. Quantitation of *Bacteroides forsythus* in subgingival plaque Comparison of immunoassay and quantitative polymerase chain reaction. *Journal of Microbiological Methods*, 39(2), pp.97–107.
- Shendure, J. & Ji, H., 2008. Next-generation DNA sequencing. *Nature Biotechnology*, 26(10), pp.1135–1145.
- Shibata, Y. *et al.*, 1994. Effective method for discriminating between oral bacterial and human alkaline phosphatase activity. *Oral Microbiology and Immunology*, 9(1), pp.35–39.
- Shulaev, V., 2006. Metabolomics technology and bioinformatics. *Briefings in Bioinformatics*, 7(2), pp.128–39.
- Silva, T.C. *et al.*, 2012. Application of an active attachment model as a high-throughput demineralization biofilm model. *Journal of Dentistry*, 40(1), pp.41–7.

- Simmler, C. *et al.*, 2014. Universal quantitative NMR analysis of complex natural samples. *Current Opinion in Biotechnology*, 25, pp.51–59.
- Siqueira, J.F. *et al.*, 2000. Checkerboard DNA-DNA hybridization analysis of endodontic infections. *Oral Surgery, Oral Medicine, Oral Pathology, Oral Radiology, and Endodontology*, 89(6), pp.744–748.
- Siqueira, J.F., Fouad, A.F. & Rôças, I.N., 2012. Pyrosequencing as a tool for better understanding of human microbiomes. *Journal of Oral Microbiology*, 4, pp.1–15.
- Siqueira, J.F. & Rôças, I.N., 2013. As-yet-uncultivated oral bacteria: breadth and association with oral and extra-oral diseases. *Journal of Oral Microbiology*, 5, pp.1–14.
- Sissons, C.H. *et al.*, 1991. A multi-station dental plaque microcosm (artificial mouth) for the study of plaque growth, metabolism, pH, and mineralization. *Journal of Dental Research*, 70(11), pp.1409–1417.
- Sissons, C.H., 1997. Artificial dental plaque biofilm model systems. *Advanced Dental Research*, 11(1), pp.110–127.
- Slots, J., 1977a. Microflora in the healthy gingival sulcus in man. *Oral Sciences*, 85(4), pp.247–254.
- Slots, J., 1977b. The predominant cultivable microflora of advanced periodontitis. *Oral Sciences*, 85(2), pp.114–121.
- Slots, J., 1977. The predominant cultivable microflora of advanced periodontitis. *European Journal of Oral Sciences*, 85(2), pp.114–121.
- Slots, J. *et al.*, 1980. *Actinobacillus actinomycetemcomitans* in human periodontal disease: a cross-sectional microbiological investigation. *Infection and Immunity*, 29(3), pp.1013–1020.
- Smith, C.J. & Osborn, M., 2009. Advantages and limitations of quantitative PCR (Q-PCR) based approaches in microbial ecology. *FEMS Microbiology Ecology*, 67(1), pp.6–20.
- Smolinska, A. *et al.*, 2012. NMR and pattern recognition methods in metabolomics: from data acquisition to biomarker discovery: a review. *Analytica Chimica Acta*, 750, pp.82–97.
- Socransky, S. & Haffajee, A., 2005. Periodontal microbial ecology. *Periodontology 2000*, 38(1), pp.135–187.
- Socransky, S. *et al.*, 1998. Microbial complexes in subgingival plaque. *Journal of Clinical Periodontology*, 25(2), pp.134–44.

- Socransky, S., 1977. Microbiology of periodontal disease — present status and future considerations. *Journal of Periodontology*, 48(9), pp.497–504.
- Socransky, S. *et al.*, 1963. The microbiota of the gingival crevice area of men - total microscopic and viable counts and counts of specific organisms. *Archives of Oral Biology*, 8(3), pp.275–280.
- Socransky, S. *et al.*, 2004. Use of checkerboard DNA-DNA hybridization to study complex microbial ecosystems. *Oral Microbiology and Immunology*, 19(6), pp.352–62.
- Socransky, S. & Haffajee, A.D., 1994. Microbial etiological agents of destructive periodontal diseases. *Periodontology 2000*, 5(1), pp.78–111.
- Solmaz, G. *et al.*, 2013. Inhibitory and disruptive effects of shiitake mushroom (*Lentinula edodes*) essential oil extract on oral biofilms. *Jundishapur Journal of Microbiology*, 6(9), pp.1–6.
- Stamm, J., 1986. Epidemiology of gingivitis. *Journal of Clinical Periodontology*, 13(5), pp.360–366.
- Stewart, P.S. & Costerton, J.W., 2001. Antibiotic resistance of bacteria in biofilms. *The Lancet*, 358(9276), pp.135–138.
- Strange, K., 2005. The end of “naive reductionism”: rise of systems biology or renaissance of physiology? *Journal of Cell Physiology*, 288(5), pp.968–974.
- Strelkova, E. A. *et al.*, 2013. Role of the extracellular polymer matrix in resistance of bacterial biofilms to extreme environmental factors. *Microbiology*, 82(2), pp.119–125.
- Sugimoto, M. *et al.*, 2012. Physiological and environmental parameters associated with mass spectrometry-based salivary metabolomic profiles. *Metabolomics*, 9(2), pp.454–463.
- Syed, S.A. & Loesche, W.J., 1978. Bacteriology of human experimental gingivitis: effect of plaque age bacteriology of human experimental gingivitis: effect of plaque age. *Infection and Immunity*, 21(3), pp.821–829.
- Takada, K. *et al.*, 2010. Characterization of a new serotype g isolate of *Aggregatibacter actinomycetemcomitans*. *Molecular Oral Microbiology*, 25(3), pp.200–206.
- Takahashi, N., 2005. Microbial ecosystem in the oral cavity: metabolic diversity in an ecological niche and its relationship with oral diseases. *International Congress Series*, 1284, pp.103–112.

- Takeda, I. *et al.*, 2009. Understanding the human salivary metabolome. *NMR in Biomedicine*, 22(6), pp.577–84.
- Tamura, S. *et al.*, 2009. Inhibiting effects of *Streptococcus salivarius* on competence-stimulating peptide-dependent biofilm formation by *Streptococcus mutans*. *Journal of Oral Microbiology*, 24(2), pp.152–161.
- Tang, G. *et al.*, 2003. Artificial mouth model systems and their contribution to caries research: a review. *Journal of Dentistry*, 31(3), pp.161–171.
- Tanner, A. *et al.*, 1996. Clinical, microbiological and immunological profile of healthy, gingivitis and putative active periodontal subjects. *Journal of Periodontal Research*, 31(3), pp.195–204.
- Tanner, A. *et al.*, 1998. Microbiota of health, gingivitis, and initial periodontitis. *Journal of Clinical Periodontology*, 25(2), pp.85–98.
- Tanner, A.C.R. *et al.*, 1979. A study of the bacteria associated with advancing periodontitis in men. *Journal of Clinical Periodontology*, 6(5), pp.278–307.
- Tanner, A.C.R. *et al.*, 1979. A study of the bacteria associated with advancing periodontitis in man. *Journal of Clinical Periodontology*, 6(5), pp.278–307.
- Trombelli, L. *et al.*, 2004. Modulation of clinical expression of plaque-induced gingivitis. *Journal of Clinical Periodontology*, 31(4), pp.229–238.
- Teles, F.R. *et al.*, 2012. Early microbial succession in redeveloping dental biofilms in periodontal health and disease. *Journal of Periodontal Research*, 47(1), pp.95–104.
- Theilade, E., 1986. The non-specific theory in microbial etiology of inflammatory periodontal diseases. *Journal of Clinical Periodontology*, 13(10), pp. 905-911.
- Thurnheer, T. *et al.*, 2001. Automated fluorescent in situ hybridization for the specific detection and quantification of oral streptococci in dental plaque. *Journal of Microbiological Methods*, 44(1), pp.39–47.
- Timmerman, M. & Van der Weijden, G., 2006. Risk factors for periodontitis. *International Journal of Dental Hygiene*, 4(1), pp.2-7.
- Toole, G.A.O. & Stewart, P.S., 2005. Biofilms strike back. *Nature*, 23(11), pp.1378–1379.
- Tsuchida, S. *et al.*, 2012. Proteomic analysis of gingival crevicular fluid for discovery of novel periodontal disease markers. *Proteomics*, 12(13), pp.2190–202.

- Ursell, L.K. *et al.*, 2012. The interpersonal and intrapersonal diversity of human-associated microbiota in key body sites. *The Journal of Allergy and Clinical Immunology*, 129(5), pp.1204–8.
- Van der Velden, U., 2005. Purpose and problems of periodontal disease classification. *Periodontology 2000*, 39(1), pp.13–21.
- Verkaik, M.J. *et al.*, 2010. Oral biofilm models for mechanical plaque removal. *Clinical Oral Investigations*, 14(4), pp.403–9.
- Vokurka, J. *et al.*, 2008. The association of MMP-9 and IL-18 gene promoter polymorphisms with gingivitis in adolescents. *Archives of Oral Biology*, 54(2009), pp.172–8.
- Waddington, R. & Embery, G., 1994. Gingival crevicular fluid: biomarkers of periodontal tissue activity. *Advances in Dental Research*, 8(2), pp.329–337.
- Wade, W.G., 2013. Characterisation of the human oral microbiome. *Journal of Oral Biosciences*, 55(3), pp.143–148.
- Wade, W.G., 2011. Has the use of molecular methods for the characterization of the human oral microbiome changed our understanding of the role of bacteria in the pathogenesis of periodontal disease? *Journal of Clinical Periodontology*, 38 (Suppl 1), pp.7–16.
- Walker, C. & Sedlacek, M.J., 2007. An *in vitro* biofilm model of subgingival plaque. *Oral Microbiology and Immunology*, 22(3), pp.152–61.
- Wall, P.K. *et al.*, 2009. Comparison of next generation sequencing technologies for transcriptome characterization. *BMC Genomics*, 10(347), pp.1–19.
- Wall-manning, G.M. *et al.*, 2002. Checkerboard DNA – DNA hybridisation technology focused on the analysis of Gram-positive cariogenic bacteria. *Journal of Microbiological Methods*, 51(3), pp.301–311.
- Wang, J. *et al.*, 2013. Metagenomic sequencing reveals microbiota and its functional potential associated with periodontal disease. *Scientific reports*, 3(1843), pp. 1–10.
- Wang, X. *et al.*, 2011. Ultra-performance liquid chromatography coupled to mass spectrometry as a sensitive and powerful technology for metabolomic studies. *Journal of Separation Science*, 34(24), pp.3451–9.
- Wang, Z. *et al.*, 2009. RNA-Seq: a revolutionary tool for transcriptomics. *Nature Reviews Genetics*, 10, pp.57–63.

- Van Der Weijden, G. *et al.*, 2002. Effectiveness of an electrically active brush in the removal of overnight plaque and treatment of gingivitis. *Journal of Clinical Periodontology*, 29(8), pp.699–704.
- Whiteley, M., Brown, E. & Mclean, R.J.C., 1997. An inexpensive chemostat apparatus for the study of microbial biofilms. *Journal of Microbiological Methods*, 30(2), pp.125–132.
- Wilson, M., 1999. Use of constant depth film fermentor in studies of biofilms of oral bacteria. *Methods in Enzymology*, 310, pp.264–279.
- Wilson, M., 1996. Susceptibility of oral bacterial biofilms to antimicrobial agents. *Journal of Medical Microbiology*, 44, pp.79–87.
- Wilson, M. *et al.*, 1996. Killing of *Streptococcus sanguis* in biofilms using a light-activated antimicrobial agent. *The Journal of Antimicrobial Chemotherapy*, 37(2), pp.377–81.
- Wilson, M. *et al.*, 1998. Effect of chlorhexidine on multi-species biofilms. *Current Microbiology*, 36(5), pp.13–18.
- Wirthlin, M.R. *et al.*, 2005. A laboratory model biofilm fermenter: design and initial trial on a single species biofilm. *Journal of Periodontology*, 76(9), pp.1443–9.
- Wirthlin, R.M. *et al.*, 2005. A Laboratory Model Biofilm Fermenter: design and initial trial on a single species biofilm. *Journal of Periodontology*, 76(9), pp.1443 – 1449.
- Wishart, D.S., 2008. Quantitative metabolomics using NMR. *Trends in Analytical Chemistry*, 27(3), pp.228-237.
- Wu, Y. *et al.*, 2009. Initial comparison of proteomic profiles of whole unstimulated saliva obtained from generalized aggressive periodontitis patients and healthy control subjects. *Journal of Periodontal Research*, 44(5), pp.636–44.
- Xu, Y.J. *et al.*, 2014. Recent developments and applications of metabolomics in microbiological investigations. *TrAC Trends in Analytical Chemistry*, 56, pp.37–48.
- Y. Li, P.W. *et al.*, 2005. Mode of delivery and other maternal factors influence the acquisition of *Streptococcus mutans* in infants. *Journal of Dental Research*, 84(9), pp.806–811.
- Yassien, M. *et al.*, 1995. Modulation of biofilms of *Pseudomonas aeruginosa* by quinolones. *Antimicrobial Agents and Chemotherapy*, 39(10), pp.2262–2268.
- Yoshimura, F. *et al.*, 1984. Characterization of a trypsin-like protease from the bacterium *Bacteroides gingivalis* isolated from human dental plaque. *Archives of Oral Biology*, 29(7), pp.559–564.

- Zarco, M.F. *et al.*, 2012. The oral microbiome in health and disease and the potential impact on personalized dental medicine. *Oral Diseases*, 18(2), pp.109–20.
- Zaura, E. *et al.*, 2009. Defining the healthy “core microbiome” of oral microbial communities. *BMC Microbiology*, 9(259), pp.1-12.
- Zaura, E., 2012. Next-generation sequencing approaches to understanding the oral microbiome. *Advances in Dental Research*, 24(2), pp.81–5.
- Zee, K.Y. *et al.*, 1996. Predominant cultivable supragingival plaque in Chinese rapid and slow plaque formers. *Journal of Clinical Periodontology*, 23(11), pp.1082–1085.
- Zhang, W. *et al.*, 2011. A practical comparison of de novo genome assembly software tools for next-generation sequencing technologies. *PloS one*, 6(3), pp.1-12.
- Zylber, L. J. & Jordan, H. V., 1982. Development of a selective medium for detection of and enumeration of *Actinomyces viscosus* and *Actiomyces naeslundii* in dental plaque. *Journal of Clinical Microbiology*, 15(2), pp.253–259.